

**On the redistribution and sorting of sand at nourishments  
Field evidence and modelling of transport processes and bed composition change**

Huisman, Bas

**DOI**

[10.4233/uuid:a2bbb49d-8642-4a32-b479-4f0091f2d206](https://doi.org/10.4233/uuid:a2bbb49d-8642-4a32-b479-4f0091f2d206)

**Publication date**

2019

**Document Version**

Final published version

**Citation (APA)**

Huisman, B. (2019). *On the redistribution and sorting of sand at nourishments: Field evidence and modelling of transport processes and bed composition change*. [Dissertation (TU Delft), Delft University of Technology]. <https://doi.org/10.4233/uuid:a2bbb49d-8642-4a32-b479-4f0091f2d206>

**Important note**

To cite this publication, please use the final published version (if applicable).  
Please check the document version above.

**Copyright**

Other than for strictly personal use, it is not permitted to download, forward or distribute the text or part of it, without the consent of the author(s) and/or copyright holder(s), unless the work is under an open content license such as Creative Commons.

**Takedown policy**

Please contact us and provide details if you believe this document breaches copyrights.  
We will remove access to the work immediately and investigate your claim.

# ON THE REDISTRIBUTION AND SORTING OF SAND AT NOURISHMENTS

Bastiaan Jan Arie Huisman



# **ON THE REDISTRIBUTION AND SORTING OF SAND AT NOURISHMENTS**

FIELD EVIDENCE AND MODELLING OF TRANSPORT  
PROCESSES AND BED COMPOSITION CHANGE



# **ON THE REDISTRIBUTION AND SORTING OF SAND AT NOURISHMENTS**

FIELD EVIDENCE AND MODELLING OF TRANSPORT  
PROCESSES AND BED COMPOSITION CHANGE

## **Dissertation**

for the purpose of obtaining the degree of doctor  
at Delft University of Technology  
by the authority of the Rector Magnificus prof. dr. ir. T. H. J. van der Hagen  
chair of the Board for Doctorates  
to be defended publicly on  
Thursday 9 May 2019 at 15:00 o'clock

by

**Bastiaan Jan Arie HUISMAN**

Civil Engineer, Delft University of Technology  
born in Sliedrecht, The Netherlands.

This dissertation has been approved by the promotor.

Composition of the doctoral committee:

Rector Magnificus,	Chairman
Prof. dr. ir. M.J.F. Stive,	Delft University of Technology, promotor
Prof. dr. B.G. Ruessink,	Utrecht University, promotor
Dr. ir. M.A. de Schipper,	Delft University of Technology, copromotor

Independent members:

Dr. E. Gallagher,	Franklin & Marshall college
Prof. dr. K.M. Wijnberg,	University of Twente
Prof. dr. ir. S.G.J. Aarninkhof,	Delft University of Technology
Prof. dr. ir. J.A. Roelvink,	IHE-Delft

dr. ir. D.J.R. Walstra has, as a supervisor, contributed significantly to the preparation of this dissertation.



*Keywords:* Coastal safety, Sand nourishment, Morphology, Bed composition, Sediment sorting, Rip-currents, Numerical modelling

*Cover:* Based on 'Baggermolens' by Bas Baan (Molenaarsgraaf, 1980)

*Printed by:* ProefschriftMaken || [www.proefschriftmaken.nl](http://www.proefschriftmaken.nl)

Copyright © 2019 by B.J.A. Huisman

The European Research Council of the European Union is acknowledged for the funding provided for this research by the ERC-advanced Grant 291206-NEMO.

ISBN 978-94-6384-037-8

An electronic version of this dissertation is available at

<http://repository.tudelft.nl/>.

# SUMMARY

Sand nourishments are essential for the maintenance of sandy coasts in various countries around the world. The sand is placed at the beach or shoreface to mitigate erosion due to sea level rise, wave induced alongshore transport gradients, diminishing sediment supply or lee-side erosion at coastal structures. Over time the nourishment will erode, but sediment will remain available for the local coastal cell. The scale of the nourishments has increased considerably in the last decades as a result of more proactive maintenance of the coast and compensation of sediment deficits due to sea level rise. Relatively small beach nourishments with volumes of 100 to 500 thousand  $\text{m}^3$  were the dominant type of nourishment up till the 90's, but in the last decades it has become common practice in some countries (e.g. in the Netherlands, United States and Australia) to use large sand buffers in shallow water seaward of the sub-tidal bar (between MSL -4m and MSL -10m; referred to as 'shoreface nourishments') with volumes of a few million  $\text{m}^3$ . Recently, even larger scale 'mega nourishments' were placed in the Netherlands which in-fact act as (temporary or maintained) land reclamations. These mega nourishments were applied as a long-term buffer for coastal erosion at two locations in the Netherlands (Sand Motor in 2011,  $\sim 21.5$  million  $\text{m}^3$  and Hondsbossche & Pettemer Zeewering in 2014,  $\sim 35$  million  $\text{m}^3$ ). The behaviour of shoreface and mega feeder nourishments and their effects on the marine environment (e.g. bed composition) are, however, not well understood. Moreover efficient methods are needed to assist coastal managers with the evaluation of the required sandy coastal maintenance measures in the coming decades. The objectives of this thesis are therefore to provide understanding of I) the sediment redistribution at large-scale nourishments and II) their impact on the bed sediment composition of the surrounding coast. Field data of the bathymetry and sediment were used in this thesis to validate numerical models, which in turn were used to quantify the contribution of the most relevant driving hydrodynamic processes. On the basis of these data it was possible to develop more efficient evaluation methods of the lifetime of large-scale nourishments and their impact on the bed composition of the surrounding coast.

## BEHAVIOUR AND MODELLING OF SHOREFACE NOURISHMENTS

Bathymetric data of 19 shoreface nourishments located at alongshore uniform sections of coast were analyzed and used to validate an efficient method for predicting the erosion of shoreface nourishments. Data shows that considerable cross-shore profile change takes place at a shoreface nourishment, while an impact at the adjacent coast is hard to distinguish. A landward skewing of the cross-shore profile is typically observed consisting of a landward movement (and increase in height) of the nourishment crest and erosion of the seaward edge of the nourishment, erosion directly landward of the shoreface nourishment (in the first 100 to 150 m) and some accretion in the inner surfzone ( $\sim$  MSL -2m). The considered shoreface nourishments provide a

long-term (3 to ~30 years) cross-shore supply of sediment to the beach, but with small impact on the local shoreline shape. An efficient modelling approach is presented using a lookup table filled with computed initial erosion-sedimentation rates for a range of potential environmental conditions at a single post-construction bathymetry, after which the erosion-sedimentation rates for a measured time-series are obtained through interpolation. Numerical modelling showed that the geometrical change of the profile by the shoreface nourishment enhances the onshore transport processes (due to increased velocity asymmetry of the waves). Cross-shore transport due to waves and water-level setup driven currents contribute most to the erosion of a shoreface nourishment in the first years after construction (i.e. 60% to 85%), while the alongshore transport contributes to a smaller extent. Most erosion of the nourishment takes place during energetic conditions ( $H_{m0} >= 3\text{m}$ ) as milder waves are propagated over the nourishment without breaking. A data-model comparison shows that the applied modelling approach can be used to accurately assess the erosion rates of shoreface nourishments in the first years after construction.

#### REDISTRIBUTION AND LIFETIME OF MEGA NOURISHMENTS

Design graphs showing the erosion rates, life span and maintenance volumes for the planning phase of projects are derived for freely developing feeder-type mega nourishments (such as the Sand Motor) and permanent mega-nourishments (i.e. land reclamation with sand). Various length-to-width ratios and volumes are considered using calibrated 2DH and 1D numerical models. The extensive set of bathymetric data at the Sand Motor was used as validation data for the numerical models. Results show that mega nourishments reshape towards a bell-shape which gradually becomes wider in alongshore direction and less pronounced in cross-shore direction. The redistributed sediment has a direct impact on the adjacent coast (i.e especially in the first kilometer) which accretes considerably in the first years after construction. The response of a mega nourishment can be described well with a model that resolves the alongshore wave-driven current, such as a shoreline model, which have the advantage that no trade-off needs to be made with respect to the schematization of the wave climate. Making a differentiation between the non-rotating foreshore and active surfzone proved to be essential for an accurate representation of the wave-driven alongshore transport in 1D coastline models. The lifetime of nourishments is mainly determined by the dimensions of the nourishment and incoming wave energy. It was found that the lifetime of the nourishment can be related to the sensitivity of the alongshore wave-driven transport to a small rotation of the shoreline, which is expressed with the Longshore transport index ( $LTI$ ).

#### OBSERVED BED COMPOSITION CHANGES AT A LARGE-SCALE NOURISHMENT

The development of the bed sediment composition, with a focus on the median grain size  $D_{50}$ , was investigated for the 'Sand Motor' at the Dutch coast. Considerable alongshore heterogeneity of the bed composition ( $D_{50}$ ) was observed as the Sand Motor evolved over time with (1) a coarsening of the lower shoreface of the exposed part of the Sand Motor (+90 to +150  $\mu\text{m}$ ) and (2) a deposition area with relatively fine material (50  $\mu\text{m}$  finer) just North and South of the Sand Motor. The alongshore heterogeneity of the  $D_{50}$  is most evident outside the surfzone (i.e. seaward of MSL -4 m), while along-



shore variation in  $D_{50}$  was relatively small in the surfzone itself (i.e. landward of MSL -4 m). Considerable bed composition change can take place also seaward of the toe of the nourishment at the natural seabed (~ up to MSL -14 m). The coarsening of the bed after construction of the Sand Motor is attributed to hydrodynamic sorting processes, as the alongshore heterogeneity of the  $D_{50}$  correlated significantly with the mean bed shear stresses ( $R^2 \sim 0.8$ ). Preferential erosion of the finer sand fractions takes place during mild to moderate wave conditions, while a reduction of the local armouring of the bed takes place during storms (i.e. a  $\sim 40 \mu\text{m}$  reduction of the  $D_{50}$  after a storm in September 2014). This is attributed to the mobilization of both the coarse and fine sediment size fractions and mixing of the top-layer of the bed with the relatively finer substrate.

#### MODELLING SORTING PROCESSES IN RELATION TO ENVIRONMENTAL CONDITIONS

The relevance of hydrodynamic conditions (e.g. horizontal tide and waves) for bed composition changes at the lower shoreface of the Sand Motor and driving sediment sorting processes were investigated using numerical modelling. A 3D multi-fraction morphological model gave a good hindcast of 2.5 year of observed spatial and temporal changes in  $D_{50}$  at the Sand Motor, for which the precise initial condition for the  $D_{50}$  of the bed was unimportant. The alongshore variation of the  $D_{50}$  in both the 2DH and 3D models correlated significantly with the measurements ( $R^2$  of 0.84 to 0.94), but the observed cross-shore  $D_{50}$  variation was only represented well in the 3D model. The model computations showed that normal wave conditions can easily suspend the fine sand fractions at the lower shoreface, while the coarser sand fractions are hardly entrained. This difference in suspension behaviour is the main cause of the observed bed composition changes at the lower shoreface. Within the surfzone the difference in suspension behaviour of the size fractions will be smaller, as the energetic conditions can suspend all size fractions. Models with multiple sediment fractions are therefore required for the assessment of the impact of large-scale nourishments (or coastal structures) on the bed composition of the lower shoreface, while a single fraction model with a representative median grain size ( $D_{50}$ ) may suffice for the modelling of morphological changes within the surfzone. Furthermore, the model shows that the extent and magnitude of the coarsening of the bed are related to the tidal contraction, which implies that large-scale bed composition changes can take place at any coastal structure which has a considerable impact on the tidal currents.

#### RECOMMENDATIONS

Ongoing urbanization and enhanced sea level rise will inevitably increase the pressure on the land use of sandy coasts in the near future. The evaluation of the efficiency of large-scale nourishments in mitigating coastal erosion and the effects of these measures on the seabed composition are therefore not just important for The Netherlands, but also for various other densely populated coastal regions around the world. The applied evaluation methods for shoreface and mega-nourishments can in principle also be used for coasts with less wave energy (e.g. sites in the Middle East, South-East Asia or Australia) or more severe waves (e.g. United States or Namibia). For this purpose, however, it is recommended to evaluate the methods for a selection of representative sites around the world.

The long-term morphological change of shoreface nourishments (>5 years after construction) is a remaining challenge, as the current measurements and models do not provide sufficient information to trace back the redistribution of sand at longer time scales. For this purpose, the evolution of a shoreface nourishment should be measured for a sufficiently long period (e.g. 10 years) and large coastal area (e.g. 5 km at both sides). In addition the current studies show that a better preservation of the sub-tidal bars is needed in numerical models to accurately represent both short-term and long-term coastal morphological change at shoreface nourishments. Detailed flow patterns at the sand bar and trough will be needed to discriminate the physical processes responsible for the net transport of sand. The behaviour of shoreface and mega nourishments also needs to be studied for more complex coasts with bays, tidal currents and coastal structures, where the influence of wave-direction and non-wavedriven currents will be more important. In order to aid coastal modelers, it is suggested to extend the current handbooks with hydrodynamic forcing conditions with site specific coastal properties such as the *LTI* parameter, which expresses the sensitivity of the wave climate to a rotation of the beach.

Questions on the effects on the marine habitat for benthos and fish have become more relevant recently as a consequence of the ongoing increase in the size of nourishments. The potential effects are, however, not yet accounted for in environmental impact assessments of coastal structures. In order to ease the evaluation of the impact of future large-scale nourishments on bed composition for such studies, it is necessary to improve the computational efficiency of the numerical models computing the multi-fraction transport rates and administration of sediment in the bed. For example, by using representative conditions, more efficient representations of the physics in the models and design graphs. When it comes to detailed hindcasts of bed composition changes due to nourishments, it is expected that improvements can still be made to the model representation of bed composition changes during storms, which will require a mixing function of the sediment in the top-layers of the bed. Regions where fine sediment moves over a coarse bed (e.g. entrance channels of tidal basins) need a weighting of the separately computed size fractions in the numerical model based on the presence of the considered fractions in the updrift supply of sediment.

# SAMENVATTING

Zandsuppleties zijn essentieel voor het onderhoud van zandige kusten. Het zand wordt op de kust geplaatst om erosie te compenseren door zeespiegelstijging, golfgedreven langstransport, afnemende toevoer van sediment door rivieren of lijzijde erosie bij constructies. Door de tijd heen zal de zandsuppletie eroderen, maar het zand blijft beschikbaar voor de kustcel waarin deze is geplaatst. De schaal van de zandsuppleties is echter aanzienlijk toegenomen sinds 1990 als gevolg van een meer proactieve wijze van onderhoud van de kust waarbij een minimum kustlijn wordt gehandhaafd én zeespiegelstijging wordt gecompenseerd. In de jaren '90 werden meestal relatief kleine strandsuppleties toegepast met volumes van 100 tot 500 duizend m<sup>3</sup>, terwijl het tegenwoordig in verschillende landen (o.a. Nederland, Verenigde Staten en Australië) al gebruikelijk is om grote zandbuffers ('vooroeversuppleties') te plaatsen op ondiep water aan de zeewaartse zijde van de brekerbank (op 4 tot 10 meter waterdiepte) met volumes van enkele miljoenen m<sup>3</sup>. Recent zijn in Nederland zelfs nog grotere suppleties toegepast ('megasuppleties') welke in feite gezien kunnen worden als (tijdelijke of door onderhoud op hun plaats gehouden) landaanwinningen. Deze megasuppleties zijn toegepast als lange-termijn zandbuffer op de Delflandse kust in 2011 (Zandmotor; ~ 21.5 miljoen m<sup>3</sup>) en bij de Hondsbossche & Pettemer Zeewering in 2014 (~ 35 miljoen m<sup>3</sup>). Het gedrag van de grootschalige vooroever- en megasuppleties en hun effect op de mariene omgeving (o.a. bodemsamenstelling) is echter nog slecht begrepen. Bovendien is er vanuit kustbeheerders behoefte aan efficiënte methodes voor het evalueren van de effecten van toekomstige zandige kustversterkingsmaatregelen, welke momenteel nog ontbreken voor deze grootschalige zandsuppleties. De doelen van dit proefschrift zijn daarom om meer inzicht te verwerven in I) de herverdeling van zand bij grootschalige zandsuppleties en II) de invloed op bodemsamenstelling van de omliggende kust. Veldmetingen van bodemhoogte en sediment worden in het project gebruikt om numerieke modellen te calibreren welke daarna inzicht geven in de belangrijkste aandrijvende hydrodynamische processen. Op basis van deze gegevens is het mogelijk om efficiënte evaluatie methodes te ontwikkelen voor de levensduur van grootschalige suppleties en hun invloed op de bodemsamenstelling van de omliggende kust.

## GEDRAG EN MODELLERING VAN VOOROEVERSUPPLETIES

Het gedrag van 19 vooroeversuppleties op langsuniforme secties kust is onderzocht én gebruikt om een efficiënte methode te valideren voor het voorspellen van erosie van vooroeversuppleties. De gegevens laten zien dat aanzienlijke kustdwarse profielveranderingen plaats vinden als gevolg van vooroeversuppleties, terwijl de invloed op de aanliggende kust (in langsrichting) moeilijk te onderscheiden is. De kustdwarse profielvorm ter plaatse van de vooroeversuppletie vervormt als een zaagtand in landwaartse richting. Erosie vindt plaats aan de zeewaartse zijde van de suppletie én in

de eerste 100 tot 150 meter direct landwaarts van de suppletie, terwijl de kruin toeneemt in hoogte en landwaarts verplaatst. Tevens vindt er aanzanding plaats in ondiep water (~ MSL -2m). De vooroever-suppleties leveren een lange termijn (3 tot ~30 jaar) bijdrage aan de sedimentbalans van de kust, maar hebben een beperkte invloed op de vorm van de kustlijn. De toegepaste efficiënte modellering maakt gebruik van een database gevuld met vooraf berekende initiële sedimentatie-erosie velden voor potentieel relevante golf- en getijcondities, welke berekend zijn voor een enkele post-constructie bodem, waarna de erosie-sedimentatie voor elk van de condities in een tijdserie middels interpolatie wordt bepaald. Numerieke modellering laat zien dat de geometrische verandering van het kustprofiel als gevolg van het plaatsen van een vooroever-suppletie zorgt voor een vergroting van de transportprocessen richting de kust (als gevolg van een verhoogde asymmetrie van de orbitaalsnelheden van de golven). Dwarstransport door golven en waterstandsverschil gedreven stroming dragen (in de eerste jaren na constructie) het meeste bij aan de erosie van vooroever-suppleties (i.e. 60% tot 85%), terwijl het langstransport een aanzienlijk kleiner deel bijdraagt. De meeste erosie vindt plaats tijdens energetische condities ( $H_{m0} >= 3\text{m}$ ) omdat de rustigere golven over de suppletie heen gaan zonder te breken. Een data-model vergelijking laat zien dat de toegepaste aanpak gebruikt kan worden om nauwkeurige berekeningen te maken van erosiesnelheden van vooroever-suppleties in de eerste jaren na aanleg.

#### HERVERDELING EN LEVENSDUUR VAN MEGASUPPLETIES

Ontwerpgrafieken met erosiesnelheden, levensduur en onderhoudsvolumes voor de planfase van projecten zijn afgeleid voor vrij ontwikkelende en permanente megasuppleties (o.a. Zandmotor of landaanwinningen). Verschillende lengte-breedte verhoudingen en volumes zijn beschouwd, waarvoor gecalibreerde 2DH en 1D modellen zijn gebruikt. De uitgebreide set met bodemhoogte gegevens bij de Zandmotor is gebruikt als validatie voor de modellen. De resultaten laten zien dat megasuppleties een klok-vorm aan gaan nemen, waarna ze geleidelijk steeds wijder worden langs de kust en minder breed in kustdwarse richting. Het herverdeelde sediment heeft een directe invloed op de omliggende kust (in het bijzonder de eerste kilometer) waar aanzienlijke aanzanding plaats vindt. Het gedrag van een megasuppletie kan goed worden beschreven met een model dat het langstransport van zand door golven berekent (i.e. een kustlijnmodel). Het is echter van groot belang om in het model een verschil te maken tussen de statische vooroever en de actieve kustlijn die meeroteert als de kustlijn (door erosie of sedimentatie) van vorm veranderd. De levensduur van megasuppleties wordt hoofdzakelijk bepaald door de afmetingen van de suppletie en de inkomende golfenergie, terwijl golfrichting een kleinere invloed heeft. De levensduur van de megasuppletie kan het beste ingeschat worden op basis van de gevoeligheid van het langstransport voor een kleine rotatie van de kusthoek, welke wordt gerepresenteerd door de Langstransportindex (*LTI*).

#### VERANDERING IN BODEMSAMENSTELLING BIJ EEN GROOTSCHALIGE SUPPLETIE

De ontwikkeling van de bodemsamenstelling, met een focus op de mediane korreldiameter  $D_{50}$ , is onderzocht voor de Zandmotor aan de Nederlandse kust. Dit laat zien dat er aanzienlijke heterogeniteit is in de bodemsamenstelling bij de Zandmotor be-

staande uit (1) een vergroving van de korreldiameter op de diepe vooroever zeewaarts van de Zandmotor (+90 to +150  $\mu\text{m}$ ) en (2) een aanzandingsgebied met relatief fijn sediment (50  $\mu\text{m}$  fijner dan omgeving) net noordelijk en zuidelijk van de Zandmotor. Deze langsheterogeniteit van de  $D_{50}$  is vooral aanwezig buiten de brandingszone (i.e. zeewaarts van MSL -4 m), terwijl de langsvariatie in  $D_{50}$  relatief klein was in de brandingszone zelf (i.e. landwaarts van MSL -4 m). Aanzienlijke veranderingen in bodemsamenstelling konden zelfs zeewaarts van de teen van de suppletie plaats vinden op de natuurlijke zeebodem ( $\sim$  tot MSL -14 m). De vergroving van de bodem na aanleg van de Zandmotor wordt toegeschreven aan hydrodynamische sorteringsprocessen, omdat de langsheterogeniteit van de  $D_{50}$  significant correleert met de gemiddelde bodemschuifspanningen ( $R^2 \sim 0.8$ ). Selectieve erosie van de fijne zandfracties vindt plaats tijdens normale golfcondities, terwijl er sprake is van een vermindering van de lokale vergroving van de toplaag van de bodem tijdens stormen (i.e. een  $\sim 40$   $\mu\text{m}$  reductie van de  $D_{50}$  na een storm in September 2014). Dit wordt toegeschreven aan de mobilisatie van zowel de grove als de fijne fracties tijdens de storm alsmede het mixen van de toplaag van de bodem met het relatief fijnere substraat.

#### MODELLERING VAN SORTERINGSPROCESSEN IN RELATIE TOT DE OMGEVINGSCONDITIES

Het belang van hydrodynamische condities voor de verandering van de bodemsamenstelling op de vooroever van de Zandmotor en daarvoor meest belangrijke drijvende sortingsprocessen zijn onderzocht met numerieke modellering. Een 3D multi-fractie morfologisch model gaf een goede reproductie van 2.5 jaar aan geobserveerde ruimtelijke en temporele veranderingen van de  $D_{50}$  bij de Zandmotor, waarbij de precieze start bodemsamenstelling onbelangrijk was. De langsvariatie van de  $D_{50}$  correleerde in zowel het 2DH als 3D model significant met de waarnemingen ( $R^2$  van 0.84 tot 0.94), terwijl de kustdwarse verdeling van de  $D_{50}$  alleen in een 3D model werd gerepresenteerd. De simulaties laten zien dat normale golfcondities de fijnere sediment fracties op de vooroever makkelijk kunnen suspenderen, terwijl de grovere zandfracties slechts beperkt omhoog getransporteerd worden. Dit verschil in suspensiegedrag is de belangrijkste oorzaak van de geobserveerde verandering in bodemsamenstelling bij de Zandmotor. Binnen de brandingszone zal het verschil in suspensiegedrag echter kleiner zijn, omdat de energie hier zo groot is dat alle zandfracties makkelijk suspenderen. Modellen met meerdere sediment fracties zijn daarom nodig voor het beoordelen van de invloed van grootschalige suppleties (of constructies) op de bodemsamenstelling van de diepe vooroever, terwijl een model met een enkele representatieve sedimentfractie genoeg kan zijn voor de modellering van morfologische veranderingen in de brandingszone. Verder laat het model ook zien dat de invloedszone en mate van vergroving van de bodemsamenstelling gerelateerd zijn aan de getijcontractie, wat betekent dat een verandering van de bodemsamenstelling kan plaats vinden bij elke kustmaatregel die invloed heeft op de getijdestroming.

#### AANBEVELINGEN

Verstedelijking en versnelde zeespiegelstijging zullen onvermijdelijk zorgen voor een toename van de druk op het landgebruik in kustgebieden in de nabije toekomst. De evaluatie van de efficiëntie van grootschalige zandsuppleties in het bestrijden van kusterosie en de invloed van deze maatregelen op de samenstelling van de zeebodem zijn

daarom niet alleen belangrijk voor Nederland, maar ook voor andere dichtbevolkte kustgebieden over de hele wereld. De toegepaste methodes voor het berekenen van de veranderingen bij vooroever- en megasuppleties kunnen in principe ook gebruikt worden voor kusten met minder golfenergie (bijv. in het Midden-Oosten, Zuid-Oost Azië of Australië) of voor heftigere condities (bijv. Verenigde Staten of Namibië). Ten behoeve hiervan wordt het echter wel aangeraden om de methodes te toetsen voor een paar geselecteerde representatieve landen/regio's van de wereld.

De lange-termijn verandering van vooroever-suppleties (>5 jaar na aanleg) is een nog bestaande uitdaging, aangezien de huidige metingen en modellen geen uitsluitel geven over de verspreiding van het zand op langere termijn. Ten behoeve hiervan zou de ontwikkeling van een vooroever-suppletie over een voldoende lange periode (bijv. 10 jaar) en groot kustlangs gebied (5 km aan beide zijden) moeten worden gemeten. Aanvullend laten de huidige studies zien dat een betere representatie van de zandbanken nodig is in numerieke modellen om zowel de korte als lange termijn morfologische verandering van vooroever-suppleties beter te representeren. Gedetailleerde stromingspatronen bij de zandbank en in de trog zijn nodig om onderscheid te maken tussen de fysische processen die verantwoordelijk zijn voor het netto transport van zand. Het gedrag van vooroever- en grootschalige suppleties op complexe kusten met baaien, constructies en getijdeinvloed moet ook beter onderzocht worden, waarbij de invloed van golfrichting en niet-golfgedreven stroming belangrijker gaat worden. Om kustmodelleers te helpen wordt voorgesteld om de huidige randvoorwaardenboeken (met hydrodynamische condities) uit te breiden met regio-specifieke morfologische karakteristieken zoals de *LTI* parameter welke de gevoeligheid van het transport weergeeft voor een rotatie van het strand.

Als gevolg van de recente toename in het volume van suppleties worden vragen over de effecten van suppleren op de mariene leefomgeving voor bodemdieren en vissen opeens actueel. De mogelijke effecten worden echter nog niet meegenomen in milieueffect rapportages voor kustmaatregelen. Om het proces van de evaluatie van de invloed van toekomstige grootschalige suppleties op de bodemsamenstelling makkelijker te maken, is het nodig om de snelheid te vergroten van de numerieke modellen met multi-fractie transport en een administratie van de samenstelling van de bodemlagen. Dit kan bijvoorbeeld door het gebruik van representatieve condities, snellere rekenmethode's en ontwerpgrafieken. Als het aankomt op gedetailleerde voorspellingen van bodemsamenstelling, dan kunnen er nog verbeteringen gemaakt worden door een betere representatie van de bodemverandering tijdens stormen, waarvoor een functie nodig is die het sediment in de top-lagen van de bodem verticaal mixt. Voor regio's waar fijn sediment over een grove toplaag beweegt (bijv. bij de toegang van een getijdebasin) is een weging nodig van de per fractie berekende transporten die afhangt van het voorkomen van de beschouwde fracties in de bovenstroomse aanvoer van sediment.

# CONTENTS

<b>Summary</b>	<b>v</b>
<b>Samenvatting</b>	<b>ix</b>
<b>1 Introduction</b>	<b>1</b>
<b>2 Behaviour and modelling of shoreface nourishments</b>	<b>7</b>
2.1 Introduction . . . . .	7
2.2 Study Area . . . . .	9
2.3 Methodology . . . . .	12
2.4 Observed Nourishment Behaviour . . . . .	16
2.5 Efficient Modelling of Shoreface Nourishments . . . . .	23
2.6 Discussion . . . . .	28
2.7 Conclusions. . . . .	32
<b>3 Redistribution and lifetime of mega nourishments</b>	<b>35</b>
3.1 Introduction . . . . .	35
3.2 Methodology . . . . .	37
3.3 Hindcast of Sand Motor mega nourishment. . . . .	42
3.4 Evolution of mega nourishments . . . . .	50
3.5 Discussion . . . . .	61
3.6 Conclusions. . . . .	65
<b>4 Observed sediment Sorting</b>	<b>67</b>
4.1 Introduction . . . . .	67
4.2 Study Area . . . . .	70
4.3 Methodology . . . . .	72
4.4 Sediment survey data . . . . .	77
4.5 Relation of $D_{50}$ with bed shear stresses . . . . .	84
4.6 Discussion . . . . .	87
4.7 Conclusions. . . . .	89
<b>5 Modelling sorting processes</b>	<b>95</b>
5.1 Introduction . . . . .	95
5.2 Study Area . . . . .	99
5.3 Methodology . . . . .	101
5.4 Hindcast of morphology and bed composition . . . . .	106
5.5 Relevance of hydrodynamic conditions . . . . .	113
5.6 Discussion . . . . .	115
5.7 Conclusions. . . . .	118

---

<b>6 Conclusions and perspectives</b>	<b>119</b>
6.1 Conclusions . . . . .	119
6.2 Discussion and perspectives . . . . .	123
<b>References</b>	<b>127</b>
<b>Acknowledgments</b>	<b>143</b>
<b>About the author</b>	<b>145</b>
<b>List of Publications</b>	<b>147</b>



# 1

## INTRODUCTION

### BACKGROUND

Many sandy coasts around the world are under threat of coastal retreat due to sea level rise (Bruun, 1962; Bird, 1985; Stive et al., 1991; Ranasinghe et al., 2013; Luijendijk et al., 2018) as well as erosion due to alongshore transport gradients (Inman, 1987; Thevenot and Kraus, 1995; Van Rijn, 1997b), diminishing sediment supply by rivers and land subsidence (Anthony et al., 2015). Beaches and dunes are, however, essential elements of the coast as they protect the hinterland against flooding and sustain other economic functions (e.g. recreation and drinking water supply). Especially the densely populated low-lying delta regions are threatened by coastal retreat, such as the Netherlands where about 26% of the land area is below sea level (Figure 1.1a; Alcamo et al., 2007), but also the deltas of the Mississippi, Mekong, Nile and Ganges-Brahmaputra rivers are vulnerable (Field et al., 2007; Cruz et al., 2007).

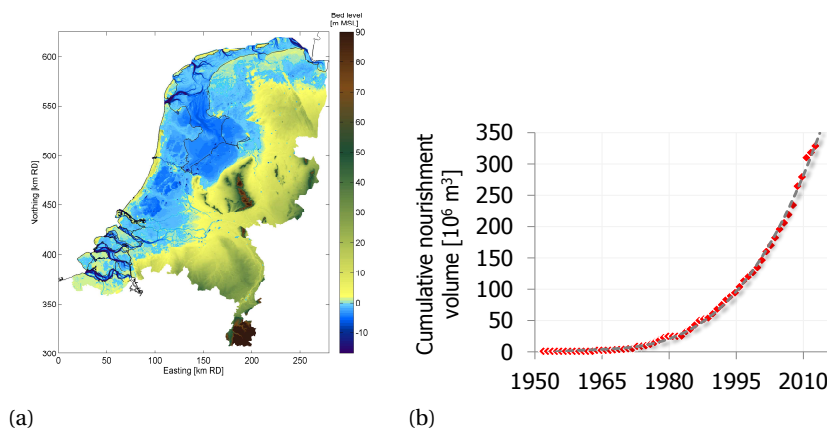


Figure 1.1: Map of The Netherlands showing the elevation of the terrain (left panel) and cumulative nourished sediment volume at the Dutch coast (right panel).

In view of anticipated sea level rise and increasing population pressure on coastal areas it is anticipated that more and more places in the world are affected by flooding (e.g. cities such as Richmond, Miami, Venice and many mega-cities in Asia; Nicholls, 2004; Hanson et al., 2011; Park et al., 2017), which will make the maintenance of sandy coasts increasingly important in the coming decades. In addition the yearly nourishment requirement of sandy beaches has increased substantially over time due to more pro-active maintenance policies (Van Koningsveld and Mulder, 2004; [Figure 1.1b](#)).

Various coastal reinforcements were constructed in the last centuries to protect sandy coasts against erosion (e.g. dikes, rock revetments, wooden pole groynes, port breakwaters and sand nourishments). Hard coastal structures, however, often have a negative impact on the adjacent coast (Komar, 1998), which is for example noticeable in the Netherlands at the port breakwaters of IJmuiden which block the natural transport of sand towards the North (Van Rijn, 1997b; Wijnberg, 2002). Sand is therefore commonly used nowadays to maintain and restore natural beaches in The United States, European countries and Australia (Leonard et al., 1990; Hanson et al., 2002; Cooke et al., 2012). Well over a 1000 sand nourishments have been applied since the 1920's in the United States East coast, Gulf of Mexico and Great Lakes at about 400 different sites (Sorensen et al., 2011; Trembanis and Pilkey, 1998; Valverde et al., 1999), while a similar number of nourishments has been applied in European countries until the year 2000 (Hamm et al., 2002). Most nourishments have been placed at the beach where they have a direct benefit for beach users and safety (e.g. Stolk, 1989; Roelse, 1990; Leonard et al., 1990; Hanson et al., 2002; Cooke et al., 2012) with volumes ranging from 50,000 to a few million m<sup>3</sup> over lengths of 1 to 10 kilometers. Over time these sand nourishments will disappear, but the sand remains beneficial for the sediment balance of the coastal cell (Hanson et al., 2002; Van Koningsveld and Mulder, 2004). A 50% reduction of beach nourishment volume typically takes place in 1 to 5 years for beach nourishments at the U.S. East coast (Leonard et al., 1990), while the erosion of the full nourishment took 5 to 15 years for many of the European cases considered by Hamm et al. (2002). The halftime of the nourishments does, however, vary substantially for nourishments. For the U.S. East coast Leonard et al. (1990) attributed this to the density of placed sand per meter length of the nourishment and the number of storms that occurred, while Dean and Yoo (1992) on the other hand present design-graphs which relate the halftime of nourishment volume only to the length and the average offshore wave height in the considered region (thus excluding the alongshore volume density of the nourishment or cross-shore width). Most recent studies do, however, use numerical models to evaluate the stability of the beach nourishments, which solve the redistribution of nourishment sand based on gradients in the wave-driven alongshore currents (e.g. using coastline models; Hanson and Kraus, 1989) and therefore implicitly include also the cross-shore perturbation size of the nourishment. Also other nourishment and regional characteristics can influence the stability of nourishments, such as recirculation of sand towards borrow areas that are created too close to the shore (at Delray beach (Florida); Hartog, 2006; Benedet et al., 2007) or the placement of relatively coarse sand at the beach (Ludka et al., 2018).

The costs of beach nourishments are substantial, amounting to an annual cost of

about 100 million U.S. dollar for the United States East coast alone (Trembanis et al., 1999) with a cost price of 0.2 to 1 million dollars per kilometer of beach nourishment. Innovative larger scale nourishments (with a volume of several million  $\text{m}^3$ ) were therefore applied a number of times in the last decades to make the coastal maintenance more cost-efficient (e.g. Van Duin et al., 2004; Van der Spek and Elias, 2013; Stive et al., 2013; see Figure 1.2a). These large-scale nourishments are placed either 1) as 'Shoreface nourishments' directly seaward of the sub-tidal bar at 4 to 10 meter below Mean Sea Level (MSL) or 2) as temporary land reclamations over the full cross-shore profile (from MSL -10 m to MSL +3 m) which feed the adjacent coast (referred to as 'Mega nourishments').

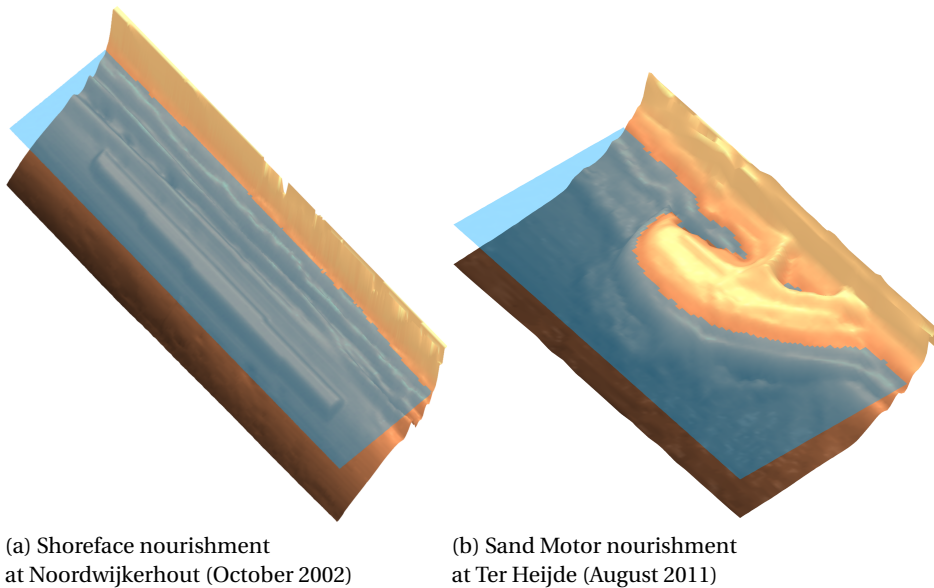


Figure 1.2: Examples of large scale sand nourishments at the Dutch coast.

The main advantage of the shoreface nourishment (compared to beach nourishments) is the ease of application, as a ship can sail to the dump locations in intermediate water depth and quickly release the sand, which can make coastal maintenance considerably more cost-effective. The actual spreading of the sand and lifetime of the shoreface nourishment has been studied in Florida and the Netherlands. The shoreface nourishments interact with the natural bars and activate alongshore and cross-shore spreading of sand (e.g. Van Duin et al., 2004; Grunnet and Ruessink, 2005; Van der Spek and Elias, 2013), but the development of the erosion over time and supply of sediment to the adjacent coast are poorly understood. The morphological changes are attributed partly to shielding of the waves by the nourishment, cross-shore transport processes and alongshore transport as a result of the wave-driven current in the considered case studies (i.e. at Egmond and Terschelling), but the general applicability of these findings is not so clear. In this respect it should be noted that the observed

lifetime of shoreface nourishments can differ considerably (i.e. with a halftime ranging from 3 to more than 10 years), which suggests that the driving forces and transport processes may be different depending on the characteristics of the shoreface nourishment or local environment. Furthermore, also the modelling of shoreface nourishments is only partly successful as the influence of artificial flattening of the natural beach profile in the models is making it difficult to identify the impacts of the nourishment (e.g. Grunnet et al., 2004). It is obvious that federal governments and municipalities demand proven effective beach nourishment methods. And as a result the lack of knowledge on the morphological behaviour and absence of a generally applicable and efficient prediction method for the sediment redistribution limits the use of shoreface nourishments in coastal maintenance practice.

Recently two mega feeder nourishments were constructed along the Dutch coast, which are even larger than shoreface nourishments and can be considered as (temporary) land reclamations. The 'Sand Motor' with a volume of  $\sim 21$  million  $m^3$  (Stive et al., 2013) was applied in 2011 at the southern section of the Holland coast, while the 'Hondsbossche & Pettemer Zeewering' nourishment at the North-Holland coast had a volume of  $\sim 35$  million  $m^3$  (Kroon et al., 2015). Mega nourishments act as a sand feeder to the coast and live much longer than the other nourishment types (De Schipper et al., 2016; Arriaga et al., 2017), while providing opportunities for other coastal functions such as nature development and recreation in the mean-time. The sheer size of these measures also results in a low price per volume unit of the sand (Brown et al., 2016). It is therefore likely that more large-scale nourishments will be planned in the near future, which will require efficient and easy-to-use methods to compute the redistribution of sediment and lifetime of these nourishments. The current numerical methods are, however, computationally intensive, which make them less practical for the evaluation of future measures. A thorough understanding of the physical processes controlling the sediment redistribution is also needed to come up with more efficient modelling methods for both the shoreface and mega nourishments, requiring the collection and analysis of field evidence as verification of the modelled alongshore or cross-shore spreading of the sand. The limited understanding of the sediment redistribution processes at large-scale shoreface and mega nourishments is therefore the first problem that is addressed in this thesis.

Numerical models can be used to obtain information on the relevance of environmental conditions (e.g. Van Rijn, 1997b; Wijnberg and Kroon, 2002) and transport processes (i.e. cross-shore or alongshore due to waves or tide). Either detailed process-based models resolving the most dominant hydrodynamic and morphological processes (Lesser et al., 2004; Reniers et al., 2004a) or less detailed semi-empirical model can be applied. These behaviour models are typically more efficient as they use prior knowledge of typical coastal behaviour and only the most relevant physics. The most relevant driving processes can be included in the modelling (e.g. hydrodynamic forcing conditions such as wave-driven and tidal currents, water level setup, infra-gravity waves, wave breaking, roller forces, boundary layer streaming or wave asymmetry and skewness), while the lesser important or static processes can be left out of consideration. For example, coastline models enforce an equilibrium profile shape and coast-

line orientation (Hanson and Kraus, 1989 and Ruggiero et al., 2010) which effectively limits the freedom of the model to the alongshore redistribution of sediment. A question is, however, whether the physics of large-scale nourishments can be captured with the more-efficient 'reduced complexity' models.

The recent upscaling of the sand nourishment volume in the last decades (i.e. to Sand Motor scale) and increasing anthropogenic pressure also comes with questions regarding the impact that is made on the natural environment (Defeo et al., 2009). Sand nourishments are generally considered less invasive than hard structures, as they consist of natural materials, but burial of marine species may take place (McLachlan, 1996; Knaapen et al., 2003). The bed sediment composition may change, directly as a result of the nourished sand or indirectly due to the altered hydrodynamic conditions (Gibson and Robb, 1992; McLachlan and De Ruyc, 1993; Alexander et al., 1993). This can affect the habitat for benthos and flat fish (Post et al., 2017). Some research has been conducted on the bed composition change of coastal profiles during storm conditions (Broekema et al., 2016). A problem is, however, that the impact of nourishments on the bed sediment composition during mild conditions is not yet explored, which is the second problem addressed in this thesis. Previous applications focused on a river bifurcation (Sloff and Mosselman, 2012) or delta developments (Geleynse et al., 2011). Most previous research on sediment sorting processes focuses either on 1) the initiation of motion of sediment grains (e.g. Wilcock, 1993) or 2) high-energy sheet-flow conditions in the swash zone where waves run-up the beach (e.g. Hassan and Ribberink, 2005). Conditions in the marine environment will, however, exceed the threshold of motion most of the time as a result of the stirring of the bed by waves, but will not reach sheet-flow conditions either. Thus leaving a void with respect to the sorting processes during the more common intermediate energetic conditions at the Dutch coast.

## RESEARCH OBJECTIVES

The objective of this thesis is to provide understanding on 1) the redistribution of sand of large-scale nourishments and 2) the impact of nourishments on the bed sediment composition. An underlying question is the sustainability of future policies to maintain the coasts and their effects on the marine environment. This thesis provides essential building blocks for the understanding of the processes and mechanisms affecting sediment redistribution at shoreface nourishments and mega nourishments, which comprises I) analyses of field observations of bathymetric and bed composition changes, II) the investigation of the driving processes and III) methods to predict changes of future coastal measures. The two objectives lead to the following research questions:

### **Objective 1: Redistribution of nourished sediment**

- Q1.1 : How do shoreface and mega nourishments redistribute over time?
- Q1.2 : What is the relative contribution of alongshore and cross-shore processes to the redistribution of shoreface and mega nourishments?
- Q1.3 : How can the lifetime of nourishments be assessed efficiently?

**Objective 2: Bed composition change at nourishments**

- Q2.1 : What impact do sand nourishments have on the bed sediment composition of the surrounding coast?
- Q2.2 : What processes affect sediment sorting at nourishments?
- Q2.3 : What are the implications of sediment sorting at mega nourishments for morphological modelling?

A combination of field measurements (i.e. bathymetric surveys and bed sediment composition samples) and numerical modelling with 1D coastline and 2DH / 3D field models is used to investigate the research questions. The recent bathymetry measurements of the large-scale Sand Motor nourishment (De Schipper et al., 2016) are used to study the morphological behaviour of the coast as well as bathymetric data for a large number of shoreface nourishments at alongshore uniform sections of the Dutch coast (e.g. Van Duin et al., 2004). Field data are used to improve and develop validated prediction methods for the erosion of shoreface and mega nourishments. This thesis provides methods to hindcast observed morphological changes with a selection of governing morphological process (e.g. due to the alongshore wave-driven current).

Sediment samples are collected and analyzed to show the impacts of the large-scale Sand Motor nourishment on the bed composition of the coast and used as validation for a numerical model. In this way the applicability of multi-fraction sediment transport computations for sandy coasts with nourishments is verified. The numerical model is then used to explore the detailed bed composition changes which could not be measured in the field, as well as the relevance of suspension transport for each of the size fractions in relation to the forcing conditions and geometrical properties of the nourishment.

## OUTLINE

This doctoral thesis discusses 1) the behaviour of shoreface nourishments ([chapter 2](#)), 2) the lifetime of mega nourishments based on morphological development of the Sand Motor ([chapter 3](#)), 3) the impact of the large-scale Sand Motor nourishment on bed composition in relation with hydrodynamics ([chapter 4](#)) and 4) modelling of sorting processes to reveal the underlying mechanisms ([chapter 5](#)). In addition the individual chapters also provide methodologies for efficient and accurate modelling of shoreface and mega nourishments. The research questions 1.1 to 1.3 are studied in [chapter 2](#) and [chapter 3](#), while the research questions 2.1 to 2.3 are considered in [chapter 4](#) and [chapter 5](#). It is noted that [chapter 2](#) to [chapter 5](#) are based on journal publications (Huisman et al., 2016; Huisman et al., 2018; Tonnon et al., 2018; Huisman et al., 2019), which were slightly modified to smoothly fit in this thesis.

# 2

## BEHAVIOUR AND MODELLING OF SHOREFACE NOURISHMENTS

*\* Shoreface nourishments are commonly applied for coastal maintenance, but their behaviour is not well understood. Bathymetric data of 19 shoreface nourishments located at alongshore uniform sections of the Dutch coast were therefore analyzed and used to validate an efficient method for predicting the erosion of shoreface nourishments. Data shows that considerable cross-shore profile change takes place at a shoreface nourishment, while an impact at the adjacent coast is hard to distinguish. The considered shoreface nourishments provide a long-term (3 to ~30 years) cross-shore supply of sediment to the beach, but with small impact on the local shoreline shape. An efficient modelling approach is presented using a lookup table filled with computed initial erosion-sedimentation rates for a range of potential environmental conditions at a single post-construction bathymetry. Cross-shore transport contributed the majority of the losses from the initial nourishment region. This transport was driven partly by water-level setup driven currents (e.g. rip currents) and increased velocity asymmetry of the waves due to the geometrical change at the shoreface nourishment. Most erosion of the nourishment takes place during energetic wave conditions ( $H_{m0} >= 3$  m) as milder waves are propagated over the nourishment without breaking. A data-model comparison shows that this approach can be used to accurately assess the erosion rates of shoreface nourishments in the first years after construction.*

### 2.1. INTRODUCTION

The preservation of sandy coastlines around the world requires regular maintenance with 'soft measures' using sand to mitigate potential erosion from natural and anthropogenic causes (Bird, 1985; Dean and Yoo, 1992; Davis et al., 2000; Hamm et al., 2002;

---

\*This chapter is based on the publication: Huisman, B.J.A., Walstra, D.J.R., Radermacher, M., De Schipper, M.A. and Ruessink, B.G.. *Observations and Modelling of Shoreface Nourishment Behaviour*. *Journal of Marine Science and Engineering*. 2019; 7(3):59.

Benedet et al., 2007; Ludka et al., 2018). Over time, these sand nourishments will disappear, but the sand will still be beneficial for the sediment balance of the coastal cell. Historically, the most common type of sand nourishment is placed at the beach from 2 meter below mean sea level (MSL) up to the dunefoot at MSL +5 m (e.g. Leonard et al., 1990; Cooke et al., 2012), but considerably larger sub-tidal nourishments (referred to as 'shoreface nourishments') are also placed nowadays to replenish the beach (Van der Spek and Elias, 2013). These shoreface nourishments are placed as relatively long (2 to 10 km) sand bodies in depths ranging from MSL -10 to -4 m, which simplifies the process of nourishing as dredging vessels can navigate towards the location where the sand needs to be placed. Investigations of the behaviour of shoreface nourishments in the Netherlands at Terschelling, Egmond and Noordwijk (Hoekstra et al., 1996; Grunnet and Ruessink, 2005; Van Duin et al., 2004; Ojeda et al., 2008) show that shoreface nourishments remain in place for a much longer period than beach nourishments. About 45% of the sediment was, for example, still in place at the Egmond 1999 nourishment after three years (Van Duin et al., 2004). The available studies showed erosion at the shoreface nourishment and some accretion in the inner surfzone (i.e. ~MSL -2 m). This is explained by Hoekstra et al. (1996) with a concept of a shoreface nourishment which acts as a submerged breakwater which retains sand from the alongshore wave-driven current, while cross-shore processes play only a subtle role. A study for Egmond (Van Duin et al., 2004) did, however, conclude that part of the accretion in the shallow nearshore zone is due to cross-shore processes on the basis of simulations with a cross-shore model capable of resolving bar migration. In addition, schematic computations by Grunnet and Ruessink (2005) indicate an enhancement of the skewness of the wave orbital motion (i.e. enhanced landward velocities of the orbital wave motion) at the nourishment resulting in onshore transport. The relative contribution of alongshore and cross-shore processes could, however, not be quantified, as 2DH models were hindered by artificial flattening of the bars (e.g. Grunnet et al., 2004), while a stable sub-tidal bar could only be maintained in cross-shore profile models (Walstra et al., 2012; Jacobsen and Fredsoe, 2014a). This is a problem since answering the questions on the driving processes at shoreface nourishments will require a method which can compute both alongshore and cross-shore profile change while keeping the natural profile (with sub-tidal bar) in place.

In addition, the representativeness of the studied shoreface nourishments for other regions is under discussion as the shoreface nourishment at Terschelling is placed inside the trough of the natural bar system (Hoekstra et al., 1996), while other shoreface nourishments (e.g. at Egmond; Van Duin et al., 2004) are placed at the seaward side of the sub-tidal bar. Furthermore, the Noordwijk nourishment eroded at a slower pace than the other nourishments (Ojeda et al., 2008). It is therefore very relevant to better understand the behaviour of shoreface nourishments at other field sites (and with different properties) to create generic knowledge and modelling methods that can be used effectively for future beach maintenance plans.

Relevant for the investigation of shoreface nourishments is the interaction with the natural bar system, which according to Van der Spek and Elias (2013) consists of a temporary blockage of the natural offshore bar migration at the Dutch coast. Land-



ward transport was even observed at the Delfland coast (i.e. southern Holland coast) by Radermacher et al. (2018) as a result of the placement of shoreface nourishments which pushed the existing bars towards the coast. It is envisioned that the delicate balance of onshore (e.g. Hoefel and Elgar, 2003; Ruessink et al., 2007) and offshore directed transport processes (e.g. due to the undertow current and long infra-gravity waves; Svendsen, 1984; Roelvink, 1993b) at natural sub-tidal bars also controls the behaviour of shoreface nourishments. Since placing a disturbance in the profile (such as a shoreface nourishment) is likely to adjust the balance of cross-shore transport processes. Model simulations by Jacobsen and Fredsoe (2014a) showed such detailed cross-shore profile changes after placement of a nourishment, which consisted of an increase of the crest height of the bar (located between MSL  $-1$  m and MSL  $-2$  m) and erosion at the landward side of the nourishment crest. Furthermore, Jacobsen and Fredsoe (2014a) found an increase of offshore losses after placement of nourishment sand in the trough region for the considered situation, but large offshore losses were not observed by Hoekstra et al. (1996) and Grunnet and Ruessink (2005) for the Terschelling nourishment which was also placed in a trough. It is uncertain what causes this discrepancy for both situations (e.g. the crest height of the bar or wave conditions), but illustrates the difficulties in finding general rules for the behaviour of shoreface nourishments.

This research aims at providing an overview of the morphological development of multiple shoreface nourishments with varying properties, which is then used to validate a modelling approach for the erosion and redistribution of sediment from the nourishments showing the relevance of the driving processes. For this purpose, the cross-shore profile change and alongshore redistribution are studied for 19 shoreface nourishments on the alongshore uniform sections of the Dutch coast. Volumetric changes are computed over time for predefined spatial regions (e.g. nourishment, trough and nearshore) and related to the geometrical properties, thus showing erosion and accretion rates for each of the spatial regions, especially the morphological development in the first 3 years after construction is studied. A modelling approach using precomputed sedimentation and erosion rates for a matrix of possible conditions is then validated against the observed rates of erosion and accretion. In this way, understanding is created of the driving processes, as well as a validated generic forecast method.

## 2.2. STUDY AREA

The Dutch coast is characterized as a sandy coast with a micro-tidal environment (Wijnberg, 2002). This study considers nourishments at four different sections of the Dutch coast ('Delfland', 'Rijnland' and 'North-Holland' and 'Terschelling'). Each of these regions has specific characteristics with respect to the bathymetry, wave conditions and sediment composition (Figure 2.1).

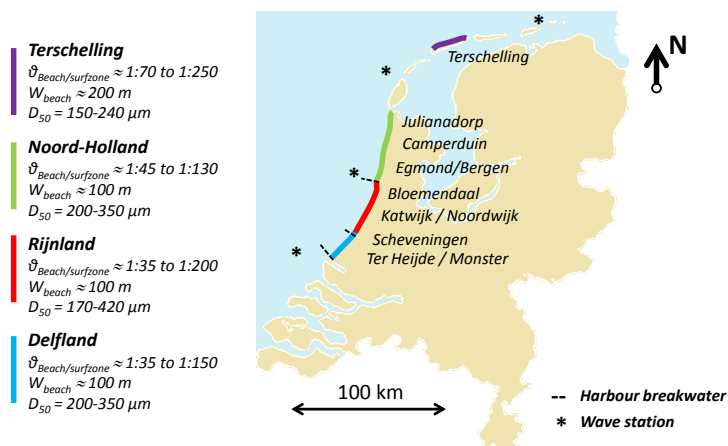


Figure 2.1: Overview of locations of considered nourishments along the Dutch coast and typical characteristics.

The Delfland and Rijnland beaches are characterized by a beach slope of 1:35 with a gradual transition to a milder slope of 1:150 to 1:200 in the surfzone (MSL to MSL  $-8$  m; Ruessink et al., 2003; Rijkswaterstaat, 2017b). The North-Holland coast has a beach slope of 1:45 to 1:60, a steeper sub-tidal profile (1:100 to 1:130) and a more complex shoreface with a large tidal channel in the North. The beach and surfzone at Terschelling are milder with a beach slope of 1:70 and a 1:200 to 1:250 slope in the sub-tidal profile. A maximum of five sand bars can be present in a single cross-shore profile at the Holland coast (Walstra et al., 2012; Wijnberg and Terwindt, 1995; Pape et al., 2010) of which the amplitude varies in seaward direction. Ruessink et al. (2003) shows that largest bar-crest amplitudes are found at water depths of about MSL  $-4$  m at the Delfland and Rijnland coast, MSL  $-5$  m at North-Holland and MSL  $-6$  m at Terschelling. The natural bars are influenced by storms which push the bar in seaward direction, while onshore movement of the bar takes place during quiet conditions (Van Enckevort and Ruessink, 2003). Over longer time-frames, they show a net offshore migration with cycle times between 3 and 15 years at the Dutch coast (e.g. Ruessink et al., 2003; Wijnberg and Terwindt, 1995; Ruessink and Kroon, 1994; Shand et al., 1999), but this behaviour is affected by nourishments as the offshore migration of the sub-tidal bar at Egmond is temporarily halted after nourishment construction (Van der Spek and Elias, 2013).

A range of shoreface nourishments was investigated in this research (Table 2.1). This comprises nourishments on alongshore uniform sections of coast, which includes the central sections of the barrier island of Terschelling. Each of the nourishments is monitored with sufficient frequency and is not influenced by other nourishments (i.e. within the first 3 to 5 years after construction). Most of the shoreface nourishments are constructed at the seaward side of the sub-tidal bar between MSL  $-8$  m to MSL  $-3$  m (e.g. Van Duin et al., 2004), with the exception of the Terschelling nourishment which was constructed in the trough landward of the sub-tidal bar (Grunnet and Ruessink, 2005).

Table 2.1: Overview of properties of the considered shoreface nourishment.

Nourishment	T0	Vol. [10 <sup>6</sup> m <sup>3</sup> ]	Density [m <sup>3</sup> /m]	L×W [km]	Depth [m MSL]	Type ****	
<i>Delfland:</i>							
Scheveningen'99	Jun-99	1.4	453	3.2×0.4	-8 to -4	B&S	near breakwater
Terheijde'97	Aug-97	0.9 **	517	1.7×0.3	-8 to -5	S	
Terheijde'01	Aug-01	3.0 (+0.8) ***	569	5.2×0.4	-9 to -5	B&S	beach 2003 & 2004
Monster'05	Nov-05	1.0 **/ ***	198	5.1×0.4	-7 to -4	S	
<i>Rijnland:</i>							
Katwijk'98	Nov-98	0.75 **	349	2.2×0.3	-7 to -5	S	
Noordwijk'98	Apr-98	1.3	414	3.1×0.5	-7 to -5	S	
Noordwijkerhout'02	Jun-02	2.6	375	7.0×0.3	-8 to -5	S	
Wassenaar'02	Dec-02	2.5	412	6.1×0.3	-8 to -5	S	
Zandvoort'04	Oct-04	1.4	278	5.0×0.4	-7 to -5	B&S	
Zandvoort-Zuid'08	Jul-08	0.5 **/ ***	191	2.7×0.2	-6 to -4	S	
Bloemendaal'08	Nov-08	1.0	531	1.9×0.3	-7 to -5	S	
<i>North-Holland:</i>							
Camperduin'02	Aug-02	2.0 **	522	3.8×0.3	-10 to -4	S	beach 2003 & 2004
Callantsoog'03	Apr-03	2.3 (+0.4) *	386	6.0×0.5	-8 to -5	B&S	beach 2004
Egmond'99	Jun-99	0.9** (+0.2)*	376	2.3×0.3	-8 to -5	B&S	beach 2001
Bergen'00	Jul-00	1.0** (+0.2)*	377	2.6×0.5	-6 to -3	B&S	
Bergen&Egmond'05	Sep-05	3.1** (+0.8)*	343	9.0×0.6	-8 to -4	B&S	
Hondsb.&Pettem.Zw.'09	Apr-09	5.7 **	423	13.5×1.0	-12 to -4	S	at revetment
Julianadorp'09	Apr-09	1.3	402	3.2×0.6	-9 to -4	S	beach 2011
<i>Terschelling:</i>							
Terschelling'93	Nov-93	2.1 **	476	4.4×0.3	-7 to -4	S	landward of bar

\* The volume of the beach nourishments is presented in-between brackets.

\*\* Measured volume in the first survey was considerably smaller than official nourishment volume (<90%).

\*\*\* Placement within a few years after a preceding nourishment.

\*\*\*\* The nourishment types are beach (B) and shoreface (S).

The wave climate of the Dutch coast is characterized by wind waves which originate either from the southwest (i.e. dominant wind direction) or the northwest (i.e. direction with largest fetch length). For Terschelling, this means that the waves predominantly approach from the northwest, because the southwestern component is shielded by land. Offshore wave data are available from an offshore platform ('Europlatform') at 32 m water depth West off the Delfland coast, the IJmuiden wave station (between Rijnland and North-Holland), the 'Eierland' wave measurement buoy in the northwest (between the islands of Texel and Vlieland) and the Schiermonnikoog North buoy (at about 40 kilometers East of Terschelling). The wave climate is characterized by average significant wave height ( $H_{m0}$ ) of about one meter in summer and 1.7 meters in winter (Wijnberg, 2002) with typical winter storms with wave heights ( $H_{m0}$ ) of 4 to 5 meters and a wave period of about 10 s (Sembiring et al., 2015). The storms originate

from the northwest and coincide with a typical storm surge of 0.5 to 2 meter. The tidal current is asymmetric with largest flow velocities towards the north during the flood ( $\sim 0.7$  m/s) and a longer period with ebb-flow in the southern direction ( $\sim 0.5$  m/s; Wijnberg, 2002). The tidal wave at this part of the North Sea is a progressive wave with largest flood velocities occurring just before high water.

The natural sediment at the Delfland, Rijnland and North-Holland coast can be characterized as medium sand at the waterline ( $D_{50}$  of 300 to 400  $\mu\text{m}$  at the Delfland coast) which gradually fines in seaward direction to a  $D_{50}$  of 150 to 200  $\mu\text{m}$  at MSL  $-8$  m and deeper (Terwindt, 1962; Van Straaten, 1965). Sediment at Terschelling is finer than at the other locations with a  $D_{50}$  of about 240  $\mu\text{m}$  at the waterline with a gradual decrease to 150  $\mu\text{m}$  at MSL  $-8$  m (Guillén and Hoekstra, 1996). Specifications from Rijkswaterstaat prescribe that the nourishment sediment is similar to the natural beach sediment (Stolk, 1989; Rijkswaterstaat, 2017a). The  $D_{50}$  at Egmond '99, Bergen '00 and Noordwijk '98 nourishments was measured, which indicated a  $D_{50}$  of respectively 228  $\mu\text{m}$ , 250  $\mu\text{m}$  and 400  $\mu\text{m}$  (Ojeda et al., 2008). However, some uncertainty is present in these measurements as the sediment size is expected to vary over the cross-shore profile of the shoreface nourishment. Nourished sediment at the Terschelling coast was slightly coarser than the natural sediment at the depth where it was applied (i.e.  $D_{50}$  about 10 to 50  $\mu\text{m}$  larger at MSL  $-4$  m to MSL  $-6$  m depth). Details on the applied sediment for the other nourishment sites are not available. The borrow areas are typically located in relative close proximity (i.e. 10 to 50 kilometers) from the coastal section where the sediment is placed, which implies that the origin of the sediment is typically similar. It is therefore expected that the grain size distribution of the nourished material matches with the native material, which is relevant for the stability of the nourished material (Krumbein and James, 1965; De Vincenzo et al., 2018), although too little field measurements of sediment at shoreface nourishments are available to understand potential sorting processes during the placement of the nourished material. For the Holland coast, it is expected that sorting processes are especially relevant outside the surfzone (i.e. where the suspension of size fractions differs for coarse and fine sand grains; Huisman et al., 2018), while shoreface nourishments are placed for a large part inside the surfzone. The importance of sorting processes at shoreface nourishments should, however, be judged per site and may need further investigation.

### 2.3. METHODOLOGY

Bathymetric surveys of 19 shoreface nourishments were studied to establish an overview of the behaviour of shoreface nourishments, with a focus on (1) cross-shore profile changes, (2) alongshore spreading (i.e. impact on the coast) and (3) a volumetric analysis of the changes. These data were then used to validate a morphological model of the erosion of the shoreface nourishment, which uses an interpolation of pre-computed sedimentation-erosion fields for a matrix of possible environmental conditions to obtain a prediction of the erosion rates at each time instance of a hindcast time-series. Such a method is considered considerably more efficient than brute-force modelling of the time-series of conditions, while artificial flattening of bar and trough features (in the numerical model) is avoided by using static underlying

bathymetries (i.e. from the first survey after construction of the shoreface nourishment).

## DATA ANALYSIS

The annual cross-shore bathymetric measurements along the Dutch coast (Jarkus data; Rijkswaterstaat, 2017b) were used as a basis for the assessment of the behaviour of the nourishments. These data provided a complete coverage of the Dutch coast from 1965 onwards. Additional bathymetry data were available at Terschelling '93 (Hoekstra et al., 1996; Grunnet and Ruessink, 2005), Egmond '99 and Bergen '00 (Van Duin et al., 2004). It is noted that the surveys did not always cover the full extent of the region with the nourishment (or the adjacent coast), in which case the regions with missing data were filled in by linear interpolation of the survey data of the preceding and following survey. The outline of the initial nourishment region was defined based on visual inspection of the sedimentation-erosion in the first post-construction survey with respect to the pre-nourishment situation.

First, the alongshore spreading of sand was determined from the changes over time in the cross-shore averaged sediment volume along the coast. Histograms were made of (1) the average volume change of the nourishments, (2) migration rate of the center of the added volume/mass of the nourishment and (3) impact on the adjacent coast. Alongshore compartments of 800 m at both sides of the nourishment were used. The extent of the regions at the adjacent coast was based on availability of suitable bathymetric data and the influence area of other nourishments. Cross-shore profile change was shown at the center of the nourishment with the aim to find the typical response(s) of the profile shape to the added sediment (e.g. influence on the bar). The temporal development of the crest height, trough depth and profile steepness of the seaward side of the nourishment were inspected from the data. The volumetric changes in predefined cross-shore regions were then quantified over a period of three years (Figure 2.2) with respect to a pre-construction 'reference' bathymetry (analogous to Walstra et al., 2013). The considered regions covered (1) the offshore area from MSL  $-10$  m to the seaward edge of the nourishment (somewhere between MSL  $-8$  m and MSL  $-3$  m), (2) the initial nourishment region (approximately from MSL  $-8$  m to MSL  $-4$  m), (3) a region of 120 m directly landward of the shoreface nourishment ( $\sim$  MSL  $-4$  m) and (4) the inner surfzone and beach (approximately from MSL  $-4$  m to MSL  $+2$  m).

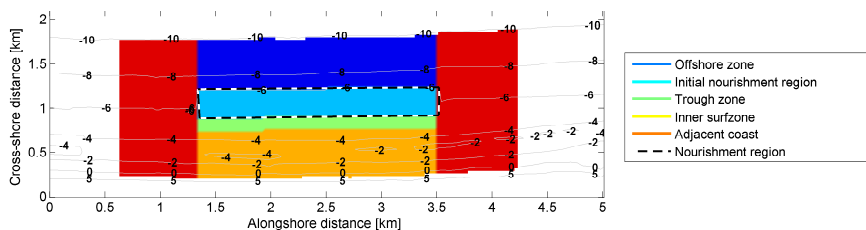


Figure 2.2: Example of defined volumetric integration regions for the Katwijk '98 shoreface nourishment. Contours with respect to mean sea level (MSL).

## NUMERICAL MODELLING

A next step was to perform numerical modelling of the morphological changes at shoreface nourishments. This was achieved using pre-computed sedimentation and erosion rates (in different regions of the nourishment) from the XBeach model (Reniers et al., 2004b; Roelvink et al., 2009) for a matrix of possible environmental conditions, which functions as a look-up table. The actual erosion rates of a hindcast time-series of wave conditions could then be obtained by interpolation of the most similar conditions in the matrix of pre-computed sedimentation-erosion rates (Figure 2.3). The first post-construction bathymetry was used for the XBeach models. Off-shore wave boundary conditions were applied with increasing wave height ( $H_{m0}$  of 1, 2, 3 and 4 m) and corresponding wave periods ( $T_p$  of 6, 8, 10 and 12 s). Each of these wave conditions was then computed for five wave directions ( $-30, -15, 0, 15$  and  $30$  degree), which were all evaluated for a range of tidal velocities ( $-1, -0.5, 0, 0.5$  and  $1$  m/s). This resulted in 100 simulations ( $4 \times$  waves,  $5 \times$  directions and  $5 \times$  tidal velocities) for each considered nourishment. An erosion rate of 0 was assumed for the situation without waves ( $H_{m0} = 0$  m). In fact, the pre-computed XBeach simulations are used as a lookup table to obtain a prediction of the erosion rates for each of the time-instances of a (measured) hindcast time-series of wave conditions. A linear interpolation was used in between the pre-computed classes.

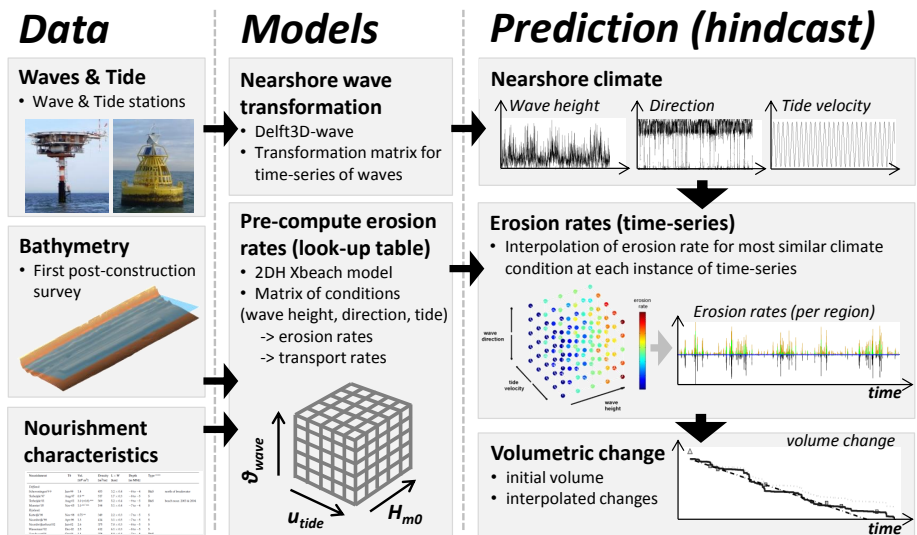


Figure 2.3: Methodology for computing volumetric change at shoreface nourishments using a lookup table of computed initial erosion rates.

The XBeach model (Reniers et al., 2004b; Roelvink et al., 2009) computes the sediment transport as a result of wave-driven currents, roller forcing, residual circulations, long (infra-gravity) waves and tidal currents (Roelvink, 1993a). Basic wave transformation processes such as refraction, shoaling, breaking of the waves and bed friction were included in the short-wave model. The surbeat mode of XBeach was used to resolve also the long (infra-gravity) waves. Sediment transport rates were computed using the

Van Thiel de Vries (2009) transport formulation. Settings of the XBeach model were based on default settings for the safety evaluations of the Dutch primary water defenses (Table 2.2), which included calibrated wave skewness and asymmetry parameters to balance the offshore transport at the Dutch coast (Van Geer et al., 2015; Bart, 2017). Other process-based area models have difficulties in maintaining the steepness of the coastal profile (e.g. Delft3D; Grunnet et al., 2004; Lesser et al., 2004). The XBeach model can also cope well with extreme wave conditions (Roelvink et al., 2009), which are expected to be relevant for the transport at a sub-tidal sand nourishment.

Table 2.2: Overview of settings used in the XBeach model.

Type	Description	Keyword	Value	Unit
Grid	Grid resolution (2DH)	$dx&dy$	5 to 30 (finest at MSL -4m)	$m$
Waves	Wave shape		Van Thiel de Vries (2009)	
	Wave skewness factor	$facSk$	0.375	
	Wave asymmetry factor	$facAs$	0.123	
	Bore-averaged turbulence	$turb$	2 (=bore avg)	
	Depth breaking parameter	$gamma$	0.541	
	Steepness breaking parameter	$alpha$	1.262	
	Minimum adaptation time scale	$Tsmin$	1	$s$
	Maximum wave steepness	$maxbrsteep$	0.4	
Roller	Maximum wave height	$gammax$	2.364	
	Breaker slope coefficient	$beta$	0.138	
Friction	Roller dissipation power	$n$	10	
	Bed friction	$Manning$	0.02	$s/m^{1/3}$
Sediment	Equilibrium sediment concentration	$form$	TRANSPOR2004 (Van Rijn, 2007a,b) Van Thiel de Vries (2009)	
	Median grain diameter	$D_{50}$	300	$\mu m$
	90th percentile grain diameter	$D_{90}$	400	$\mu m$
	Porosity	$por$	0.4	
	Density of the sediment	$\rho_s$	2650	$kg/m^3$
	Density of the water	$\rho_w$	1025	$kg/m^3$

The prediction (or hindcast) of the erosion/accretion rates was made for five shoreface nourishments (Ter Heijde '97, Katwijk '98, Noordwijk '98, Noordwijkerhout '02 and Egmond '99) for the first 2 to 3 years after construction. The matrix of pre-computed sedimentation-erosion rates was used to obtain the erosion rate for each time instance of the hindcast period. For this purpose, an interpolation was made of the computed erosion rates for the most similar conditions in this matrix (considering wave height, direction and tide velocity). Analyses were then made of the influence of environmental conditions (tidal currents, wave height and direction) on the erosion of the nourishment and the contribution of cross-shore and alongshore transport processes.

The hindcast time-series of wave boundary conditions were derived using the wave energy transport modelling software SWAN (Booij et al., 1999). For this purpose, a

dedicated model was used for the Holland coast and Waddenzee (Figure 2.4) to transform offshore wave climate conditions to the offshore model boundary of each considered nourishment (i.e. at about MSL  $-8$  m). The grid resolution of this large-scale SWAN wave model ranged from 50 m in the nearshore to 3 km at the offshore boundary. The model applied a long-term averaged wave climate with 391 conditions at the offshore boundary, which was based on a 21 year time-series (January 1979 until December 2000) of wave conditions at the 'Europlatform', 'IJmuiden', 'Eierland' and 'Schiermonnikoog' measurement stations.

The wave conditions were validated at the nearshore non-directional wave station 'Noordwijk' (Figure 2.4;  $x = 80443$  m RD,  $y = 476683$  m RD). The computed significant wave height agreed very well with the measurements ( $R^2 = 0.96$  with a standard deviation of 0.11 m), while also the peak wave period was well represented ( $R^2 = 0.76$  with a standard deviation of 0.53 s). Tide conditions were derived from a M2 fit of tidal currents from an operational tide and surge model for the Netherlands (Rijkswaterstaat, 1999; Spee and Vatvani, 2009), but are expected to have a smaller impact than the wave-driven transport processes (Van Duin et al., 2004).

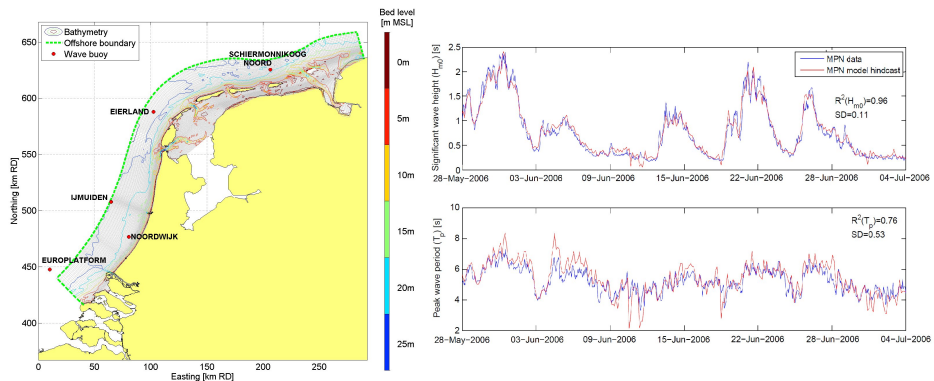


Figure 2.4: SWAN model domain for the derivation of nearshore wave boundary conditions (left panel). Wave measurement stations are shown as red markers. Hindcast for Noordwijk (right panels).

## 2.4. OBSERVED NOURISHMENT BEHAVIOUR

Post-construction morphological change of the considered shoreface nourishments is shown in Figure 2.5 with respect to the pre-construction situation. A decrease in the volume (i.e. fading of the yellow and orange colours) is visible for most nourishments within the bounds of the initial nourishment area, which is demarcated as a black line. While some nourishments erode substantially within a few years (e.g. Katwijk '98 and Bergen '00), others hardly erode over a long period (e.g. Ter Heijde '01 and Terschelling '93). In addition, alongshore bands of erosion and accretion can be seen landward of the nourishment (i.e. shown in blue and yellow), which indicate a trough directly landward of the nourishment and accretion in the inner surfzone ( $\sim$ MSL  $-2$  m).



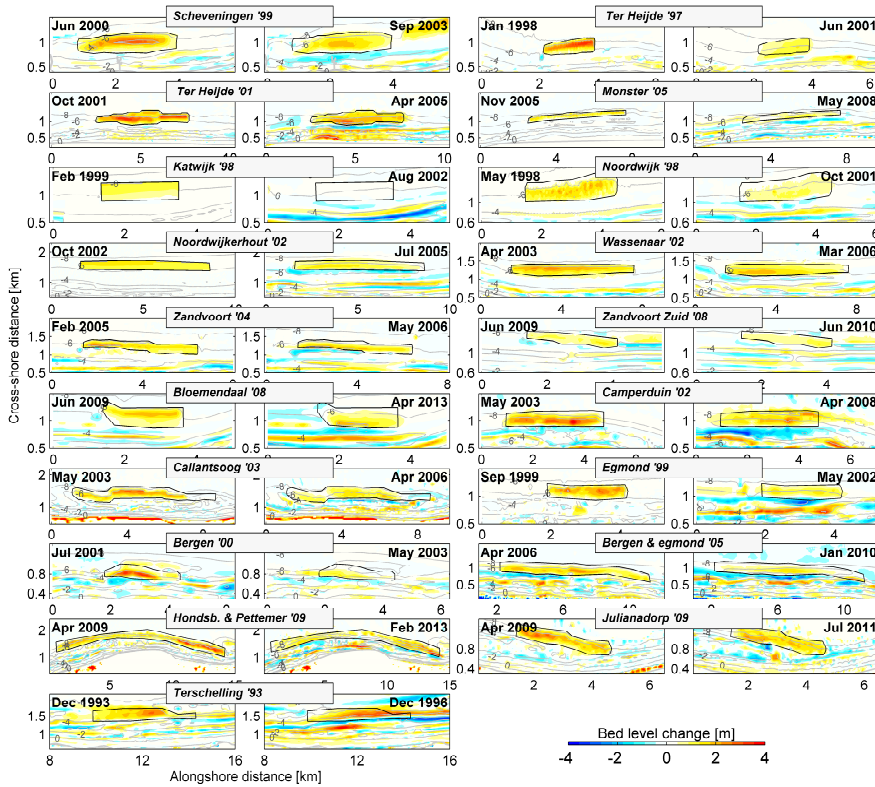


Figure 2.5: Bathymetric change of 19 nourishments with respect to the pre-construction situation for a moment shortly after construction (1st and 3rd column) and after 2 to 6 years (2nd and 4th column). The initial nourishment region is demarcated with a black line. Depth contours are indicated as gray lines with depth annotations with respect to MSL. The horizontal and vertical directions correspond with the alongshore and cross-shore direction, with the landward side at the bottom of each plot (the right side is northeast). Note that the scale has been distorted to fit the figure.

A cross-shore integration of the sediment volume (from MSL  $-10$  m to MSL  $+2$  m) is made for all considered coastal sections and exemplified for Ter Heijde '97, Wasseenaar '02, Egmond '99 and Terschelling '93 (Figure 2.6). The average erosion rate of the cross-shore profiles with the nourishment was  $28 \text{ m}^3/\text{m}/\text{yr}$  for the 19 considered cases (see  $\Delta \bar{v}_{center}$  in Figure 2.6e) with a standard deviation ( $SD$ ) of  $27 \text{ m}^3/\text{m}/\text{yr}$ . The preservation of sediment in the cross-shore profile can therefore differ substantially between sites. For some sites, a net increase in the sediment volume (in the full cross-shore profile) was found after placement of the nourishment (Zandvoort–Zuid '08 and Bloemendaal '08). More erosion took place on the southern ends of the coastal sections with the nourishments (i.e. within inner dashed boundaries) resulting in an alongshore shift of the center of gravity ( $\Delta x_{center}$  in Figure 2.6f) of the sediment volume towards the North (e.g. at Ter Heijde '97). A southward movement of the center of gravity is observed only for Bergen '00 and Noordwijkerhout '02. The eroded sediment can often not be traced back at the adjacent coastal sections ( $\Delta \bar{v}_{adj}$  in Figure 2.6g). Considerable erosion ( $>30 \text{ m}^3/\text{m}/\text{yr}$ ) can take place directly adjacent to the coastal

section of the nourishment (e.g. Noordwijk '98, Camperduin '02, Julianadorp '09 and Terschelling '93), but also moderate accretion (10 to 30 m<sup>3</sup>/m/yr) is observed at some adjacent coastal sections (e.g. Ter Heijde '97, Scheveningen '99 Bergen '00 and Hondsbossche & Pettemer Zeewering '09). It is expected that sediment has been moved out of the monitoring area, as a closed balance could not be obtained.

2

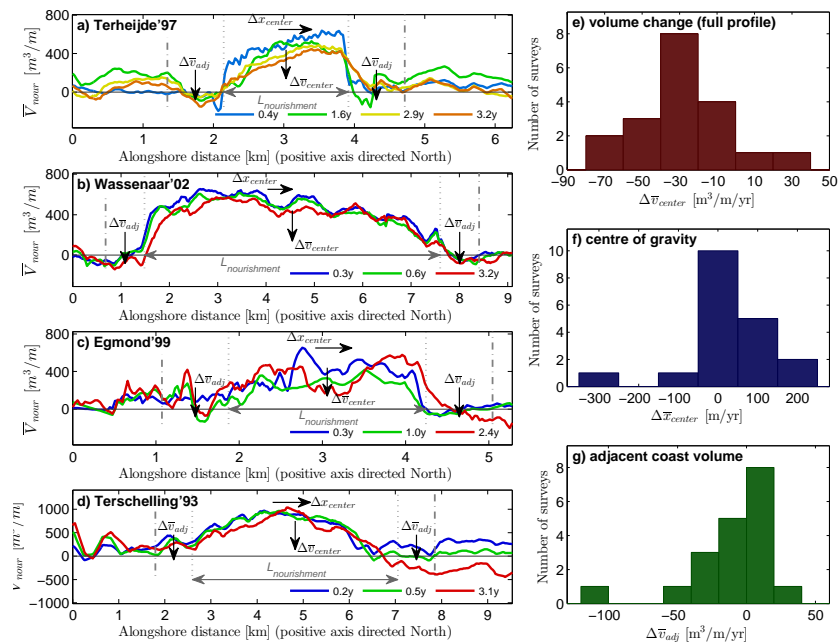


Figure 2.6: Overview of the alongshore distribution of the added nourishment volume along the coast in the zone from MSL  $-10$  m to MSL  $+2$  m at 4 representative nourishments from each of the coastal sections. The initial post-construction situation is shown in blue, which gradually changes towards red for the latest considered survey (in red). Dashed vertical lines show the initial extents of the considered nourishment and extent of the adjacent coast regions.

An overview of the cross-shore profile changes at the center of the shoreface nourishments (Figure 2.7) is shown for four selected nourishments at the Delfland, Rijnland, North-Holland and Terschelling coast (Ter Heijde '97, Wassenaar '02, Egmond '99 and Terschelling '93), which exemplify the observed behaviour for other nourishments. The cross-section data show that a landward shift and increase in the height of the 'nourishment crest' can be observed for the post-construction profiles ( $\Delta x_{crest}$ ), which is most visible for the relatively short Ter Heijde '97 nourishment. After one to two years, the nourishment crest attains a depth of about MSL  $-4$  m to  $-5$  m and a cross-shore position that ranges between  $x = 400$  and  $x = 800$  m from the shoreline. This cross-shore location is in line with the cross-shore position and depth at which highest bar amplitudes are present in the cross-shore profile at the Holland coast (Ruessink et al., 2003). It is noted that the observed onshore migration of the nourishment crest in the first years after construction is opposite to the natural offshore directed bar cycle. After four to five years, the natural bar cycle takes over again

and starts to move the bar in offshore direction.

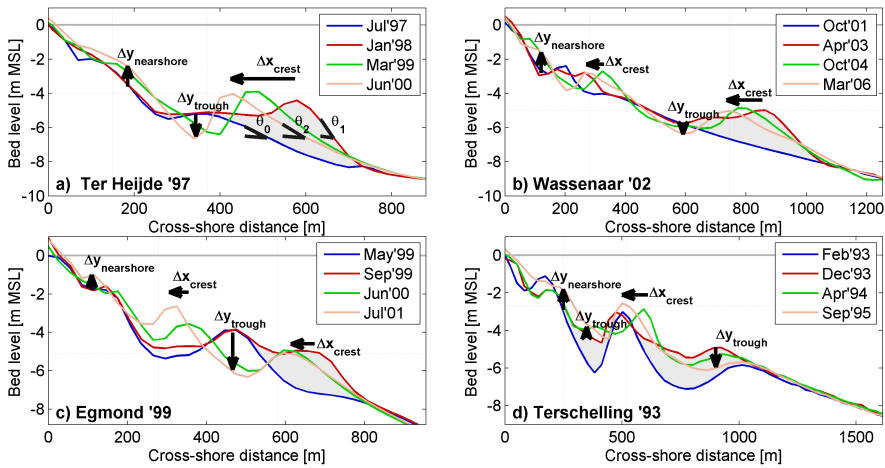


Figure 2.7: Cross-shore profile changes at 4 representative nourishments for four moments in time. The pre-construction situation is shown in blue. The initial nourishment (at the moment of the first post-construction survey) is shown as a grey area in the plots.

On the other hand, the seaward side of the nourishments was eroding. As a result, the seaward facing slope of the nourishment had the tendency to become milder (from  $\theta_1$  to  $\theta_2$ ) and therefore more similar to the pre-construction profile slope ( $\theta_0$ ). The seaward sides of all 19 considered nourishments had an average profile slope of 1:50 with a standard deviation (*SD*) of 33 (for the first post-construction survey), and were therefore much steeper than the natural profile slope of 1:100 to 1:200. The seaward facing side of all of the nourishments gradually became milder over time with an average slope of 1:80 for the considered nourishments after  $\sim 3$  years (with a *SD* of 48), but remained steeper than the natural profile. The profile change is consistent over the length of the nourishment, which suggests that sediment is transported onto the nourishment in the cross-shore direction.

The landward facing slope of the nourishment became steeper in the first years due to an increase in crest height of the nourishment and the development of a trough at the landward side ( $\Delta y_{trough}$ ; between MSL  $-4$  m and  $-6.5$  m in Figure 2.7) with a cross-shore extent of 100 to 150 m. The mean depth of the trough with respect to a long-term averaged profile was 0.5 to 2 m, which was within the bounds of the natural bar-migration cycle. However, a considerable erosion of up to 4 m has taken place for the Egmond '99 nourishment where a trough developed at the location of the existing bar (see Figure 2.7). Most pronounced troughs developed for nourishments at the North-Holland coast. When considering all the nourishments, the trough depth seemed to be related to regional characteristics rather than a geometry related property (e.g. the length or volume of the nourishment). It can also be seen from Figure 2.7 that some interaction of the shoreface nourishment with the natural bars took place in the measurements. Most of the 19 considered nourishments had only a small interaction with the natural bars, while a few show a landward push of the natural bar

(e.g. Bergen & Egmond '05 and Bloemendaal '08). At Egmond '99, the natural bar is pushed towards the coast resulting in two bars, while the nourishment merged with the existing bar at Ter Heijde '97. The Wassenaar '02 site shows the creation of a small nearshore bar, which can be considered as an in-between situation. The Terschelling '93 nourishment differed from other nourishments in the respect that accretion took place in the trough, but on the other hand showed a landward movement of the bar crest as for the other sites.

A quantitative analysis of the volume change in the predefined cross-shore regions (see Figure 2.2) shows a decrease of the nourishment volume  $V_{nour}$  (dark gray markers in Figure 2.8) and volumetric changes in the seaward, trough and nearshore regions ( $V_{seaward}$ ,  $V_{trough}$  and  $V_{nearshore}$ )).

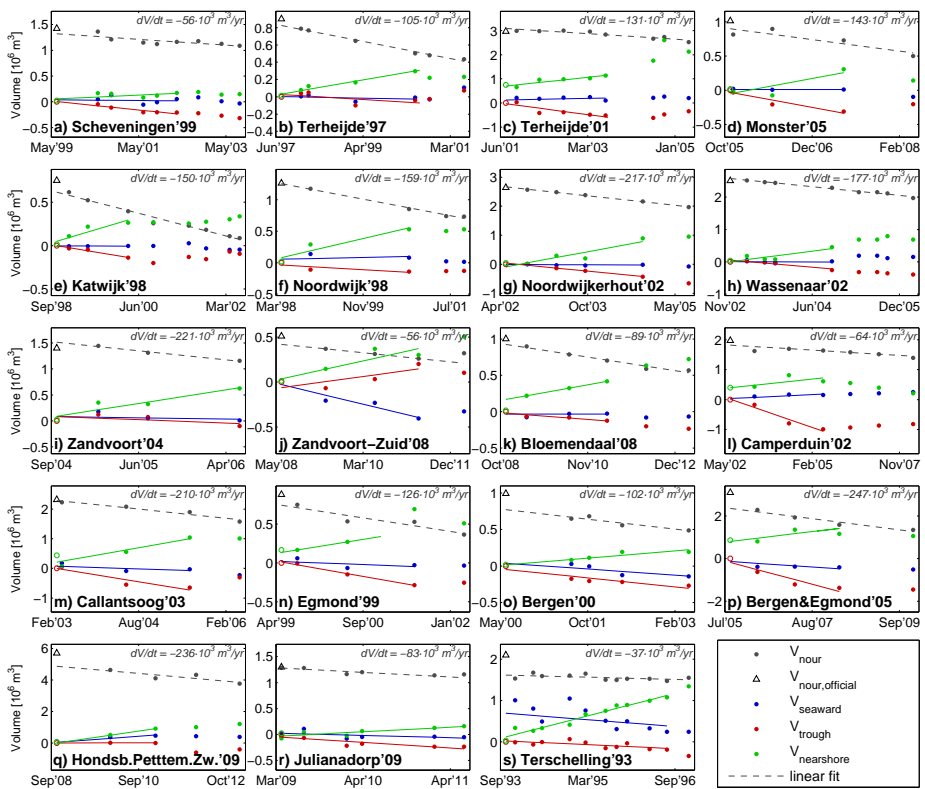


Figure 2.8: Overview of measured volume change at the 19 considered nourishments. The measured volume change is shown for the initial nourishment region (gray marker), the trough region in the first 120 m directly landward of the nourishment (red marker), the shallow nearshore region (green marker) and the offshore region (blue marker). A linear trend is fitted through the measured volumes in the initial nourishment region (dashed gray line, with trend  $dV_{nour}/dt$ ) and for the first three-year development of the other regions (colored lines). A triangle marker represents the official nourishment volume ( $V_{nour,official}$ ) from Rijkswaterstaat records.

The measured change in  $V_{nour}$  can be represented reasonably well with a linear trend for most nourishments (i.e. dashed gray line in Figure 2.8). For some nourishments, a discrepancy is present between the initial nourishment volume that is computed from the bathymetric measurements and the official nourishment volume. For example, a much larger volume was nourished at Bergen & Egmond '05 than could be shown in the measurements. The multi-year average rate of erosion ( $dV_{nour}/dt$  using the linear trend in the measurements) varied from 37,000 to 247,000  $m^3/yr$ . The erosion rate per alongshore length unit ( $d\bar{v}_{nour}/dt$ ) was on average 34  $m^3/m/yr$  with a  $SD$  of 17  $m^3/m/yr$ . The least erosion took place at Terschelling (about 8  $m^3/m/yr$ ). The largest erosion was observed at Katwijk '98 (about 70  $m^3/m/yr$ ).

The considered shoreface nourishments have an estimated halftime of the nourishment volume varying from three years for Katwijk '98 to a theoretical halftime of  $\sim 30$  years for the Terschelling '93 nourishment (based on a linear extrapolation of the computed erosion rate; see Figure 2.8). The volume of sediment remaining in the initial nourishment region after three years ranged from 26% (at Katwijk '98) to  $\sim 90\%$  (at Scheveningen '99, Ter Heijde '01, Camperduin '02 and Terschelling '93) with an average of 68% for all considered nourishments with a  $SD$  of 17%. It should, however, be noted that some of the more persistent shoreface nourishments in this study were preceded by earlier nourishments (e.g. Ter Heijde '01), which may have lengthened the lifetime of the nourishment.

Geometrical properties have an influence on the erosion rates, as the inverse alongshore length of the nourishment correlates significantly with the erosion rate per meter length of the nourishment (with  $R^2$  of 0.4; see Figure 2.9). Apparently, the shorter nourishments experience a relatively larger loss (per alongshore length unit) than longer nourishments. The cross-shore width and depth of the nourishment crest are, however, not significantly correlated to the erosion rate (Figure 2.9).

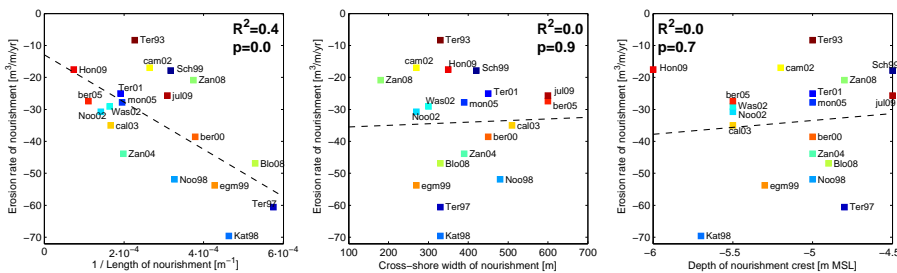


Figure 2.9: Correlation of the erosion rate of the nourishment region with geometrical properties of the shoreface nourishment (i.e. alongshore length, width and depth of the nourishment crest).

The volumetric changes in the nearshore region landward of the shoreface nourishments (i.e.  $V_{trough}$  and  $V_{nearshore}$ ) are also influenced by the construction of the nourishment (Figure 2.8), while sediment volume in the seaward region ( $V_{seaward}$ ) is hardly

affected by the nourishment, which is not unexpected given that the depth of closure is approximately at the toe of the nourishment at 9 m water depth (Hallermeier, 1981; Hinton and Nichols, 1998). A linear trend of accretion is generally observed in the inner surfzone ( $V_{nearshore}$ ) in the first three years after construction of the nourishment, while an erosive trend is observed in the region directly landward of the nourishment ( $V_{trough}$ ). The accretion in the nearshore ( $V_{nearshore}$ ) was on average  $46 \text{ m}^3/\text{m}/\text{yr}$  with a  $SD$  of  $19 \text{ m}^3/\text{m}/\text{yr}$  over the first three years after construction, while the erosion of the trough ( $V_{trough}$ ) was about  $32 \text{ m}^3/\text{m}/\text{yr}$  with a  $SD$  of  $26 \text{ m}^3/\text{m}/\text{yr}$ , meaning that the volume changes in the trough and nearshore regions are of similar magnitude as the changes in the initial nourishment region. Typically, the volumetric changes in the trough and inner surfzone become smaller after three to four years with a small tendency to return to the original situation (see Camperduin '02 in Figure 2.8). It is noted that the Zandvoort–Zuid '08 nourishment behaved somewhat different as considerable accretion was observed in the trough zone. The accretion in the nearshore region at Terschelling '93 is considerably larger than the erosion from the nourishment.

A relation between the rate of volumetric change in the nearshore region (in the first three years after construction) and the erosion rate of the nourishment region (Figure 2.10;  $R^2 = 0.6$ ) suggests that the shoreface nourishments have a considerable positive impact on the nearshore sediment budgets. Nearshore accretion may even exceed the erosion in the initial nourishment region, which shows that a supply from the trough region or adjacent coast is present. The rate of erosion in the trough region is, however, not correlated to the erosion of the nourishment (see right panel in Figure 2.10), but does show that an erosion of 20 to  $60 \text{ m}^3/\text{m}/\text{yr}$  is typically present in the trough in the first three years after construction of the nourishment.

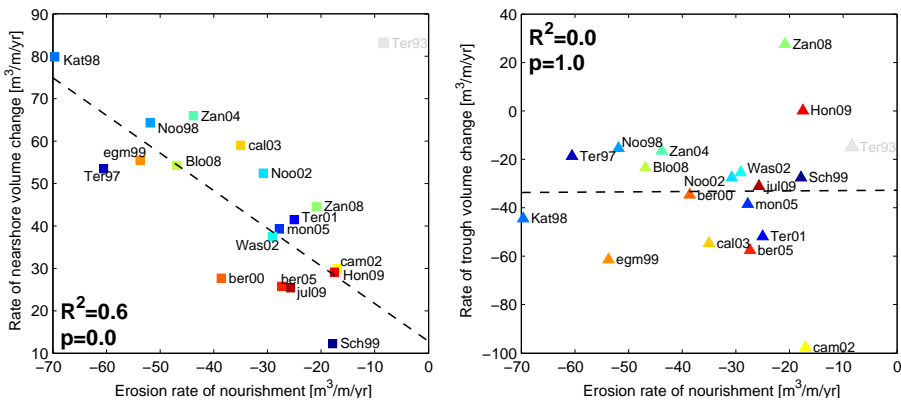


Figure 2.10: Correlation of erosion rate of the nourishment region with the rate of nearshore accretion and erosion of the trough area.

## 2.5. EFFICIENT MODELLING OF SHOREFACE NOURISHMENTS

The XBeach numerical model is used to assess the impact of hydrodynamic processes acting at the shoreface nourishment and for pre-computing the erosion rates for a matrix of wave heights ( $H_{m0}$  ranging of 1, 2, 3 and 4 m), directions ( $-30^\circ$ ,  $-15^\circ$ ,  $0^\circ$ ,  $15^\circ$ ,  $30^\circ$ ) and tide conditions ( $-1$ ,  $-0.5$ ,  $0$ ,  $0.5$  and  $1$  m/s; see Section 2.3). The erosion rates of five shoreface nourishments over the first 2.5 years were then reconstructed at each time-instance of a (measured) hindcast time-series of wave conditions using an interpolation of the pre-computed erosion rates. The Ter Heijde '97 nourishment is used as an illustration case, since measurements show a clear morphological development over time. In addition also four other nourishments (Katwijk '98, Noordwijk '98, Egmond '99 and Noordwijkerhout '02) are modelled to provide information on the consistency of the results for nourishments with a different size or location along the coast.

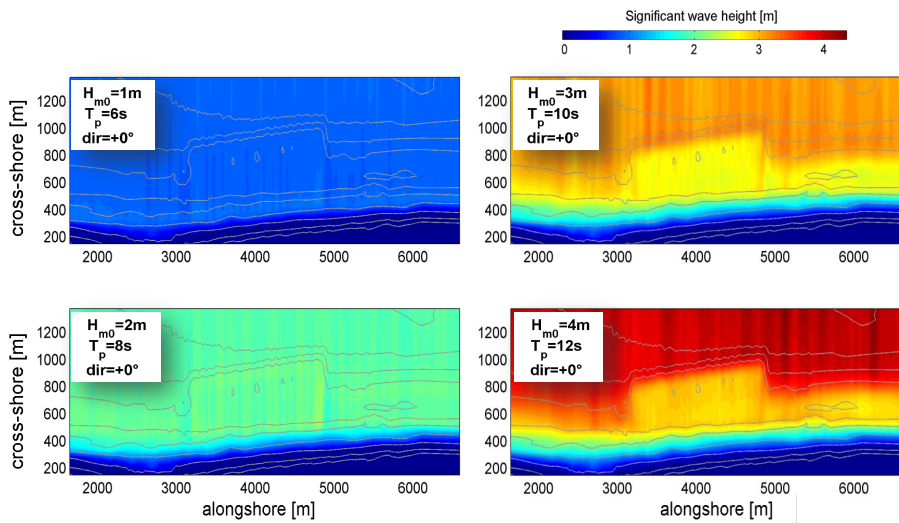


Figure 2.11: Modelled wave transformation for four shore-normal wave height classes at the Ter Heijde '97 shoreface nourishment using the XBeach model (using January 1998 bathymetry survey).

Results of the illustration case (Ter Heijde '97) show that the smaller waves are propagated without breaking over the shoreface nourishment Figure 2.11, while larger waves (partially) break at the shoreface nourishment. A substantial part of the wave energy is therefore transmitted to the landward side during mild conditions (e.g. significant wave height  $< 1$  m, occurring 64% of the time). Obliquely incident waves induce similar wave patterns, but with the shadow area shifted somewhat downdrift of the nourishment. Onshore currents are present at the crest of the nourishment, while a strong offshore directed current is present at both lateral sides of the nourishment during shore-normal incident waves with  $H_{m0} \geq 3$  m (see left panels in Figure 2.12). This rip current is only present at the updrift side for moderately oblique incident waves (from  $15^\circ$ ) while the rip currents are absent during very oblique wave incidence. In

that situation, the lateral sides are influenced by the alongshore current. The alongshore current velocities landward of the nourishment during obliquely incident wave conditions (from  $15^\circ$ ) are hardly reduced for mild to moderate wave conditions ( $H_{m0} < 2$  m), while a considerable reduction of longshore current velocities is found landward of the nourishment for energetic conditions ( $H_{m0} \geq 3$  m from  $15^\circ$ ).

2

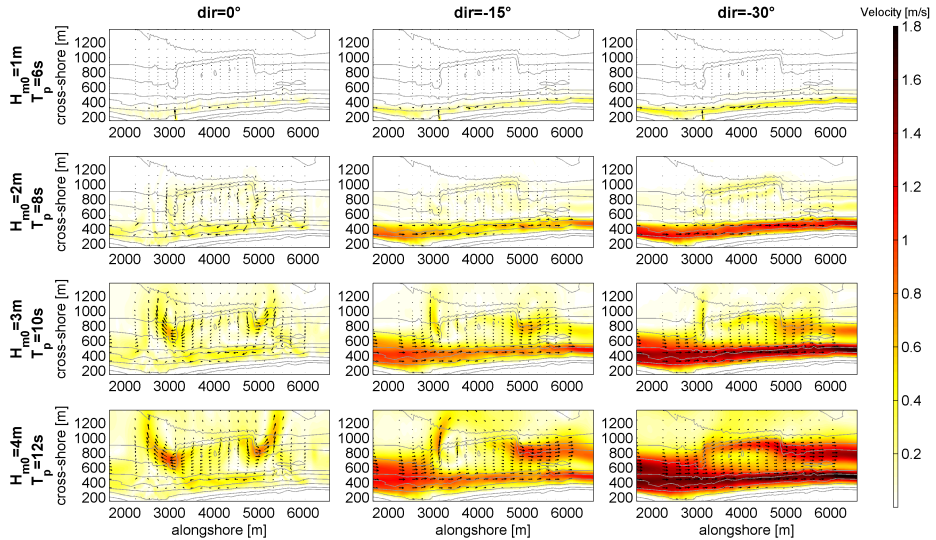


Figure 2.12: Modelled impact of Ter Heijde '97 shoreface nourishment on the flow patterns depending on the offshore wave height and direction for the first survey moment after construction (T1; January 1998).

The initial transport rates for each individual condition of the 2.5 year hindcast time-series were derived from the computed matrix of XBeach computations (for a range of environmental conditions) using an interpolation of the most similar conditions (see Figure 2.3). The resulting transport rates for the Ter Heijde '97 nourishment Figure 2.13, as shown relative to the pre-nourishment situation) show a transport away from the initial nourishment region in both the alongshore and cross-shore direction. In addition, a reduction of the alongshore transport rates is present in the shadowed zone nearshore of the shoreface nourishment, which results in a convergence of the transport at the coast. This shielding of the waves by the nourishment takes place especially during the more energetic wave conditions.



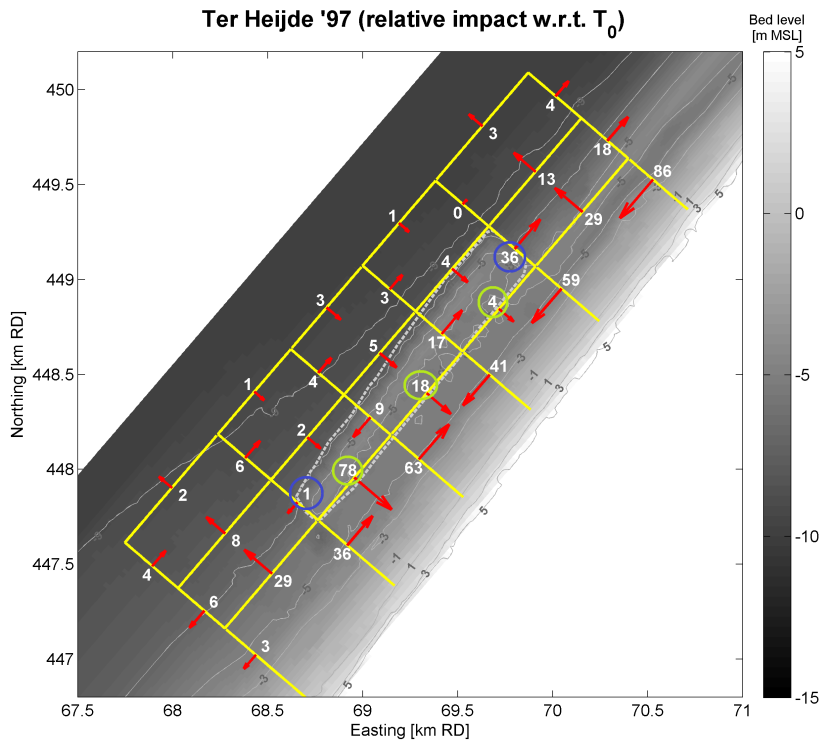


Figure 2.13: Computed year-averaged transport rates (in  $10^3 \text{ m}^3/\text{yr}$  w.r.t. pre-nourishment situation) at Ter Heijde '97 shoreface nourishment based on XBeach simulations. The dashed gray line indicates the initial nourishment region. Cross-shore losses from the nourishment are indicated with the green circles, while the alongshore losses are marked with blue circles.

In addition, the volume change of the Ter Heijde '97 nourishment Figure 2.14 was reconstructed using (at each moment of the actual hindcast time-series) an interpolation of the computed initial erosion rates from the matrix of XBeach computations for the predefined environmental conditions. The trend in the computed volumetric change of the nourishment and inner surfzone (i.e. trough and nearshore zone combined) was similar to the observations, while the model was using just the initial transport computations for a single post-construction bathymetry. This is surprising knowing that various properties of the bathymetry change over time. Apparently, the most important parameters for the erosion of the nourishment do not change substantially in consecutive measured bathymetries. It is envisioned that the use of more measured bathymetries may be even more accurate, but these are in practice not available when a prediction is made of the performance of shoreface nourishments (i.e. prior to the construction). Relevant for practical applications is also that the longer-term trend in the nourishment volume can be represented with an average climate (see dash-dot line). The volume changes of the region seaward of the nourishment and at the adjacent coast show a larger deviation from the measurements, which vary considerably over time, but do still represent the trend reasonably well.

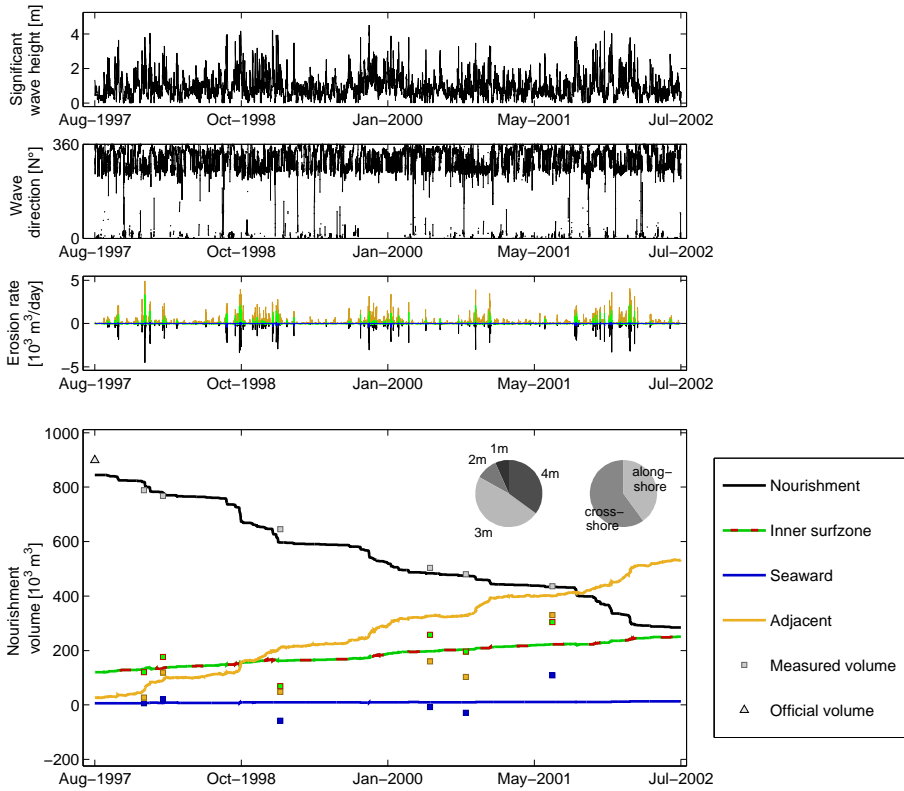


Figure 2.14: Modelled and observed volumetric change of the initial nourishment area, inner surfzone, seaward of the nourishment and at the adjacent coast of the Ter Heijde '97 shoreface nourishment. Observations are shown with square markers. The relative contribution of wave height, wave incidence angle and cross-shore/alongshore erosion of the shoreface nourishment are shown in pie charts. Left pie chart: contribution of wave height classes. Right pie chart: contribution of cross-shore and alongshore transport to the total erosion of the nourishment.

Similarly, a prediction was made of the volumetric changes at the Katwijk '98, Noordwijk '98, Noordwijkerhout '02 and Egmond '99 shoreface nourishments (Figure 2.15), which showed the same trend in the erosion volume of the initial nourishment area as the measurement data. In particular, the initial nourishment region, seaward region and inner surfzone were predicted well. Less agreement with measurements was present for the adjacent coast, although Katwijk '98 was still well represented. In addition, the more energetic wave conditions ( $H_{m0} = 3$  m) contribute to the erosion of the nourishment, as can be seen from the left pie-charts in Figure 2.14 and 2.15, which is in line with the expected transmission of wave energy over the nourishment during mild conditions. This erosion of the nourishment takes place for about 60% to 85% due to cross-shore transport.

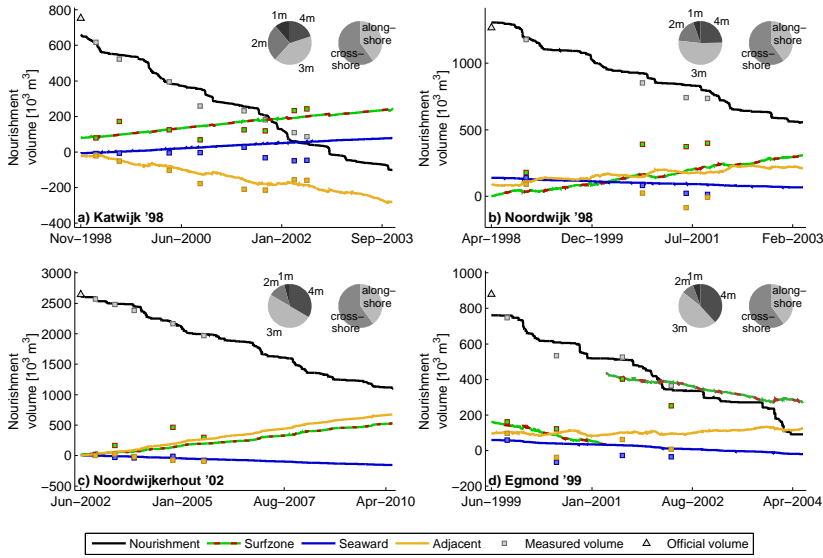


Figure 2.15: Modelled and observed volumetric change of the Katwijk '98, Noordwijk '98, Noordwijkerhout '02 and Egmond '99 shoreface nourishments. Four different regions are shown: (1) the initial nourishment area, (2) inner surfzone, (3) seaward of the nourishment and (4) the adjacent coast. Observations are shown with square markers. The relative contribution of wave height, wave incidence angle and cross-shore/alongshore erosion of the shoreface nourishment are shown in pie charts. Left pie chart: contribution of wave height classes. Right pie chart: contribution of cross-shore and alongshore transport to the total erosion of the nourishment.

A quantification of the capability of the model to compute the initial volumetric changes (in the first three years) at the shoreface nourishments is provided in Figure 2.16, which shows a similar trend of the volume in the initial nourishment region ( $R^2 = 0.9$ ) and inner surfzone ( $R^2 = 0.8$ ) as the measurements. The seaward region is reasonably well resolved ( $R^2 = 0.6$  with  $p = 0.11$ ), while impacts on the adjacent coast are more difficult to predict ( $R^2 = 0.3$  with  $p = 0.33$ ). The number of cases is, however, still small.

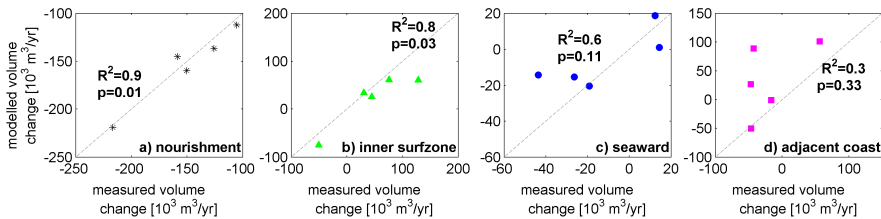


Figure 2.16: Modelled and observed rate of change of the volume of predefined regions of the Ter Heijde '97, Katwijk '98, Noordwijk '98, Noordwijkerhout '02 and Egmond '99 shoreface nourishments. Four different regions are shown: (1) the initial nourishment area, (2) inner surfzone, (3) seaward of the nourishment and (4) the adjacent coast. A linear fit and coefficient of determination ( $R^2$ ) and probability value ( $p$ -value) are provided.

## 2.6. DISCUSSION

Bathymetric surveys at 19 shoreface nourishments show that shoreface nourishments (with a lifetime of 3 to ~30 years) are quite persistent compared to beach nourishments. The larger shoreface nourishments were only partly eroded after three years with 40% to 80% of volume still in the initial nourishment region. This is in line with the findings of Van Duin et al. (2004) who showed that about 45% of the sediment remained after three years in the initial nourishment region at the Egmond '99 nourishment. Measurements show that a rather linear decrease of the volume in the initial nourishment region takes place for the considered shoreface nourishments. The observed behaviour is clearly different from beach or mega nourishments (e.g. Sand Motor, De Schipper et al., 2016), which act as coastline perturbations that gradually spread along the coast over time as a result of gradients in the wave-driven alongshore transport. The beach and mega nourishments are, however, almost exclusively influenced by the alongshore wave-driven current which induces transport gradients depending on the local coastline orientation (Benedet et al., 2007; Hanson and Kraus, 1989; Larson and Kraus, 1991; Luijendijk et al., 2017), while a much smaller influence of the wave-driven alongshore transport is observed at the shoreface nourishments.

Alongshore transport takes place at the seaward side of the shoreface nourishment during (obliquely incident) stormy conditions ( $H_{m0} \geq 3$  m; Figure 2.11), but causes only 15 to 40% of the erosion of the shoreface nourishment as smaller waves are propagated without breaking over the shoreface nourishment. Instead the erosion of a shoreface nourishment is controlled by onshore transport of sediment contributing 60 to 85% for the five modelled nourishments in this study (Figures 2.14 and 2.15). However, relatively speaking, the shorter nourishments do experience a larger impact of the longshore transport, which acts at the lateral ends (as shown from the relation between length and erosion per alongshore length unit in Figure 2.9). Onshore currents are present at the middle section of the nourishment as a result of mass transport by the waves, wave skewness induced velocity asymmetry and residual circulations (Figures 2.12 and 2.17), which also feed the strong seaward directed currents at the lateral sides of the nourishment.

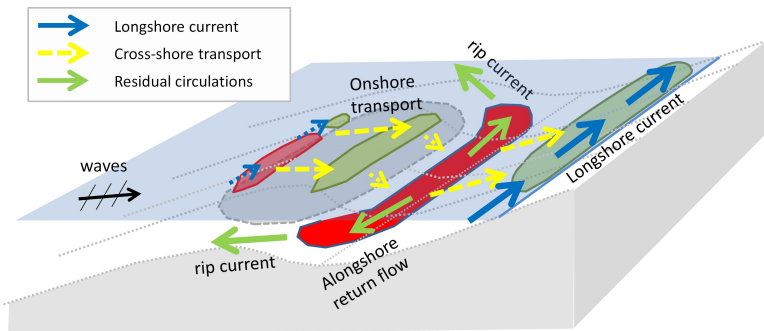


Figure 2.17: Illustration of mechanisms for sediment redistribution at shoreface nourishments. Areas with erosion and sedimentation of the bed are shown as red and green regions.

Computations of the impact of the Ter Heijde '97 nourishment on the wave asymmetry and skewness (i.e. the difference between the post-construction and T0 situation;  $\Delta Asymmetry$  and  $\Delta Skewness$ ) suggest that the geometrical change of the profile affects the velocity asymmetry of the wave orbital motion (see Figure 2.18), thus providing at least a partial contribution to the cross-shore transport in shoreward direction (analogous to Grunnet and Ruessink, 2005). The contribution of wave skewness and asymmetry was also confirmed by a simulation with disabled wave skewness and asymmetry, which showed only half of the erosion at the shoreface nourishment and an absence of accretion in the nearshore. From Figure 2.18, it is also shown that the T2 survey (in August 1998), which has a more pronounced trough and bar crest, has a larger impact on the wave skewness and asymmetry in the trough area than the T1 survey while the influence on the skewness and asymmetry at the nourishment crest is similar. This suggests that an internal feedback mechanism may take place during the development of the trough.

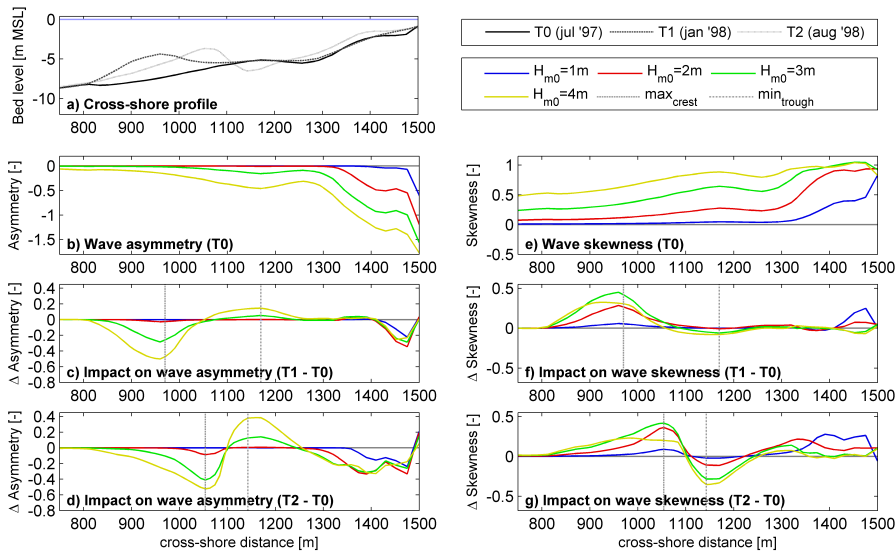


Figure 2.18: Modelled relative impact of Ter Heijde '97 shoreface nourishment on the wave skewness and asymmetry for January and August 1998 bathymetries (T1 and T2) with respect to the pre-nourishment situation (T0). (a) bathymetry for T0 to T2; (b) wave asymmetry for T0 situation; (c and d) impact on wave asymmetry for time instances T1 and T2; (e) wave skewness for T0 situation; (f and g) impact on wave skewness for time instances T1 and T2.

In practice, this means that the actual magnitude of the cross-shore transport in the applied method depends (to some extent) on settings for wave skewness and asymmetry ( $facSk$  and  $facAs$ ) in the XBeach model, which requires a calibration for the pre-nourishment situation. The current study used the default calibration settings for safety assessments of the Holland coast (Van Geer et al., 2015) for all considered cases.

Findings in this study are in line with Grunnet and Ruessink (2005) who computed a considerable enhancement of onshore transport for the Terschelling '93 nourishment. Onshore transport of sediment is expected to take place at the seaward side of any shoreface nourishment moving sediment to the 'nourishment crest'. Most nourishments therefore develop a 'triangular' landward skewed shape in the first year(s) after construction, which can be perceived as a migration of the nourishment in landward direction. This process is expected to continue until the moment that the sediment source at the seaward toe of the nourishment depletes (i.e. when the seaward slope gets milder), which happens typically after two to four years. The crest of the shoreface nourishment will then become less pronounced (i.e. lower and more rounded) and the natural offshore bar cycle resumes.

A short steep back slope is present on the landward side of the shoreface nourishment, where a trough develops over time with a depth of 0.5 to 4 m with respect to the pre-nourishment situation. Sediment from the nourishment which reaches the trough (i.e. the loss from the initial nourishment region) moves either (1) to the sides of the nourishment by water-level gradient driven currents which expel sediment with rip currents at the lateral sides during shore-normal to mildly oblique wave conditions (see Figures 2.12 and 2.17) or (2) towards the shallow nearshore zone as a result of enhanced onshore transport (Figure 2.18). The correlation of the erosion in the area directly landward of the nourishment and accretion in the shallow nearshore zone ( $R^2 = 0.6$ ; Figure 2.10) suggests that most of the sediment that initially accretes in the shallow nearshore zone originates from the erosion in the 'area directly landward of the nourishment' rather than the supply from the shoreface nourishment itself. The erosion in the region landward of the nourishment (at about MSL  $-4$  m) is therefore considered beneficial for the accretion near to the waterline in shallow water. After about three years, the area landward of the nourishment fills up and nearshore accretion decreases again when onshore sediment supply diminishes, which is the case for Camperduin '02 and Egmond '99 (Figure 2.7). In addition, wave shielding by the nourishment may also contribute to accretion in the shallow nearshore zone, although an effect is only expected during the energetic wave conditions ( $H_{m0} \geq 3$  m; Figure 2.11), while the wave-driven current is likely to spread sediment alongshore during mild to moderate conditions. This aligns with Van Duin et al. (2004) who recognize the difference in impact of the wave shielding by the nourishment for mild and energetic conditions. The part of the sediment from the shoreface nourishment that is not transported to the shallow nearshore is spread over a large area by the rip currents at the lateral ends of the nourishment, which explains the lack of visible accretion at the coast directly adjacent to the shoreface nourishment. However, this offshore transported sand will eventually end up in the surfzone as a result of onshore transport.

The applied simplified XBeach modelling method provides a good representation of the trend of the erosion of the shoreface nourishment (with  $R^2 = 0.9$ ) and subsequent nearshore accretion rates (with  $R^2 = 0.8$ ) using just the initial erosion rates for a single post-construction bathymetry. It is envisioned that the use of more measured bathymetries may be even more accurate, but these are in practice often not available when a prediction is made of the performance of shoreface nourishments. This is

considerably more efficient than a modelling approach using a brute-force morphological hindcast (e.g. Luijendijk et al., 2017) or reduced wave climate (e.g. Van Duin et al., 2004 or Hartog et al., 2008). Some uncertainty will always remain as the precise occurrence of conditions will not be available for future forecasts (e.g. yearly variation in storminess), but still the method proved to be rather robust even when a measured bathymetry of one year later is applied or when an average wave climate is used. The method is therefore of practical use for future morphological forecasts of shoreface nourishments. In fact, the applied measured bathymetries are considered more realistic than the model-generated bathymetries of morphodynamic model studies, which show a considerable flattening of the bar features (e.g. Van Duin et al., 2004; Grunnet et al., 2004) and suggests that a realistic crest height is essential for an accurate reproduction of the onshore sediment transport. The current model also has a good representation of the accretion in the inner surfzone, while volumetric changes seaward of the nourishment and at the adjacent coast are more difficult to predict. This is expected to relate to the chosen approach using only the initial morphological changes, which disregards the feedback from accretion at the adjacent coast on the local accretion. As a result, the computed changes at the adjacent coast are expected to be larger than the actual accretion because sediment will in practice be spread over a larger area. The model for Ter Heijde '97 even predicts a local reduction of the skewness and asymmetry at the location of the trough, which can promote the growth of the trough depth (Figure 2.18). The applied approach (using hydrostatic assumptions and 2DH processes) still cannot fully capture the processes at the interface of the bar and trough area, where complex 3D currents, turbulence (from breaking waves penetrating to the bed) and phase lags between wave stirring and advection play a role (e.g. Roelvink and Stive, 1989; Hsu and Liu, 2004; Van der Zanden et al., 2016; Brinkkemper et al., 2018). This may be resolved using detailed Navier Stokes models (including these processes) which generate more realistic sub-tidal bars and troughs (e.g. Jacobsen and Fredsoe, 2014b), but these models cannot easily be applied at the scale of a shoreface nourishment. In fact, a parameterization of the complex processes at the bar will be needed to improve the performance of morphological models in predicting bar-trough features. In addition, the models using Boussinesq type wave parameterization may need to be explored (e.g. Karambas and Samaras, 2014). It is noteworthy that qualitatively realistic behaviour is obtained with the UNIBEST-TC model for cross-shore profiles that uses a parameterization of the transport processes (Walstra et al., 2012; Ruessink et al., 2007). The development of sub-tidal bars is, however, still a field of research that is heavily debated on and not a principal aim of this research. In practice, this means that the current modelling approach is less suitable for evaluating the precise erosion depth of a trough (e.g. for landfalls of power and communication cables). The applied modelling approach can, however, be used to predict the lifetime of shoreface nourishments and redistribution of the sediment, which is essential for efficient placement of future coastal maintenance measures.

This research also sheds light on the applicability of shoreface nourishments, as the functioning of this measure and lifetime is better understood. The shoreface nourishment is a very cost-effective solution to replenish a large volume of sand at the coast (about two to five times cheaper per  $m^3$  than beach nourishments), of which almost

all sand contributes to the sediment balance of the coastal cell in which it is placed (i.e. hardly any offshore transport). The shoreface nourishment feeds the coast especially during storms, thus, effectively, providing a sub-tidal buffer volume to mitigate storm erosion. It should, however, be kept in mind that the shoreface nourishment does not provide a quick solution to restore a too narrow beach, as it will take time before the inner surfzone benefits from the sand. In addition, the low visibility of the measure can be an issue for (local) governments who would like to see their coastal investment from land. The possible presence of large-scale rip-currents, on the other hand, is in practice not really a drawback for swimmer safety as these rip currents occur especially for wave heights of over three meters when hardly any swimmers will be in the water.

## 2.7. CONCLUSIONS

The objective of this research was to examine (1) the behaviour of shoreface nourishments, (2) the contribution of processes driving the morphological changes and (3) an efficient method to predict the evolution of shoreface nourishments. Morphological data of 19 sub-tidal sand nourishments at the Dutch coast and numerical modelling with XBeach were used for this purpose.

Field measurements show that considerable cross-shore profile change takes place at shoreface nourishments, while alongshore redistribution is hard to distinguish. In this respect, the shoreface nourishment behaviour is very different from a beach or mega nourishment, which is moved predominantly by the alongshore wave-driven current. The shoreface nourishments are more persistent compared to beach nourishments with on average ~68% of volume still in the initial nourishment region after three years, but considerable variation is present in the halftime of the considered shoreface nourishments (ranging from 3 to ~30 years). The cross-shore shape of the shoreface nourishment skews in landward direction over time as a result of transport from the (eroding) seaward side of the nourishment (between MSL -8 m and MSL -4 m) to the landward side of the nourishment crest (at about MSL -4 m). This onshore transport is due to water-level setup driven residual circulations as well as a local increase of the skewness and asymmetry of the wave orbital motion due to the geometrical change of the cross-shore profile by the nourishment. The dominance of the onshore directed transport is expected to last until the seaward slope of the nourishment becomes milder (i.e. more similar to the natural coast, as observed in measurements in the first years after construction). For most of the nourishments, a trough developed landward of the shoreface nourishment (i.e. where the pre-existing natural sand bar was located) with a cross-shore width of 100 to 150 m resulting in 0.5 to 4 m erosion. The eroded sediment from the trough region is transported to the shallow nearshore region between MSL -3 m and MSL resulting in local accretion.

A validation of the erosion and accretion rates for five shoreface nourishments showed that a good hindcast of volume change of the nourishment area and inner surfzone can be achieved with the XBeach model using a lookup table with a matrix of initial sedimentation-erosion rates for a range of potential environmental conditions.



The method uses a single post-construction bathymetry for all simulations, which is considerably more efficient than a brute-force morphological hindcast. This is remarkable in view of the considerable morphological changes that take place at a shoreface nourishment. It is envisioned that the use of more measured bathymetries may be even more accurate, but these are, in practice, often not available when a prediction is made of the performance of shoreface nourishments. Using the model, it is shown that cross-shore transport (for shore-normal waves) is governing the first year erosion rates of the nourishment (contributing about 60 to 85% to the erosion), while alongshore transport contributes about 15 to 40% to the erosion. Most erosion of the nourishment takes place during energetic wave conditions (about 60% to 80% for waves  $> H_{m0} = 3$  m) as the mild to moderate wave conditions are propagated without breaking over the nourishment. Tidal currents and the oblique incidence of the waves hardly affect the erosion rates, but may contribute to some extent for a nourishment that is placed in deeper water. In addition, the numerical model shows that strong rip currents can be present at both lateral sides of the shoreface nourishment for relatively shore-normal waves ( $<15^\circ$ ). These rip currents spread the sediment from the nourishment over a large area (i.e. at some distance from the sides of the nourishments and partially in offshore direction) during moderate and energetic wave conditions, which explains the absence of a clear accretion directly adjacent to the nourishment.



# 3

## REDISTRIBUTION AND LIFETIME OF MEGA NOURISHMENTS

*\* Mega nourishments, aiming at providing long-term coastal safety, nature qualities and recreational space, have been applied recently at the Holland coast and are considered at various other places in the world. Methods to quickly evaluate the potential and lifetime of these coastal mega nourishments are therefore very much desired, which is the main objective of this research. Design graphs for erosion rates, life span and maintenance volumes are derived for freely developing feeder-type mega nourishments (such as the Sand Motor) and permanent mega nourishments (i.e. land reclamation with sand) using calibrated 2DH (Delft3D) and 1D (UNIBEST-CL+ and LONGMOR) numerical models. The extensive set of bathymetric data at the Sand Motor was used as validation data for this purpose. Making a differentiation between the non-rotating foreshore and active surfzone proved to be essential for an accurate representation of the wave-driven alongshore transport in 1D coastline models. The lifetime of nourishments is mainly determined by the dimensions of the nourishment and incoming wave energy.*

### 3.1. INTRODUCTION

In the Netherlands, coastal dunes and beaches form a major part of the first line of defense against flooding by the sea. In 1990 the Dutch government decided on a policy of "Dynamic Preservation Policy" to stop structural erosion of the coast, using nourishments as the preferred intervention to maintain the 1990 coast line (Mulder and Tonnon, 2010). In 2000 it was decided to extend the policy and also maintain the sand volume in the so-called Coastal Foundation, defined as the area between the -20 m depth contour and the landward boundary of the dune area. The annual average

---

\*This chapter is a modified version of the publication: Tonnon, P.K., Huisman, B.J.A., Stam, G.N. and Van Rijn, L.C. (2018). Numerical modelling of erosion rates, life span and maintenance volumes of mega nourishments. *Coastal Engineering*, 131:51-69. The contribution of Bas Huisman consisted of software coding, coastline modelling, analyses of the lifetime of nourishments, derivation of design rules, reporting and discussion of the results.

nourishment volume since 1990 of about 6 million m<sup>3</sup> was raised to 12 million m<sup>3</sup> (see e.g. Van Koningsveld and Mulder, 2004). Since 2000, the dominant nourishment methodology has changed from beach nourishments with a typical volume of several hundred thousand m<sup>3</sup> of sand to more cost-effective and less disturbing shoreface nourishments with a typical volume in the order of one to several million m<sup>3</sup> (Van der Spek et al., 2007). An update of the sediment balance of the coastal foundation taking into account sea level rise (De Ronde, 2008) concludes that in order to maintain the active sand volume of the coastal foundation - the yearly nourishment volumes require upscaling from 12 to 20 million m<sup>3</sup> per year. Moreover, considering worst-case sea level rise scenarios, the authoritative commission on delta safety in The Netherlands (Deltacommissie, 2008) advises to pro-actively raise nourishment volumes up to 85 million m<sup>3</sup> per year until the year 2050. The extra buffer this would create, might be beneficial to different societal functions.

Recently mega nourishments have been carried out in the Netherlands near Ter Heijde (Stive et al., 2013) and near Petten (Kroon et al., 2015). Near Ter Heijde, about 21 million m<sup>3</sup> of sand was dumped (i.e. 19 million m<sup>3</sup> in 2011 and 2 million m<sup>3</sup> in the dunes in 2010) to protect the rather small beach-dune system at that location and for nature and recreational purposes. This mega nourishment known as the Sand Engine, was constructed in the shape of a hook of approximately 2.5 kilometer in alongshore length and 1 kilometer in cross-shore width. The mega nourishment near Petten consists of about 35 million m<sup>3</sup> of sand and is about 10 kilometers long and 350 to 550 m width in cross-shore. Both mega nourishments provide protection for a large stretch of coast over an estimated timescale of at least 20 years, reducing the required maintenance volumes and nourishment frequencies. This is not only cost effective, but also preserves local ecology. They also offer opportunities for nature and recreation. Both nourishments differ in the aspect that the Sand Engine near Ter Heijde is created as a temporary coastal feature that may freely evolve, while the mega nourishment near Petten (being part of the Dutch primary coastal defense) needs to be nourished to maintain its size and shape. A distinction can therefore be made between two types of mega nourishments:

1. Permanent mega nourishments (or beach extensions) that are designed to preserve momentaneous safety levels and need to maintain their size and shape and thus need to be nourished (Petten)
2. Feeder-type mega nourishments that may erode freely, thus feeding adjacent beaches and dunes with sand for a more natural, dynamic growth (Ter Heijde).

The design and impact assessment studies of both types of mega nourishments generally require detailed morphological studies, either to determine the nourishment requirements to maintain their size and function (mega nourishments for safety such as near Petten) or to determine the evolution and life span (mega nourishments such as near Ter Heijde).

This chapter focuses on providing model-based estimates of erosion rates, life span and maintenance volumes of mega nourishments of various dimensions that can be

used in project initiation phases and feasibility studies. First 2DH process-based and 1D coastline models are calibrated on measurement data of the mega nourishment near Ter Heijde, The Netherlands. Then design graphs for erosion rates and life span of mega nourishments are derived based on a series of 1D and 2DH computations for mega nourishments with various width over length ratios and volumes. Next, long-term effects and nourishment requirements to maintain the shape and size of mega nourishments are investigated.

### 3.2. METHODOLOGY

Data on the morphodynamic evolution of mega nourishments is scarce and only a few years of data are available for the mega nourishment near Ter Heijde, The Netherlands. Therefore this chapter applies numerical models to study the morphodynamic evolution, erosion rates and life span of mega nourishments. Typical model approaches that are used for the evaluation of nourishments are coastline models (e.g. Szmytkiewicz et al., 2000) and coastal area models. Coastline models assume gradually varying flow conditions, more or less parallel depth contours and a constant cross-shore profile and originate from analytical solutions of the diffusion equation to small amplitude departures for a rectilinear coast (Pelnard-Considere, 1956). Coastal model such as Delft3D (Lesser et al., 2004) resolve variations in both horizontal dimensions (De Vriend et al., 1993; Nicholson et al., 1997). Both type of models have their specific strong points and draw backs (see Table 3.1). In general, this comes down to a selection of either a fast model with limited detail (coastline models) or a more detailed description with large penalties on computational efficiency (coastal area models). In long-term applications, the latter model type often requires simplifications or input filtering techniques. Some relevant model characteristics of coastline models are discussed by (Capobianco et al., 2002) while the reduction of climate conditions is described by (Walstra et al., 2013).

Table 3.1: Overview of advantages and disadvantages of coastline and area models

Model type	Advantage	Disadvantage
Coastline	<ul style="list-style-type: none"> <li>- Fast model allowing for the application of a full wave climate</li> <li>- Time-series of wave conditions</li> </ul>	<ul style="list-style-type: none"> <li>- Less suitable for investigation of detailed morphology</li> <li>- Includes the wave-driven current only</li> </ul>
Coastal area	<ul style="list-style-type: none"> <li>- Detailed sediment transport patterns and morphology</li> <li>- Inclusion of tidal forcing and wind driven currents</li> </ul>	<ul style="list-style-type: none"> <li>- Computationally intensive; requires reduction of forcing conditions</li> </ul>

Both model approaches have been applied for the evaluation of nourishments. Detailed process-based models (Delft3D) were, for example, applied at the Dutch coast by Van Duin et al. (2004) at Egmond and Grunnet et al. (2005) at Terschelling. Ruggiero

et al. (2010) uses the coastline model UNIBEST-CL+ to assess long-term coastline evolution at the West coast of the US, while other coastline models like GENESIS (Hanson and Kraus, 1989) are also widely applied in the coastal engineering community. For example by Larson and Kraus (1991), for a theoretical analysis of the fate of beach fill material (for small nourishments) and by Thevenot and Kraus (1995) for the evolution of longshore sand waves on Southampton beach in New York state.

In this chapter, we apply both models to study the morphodynamic evolution of mega nourishments. A detailed Delft3D coastal area model is applied for the short-term evolution, while the coastline models UNIBEST-CL+ (WL | Delft Hydraulics, 1994; Deltares, 2011) and LONGMOR (Van Rijn et al., 1995) are used for the evaluation of mega nourishments on longer time scales. Both the mega nourishment near Ter Heijde and a range of idealised nourishment configurations have been modelled using these models. Design graphs and simple formulations for maximum erosion and half time (life span) of freely evolving nourishments and for initial erosion rates and long-term maintenance of permanent beach reclamations are derived based on these model results.

### DELFT3D

Delft3D is a coastal area model that solves the shallow water equations and the advection-diffusion equation for sediment. In this coastal morphodynamic application, a depth-averaged (2D) Delft3D hydrodynamic model is coupled to a SWAN spectral wave model. Delft3D applies the online morphology functionality to compute sediment transport and bed changes after each time step (Lesser et al., 2004). Non-cohesive sediment transport is modelled following Van Rijn (2007a) and Van Rijn (2007b). In order to speed up the simulations and achieve reasonable computational times (in the order of days), a morphological scale factor (Ranasinghe et al., 2011) was applied in combination with the so-called *mormerge* or parallel-online method (Roelvink, 2006). In this approach, all representative wave conditions are run in parallel and the bathymetry is updated every time step using a weighted average (based on the occurrence of the wave conditions) of the computed bed changes for each individual wave condition. The typical sediment at the Sand Motor has a  $D_{50}$  of 200 to 400  $\mu\text{m}$  (see [chapter 4](#)).

### UNIBEST-CL+

UNIBEST-CL+ is a 1D coastline model consisting of two modules (WL | Delft Hydraulics, 1994; Deltares, 2011; McCall et al., 2014). The longshore transport module calculates the tide- and wave induced longshore currents and resulting sediment transport rates. It uses a built-in wave transformation and decay model (Battjes and Janssen, 1978; Battjes and Stive, 1984) to model wave propagation over a constant cross-shore beach profile. Longshore transport rates are computed for a range of coastline angles, resulting in transport rates as a function of coast orientation which are schematized in a so-called  $Q_s - \varphi$  relation. The coastline module uses the  $Q_s - \varphi$  relation obtained from the longshore transport module to calculate the alongshore transport on each stretch of coast. Based on the gradient of the alongshore transport, the coastline changes are being calculated after which the longshore transport rates are updated and the

procedure is repeated. Wave angles in the model are limited to the angle of maximum transport (i.e. about 42 degrees) to prevent coastline instabilities for situations with high-wave angle incidence (Ashton et al., 2001; Arriaga et al., 2017), which can be present temporarily along the initial strong curvature of the shoreline at the mega nourishment.

A uniform beach profile is assumed to be present in coastline models, which is also used for the computation of the wave transformation towards the shore. In UNIBEST, a so-called dynamic boundary can be specified that defines the part of the coast (i.e. most seaward cross-shore extent) that rotates over time with the coastline (due to transport gradients) while the foreshore orientation remains static. This rotation of the cross-shore profile affects wave refraction and nearshore waves. This option is not available in traditional coastline models in which the entire profile is rotated along with a coastline reorientation.

### LONGMOR

The 1D model LONGMOR is a coastline model which computes the mean position of the coastline at every time-step directly from the gradients of the longshore transport (Van Rijn, 1993; McCall and Van Santen, 2013). LONGMOR computes the longshore transport and the longshore transport gradient at each location based on the specified wave climate, rather than making use of the  $Q_s - \varphi$  curve. This implies that the model is sensitive to wave chronology effect; wave directions are therefore ideally specified in alternating or random order. LONGMOR does not apply the dynamic boundary used in UNIBEST-CL+ and the rotation of the coastline is therefore assumed to affect the whole cross-shore profile (i.e. all depth contours up to the offshore boundary).

### MODEL SET-UP AND PARAMETER SETTINGS

The model set up and parameter settings for the Delft3D, UNIBEST-CL+ and LONGMOR models applied to model both the Sand Motor and a range of mega nourishments with various width over length ratios and volumes are summarized in [Table 3.2](#). Sediment at the Dutch coast generally consists of 200 to 300  $\mu\text{m}$  sand (Kohsiek, 1984; Van Straaten, 1965) which fines in the offshore direction. Medium size sand was also used for the construction of the Sand Motor (see [chapter 4](#)). Schematized tidal forcing, wave conditions and cross-shore profiles representative for the central Dutch coast are applied.

Table 3.2: Input parameters for all three models

Parameter	Delft3D	UNIBEST-CL+	LONGMOR
Model type	Process-based. Two dimensional depth averaged model (2DH)	Equilibrium based. 1D coastline model	
Model domain	Flow grid : 24 x 3.8 km, Wave grid: 33 x 3.9 km, $dx = 20 \times 20$ m in area of interest.	180 km length with $dx = 50$ m in area of interest.	35 km length with $dx = 50$ m.
Model time	5 years	200 years	20 years
Time step	0.25 minutes	100 steps per year	3.6 minutes
Bathymetry	Equilibrium Dean profile with constant slope near waterline (Dean-Moore-Wiegel profile; Stive et al., 1993)		No profile. Using bulk transport formulation with wave height at breaker line
Boundary condition	1:50 nour. slope Water level (harmonic) at 19m depth [offshore]	1:50 nour. slope Wave conditions at 6.3m depth [nearshore]	Wave conditions at 19m depth [offshore]
Wave forcing	Lateral boundaries: Neumann (harmonic) 10 representative offshore wave conditions based on 23 years of observations at Noordwijk	Fixed coastline position at both sides. Far away from area of interest 269 (modelled) nearshore wave conditions near Noordwijk	10 representative offshore wave conditions based on 23 years of observations at Noordwijk
Tidal forcing	tidal component: $M2=0.80$ m and $M4=0.22$ m		No tidal forcing
Morphological Factor	372.07 for all wave conditions combined	1 on 1 timescale for hydrodynamics and morphology	
Active height	Implicitly by process formulations in Delft3D	8.5m for Sand Motor case, 7m for artificial cases	10m (from -7m to +3m MSL)
Seawater	Temperature: 15 °C; Density = 1025 kg/m <sup>3</sup> ; Salinity ≈ 34 ‰		
Sediment characteristics	$D_{10}=150\mu\text{m}$ , $D_{50}=200\mu\text{m}$ , $D_{90}=300\mu\text{m}$ , $D_{SS}=200\mu\text{m}$ , Porosity = 40%, Density = 2650 kg/m <sup>3</sup> (note that LONGMOR uses only the $D_{50}$ of the grain size distribution)		
Sediment transport	TRANSPOR2004 (Van Rijn, 2007a and Van Rijn, 2007b)		Parameterized bulk transport formulation (Van Rijn, 2014)

### WAVE CLIMATES AND NET LONGSHORE TRANSPORT RATES

Representative wave and wind forcing conditions were derived from a 23-year data set at measuring station Noordwijk at the central part of the Dutch coast. For UNIBEST, a nearshore wave climate with 269 wave conditions was generated using a SWAN model for the central part of the Dutch coast. For Delft3D and LONGMOR, ten representative offshore wave conditions were derived by binning the measured, offshore wave times series into 5 wave directional classes of 30° and two wave height classes (0 to 1.5 m and 1.5 to 4 m). For each of the ten wave conditions the probability of occurrence and the representative wave period and mean wind speed and direction were determined, see Table 3.3. In order to set the total probability of occurrence to 100%, the proba-



bility of occurrence of offshore directed waves was distributed over the 5 lower wave conditions ( $w01$  to  $w05$ ). The peak period  $T_p$  was calculated from the significant wave period  $T_s$  by using the relation  $T_p = 1/0.95 \cdot T_s$ . Wave roses of the full and reduced wave climate are presented in Figure 3.1.

Table 3.3: Wave and wind conditions derived from the dataset of 23 year wave and wind observations near Noordwijk

# of cond.	Sign. wave height ( $H_{m0}$ ) [m]	Peak wave period ( $T_p$ ) [s]	Wave direction ( $\theta_{dir}$ ) [ $^{\circ}N$ ]	Wind speed ( $w_s$ ) [m/s]	Wind direction ( $w_{dir}$ ) [ $^{\circ}N$ ]	Occurrence [%]
$w01$	1.08	5.24	240	8.87	217.1	19.544
$w02$	2.43	6.89	241.4	14.61	228.9	3.14
$w03$	0.89	5.24	267.7	6.61	243.4	16.174
$w04$	2.64	7.22	267.5	13.31	367.8	2.08
$w05$	0.84	5.67	299.5	5.29	278.8	17.174
$w06$	2.61	7.46	299.6	12.21	293.8	2.02
$w07$	0.82	5.94	328.3	4.9	358	23.604
$w08$	2.64	7.94	326.4	11.7	339	2.19
$w09$	0.72	5.16	354.3	6.22	56.1	13.954
$w10$	2.24	7.03	353	12.52	32.7	0.12
<b>SUM:</b>						<b>100</b>

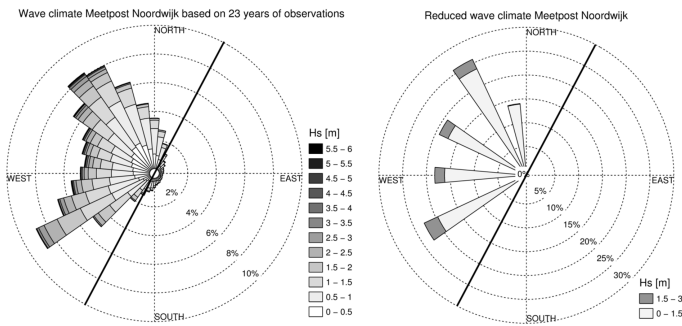


Figure 3.1: Wave rose of the full wave climate (left) and reduced wave climate (right), solid black line represents coastline

For a fair comparison between the models applied in this study, all models were calibrated on a net annual alongshore transport of  $200,000 \text{ m}^3/\text{year}$ , being the average alongshore transport in the surf zone for the central part of the Dutch coast (Van Rijn, 1997b).

### 3.3. HINDCAST OF SAND MOTOR MEGA NOURISHMENT

The Delft3D, UNIBEST and LONGMOR models are calibrated with field data for the Sand Motor mega nourishment as constructed at the Holland coast (Delfland section) a few kilometers south of The Hague from June until August 2011 (Stive et al., 2013; De Schipper et al., 2016; Luijendijk et al., 2017). In total, a volume of 19 million cubic meters of sand has been nourished in order to create the large scale nourishment with approximate dimensions of 2.5 km alongshore length and 1 km cross-shore extent (see Figure 3.3a). The shore-normal of the undisturbed coastline before construction of the Sand motor is about  $310^{\circ}\text{N}$ , but is shown rotated with the alongshore direction from left to right in the figures here for practical reasons.

#### BATHYMETRIC DATA

Between the moment of completion of the Sand Motor (August 2011) and September 2014 (i.e. the moment this chapter was written), 25 bathymetric surveys have been carried out using a real-time kinematic differential global positioning system (RTKDGPS) and (for sub-areal parts) a single beam echo sounder mounted on a waverunner jetski. Figure 3.3 shows the bathymetry of the Sand Motor after construction (survey 1 - August 2011: Figure 3.3a) and after 3 years (survey 25 – September 2014: Figure 3.3b).

For each survey, the volume change of the Sand Motor Peninsula (red polygon in Figure 3.3a) with respect to the first measurement has been computed. It was found that in the first 3 years a total volume of 2.8 million  $\text{m}^3$  has disappeared from the initial area, which is approximately 17% of the initial volume of the Sand Motor Peninsula as measured ( $16.35 \cdot 10^6 \text{ m}^3$ ). Approximately  $1.23 \cdot 10^6 \text{ m}^3$  of sediment loss occurred in the first six months after completion,  $1.54 \cdot 10^6 \text{ m}^3$  in the first year and  $2.04 \cdot 10^6 \text{ m}^3$  in the first 2 years. It is assumed that the sediment is mainly redistributed towards the dune area and to the adjacent coast.

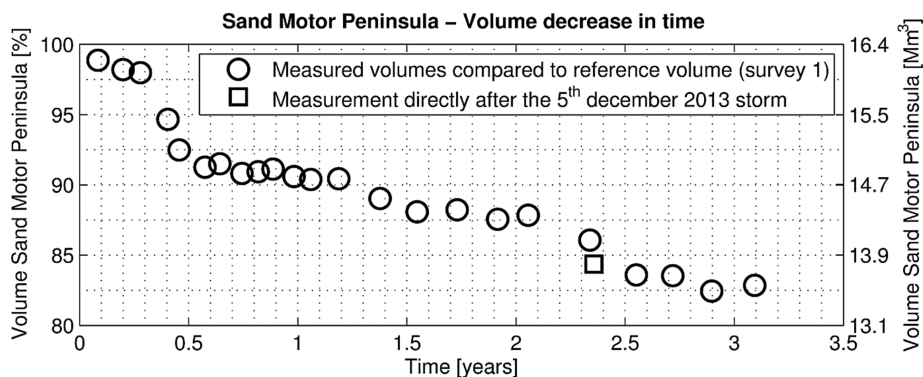


Figure 3.2: Volume decrease in time for the Sand Motor Peninsula (red polygon)

Figure 3.2 shows the volume decrease of the Sand Motor Peninsula, in which all surveys are displayed. Bathymetric surveys were carried out right before and after (rectangular marker in Figure 3.2) the severe storm of 5 December 2013. These measurements indicate that that nearly 280,000 m<sup>3</sup> of sand was eroded from the Sand Motor peninsula. A considerable amount of sand is expected to be transported alongshore away from the Sand Motor, while a (smaller) part of the sand has been brought off-shore by high undertow velocities.

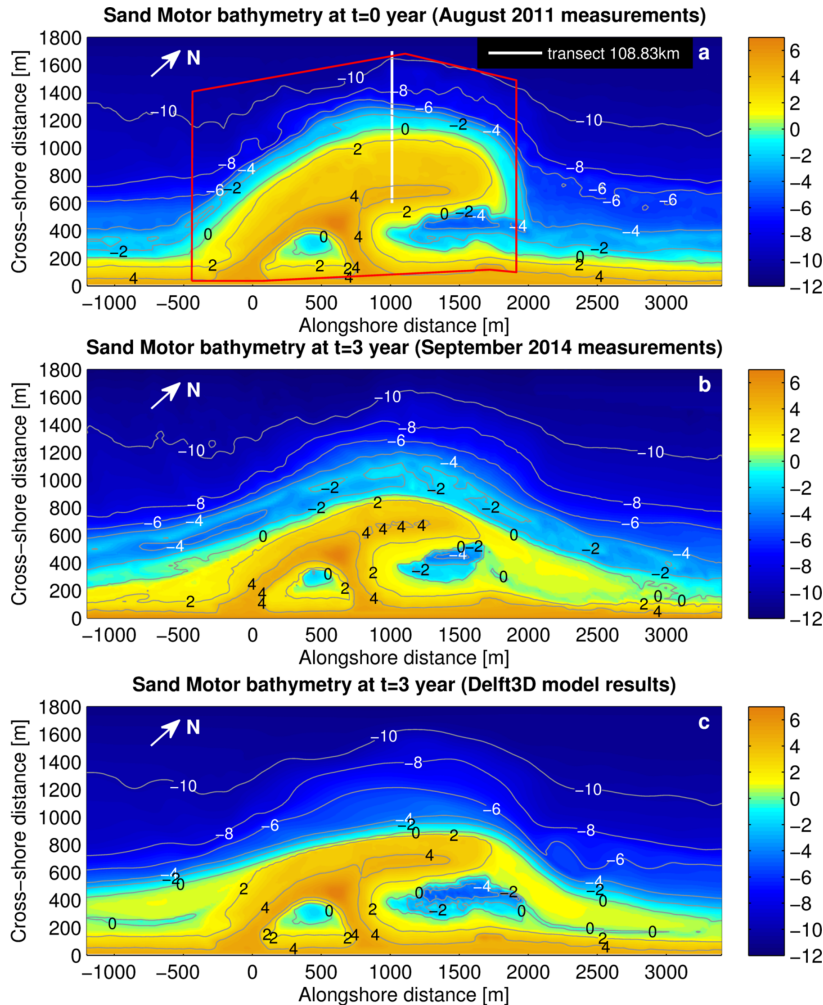


Figure 3.3: Top view of the Sand Motor nourishment. Bathymetry measurements (panel a: August 2011; panel b: September 2014) and Delft3D model results (panel c). Depth with respect to MSL. The white line in panel a depicts transect 108.83 for which the cross-shore profile is shown later. The red polygon shows the area called 'Sand Motor Peninsula' for which volume calculations are carried out.

### CALIBRATION DELFT3D

The Delft3D model of the Sand Motor mega nourishment was run for 5 years. After 3 years, a good resemblance between modelled and measured bathymetry was observed (Figure 3.3b and c). At the eastern part, the spit growth is correctly predicted as well as the formation of the channel, although the shape of the channel is slightly different. Large erosion can be observed at the top of the Sand Motor as well as accretion of sediment on both adjacent sides, which is in good agreement with the measurements. However, the model predicts a steeper cross-shore profile which was not shown in the measurements and the overall shape of the nourishment is slightly different than measured. The measurements show a much more symmetrical shape than the model results, in which the latter is shifted to the right. The reduction in seaward extent of the Sand Motor model is in good agreement with the measurements.

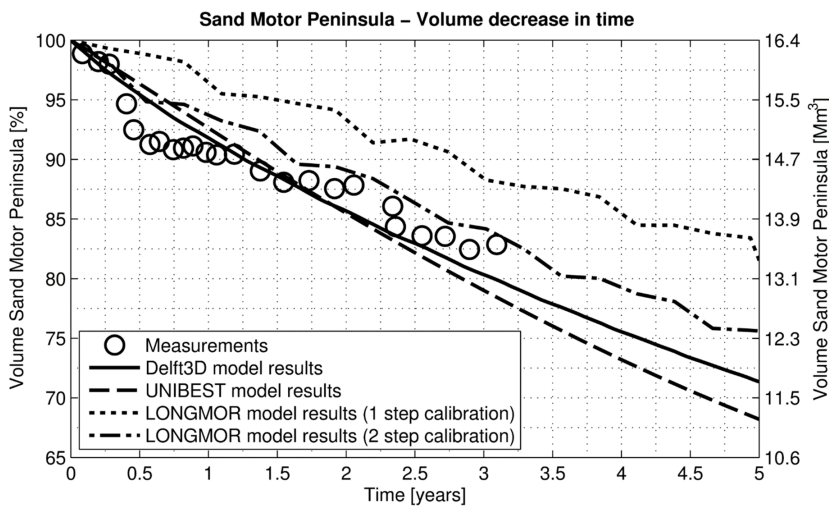


Figure 3.4: Observed and modelled volume decrease at the Sand Motor Peninsula

Figure 3.4 shows the measured volume decrease in time for the Sand Motor Peninsula, combined with computed results for Delft3D (solid black line), UNIBEST (dashed black line) and LONGMOR (dotted black line and dash-dotted black line). The UNIBEST and LONGMOR results are discussed later in current section. Overall, the Delft3D result is in good agreement with the measurements and it is concluded that the Delft3D model is capable of predicting volume decrease in time for mega nourishments. The underestimation of the volume decrease in the first year is attributed to the application of a yearly averaged wave climate. Especially in the second part of the first year, a number of consecutive winter storms resulted in larger long-term averaged erosion of the Sand Motor. Over the course of a few years, results with the year-averaged wave climate are more in line with measurements. It is noted that due to the use of the *mormerge* approach, the results do not respond to the individual wave conditions of the wave climate used, but show a gradual, averaged response.

Figure 3.5 shows the cross-shore profiles at transect 108.83 km (see Figure 3.3a) for the first 3 years according to the Delft3D model results (upper plot) and measurements (lower plot). The shown measurements are carried out on August 2011, August 2012, August 2013 and September 2014. It can be seen from the model results that during a period of 3 years the mean water line moved approximately 250m towards the shore, which is in very good agreement with the measurements. Although the seaward extent reduction is calculated correctly, measurements show a considerable amount of sand being placed between a cross-shore distance of 1000 to 1200m, which is not present in the model results. The absence of this berm is due to the used computation type (2DH), the absence of infragravity waves and the *mormerge* approach, in which the latter causes a smoothed profile due to averaging over 10 wave conditions. However, in general, the model results are in good agreement with the measurements. Based on the good agreement between modelled and measured erosion volumes and shoreline retreat, it is concluded that Delft3D can be applied to study the evolution of series of mega nourishments with various dimensions.

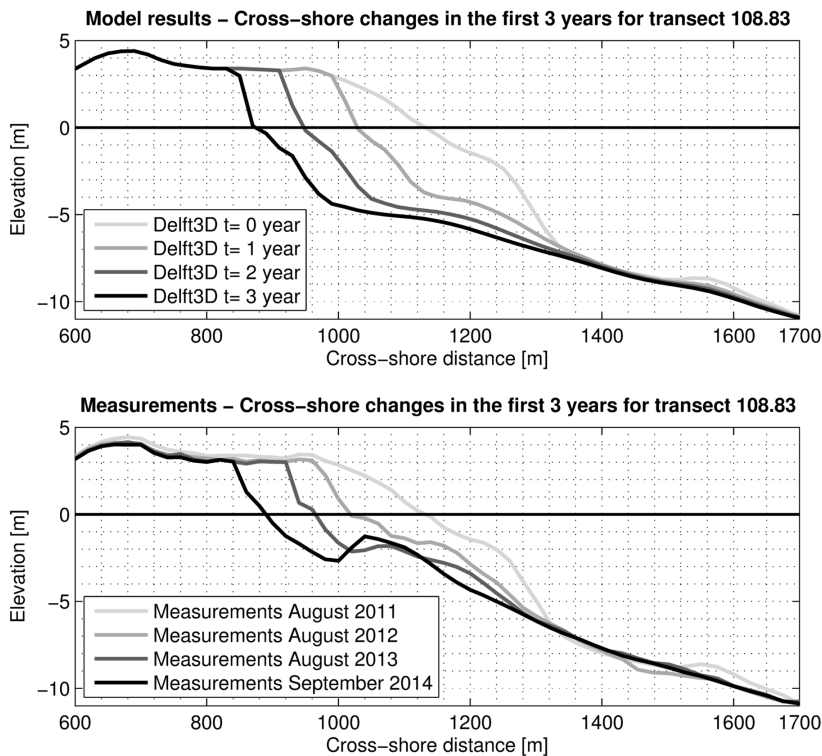


Figure 3.5: Cross-shore profiles at transect 108.83 km. Model results (upper) and measurements (lower)

### CALIBRATION 1D LINE MODELS

In order to compare model results and measurements, the initial Sand Motor shape is implemented in the UNIBEST model (Figure 3.6b). It is noted that detailed characteristics such as 'the hook' at the East of the Sand Motor cannot be implemented because of the strong curvature in coastline. The initial volume of the Sand Motor Peninsula is accounted for by using an active height of 8.5m. The model input parameters are given in Table 3.2. The cross-shore profile extends to a water depth of 6.3m on which a detailed nearshore wave climate consisting of 269 wave conditions is imposed. This boundary is also used as the dynamic boundary, which means that the coast rotates with the shoreline over time. In the first months of the simulation, wave angles may locally exceed 45 degrees due to the strongly curved coastline. In these cases, transports rates are limited to the maximum transport (at about 42 degrees) to prevent instabilities. The net alongshore sediment transport of the UNIBEST model was 200,000 m<sup>3</sup>/year for a straight coastline. Calibration of the transport rates or wave angles was therefore not necessary with the UNIBEST model. The computed and measured volume decrease over time is very similar to the transport rates computed with the Delft3D model (see Figure 3.4; with UNIBEST results represented by the black dashed line). This is remarkable since cross-shore processes and tidal forcing are not taken into account within the UNIBEST model, but is also in line with findings by Luijendijk et al. (2017) who found that volume changes at the Sand Motor are predominantly the result of the alongshore wave-driven currents. The good UNIBEST results for the Sand Motor case illustrate that this model can be used to study erosion rates, life span and maintenance volumes of mega nourishments. The effect of using different wave climates in the Delft3D and UNIBEST models and the effect of using a dynamic boundary in UNIBEST is discussed further at the end of this section.

As is the case for UNIBEST, the rather steep alongshore coastline profile of the Sand Motor may lead to coastline instabilities due to the large relative wave angles (>45°) occurring at that part. The parameterized alongshore transport formulation (van Rijn, 2014) used in LONGMOR varies with  $\sin(2\theta_{br})$  and the alongshore transport will therefore decrease for relative wave angles larger than 45°, which may lead to coastline instabilities. The coastline position is numerically computed from an explicit Lax-Wendroff scheme including a smoothing-parameter to suppress numerical oscillations of the computed coastlines. The value of the smoothing parameter  $\alpha$  (in the range of 0.0001 to 0.001) can be determined by trial and error. Figure 3.4 shows the calculated volume of the Sand Motor Peninsula according to the LONGMOR model (dotted black line) using the same wave climate with 10 offshore wave conditions as is used in Delft3D. The offshore wave heights are converted to wave heights at the breaker line by a refraction analysis assuming shore-parallel depth contours. Similar to the other models, LONGMOR is calibrated to a net annual alongshore transport of 200,000 m<sup>3</sup>/year for a straight coastline. As can be seen from the figure, the LONGMOR model significantly underestimates the volume decrease in time with respect to the measurements (approximately 30%). This discrepancy between the Delft3D and LONGMOR result has the following causes:

- Different wave refraction seaward of the active surf zone. The depth contours outside the surf zone rotate with the coast in the LONGMOR model, while the Delft3D model uses a more realistic (almost stationary) foreshore orientation.
- Wave focusing resulting in enhanced wave heights at both seaward corners is neglected.
- Cross-shore transport gradients which may be relatively large during the initial years due to the presence of the relatively steep beach profiles are neglected in LONGMOR.

The results of the 1D LONGMOR-model can be significantly improved by calibration of the schematized wave climate (by slightly adjusting the wave angles and durations) using measured erosion volumes, which is only possible if substantial validation data are available. The resulting wave climate is slightly more asymmetric than the wave climate used in the Delft3D-model runs. The net annual alongshore transport is kept constant at 200,000 m<sup>3</sup>/year to the north by slightly adjusting the sediment transport coefficients. Figure 3.4 shows the computed volume decrease as a function of time for this so called 2-step calibrated LONGMOR model (dash-dotted black line). The measured initial erosion volumes after 3 years are reasonably well simulated, but the measured erosion after 0.5 and 1 year are underestimated. This result shows that a 1D coastline model following a traditional approach without a dynamic boundary can be calibrated if measurement data are available, which is the case even for mega nourishments (such as the Sand Motor) with a relatively large seaward extent of about 1 km over a short alongshore distance.

### SENSITIVITY FOR WAVE CLIMATE CONDITIONS

Very similar transport rates can be obtained using a full (269 conditions) and reduced wave climate (10 wave conditions) in Delft3D and UNIBEST (Figure 6, panel a). The modelled morphological development of the Sand Motor for each of these sets of boundary conditions is very similar and also in line with the observed development (Figure 3.6c). It is noted that the cross-shore profile in the UNIBEST model was extended to a depth of 19 m in order to apply the representative offshore wave climate used in the Delft3D model in UNIBEST. Transport rates from LONGMOR (using the reduced wave climate) are significantly smaller and as a consequence, the modelled morphological development of the Sand Motor lags behind the observed development. This underprediction of transport rates and morphological development is attributed to the traditional representation of wave refraction on the foreshore in LONGMOR (see next Section). As discussed in the previous section, the results of LONGMOR can significantly be improved by calibration using measured erosion volumes.

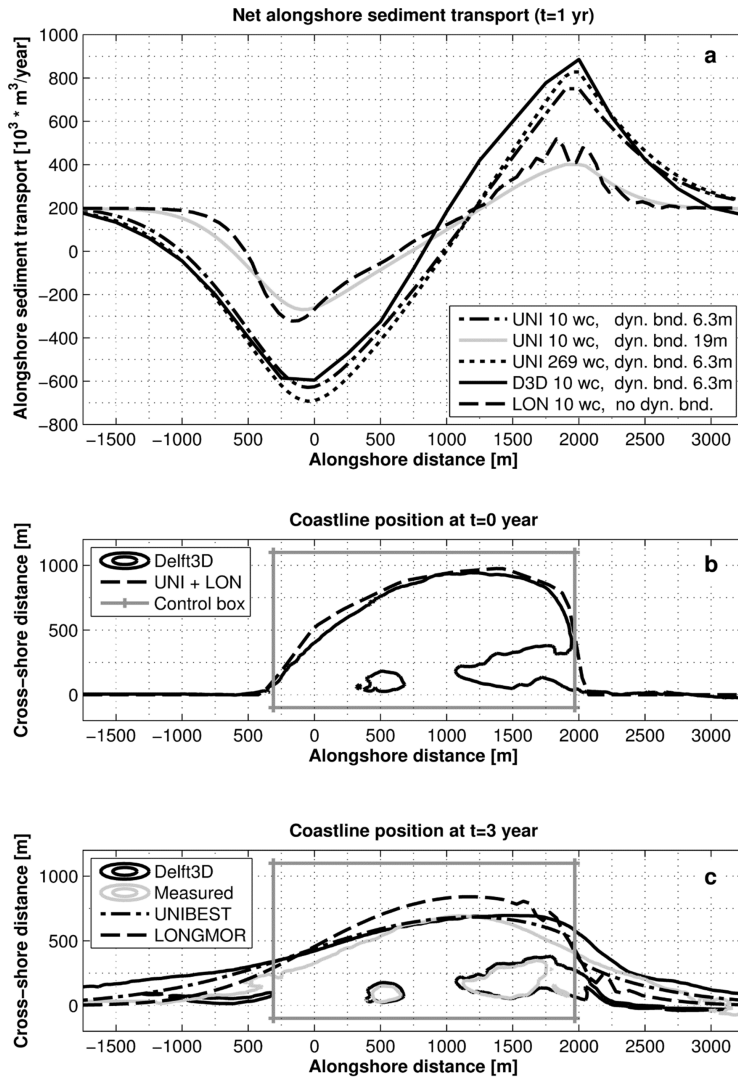


Figure 3.6: Computed alongshore sediment transport with the Delft3D, UNIBEST and LONGMOR models at  $t=1$  year (panel a), initial coastline position (panel b) and coastline position at  $t=3$  year for the Sand Motor (panel c). *wc* = wave conditions

### IMPACT OF WAVE REFRACTION ON FORESHORE

The magnitude of the modelled wave-driven alongshore transport at the Sand Motor with a coastline model (e.g. UNIBEST or LONGMOR) depends on the assumptions made for the position of the 'dynamic boundary', which defines the part of the coast that rotates in the same way as the shoreline. A considerably lower transport is computed when it is assumed that the whole profile (till deep water at 19m; e.g. LONGMOR) rotates dynamically compared to the assumption of only re-orientation in the nearshore zone (i.e. till 6.3 m; Figure 3.6, panel a). Subsequently, it was also observed



that modelled erosion volumes for the Sand Motor Peninsula (Figure 3.7) were under-predicted using an offshore position of the 'dynamic boundary'. The UNIBEST model with a nearshore position of the 'dynamic boundary' better represents the computed Delft3D and observed erosion volumes than models using an offshore position of the 'dynamic boundary' (such as LONGMOR; Figure 3.7).

This observed impact on the transport magnitude results from the difference in wave refraction over the deep water section of the cross-shore profile as a result of the different re-orientation of the profiles. Typically, a dynamic boundary definition in deep water (e.g. 19m water depth) will result in a re-orientation of the full profile towards the average wave incidence angle, which means that individual wave conditions will become more shore-normal due to refraction on the foreshore, which will not take place for a situation with a non-rotating foreshore (i.e. with 'dynamic boundary' in the nearshore). This will in turn reduce the sediment transport since the sediment transport is directly dependent on the incoming wave angle ( $Q_s - \varphi$  relation). It is noted that the UNIBEST and LONGMOR models represent similar physics when the dynamic boundary of the UNIBEST model is placed in deep water.

It was observed that a similar representation of the transport rates could be achieved with either nearshore or offshore wave climate conditions when a realistic setting is applied for the location of the 'dynamic boundary'. There is no generic position setting for the dynamic boundary, which is valid for every coastal region, since this parameter setting depends on the active region and time scales that are investigated with the model. Typically, the position of the 'dynamic boundary' will coincide with the position of depth-of-closure of the considered cross-shore profile. The optimal setting for the dynamic boundary for the Sand Motor case was at a water depth of 6.3m.

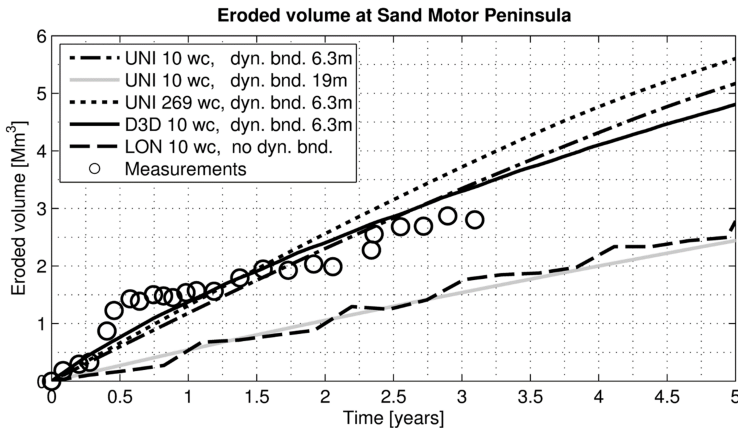


Figure 3.7: Eroded volume Sand Motor Peninsula; Measurements and model results

It is noted that traditional 1D coastline models, such as LONGMOR, do not include a 'dynamic boundary' concept and will therefore consistently underestimate along-shore transport rates. Consequently, the morphological evolution of large scale nour-

ishments is underestimated. In short it is recommended for coastal modelling studies to apply a 'dynamic boundary' concept to provide a realistic representation of the wave refraction on the foreshore.

### 3.4. EVOLUTION OF MEGA NOURISHMENTS

Information on the morphological evolution of mega nourishments is often not available in the initial phases of projects, as models are applied only for the final design and/or impact assessment study. Details on erosion rates, lifetime and maintenance volumes of mega nourishments would, however, be very useful. For this reason relations and design graphs were derived based on a series of 1D and 2DH computations for two types of mega nourishments:

- Feeder-type mega nourishments that may erode freely thus feeding adjacent beaches. A design graph and relation for the half-time is provided in order to estimate the life span of these type of nourishments
- Permanent mega nourishments (or beach extensions) that are designed to preserve momentaneous safety levels and which are kept in place by regular sand nourishments. Design graphs and relations for erosion rates and maintenance volumes are provided.

The design graphs and relations are based on a series of mainly UNIBEST-CL+ computations for a wide range of idealised nourishment configurations. These configurations cover the most relevant physical properties of the nourishment such as nourishment shape, size and adopted maintenance strategy. The ability of the UNIBEST-CL+ model to assess the morphological development of the nourishments has been verified by means of an inter-comparison with the Delft3D model.

#### IDEALISED MEGA NOURISHMENT CONFIGURATIONS

The evaluated dimensions of the nourishments were chosen such that they span the range of potential nourishment configurations. Most relevant parameters are the seaward extent (333m; 667m; 1000m), the width to length ratio (1:2.5; 1:5; 1:10) and the net annual alongshore transport  $Q_s$ , which can be considered a proxy for the wave climate intensity (100,000 m<sup>3</sup>/year; 200,000 m<sup>3</sup>/year; 400,000 m<sup>3</sup>/year). This means that 9 different idealized nourishment configurations were tested (Figure 3.8). Note that the nourishment with a cross-shore width of 667m and a  $L/W$  ratio of 1:5 is referred to as the reference nourishment.

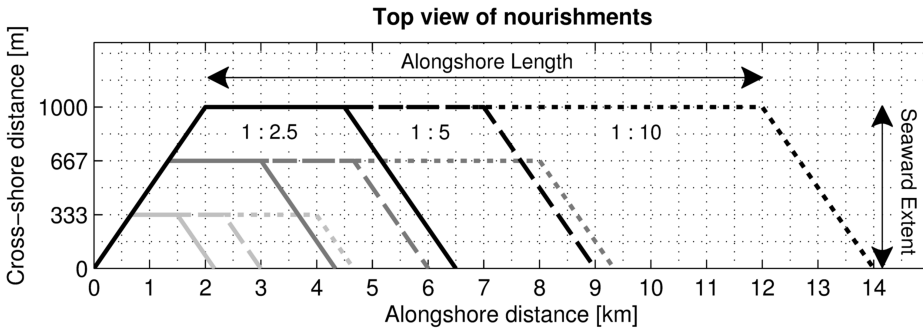


Figure 3.8: Top view of nourishments (note that the x- and y-axis do not have the same scale)

The alongshore length is specified at the seaward side of the nourishment. From there, the nourishment will attach to the adjacent coast with a width to length ratio of 1:2. The alongshore length of the nourishment may also be computed from the alongshore distribution of the sand for more complex nourishment shapes. The mean cross-shore width within the nourishment area (i.e. half of the  $L_{alongshore}$  to both sides) should then be computed as follows:

$$L_{alongshore} = 2 \cdot \frac{\int Y_{cst} |x - x_{center}| dy}{\int Y_{cst} dy} \tag{3.1}$$

with  $Y_{cst}$  the seaward extent of the nourished shoreline with respect to the natural equilibrium coastline position [m],  $x$  the alongshore position [m] with respect to the centerline of the nourishment ( $X_{center}$ ) and  $L_{alongshore}$  the effective length of the nourishment. The applied mega nourishments have an elevation of MSL +2m and a cross-shore slope of 1:50, which attached in deeper water to an equilibrium profile (Dean profile). Table 3.4 shows the nourishment dimensions and volumes for both UNIBEST and Delft3D. It is noted that a difference in sand volumes can be present between Delft3D and UNIBEST which is equal to the volume of sediment that is nourished below the active zone of the cross-shore profile (i.e. below MSL -8m at the Sand Motor). UNIBEST assumes a uniform cross-shore distribution, while Delft3D applies more volume in deeper water for larger nourishments.

Table 3.4: Overview of nourishment dimensions and volumes

Nour [#]	Seaward extent [m]	Width over length ratio [-]	Alongshore length [m]	UNIBEST volume [ $10^6 \text{ m}^3$ ]	Delft3D volume [ $10^6 \text{ m}^3$ ]
1	333	1:2.5	833	3.11	2.7
2	333	1:5	1665	5.01	4.31
3	333	1:10	3330	8.93	7.56
4	667	1:2.5	1668	12.45	13.44

Besides the nourishment dimensions, also the net annual alongshore transport  $Q_s$  has been varied in the UNIBEST-CL+ coastline model by means of adjusting the magnitude of the  $Q_s - \varphi$  curve, which effectively means that the sensitivity of the longshore transport for small changes in coastline orientation is varied. Net alongshore transport rates of 100, 200 and 400 thousand  $\text{m}^3/\text{year}$  were used in combination with a constant equilibrium wave angle of about  $-6.6^\circ$  with respect to the coast normal.

A more generic parameter to describe the sensitivity of the longshore transport for small changes in coastline orientation is used herein, which is referred to as longshore transport intensity (*LTI*). The *LTI* is defined as the variation of the net longshore transport for a small change of the coastline orientation ( $\partial Q_s / \partial \theta$ ). A change in the longshore transport intensity (*LTI*) effectively means that the intensity of the wave conditions is varied. The longshore transport intensity parameter can be approximated for a given wave climate and given coastline orientation by a simple relation which is defined as follows:

$$\frac{\partial Q_s}{\partial \theta} \approx \frac{Q_s}{\Theta \cdot \cos(2\Theta)} \quad (3.2)$$

with  $Q_s$  net longshore sediment transport [ $\text{m}^3/\text{year}$ ],  $\theta$  the coastline orientation [ $^\circ$ ] and  $\Theta$  a relative difference between coast orientation and angle of average wave incidence [ $^\circ$ ] which is larger than zero and from a low wave incidence angle (i.e.  $<40^\circ$ ). Alternatively,  $\partial Q_s / \partial \theta$  can be directly be derived from computed net longshore sediment transport ( $Q_{s,\text{net}}$  [ $\text{m}^3/\text{year}$ ]) for a coastline orientation which was modified by  $+/-1^\circ$  ( $Q_{s,\text{net}+1^\circ}$  and  $Q_{s,\text{net}-1^\circ}$ ) from which *LTI* is computed as follows:  $LTI = 0.5 \cdot [|Q_{s,\text{net}} - Q_{s,\text{net}+1^\circ}| + |Q_{s,\text{net}} - Q_{s,\text{net}-1^\circ}|]$ . The average Holland coast is characterised by an *LTI* of  $30,000 \text{ m}^3/\text{year}/^\circ$  (i.e. net transport of  $200,000 \text{ m}^3/\text{year}$  and  $\Theta$ -parameter of about 6.6 degrees from the shore-normal). Besides the reference climate condition, the *LTI*-value was also varied in the range of  $15,000$  to  $60,000 \text{ m}^3/\text{year}/^\circ$  (i.e.  $Q_s = 100,000$  to  $400,000 \text{ m}^3/\text{year}$  with  $\Theta$  of about 6.6 degrees from the shore-normal). It is noted that the sensitivity of the longshore transport for small changes in coastline orientation can only be defined when both the net transport and equilibrium wave angle are known, because the net transport alone is insufficient to describe the local wave climate. For example, a net longshore transport of zero for the undisturbed section of the coast does not mean that the coastal erosion of the land reclamation is zero.

### INITIAL ALONGSHORE TRANSPORT RATES

For practical reasons the Delft3D model was applied only for the short term computations (i.e. up to 5 year) and acts as a reference for the applied coastline models. An inter-comparison of the computed alongshore transport rates in Delft3D and UNIBEST shows that the models provide very similar results (see Figure 3.9). The transport peaks at the edges of the nourishment are very similar. The only difference between the computed alongshore transport rates is present at the straight middle section of the nourishment (i.e. at  $x = 10 \text{ km}$ ), which has a substantially larger computed transport in the Delft3D simulations (about  $300,000 \text{ m}^3/\text{year}$  for the Delft3D simulation and  $200,000 \text{ m}^3/\text{year}$  for the UNIBEST simulation). These larger sediment

transport rates at the middle section are solely the result of the steeper cross-shore nourishment profile (1:50), as was found from UNIBEST simulations with the nourishment profile shape which gave similar results as Delft3D. The locally larger transport rates are expected to erode relatively more sand from the updrift side than from the downdrift side of the nourishment in the first months until a more natural cross-shore profile has developed (see development of cross-shore profile in Figure 3.5). The total losses from the nourishment area are not expected to be influenced, which means that no effect on the lifetime of the nourishment is expected.

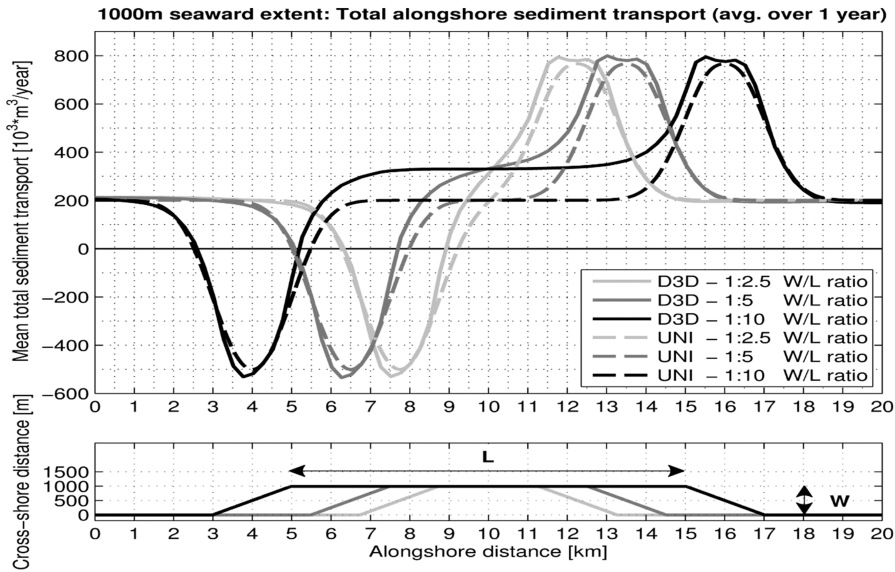


Figure 3.9: Net alongshore sediment transport versus alongshore distance for the 1000m seaward extent nourishments.  $W$  = seaward extent;  $L$  = alongshore length

### FEEDER-TYPE MEGA NOURISHMENTS

The temporal evolution of a feeder-type mega nourishment is evaluated on the basis of the remaining sand volume in the nourishment area, which also includes half of the transition slope from the nourishment to the coast (see example in Figure 3.10). Note that nourishment volumes in the coastline models were obtained by multiplying the coastline position with the active height of the profile (7m for all nourishments). Additionally, also the transport rates are evaluated as they provide insight in the accretion and erosion zones (i.e. zones with gradients). For this purpose the time-averaged transport rates up to a depth of 10m were extracted from the Delft3D model.

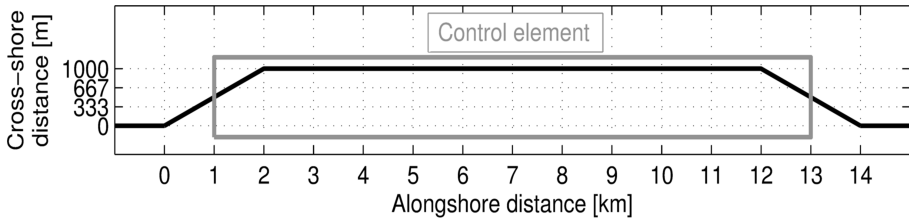


Figure 3.10: Illustrative example of a control element as used for the volume calculations

### MORPHOLOGICAL RESHAPING

The morphology of feeder-type mega nourishments quickly changes into a 'bell shape' (see Figure 3.11 for a UNIBEST-CL+ result), which is in-line with the aim of these nourishments to feed the adjacent coasts. As expected, the erosion starts at the edges of the nourishment and progresses inward over time. These edges coincide with the peaks and troughs in the alongshore transport rates (see Figure 3.9).

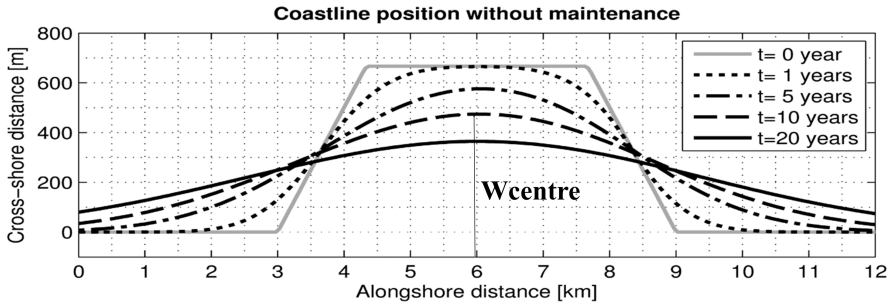


Figure 3.11: Coastline position for the first 20 years without maintenance

The maximum erosion at the center of the freely evolving nourishment is a relevant parameter for the design process. This holds especially for relatively short nourishment configurations for which the erosion is more likely to progress to the center of the nourishment. Model simulations for the different nourishment configurations (Table 3.4) show that the length of the reclamation ( $L_{nour}$ ) is the most governing parameter for the resistance against erosion, while also the longshore transport intensity ( $\partial Q_s / \partial \theta$ ), active height and the time since construction ( $T$ ) determine the magnitude of the erosion at the centerline. Noticeable is that cross-shore width was not important for the retreat at the center of the nourishment (but very relevant for erosion at the sides). The maximum computed retreat at the center of the beach reclamation could be captured by means of a simple formulation (equation 3.3), which had a good representation of the computed retreat with an  $R^2$  of 0.97 (Figure 3.12).

$$W_{center} = W_{ini} \cdot (1 - e^{-y}) \quad T > 0 \quad (3.3)$$

$$y = L_{nour} / (4.28 \cdot (\frac{\partial Q_s}{\partial \theta} \cdot \frac{T}{h_{active}})^{0.6}) \quad (3.4)$$

With  $W_{center}$  the minimum cross-shore width at the center of the nourishment [ $m$ ],  $W_{ini}$  the initial cross-shore width of the nourishment [ $yr$ ],  $L_{nour}$  the initial length of the nourishment [ $m$ ],  $T$  the time since construction of the nourishment [ $yr$ ],  $h_{active}$  the active height of the nourishment [ $m$ ] ( $\approx V_{ini} / (L_{nour} \cdot W_{ini})$ ) and  $\partial Q_s / \partial \theta$  the long-shore transport intensity parameter ( $LTI$ ) [ $m^3/year/^\circ$ ].

The interpretation of the results of the formulation for coastline retreat at the center of the nourishment (eq. 3.3) is considered a good estimate for the potential erosion over multiple years (see Figure 3.12). Seasonal variability of the wave conditions is, however, not directly accounted for in the yearly averaged longshore transport intensity, which means that situations with considerable temporal variability in the wave climate conditions (e.g. due to storms on shorter time scales) may require the use of a conservative estimate of  $LTI$  which is representative for the shorter period of time. It is also noted that the coefficient in equation 3.3 with a value of 4.28 contains various physical aspects which have not been accounted for explicitly, such as the profile shape and sediment properties. The formulation is applicable for land reclamations which cover the full cross-shore width of the active zone, which means that different (quicker) coastline retreat may take place for nourishments which are placed only at the waterline or on the sub-tidal bar. Situations which deviate considerably from the Dutch coastal situation (i.e. typical profile steepness and 250  $\mu m$  sand) may need to be accounted for by upscaling this parameter (e.g. adjusting this parameter equivalent to the impact on net sediment transport rates that is expected from deviating the considered physical parameter). The sand diameter effect (say 0.2 to 0.5 mm sand) is assumed to be partly represented by the range of  $LTI$ -values used.

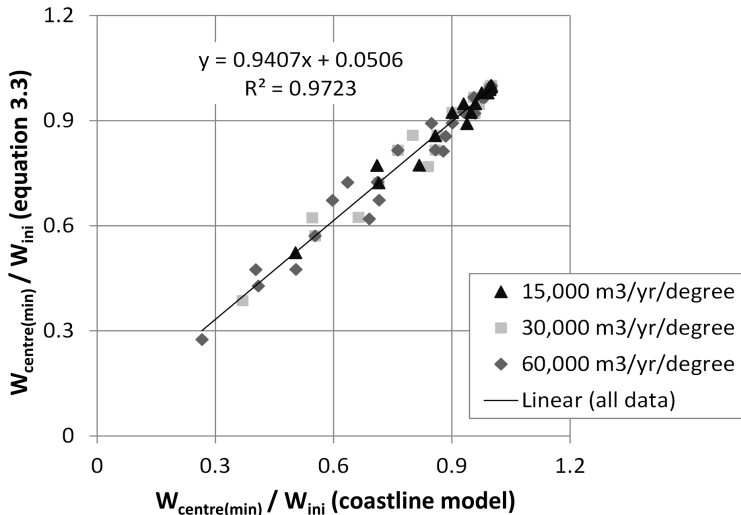


Figure 3.12: Inter-comparison of computed  $W_{center} / W_{ini}$  ratio from coastline model and Equation 3.3

## LIFE TIME

The lifespan of a nourishment can either be defined by a certain threshold value (for the cross-shore coastline position or volume) or by the half-life of the nourishment. The latter is preferred since the definition of a threshold can be arbitrary. The half-life is defined as the amount of time it takes for the nourishment to reduce to 50% of its initial volume. Results are shown for a representative climate for the Holland coast ( $\partial Q_s/\partial\theta = 30,000 \text{ m}^3/\text{yr}/\text{degree}$ ) and a more severe wave climate ( $\partial Q_s/\partial\theta = 60,000 \text{ m}^3/\text{yr}/\text{degree}$ ) for width over length ratios of 1:2.5 to 1:10 (Figure 3.13). Note that the quiet wave climate conditions ( $\partial Q_s/\partial\theta = 15,000 \text{ m}^3/\text{yr}/\text{degree}$ ) were not shown as they provided a similar but slower response.

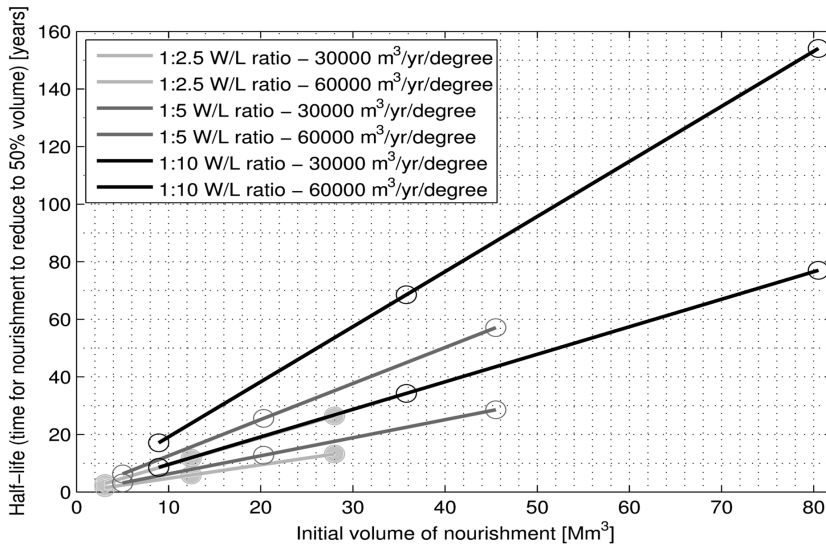


Figure 3.13: Half-life of each nourishment plotted against its volume. Note that the  $T_{1/2}$  for the 1:2.5 ratio are shown with filled circular markers.

A linear relation between the initial volume and the half-life of a nourishment is found (Figure 3.13) from the UNIBEST simulations. It appears that lifetime scales linearly with the nourishment volume ( $V_{ini}$ ) and geometry of the nourishment ( $W/L$  ratio). Note that a longer alongshore nourishment retains more sand in the initial nourishment area than a shorter nourishment with the same volume, since the coastline angles are closer to the natural orientation for longer nourishments. It is noted that simulations with a similar  $LTI$  (e.g.  $30,000 \text{ m}^3/\text{yr}/\text{degree}$ ) gave the same half-time of the nourishment even when the net transport rate and coast angle combination was very different. For example  $200,000 \text{ m}^3/\text{yr}$  and  $6.6^\circ$  gave same result as  $300,000 \text{ m}^3/\text{yr}$  and  $10^\circ$  (i.e.  $30,000 \text{ m}^3/\text{yr}/\text{degree}$  line in Figure 3.13). Hence, longshore transport intensity parameter ( $\partial Q_s/\partial\theta$ ) is considered a very relevant parameter to the actual lifetime of the nourishment.

A formulation (Equation 3.5) that describes Figure 3.13 can be used to estimate the



half time of nourishments at the Holland coast. The impact of the wave climate, cross-shore profile and sediment are confined in the constant ( $1.91 \cdot 10^{-2}$  per degree) and  $\partial Q_s / \partial \theta$  term, which scales with the longshore transport intensity ( $LTI$ ).

$$T_{1/2} = 1.91 \cdot 10^{-2} \cdot V_{ini} \cdot (0.2 \cdot L_{ini} / W_{ini} + 1) \cdot \left( \frac{\partial Q_s}{\partial \theta} \right)^{-1} \quad (3.5)$$

With  $T_{1/2}$  the half-time of the nourishment volume [yr],  $V_{ini}$  the initial volume of the nourishment [ $m^3$ ],  $L_{ini}$  the initial length of the nourishment [m],  $W_{ini}$  the initial cross-shore width of the nourishment [m] and  $LTI$  the longshore transport intensity parameter [ $m^3 / yr / degree$ ] which is defined as the sensitivity of net transport rate  $Q_s$  for rotation of the coastline  $\theta$ ). The half time of the nourishment ( $T_{1/2}$ ) can also be used to compute the remaining volume ( $V_t$ ) or losses at a moment in time after construction (T).

$$V_t = V_{ini} \cdot e^{-\frac{T}{T_{1/2}}} \quad (3.6)$$

The formulation for the lifetime of freely evolving nourishments is applicable for coastlines with relatively low-angle wave impact. This means that the undisturbed coastline orientation is within  $20^\circ$  of the equilibrium orientation. Asymmetric reshaping of the nourishment is expected for cases with large angles of relative wave incidence (Arriaga et al., 2017), as the sensitivity of the transport for coastline reorientation may be significantly different at one side of the nourishment than for the other side. Instability may even occur for very high angles of wave incidence (Ashton et al., 2001).

It is noted that above half time assessment implicitly assumes that all sediment will be mobilised on the longer-term by the alongshore wave-driven current, which means that sediment should be placed equally over the active part of the cross-shore profile. In practice, however, a small part of the nourishment sand may remain at the location of the nourishment, as sand may have been nourished outside the active zone. The sediment in deeper water may even affect wave refraction in such a way that a permanent seaward protrusion remains as a result of focusing of the waves (i.e. wave directions towards center of the nourishment). Consequently, slightly more sand is expected to remain in the nourishment area of large scale sand nourishments at the end of its lifetime than predicted by the formulation.

### PERMANENT MEGA NOURISHMENTS

Both the UNIBEST and LONGMOR models were used to explore the maintenance volumes of permanent mega nourishments, which need to be maintained on a regular basis. The required total maintenance volume over the lifetime depends on the 1) frequency of the maintenance with nourishments, 2) seaward extent of the beach reclamation and 3) longshore transport intensity ( $LTI$ ). It is also noted that initial rates of erosion are generally larger than the long-term average erosion for beach reclamations that are not maintained regularly. The UNIBEST and LONGMOR models were used to explore the effects of various maintenance intervals (2 and 5 years) for one

case (type 5) which has a seaward extent of 667m, a width over length ratio of 1:5 and an alongshore length of 3335m at the seaward side and 6000m at the landward side. A yearly-average wave climate with a longshore transport intensity of  $30,000 \text{ m}^3/\text{yr}/^\circ$  was also applied (similar as for the freely evolving nourishment). The required maintenance volumes of the permanent type are assessed for maintenance frequencies of 2 and 5 years. These were then generalised to other maintenance frequencies on the basis of available model simulations.

## 3

#### INFLUENCE OF MAINTENANCE FREQUENCY

The required total maintenance volume ( $V_{20, \text{yr}}$ ) for the reference nourishment ( $B=667\text{m}$ ) depends considerably on the frequency of the maintenance (see Table 3.5). In general, a reduction of the long-term average maintenance volumes will take place with an increase of the maintenance interval. A low maintenance volume requirement will be obtained if the beach reclamation is restored only after 20 years of free erosion, which requires a nourishment of  $9.2 \cdot 10^6 \text{ m}^3$  in the control area (see Figure 3.10). However, the coastline may have retreated in such a way over that period that maintenance needs to be carried out earlier. The total maintenance volume is largest for a continuous maintenance scheme, but does not differ much from a 1 year interval scheme. A more realistic 5 year interval scheme has significantly smaller maintenance volumes.

Table 3.5: Maintenance scheme and corresponding maintenance volumes after  $t=20$  years

Maintenance scheme	Cumulative maintenance volume after 20 years [ $10^6 \text{ m}^3$ ]	Volume in first maintenance period [ $10^6 \text{ m}^3$ ]
Continuous	16.8	1.32 (avg. 1st year)
1 year interval	15.3	1.23
2 year interval	14.6	2.19
5 year interval	13.1	4.24
20 year interval	9.2	-

An advantage of frequently maintained mega nourishments is the relatively quick development of coastal arches on both flanks (Figure 3.14). It is noted that the approach for nourishing was slightly different in the LONGMOR model which nourishes only the junctions of the beach reclamation while the UNIBEST model restores the original coastline.

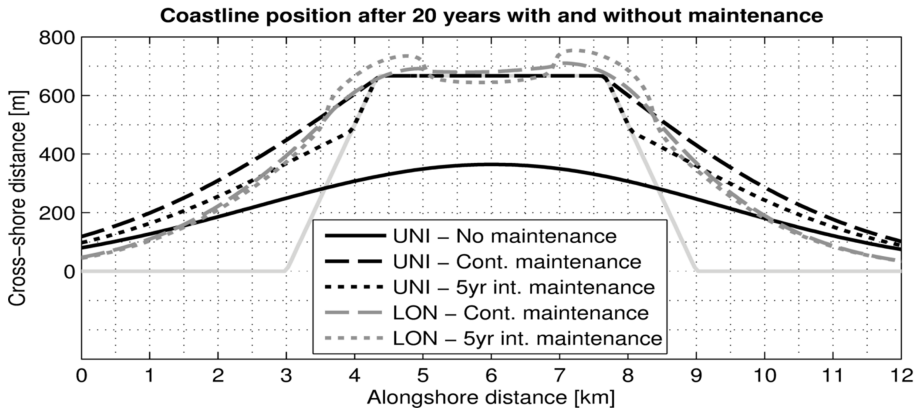


Figure 3.14: Coastline position at  $t = 20$  years with and without maintenance

Figure 3.15 shows the maintenance schemes in a more visual way, by plotting the supplied maintenance volumes in time. It can easily be seen that a shorter maintenance period requires a greater nourishment volume at  $t = 20$  year.

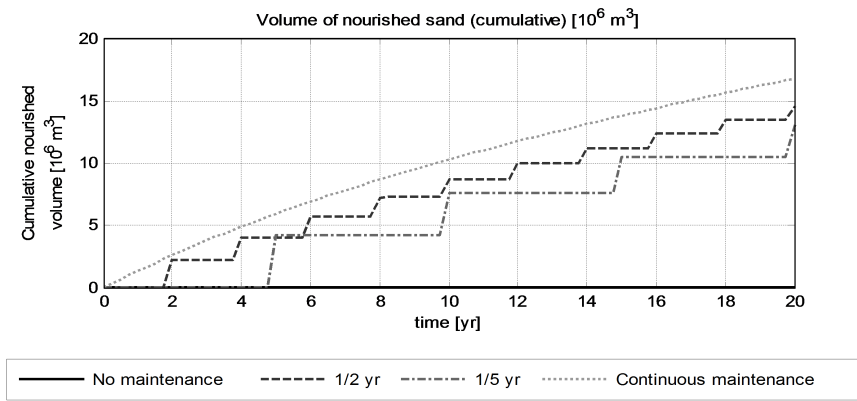


Figure 3.15: Eroded and supplied volume in time for continuous, 2yr and 5yr maintenance intervals

**INITIAL EROSION RATES**

The initial erosion rates averaged over the first 2 and first 5 years at a permanent mega nourishment depend both on the cross-shore extent as well as on the longshore transport intensity (*LTI*). Figure 3.16 and Figure 3.17 show the erosion rates averaged over the first 2 years and erosion rates averaged over the first 5 years respectively. The erosion rate averaged over the first two years for a cross-shore width of 1000m is similar as found from Sand Engine data (i.e. black triangle, Figure 3.16).

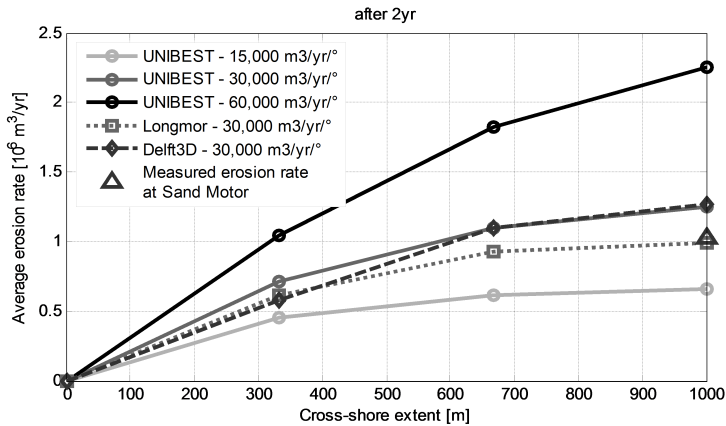


Figure 3.16: Erosion rates (averaged over 2 years) plotted against the seaward extent

It is noted that Delft3D, UNIBEST and LONGMOR simulations provide very similar results again. This indicates that the wave driven alongshore current, which is present in all models, is dominant for nourishment redistribution. Processes such as tidal flow, flow contraction, wave focusing, cross-shore sediment transports are of smaller relevance. Small differences between the coastline models (LONGMOR and UNIBEST) are likely to be caused by small differences in the applied wave climates, differences in alongshore transport formulations and different numerical computation schemes.

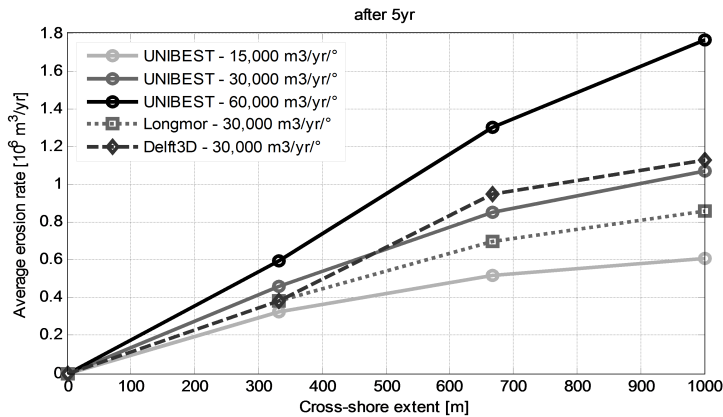


Figure 3.17: Erosion rates (averaged over 5 years) plotted against the seaward extent

### LONG-TERM MAINTENANCE VOLUMES

The actual long-term maintenance volumes are typically smaller than the initial losses, as the coastline develops a more gradual shape over time adjacent to the beach reclamation. This is shown clearly from Table 3.5 which indicates that long-term losses (over 20 years) for the reference nourishment are in the order of 0.7 times the initial

rate of losses. This factor can, however, differ considerably (from 0.4 to 0.9) depending on the size of the nourishment (i.e. cross-shore width and length) and the average longshore transport intensity ( $\partial Q_s / \partial \theta$ ). Additionally also the maintenance interval affects the required nourishment volumes. An overview of the long-term average required maintenance volumes over a 20 year period is shown in Figure 3.18. A conservative estimate of the short-term longshore transport intensity parameter may be used to account for (temporary) more energetic wave conditions or deviations in the profile shape and sediment size.

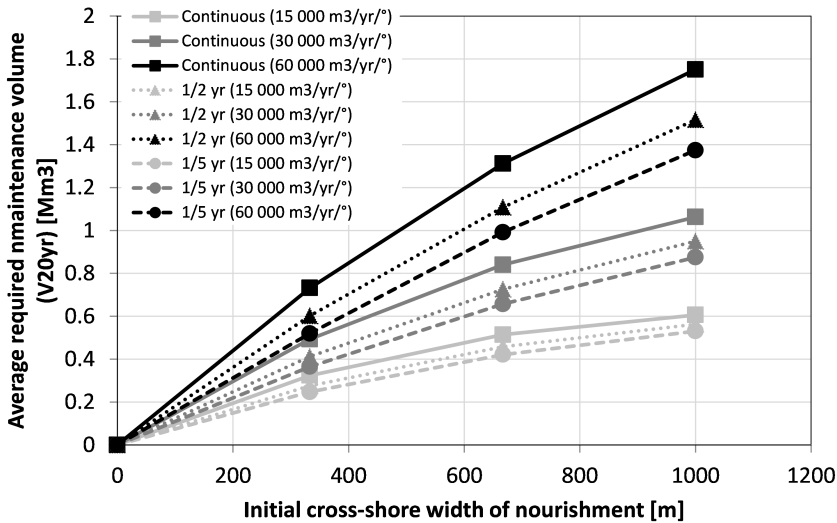


Figure 3.18: Average maintenance volumes (over the first 20 years) plotted against the seaward extent (UNIBEST results)

It is noted that cross-shore width of the nourishment had a considerable influence on the required long-term maintenance volumes, while the alongshore length was irrelevant for land reclamations since they are typically maintained before erosion is taking place at the center of the nourishment. This is in contrast with the formulations for the lifetime ( $T_{1/2}$ ) of the freely evolving nourishment and coastline retreat at the center ( $W_{center} / W_{ini}$ ), which were determined predominantly by the length of the nourishment (see equations 3.3 and 3.5).

### 3.5. DISCUSSION

Alongshore redistribution of sediment at the Sand Motor was modelled with the numerical models Delft3D, LONGMOR and UNIBEST, which provided a good representation of the observed morphological changes. The modelled erosion in the first 1.5 year after construction of the Sand Motor was similar to the observed 1.8 million cubic meter of erosion in this period (De Schipper et al., 2016). These models have been used to produce design graphs for the erosion rates, life span and maintenance volumes of mega nourishments. The present results are valid for wave-dominated open sandy

coastlines with medium sand in the range of 0.2 to 0.4 mm and a regular foreshore with shore-parallel depth contours (i.e. beyond the 8m depth contour). The mega nourishment should be placed far away from structures. Furthermore, the shape of the nourishment should be approximately trapezoidal with a maximum seaward extent of 1 km, maximum alongshore length of 10 km and side slopes of 1 to 2. The current study focuses on coasts with meso-tidal conditions (tidal range < 2 m; nearshore currents < 0.3 m/s) which are dominated by waves with a small angle of wave incidence (i.e. <30 degrees with shore-normal at the point of wave breaking). Instabilities may occur at coasts with persistent high-angle waves (e.g. alongshore sandwaves or spit formation; Ashton et al., 2001; Falques and Calvete, 2005) which are not considered in this chapter.

The ability of the coastline models to represent the coastal evolution of the Sand Motor suggests that transport gradients due to the alongshore wave-driven current are the governing morphological process. This is in-line with findings in other literature on the relevance of tide and waves (Van Duin et al., 2004; Luijendijk et al., 2017). It is noted that other processes can be present during storm conditions, such as long (infra-gravity) waves (Van Thiel de Vries et al., 2008) and transport to deeper water by the undertow current. These cross-shore components were not taken into account in the UNIBEST model and are only partly accounted for in Delft3D (due to the parallel online approach, 2DH calculation method). Effects of these cross-shore processes on the evolution of the Sand Motor and lifetime of other land reclamations is, however, considered small since eroded sediment by storm conditions typically remains within the active zone where the alongshore redistribution of sediment takes place. For example, flume tests of dune erosion have shown that deposition most often takes place only a few meters below the storm surge water-level. A restoration of the beach profile is likely to take place after the storms, which brings the sediment back to the depth-zone with the alongshore wave-driven current (Ruessink et al., 2007; Walstra et al., 2012; Walstra, 2016). Moreover the validation of coastline evolution with the Sand Motor case shows a good prediction with only wave-driven transport component.

The representation of the wave climate conditions is of relevance for the temporal evolution of a land reclamation (or nourishment). The application of a long-term average wave climate in this study results in a gradual erosion over time, which means that short-term variations in transport as a result of varying wave conditions are not represented. Consequently, the computed lifetime and transport rates in the Delft3D and UNIBEST models in this study are less applicable on the short-term (i.e. seasonal or 1 year), but are considered valid for multi-year periods which is shown by the reasonable agreement of the erosion at the Sand Motor after 1.5 year. If a short period (seasons) is considered the user should account for the possible larger persistence of the extreme conditions in the climate schematization (*LTI*). The input reduction of the wave climate for the Delft3D simulations (i.e. 10 conditions instead of 269 conditions) was also shown to have a much smaller impact than other aspects such as the refraction of waves on the lower shoreface. For practical applications it is, however, considered relevant to include the longshore transport intensity parameter (*LTI*) also

in methods for reduction of the number of wave climate conditions to a representative set (Walstra et al., 2013), since it is relevant for lifetime and reshaping of nourishments. In many cases this is implicitly done by including sufficient wave height and directional bins in the climate schematization, but a greater reduction of the number of climate conditions may be achieved when *LTI* is taken into account explicitly.

The wave climate (represented with the *LTI*-parameter) is considered the most dominant parameter for the lifetime of land reclamations on sandy coasts far away from structures (i.e. not affected by the wave sheltering of structures). Consequently, the wave direction was not included in the formulations for the lifetime of the land reclamation. This low relevance of the wave direction is the result of the accretion of sediment on the updrift side of a nourishment in case of situations with oblique wave incidence, which compensates for the additional losses at the downdrift side of the nourishment. Land reclamations near structures require detailed studies to include wave shielding effects. It should, however, be noted that a land reclamation which is placed at the beginning of a beach section or close to a structure (instead of in the middle of a beach section) is affected both by 1) shielding of wave conditions by the structure which reduces the erosion and 2) a larger influence of the wave direction as it can result in enhanced erosion when the waves are directed away from the shielded area where the land reclamation is placed (or vice versa when waves are directed towards the structure). Furthermore, the spatial variation in the climate conditions (i.e. wave energy) in the region with the reclamation can result in enhanced or reduced erosion. In this case it is best to take a conservative (i.e. high) estimate of the wave energy as a proxy for the whole reclamation. Current studies furthermore consider a situation where similar sediment is applied for the nourishment as for the adjacent coast, since situations with rocky foreshores or variations in sediment can induce either additional downdrift erosion as a result of blockage of the transport by a reclamation with coarse sediment (Dean and Yoo, 1992) or a quick mobilization of the sediment of the reclamation if it is finer than the natural sediment. Effects of spatial varying sediment on alongshore wave-driven transport are, however, expected to be small for mega nourishments at the Holland coast which consist of medium sand, such as the Sand Motor, since the behaviour of the size fractions is very similar in the nearshore region (see [chapter 5](#)).

Morphological changes as a result of alongshore redistribution of sand result in re-orientation of the coastline and subsequently in an adjusted transformation of the waves. Especially the nearshore region is influenced on short and intermediate timescales (i.e. from MSL -5m to MSL +2m at the Sand Motor). This feedback from morphological changes to wave forcing conditions is implicitly accounted for by the bed updating of the Delft3D model, but should be explicitly defined in coastline models for accurate reproduction of the wave transformation. This means that nearshore re-orientation should be fed back to the wave transformation, while the offshore bathymetry (and coastline orientation) should remain stable. An implicit assumption of some coastline models (e.g. LONGMOR or Genesis, Hanson and Kraus, 1989) that the coastline re-orientation affects the full profile until deep water (e.g. until 25 m depth) is not considered realistic at engineering timescales and may

lead to an over-estimation of wave refraction on the lower shoreface and subsequent under-estimation of the transport rates. An approach with a separately defined orientation of the static offshore and active nearshore part of the cross-shore profile in the UNIBEST model therefore provided a much better prediction of the transport rates and lifetime of the Sand Motor. A division between the offshore and nearshore part is typically made at the position of the depth-of-closure, since this an estimate of the ultimate cross-shore position of sediment redistribution on monthly to yearly timescales. The applied active height of the profile should also be defined explicitly in coastline models, which relates both to the local wave climate conditions (which mobilize sediment until the 'depth-of-closure') as well as to the dry beach profile that is evolving over time. The active height has a large impact on the computed coastline evolution and hence the diffusiveness of the nourishment. This active height is used for the translation of sediment budgets to coastline changes. In the considered cases the active height is set to a fixed value of 7 m. It is observed that a change of this active height by 1m typically has a linear effect on the modelled nourishment volume and therefore on the diffusiveness of the nourishment. It is noted that the active height depends on the time-frame for which the model is used. For instance, in 20 years time, sediment at larger depths can be mobilised compared to a time-frame of 1 year. However, this dependency is currently not incorporated in the rule of thumb.

The parameterization of the lifetime of a land reclamation based on the longshore transport intensity parameter (*LTI*) relates to work by other researchers on 'diffusion' of coastal perturbations (Pelnard-Considere, 1956; Dean and Yoo, 1992; Huisman et al., 2013; Arriaga et al., 2017) which have also shown that the parameter for alongshore redistribution was influenced by parameters such as wave height, profile steepness and active height of the zone with alongshore transport. The current approach with the *LTI* adds to this a simple approach to quantify this parameter from the 'yearly net alongshore transport' and 'average wave incidence angle relative to the coast orientation', which are two key figures of the considered coast which are often known from literature and therefore applicable in initial assessments. The *LTI* parameter also shows that a coastline cannot be characterized from the net (or gross) alongshore transport rates alone (i.e. without the angle of wave incidence), which shows that the coastal morphological behaviour of sandy land reclamations is determined mainly from the wave energy. It is also very useful that a characterization with *LTI* is less dependent on the actual location along the coast than the net transport rates, since it is not affected directly by the orientation of the coastline. It is therefore also considered useful to classify coasts along the world with an *LTI* parameter, which can be used as a 'morphological boundary condition' for initial assessments, similar to hydraulic boundary conditions which were for example assessed (e.g. Van Rijn, 1997b; Wijnberg, 2002).

The formulations in this research provide a first estimate of the lifetime and losses of land reclamations on the basis of available information on typical wave angles and net yearly transport rates, which should aid the decision process and feasibility studies of coastal managers. Even for some situations with more complex climate conditions than considered in the current studies (e.g. with temporal variability in conditions or spatial varying wave energy) an estimate can be made by assuming conserva-



tive climate conditions. Complex situations with spatially varying sediment or coastal structures do, however, require a more detailed assessment of the behaviour of a land reclamation (e.g. with a process based model) as is also the case in the design phase of a study. It is envisaged that the basic engineering formulations can provide input to other fields of research which would otherwise only use initial assumptions on the behaviour of the reclamation from previous experience (e.g. economic science or ecological studies).

### 3.6. CONCLUSIONS

In this chapter relations and design graphs for erosion rates, life time and maintenance volumes of both feeder-type and permanent mega nourishments were derived using numerical models. Both 2D process-based (Delft3D) and 1D coast line models (UNIBEST, LONGMOR) were calibrated and validated on measurement data of the mega nourishment near Ter Heijde (The Netherlands) and were then applied to model a series of mega nourishments with various width over length ratios and volumes.

- The morphological evolution of the Sand Motor could be reproduced both with a process-based numerical area model (Delft3D) as well as with a 1D coastline model (UNIBEST). The Delft3D results showed detailed predictions with realistic spit growth, channel formation and sedimentation and erosion volumes, but predicted a steeper cross-shore profile and less symmetrical plan form shape in comparison with measurements.
- Modelled erosion rates in UNIBEST were in line with observations at the Sand Motor. LONGMOR underestimated measured erosion volumes (with approximately 30%) due to the traditional representation of wave refraction on the foreshore. The LONGMOR results can, however, be improved by calibration on measured erosion volumes, which is only possible if a substantial amount of measurement data are available.
- The magnitude of the modelled wave-driven longshore sediment transport rate in 1D coastline models depends on the representation of wave refraction on the foreshore. A much more precise representation of transport rates at the Sand Motor was obtained when a so-called 'dynamic boundary' was applied (i.e. in the UNIBEST model), which defines the extent of the nearshore part of the coast that rotates with the shoreline while the orientation of the foreshore remains static. Traditional 1D coastline models (e.g. LONGMOR) assume that the entire profile rotates and consequently underestimate alongshore sediment transport rates as incident waves refract over the entire profile and thus become more shore-normal (resulting in lower alongshore sediment transport rates). With a non-rotating foreshore (i.e. with a 'dynamic boundary' in the nearshore), waves will refract somewhat less, resulting in larger sediment transport rates.
- A realistic prediction of volumetric change and transport rates can be obtained either with a full (269 conditions) and a well-defined reduced wave climate (10 wave conditions) with the Delft3D and UNIBEST models.

The relations and design graphs for erosion rates, life time and maintenance volumes can be used for initial estimates in project initiation phases and feasibility studies.

However, design phases and impact assessment studies require more extensive modelling. To account for local variations in longshore sediment transport and wave climate, the relations and design graphs were derived for various values of longshore transport intensity ( $LTI$ ) which describes the sensitivity of the longshore transport for small changes in coastline orientation. It is noted that the net transport alone is insufficient to describe the response of interventions. For example, a net longshore transport of zero for the undisturbed section of the coast does not mean that the coastal erosion of a mega nourishment is zero.

## 3

- A linear relation is found between the half time of freely evolving mega nourishments and the initial nourishment volume and width over length ratio. Furthermore, the halftime of the nourishment is negatively correlated with wave climate intensity.
- Erosion rates of considered realistic size mega nourishments (with regular 1/1 year to 1/5 year maintenance and Holland coast wave climate) mainly depend on the seaward extent of the nourishment. Additionally, the erosion rates are also very sensitive to the wave climate intensity.
- Maintenance volumes at permanent mega nourishments are considerably lower if maintenance frequency is reduced. However, a lower maintenance frequency results in larger coastline retreat between the maintenance operations. Coastline retreat at the center of a (freely evolving) mega nourishment is related to the length of the nourishment, wave climate intensity, active height and maintenance interval.

# 4

## OBSERVED SEDIMENT SORTING

*\* Bed sediment composition, with a focus on the median grain size  $D_{50}$ , was investigated at a mega nourishment (The 'Sand Motor') at the Dutch coast (~21.5 million  $m^3$  sand). Considerable alongshore heterogeneity of the bed composition ( $D_{50}$ ) was observed as the Sand Motor evolved over time with (1) a coarsening of the lower shoreface of the exposed part of the Sand Motor (+90 to +150  $\mu m$ ) and (2) a deposition area with relatively fine material (50  $\mu m$  finer) just North and South of the Sand Motor. The coarsening of the bed after construction of the Sand Motor is attributed to hydrodynamic sorting processes, as the alongshore heterogeneity of the  $D_{50}$  correlated well with the mean bed shear stresses. Preferential erosion of the finer sand fractions takes place during mild to moderate wave conditions, while a reduction of the local armouring of the bed takes place during storms. A ~40  $\mu m$  reduction of the  $D_{50}$  was observed after a storm in September 2014, which is attributed to the mobilization of both the coarse and fine sediment size fractions and mixing of the top-layer of the bed with the relatively finer substrate.*

### 4.1. INTRODUCTION

Spatial heterogeneity of bed sediment composition is observed at many coasts around the world (Holland and Elmore, 2008), but seldom accounted for in morphological or environmental impact studies of coastal interventions (e.g. modelling of sand nourishments; Capobianco et al., 2002). Knowledge of the potential spatial variability of the bed sediment (i.e. grain size and grading) is however considered essential for the understanding of the ecological impact of large-scale coastal interventions. Firstly, bed composition changes affect the ecological habitats for benthic species and fish (e.g. McLachlan, 1996; Knaapen et al., 2003). Small changes in the top-layer (i.e. centimeters) grain size can, for example, significantly affect the burrowing ability of juvenile plaice (Gibson and Robb, 1992). Secondly, long-term morphological changes may be affected by bed coarsening when finer sand fractions are predominantly eroded

---

\*This chapter is based on the publication: Huisman, B.J.A., De Schipper, M.A., Ruessink, B.G. (2016). *Sediment sorting at the Sand Motor at storm and annual time scales. Marine Geology*, 381:209-226

(Van Rijn, 2007c). Furthermore, the development of the morphology of rip-bar systems was found to be inter-related with the bed sediment (Gallagher et al., 2011; Dong et al., 2015).

Spatial heterogeneity of the bed composition of natural coasts is characterized by a fining of sediment grain size in the offshore direction with coarsest sediment being found in the swash zone (Inman, 1953; Sonu, 1972; Liu and Zarillo, 1987; Pruszkak, 1993; Horn, 1993; Stauble and Cialone, 1996; Kana et al., 2011). In the presence of sub-tidal bars the spatial pattern of the bed sediment composition can vary between different studies. Generally, coarser sediment is observed in the bar troughs and finer sediment on bar crests (Moutzouris et al., 1991; Katoh and Yanagishima, 1995), but Van Straaten (1965) observed coarser material on the bar crests for the Dutch coast. Considerable spatial heterogeneity of the sediment grain size was also observed at rip-bar systems with coarser surface sediment in the rip-channel and finer sediment at the head of the transverse bar (MacMahan et al., 2005; Gallagher et al., 2011). Gallagher et al. (2011) applied a mobile digital imaging system which derived  $D_{50}$  from 2D autocorrelation of macro images of the surface sediment (Rubin, 2004).

The impact of storm conditions at natural coasts consists of a coarsening of the sediment grain size. Most prominent coarsening of the median grain diameter ( $D_{50}$  up to 100  $\mu\text{m}$  coarser) during a storm event with  $H_{m0} = 4\text{m}$  was observed in the swash zone (Stauble and Cialone, 1996). This coarsening gradually decreases in the offshore direction. Terwindt (1962) observed a quite uniform coarsening of  $\sim 30 \mu\text{m}$  from 2 to 15 meter water depth at the coast of Katwijk (The Netherlands) after a moderate summer storm ( $H_{m0} \sim 2\text{m}$ ). Numerical modelling of cross-shore transport sorting during storms also shows coarsening of the nearshore zone and subsequent fining of the offshore sediment at the toe of the deposition profile (Reniers et al., 2013; Sirks, 2013; Broekema et al., 2016). Seasonal variability of the cross-shore distribution of the grain size was observed by Medina et al. (1994), who show that nearshore bed composition is coarsening in winter ( $H_{m0, \text{winter}} \sim 4\text{m}$ ) and restoring to a finer bed composition in summer ( $H_{m0, \text{summer}} \sim 1\text{m}$ ). The largest annual variability in the measured  $D_{50}$  was observed in the swash zone (up to 200  $\mu\text{m}$ ) at mean sea level (MSL) which gradually decreases to a variability of  $\sim 20 \mu\text{m}$  at MSL-8m. Seasonal variability of the  $D_{50}$  was, however, found to be almost negligible for a nourishment at the Dutch barrier island of Terschelling (Guillén and Hoekstra, 1996). Guillén and Hoekstra (1996) observed an 'equilibrium distribution' of the size fractions, which means that the cross-shore bed composition of each size fraction will be restored over time by the hydrodynamic processes to the natural equilibrium situation. An influence of the width of the littoral zone (which depends on the wave conditions) on the location of transitions in the cross-shore spatial variability in  $D_{50}$  of the sediment was suggested by Guillén and Hoekstra (1997).

The impact of the wave-driven longshore current on the alongshore heterogeneity of the bed composition was investigated by McLaren and Bowles (1985) with a focus on the changes of the sediment grain size distribution (size, standard deviation and skewness) along the transport path. A coastal section down-drift from a cliff was studied

by McLaren and Bowles (1985) as well as some riverine cases. McLaren and Bowles (1985) observed two typical spatial patterns of changes of the grain size distribution in the direction of the transport, which were either finer, better sorted and more negatively skewed (abbreviated as FB-) or coarser, better sorted and more positively skewed (CB+). Other studies do, however, suggest that only a better sorting provides a consistent proxy for the pathways of the sediment (Gao and Collins, 1992; Masselink, 1992). The alongshore gradients in the  $D_{50}$  were generally quite small at the Rhone Delta ( $\sim 10 \mu\text{m}$  per kilometer; Masselink, 1992) and therefore seldom larger than the natural variability of the  $D_{50}$  (Guillén and Hoekstra, 1997). In general it can be stated that the literature on the impact of the littoral drift on the spatial variability of the bed composition is scarce, which holds especially for cases with large-scale interventions where sand is expected to diffuse alongshore.

The geological history (e.g. presence of former river bed deposits) also influences the spatial heterogeneity of the local bed composition but at a very large time-scale (millenia or longer; Eisma, 1968; Van Straaten, 1965). The geological situation is therefore often seen as an initial condition of the bed which determines the mean bed composition in the region (Medina et al., 1994; Guillén and Hoekstra, 1996). In general it can be stated that the relevance of the geological history is largest in areas where hydrodynamic forcing conditions are weaker (e.g. at deeper water) and subsequently the time scale of sediment redistribution is long (i.e. months to years).

Spatial variability of the grain size (on cross-shore profiles or alongshore) is often the result of differences in the behaviour of sediment grain size fractions for the same hydrodynamic forcing conditions (Richmond and Sallenger, 1984) which takes place at the spatial scale of sediment grains. A differentiation can be made in sorting due to transport, suspension and entrainment of the grains (Slingerland and Smith, 1986). The transport sorting process is induced by the difference in magnitude of the transport for fine and coarse size fractions (Steidtmann, 1982). A larger proportion of the finer size fractions of the sediment mixture is transported away from an erosive coastal section than transported away for the coarser size fractions. Differences in sediment fall velocity may for specific situations induce suspension sorting (Baba and Komar, 1981). The spatial scale of the area over which sediment is deposited is larger for smaller grains. Additionally the difference in the weight and size of the particle may induce preferential entrainment of the finer sand grains for regimes that are close to the critical bed shear stress of the sand (Komar, 1987). These processes may act together and induce a 'preferential transport' of (fine) sediment size fractions at locations where substantial gradients in the hydrodynamic forcing conditions are present. It is envisaged that the 'Sand Motor' nourishment (Stive et al., 2013) provides an ideal case study site to investigate these processes given the large gradients in wave energy and longshore transport.

The objective of this work is to investigate the spatial heterogeneity of the surface bed composition, with a focus on the median grain size ( $D_{50}$ ), at the large-scale 'Sand Motor' nourishment (Stive et al., 2013). Sediment sampling surveys were carried out at the Sand Motor shoreface and related to modelled hydrodynamic forcing condi-

tions (i.e. mean and maximum bed shear stresses). Both (half-)yearly and bi-weekly measurements were carried out to assess the bed composition changes at annual and storm time scales.

## 4.2. STUDY AREA

The 'Sand Motor' nourishment was constructed on the southern part of the Holland coast (the Netherlands) between April and August 2011 with the aim of providing a 20-year buffer against coastal erosion (Stive et al., 2013). A total of 21.5 million  $\text{m}^3$  of sediment was dredged for the creation of two shoreface nourishments and a large peninsula of 17 million  $\text{m}^3$  (De Schipper et al., 2016). The plan-form design of the Sand Motor comprised of a hook-shape with a dune lake and open lagoon on the northern side (Figure 4.1). The alongshore extent of the Sand Motor was initially about 2.5 km. The emerged part of the Sand Motor was about 1 km wide at the Sand Motor peninsula (i.e. measured at MSL with respect to the original coastline). The initial submerged cross-shore profile slope at the center of the Sand Motor was about 1:30 and extended up to MSL -10m (De Schipper et al., 2016). This was considerably steeper than the cross-shore profile before construction of the Sand Motor which was characterized by an average beach slope which ranged from 1:50 in shallow water (up to MSL -4m) to 1:400 (beyond MSL -10m).

4



Figure 4.1: Aerial photograph of the Sand Motor after completion (September 2011). Note the clouds of fine-grained material moving to the North. Picture courtesy of Rijkswaterstaat / Joop van Houdt

The hydrodynamics, morphology and sediment composition of the Sand Motor were monitored extensively after its implementation. This consisted of in-situ measurements such as bathymetry surveys (with 1 to 3 month intervals), (half-)yearly sediment sampling and measurements of hydrodynamic forcing conditions (e.g. using ADCPs and directional wave buoys). The bathymetry surveys show that sediment was redistributed from the Sand Motor peninsula to the adjacent coast (Figure 4.2), which resulted in a transition from the initial blunt shape to a smooth plan-form shape. Erosion of  $\sim 1.8$  million  $\text{m}^3$  was observed at the peninsula in the first 18 months (De Schipper et al., 2016). Substantial accretion was especially observed during the first winter months after construction. A large spit was formed at the northern side of the Sand Motor, which partially blocked the lagoon entrance. From the following spring and summer onward the changes became more moderate as the nourishment evolved further and wave conditions became milder. It is noted that even after the first years the Sand Motor remained a large coastal disturbance. The nearshore bathymetry at the Sand Motor is characterized either by sections with a longshore uniform bar-trough system or transverse bars.

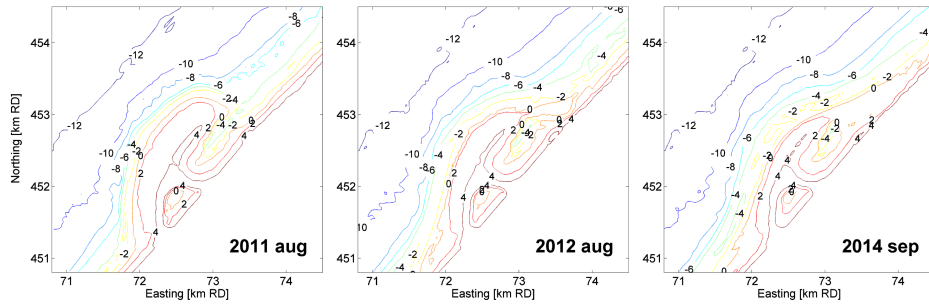


Figure 4.2: Sand Motor bathymetry directly after construction, after 1 year and after 3 years (bed level with respect to mean sea level).

The sediment composition of the Sand Motor was measured during construction and had an average  $D_{50}$  of  $\sim 278$   $\mu\text{m}$ . Beach and dune sediment of the adjacent coast generally consisted of fine sands (100 to 200  $\mu\text{m}$ ), while moderate sized sand was found in the swash and surf (200 to 400  $\mu\text{m}$ ) and finer sands in the offshore direction (100 to 300  $\mu\text{m}$ ) till 8 to 10 meter depth (Van Straaten, 1965; Janssen and Mulder, 2005). However, patches with coarse material (i.e.  $>500$   $\mu\text{m}$ ) can occasionally be found in deeper water North of the Sand Motor (Wijsman and Verduin, 2011).

The Holland coast wave climate is characterized by wind waves which originate either from the South-West (i.e. dominant wind direction) or the North-West (i.e. direction with largest fetch length). The wave climate is characterized by average significant wave heights at offshore stations of about 1 meter in summer and 1.7 meter in winter (Wijnberg, 2002) with typical winter storms with wave heights ( $H_{m0}$ ) of 4 to 5 meter and a wave period of about 10 seconds (Sembiring et al., 2015). The most severe storms originate from the North-West and coincide with storm surges of 0.5 to 2 meter. Storms from the South-West induce either a small storm surge or set-down of the wa-

ter level of some decimeters. Offshore wave data are available in the present study at an offshore platform ('Europlatform') at 32 m water depth. The tidal wave at this part of the North Sea is a progressive wave with largest flood velocities occurring just before high water. The mean tidal range is about 1.7 m at the nearby port of Scheveningen, while the horizontal tide is asymmetric with largest flow velocities towards the North during flood (~0.7 m/s) and a longer period with ebb-flow in southern direction (~0.5 m/s; Wijnberg, 2002). Tidal flow velocities at the Sand Motor peninsula are enhanced as a result of contraction of the flow (Radermacher et al., 2015).

### 4.3. METHODOLOGY

Field surveys of bed sediment composition were carried out before, during and after construction of the Sand Motor over a time-frame of 4 years (Table 4.1) with the aim of assessing both the short-term (i.e. weekly) and long-term (i.e. annual) changes of the median grain size at the Sand Motor. Surfzone and shoreface sediment samples were collected at multiple cross-shore transects with a Van Veen grab sampler (Figure 4.3).

Table 4.1: Overview of bed composition surveys at the Sand Motor

ID	Date	Executed by	Number of transects	Samples per transect	Total number of samples <sup>*1</sup>	Repetition of sampling
T0	Oct' 2010	IMARES	6	6 - 8	42	1x
T1	Apr'-Nov' 2011	Contractor	_*2	_*2	25	1x
T2	Aug' 2012	IMARES	6	11 - 12	67	1x
T3	Feb' 2013	Delft university	6	7 - 10	165 <sup>*3</sup>	3x in 1 survey
T4	Oct' 2013	IMARES	12	6 - 9	93	1x
T5	Feb' 2014	Delft university	7	9 - 25	144	1x
T6	Sep'-Oct' 2014	Delft university	4	11 - 21	111	4x <sup>*4</sup>

<sup>\*1</sup> Only the sample locations between MSL and MSL-10m.

<sup>\*2</sup> T1 sample locations were scattered over the dry beach of the Sand Motor

<sup>\*3</sup> Each location was sampled three times (i.e. 3x 55 samples)

<sup>\*4</sup> The transect at the center of the Sand Motor was sampled four times over a period of six weeks.

Sediment sampling was performed on cross-shore transects spaced about 500 to 1000 meter apart in the alongshore direction (Figure 4.3). A higher sampling resolution was obtained in the cross-shore direction than alongshore, since bed composition is generally more variable in the cross-shore direction (Van Straaten, 1965). Typically about 5 to 12 samples were taken for each transect at 1 to 10 meter below MSL and a few samples on the dry beach (typically in the swash zone). In this research the inter-comparison of the sediment data took place for pre-selected transects (A, B, D, E, F and G). Unfortunately sample transects for surveys T0, T2 and T4, which were collected within a different monitoring programme by Imares, were not co-located and therefore require interpolation of from the nearest transects which is relevant for transect B.



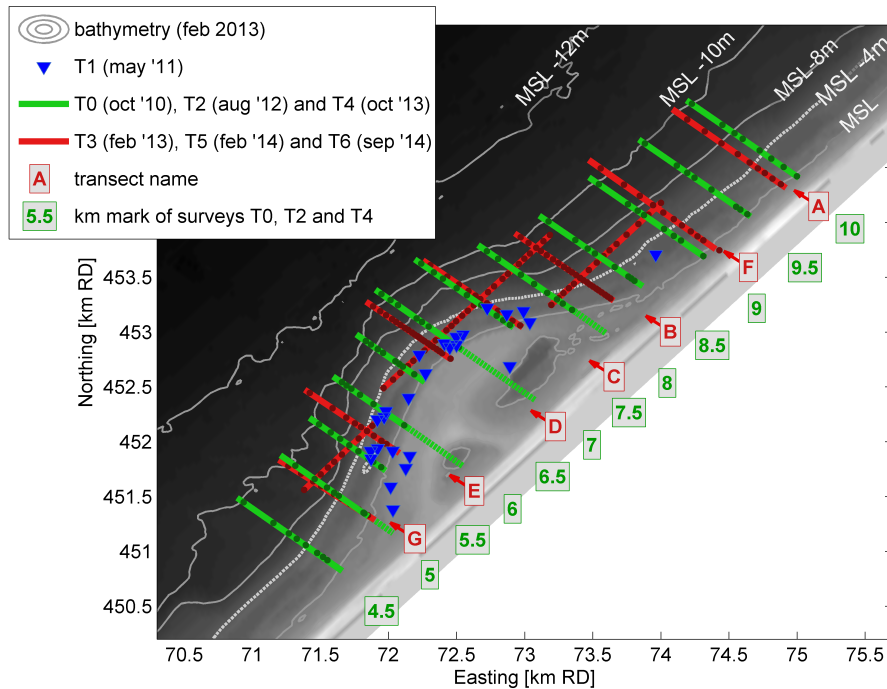


Figure 4.3: Overview of sample locations for the seven field measurement surveys and the labeling of transects. Approximate locations for the T4 and T5 survey are presented as coloured dots on the transect lines. Note that part of the samples of the pre-construction survey T0 were collected at the location of the Sand Motor (dashed green lines). The de-division between offshore and nearshore samples (as used in this research) is made at the MSL -4m contour (i.e. white dashed line).

The dry beach and swash zone samples were collected from land during low water. Sampling at the other locations took place from a ship. Nearshore points (up to MSL -2m) were sampled during high tide, since sufficient water depth was needed for the vessel to navigate. The ship GPS was used to precisely navigate to the predefined location of each sample. The local water depth at the sample location was read from the onboard Sonar. A stainless steel Van Veen grab sampler with clam-shell buckets with a radius of about 15 cm was applied for the sampling. It is lowered by hand on a rope in open position and closes when it hits the bed. A layer of 5 to 10 cm of the top-layer of the bed is then excavated when the rope is pulled. The full samples were stored in labeled bags. Some of the surveys aimed at specific goals. Three samples were collected at every location during the T3 survey to assess the impact of the sediment analysis method (mechanical sieving or Laser diffraction) on the obtained median grain diameters. Cross-shore gradients in the bed composition were assessed on the basis of detailed transects during the T5 survey (typically about 25 m to 30m resolution between samples). Small timescale variations were measured during the T6 survey on a single transect at the center of the Sand Motor (i.e. transect D in Figure 4.3), which was measured bi-weekly over a period of 6 weeks.

### SIEVING AND TREATMENT OF SEDIMENT SAMPLES

The analysis of the grain size distribution of the samples was performed with a Laser diffraction device ('Malvern'; Weber et al., 1991) for the T0, T2 and T4 surveys and with mechanical sieving for the other surveys. The dry sieving method was applied according to BS812 (1975) standards. Wet sieving and pre-treatment with acid were applied for a selection of the T3 samples, which was relevant for a few samples North of the Sand Motor with a small but significant silt content. Either wet or dry sieving of these samples did, however, have a negligible impact on the transect-averaged parameters used in this research. The weight percentiles of the full grain size distribution were determined. Derived properties of the grain size distribution such as the graphical sample standard deviation ( $\sigma_I$ ) and graphical skewness ( $Sk_I$ ) (Folk and Ward, 1957) were computed from the  $\phi$  values of the sediment (where  $\phi = -\log_2(D)$ , with  $D$  being the grain diameter in millimeters). A weighted average of the median grain size per cross-shore transect (referred to as  $D_{50TR}$ ) was used to analyse the alongshore spatial heterogeneity of the bed. The  $D_{50TR}$  is defined as follows:

$$D_{50TR} = \frac{1}{L} \sum_{i=1}^n D_{50,i} \Delta x_i \quad (4.1)$$

The contribution of each sample (landward of the MSL-10m contour) is computed by multiplying the median grain size of the sample ( $D_{50,i}$ ) with the representative cross-shore extent ( $\Delta x_i$ , i.e. half of distance to neighboring samples). The summed  $D_{50}$  contribution of each sample is divided by the length of the considered transect ( $L$ ). Similarly, a transect-averaged median grain size was computed for the nearshore and offshore part of the cross-shore profile (respectively  $D_{50TR,ns}$  and  $D_{50TR,off}$ ) to examine alongshore heterogeneity at different sections of the cross-shore profile. The offshore and nearshore part of the profile were demarcated by the MSL -4m contour (Figure 4.3).

A correction was applied to the Laser diffraction (LD) sample data to make them comparable to mechanical sieving data, since the Laser diffraction analysis typically provides larger  $D_{50}$  values for the same samples (e.g. Konert and Vandenberghe, 1997). This correction was based on a linear fit of the median grain diameter determined using the T3 survey which was both analysed with Laser diffraction and mechanically sieving. The correction function reads as follows :

$$D_{50,sieve} = 0.899 \cdot D_{50,LD} + 10.06 \quad (4.2)$$

The available  $D_{50}$  measurements of the T3 survey and linear fit ( $R^2$  of 0.89) are presented in Figure 4.4. Similar relations were applied by Rodríguez and Uriarte (2009) and Zonneveld (1994).

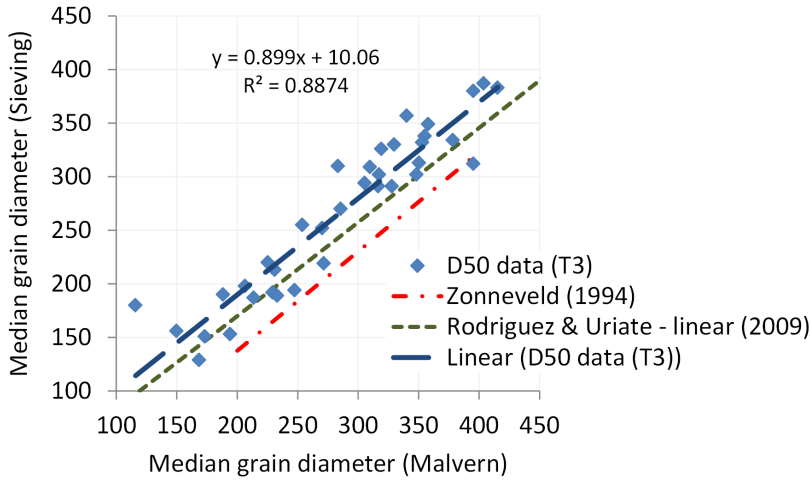


Figure 4.4: Re-analysis of  $D_{50}$  of T3 survey with Laser diffraction and Mechanical sieving and resulting correction factor.

The T3 survey data with mechanically sieved and corrected Laser diffraction samples provided a proxy for the accuracy of the analysis methodology. The standard deviation of the difference in  $D_{50}$  between the corrected Laser diffraction samples and mechanically sieved samples (of the same physical samples) was  $12 \mu\text{m}$  (Figure 4.4) and is considered a quantification of the uncertainty in the  $D_{50}$  due to the analysis methodology. Similarly, also the difference between two mechanical sieved data sets (from same T3 samples) was determined which was  $15 \mu\text{m}$  ( $R^2$  of 0.83). The inaccuracy in the sampling method was considered similar for mechanical sieving or Laser diffraction analyses. An estimate of  $30 \mu\text{m}$  (i.e.  $2x$  STD of the mechanically sieved sample sets) was therefore made for the 95% confidence interval in the mechanical sieving or Laser diffraction analysis. The inaccuracy of  $D_{50\text{TR}}$  was also determined from the considered data sets (for Laser diffraction and mechanical sieving) which was considerably smaller than for the individual samples. The 95% confidence interval of the  $D_{50\text{TR}}$  was found to be  $\pm 11 \mu\text{m}$  on the basis of a re-analysis of the T3 survey with a Laser diffraction device.

### CLIMATE CONDITIONS

Time-series of wave conditions for the T0 to T6 survey were derived from the 'Europlatform' measurement station (see wave height and wave direction in Figure 4.5). The wave conditions were considered typical for the Dutch coast (Wijnberg, 2002) with an average significant wave height ( $H_{m0}$ ) of 1.1 m for all considered survey periods. Considerable temporal variation in the magnitude and direction of the waves was, however, observed for the period of the measurements and preceding month.

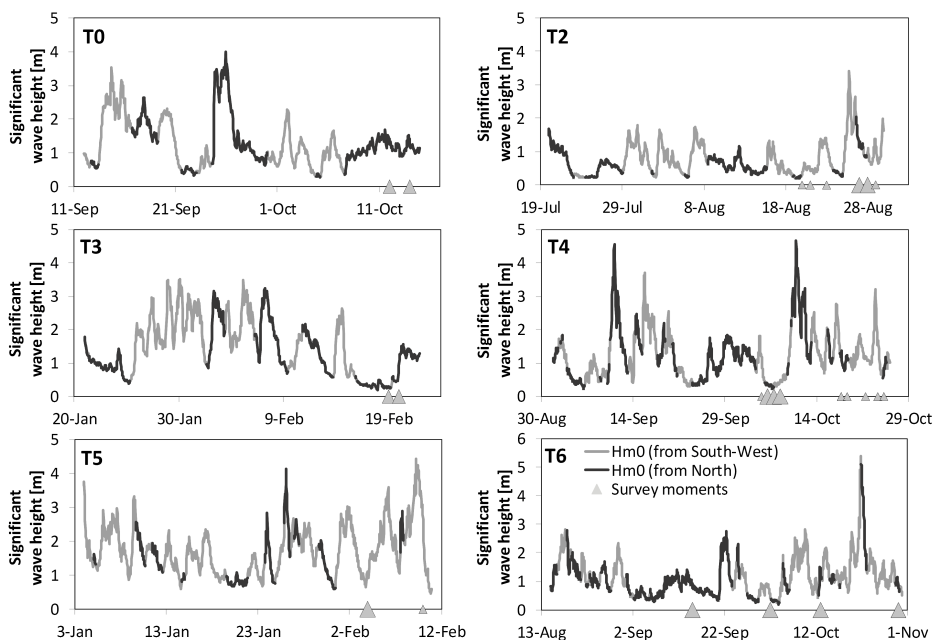


Figure 4.5: Offshore significant wave height ( $H_{m0}$ ) at 'Europlatform' measurement station for the surveys T0 and T2 to T6 (and preceding month). The grayscales of the lines indicate waves originating from the West ( $< 312^\circ\text{N}$ ) or North ( $> 312^\circ\text{N}$ ). Larger survey markers represent moments at which most of the surfzone samples were collected.

Sampling of the sediment typically took place during quiet and moderate wave conditions ( $H_{m0}$  from 0.3 to 1.5 m with an average  $T_{m02}$  of about 4 seconds). Occasional storm events (i.e. offshore wave height from 3 to 5.4 m) were observed both in the winter and summer surveys. The largest storm event in the considered survey periods was observed on 22 October 2016 (during T6 survey). This event had an offshore significant wave height ( $H_{m0}$ ) of about 5 m and originated from the North-West ( $\sim 310^\circ\text{N}$ ). It is noted that the T2 survey measurements were taken only a few days after a storm event on 25 and 26 August 2012 (offshore  $H_{m0}$  of 3.3m) which approached the coast from the West ( $\sim 263^\circ\text{N}$  at MSL -8m). This storm followed a month with relatively quiet conditions.

### HYDRODYNAMIC MODELLING

In this research we explored how observed bed composition changes relate to local hydrodynamic forcing conditions at the Sand Motor. For this purpose a Delft3D model (Lesser et al., 2004) was setup to hindcast wave and tide conditions at the Sand Motor. The Delft3D model applies the shallow water equations for the flow computations. The wave energy transport model SWAN was used for the wave modelling (Booij et al., 1999). The model domain includes the Sand Motor and adjacent coast (Figure 4.6). Time-series of wave conditions were derived from the 'Europlatform' wave measurement station for each of the survey periods. Tide conditions were derived from an operational model for the North Sea (CoSMoS, Sembiring et al., 2015) and applied on the

boundaries of the model. The modelled hydrodynamics were validated by Luijendijk et al. (2017) by means of a comparison with wave measurements at a nearshore wave buoy and current velocities at two ADCP stations. These comparisons showed that nearshore waves and tidal flow velocities were well predicted. Detailed settings of the model are described by Luijendijk et al. (2017). Bed shear stresses as a result of currents and waves ( $\tau_{cw,mean}$  and  $\tau_{cw,max}$ ) were computed with the method of Van Rijn et al. (2004) (Appendix A).

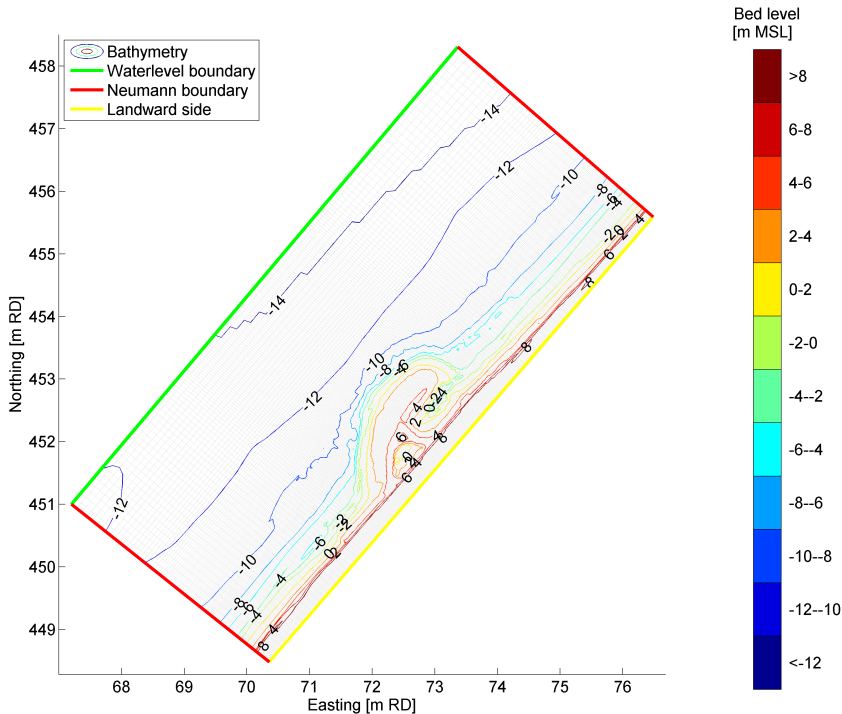


Figure 4.6: Model domain with initial Sand Motor bathymetry of August 2011 and boundary conditions.

A hindcast of the wave and tide conditions was made for the month preceding each of the surveys (T0 to T6) using the most recently surveyed bathymetry. A time-series of a full month was used to make sure that both normal and storm conditions are included. The time-series of  $\tau_{cw,mean}$  and  $\tau_{cw,max}$  were averaged over the considered month at every grid-cell to obtain a spatial field of time-averaged mean and maximum bed shear stresses. These time-averaged bed shear stresses ( $\bar{\tau}_{cw,mean}$  and  $\bar{\tau}_{cw,max}$ ) were then correlated to the  $D_{50TR}$  at predefined cross-shore transects of the surveys.

#### 4.4. SEDIMENT SURVEY DATA

Short-term temporal and spatial variability of the bed sediment composition at the Sand Motor peninsula was investigated on the basis of the T6 survey measurements. The observed short-term temporal variability of the  $D_{50}$  during the T6 survey provided

a proxy for the short-term temporal variability of the  $D_{50}$  in the half-yearly bed sediment surveys at the Sand Motor (T0 to T6).

### SHORT-TERM VARIABILITY OF BED SEDIMENT COMPOSITION

Cross-shore bed sediment composition at the center of the Sand Motor (transect D) was quite similar for the different measurement occasions of the T6 survey (Figure 4.7). The sediment at transect D was typically medium sand. All measurements contained a peak with coarser sand ( $D_{50}$  of about 370 to 420  $\mu\text{m}$ ) in the bar trough,  $\sim 300 \mu\text{m}$  sediment on the seaward side of the bar in intermediate water depths (from MSL-3m to MSL-5m) and 320 to 370  $\mu\text{m}$  sand in deeper water. The transect-averaged  $D_{50}$  ( $D_{50\text{TR}}$ ) of transect D of the T6 survey was on average 331  $\mu\text{m}$ , while  $D_{50\text{TR,off}}$  and  $D_{50\text{TR,ns}}$  were respectively 338 and 320  $\mu\text{m}$  for this transect.

4

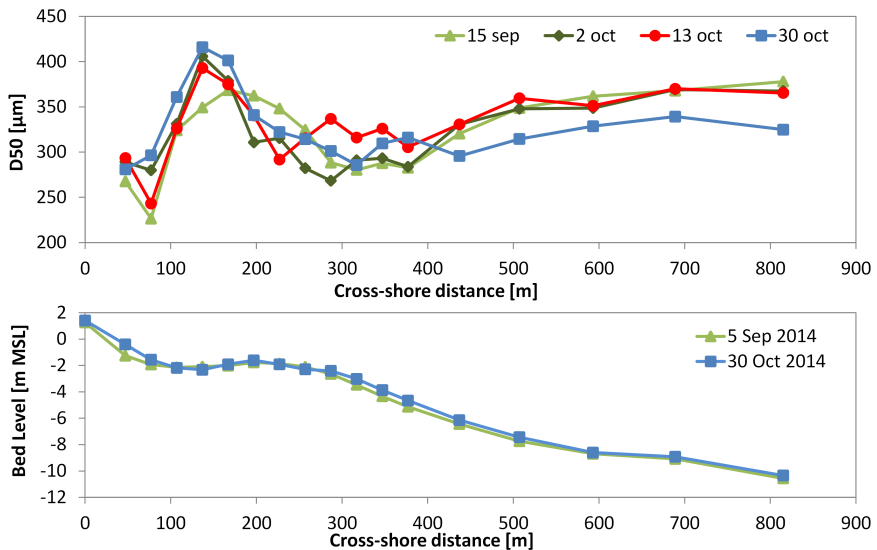


Figure 4.7: Measured median grain diameter ( $D_{50}$ ) and bed level at transect D of the T6 measurement survey (i.e. center of Sand Motor)

The most significant change in the bed composition consisted of a finer  $D_{50}$  of 30 to 40  $\mu\text{m}$  at deeper water (from MSL -6m to MSL -11m) in the October 30 measurements, which was a post-storm survey after the October 22 storm. The transect-averaged bed composition ( $D_{50\text{TR}}$ ) was slightly finer for the October 30 measurements with a  $D_{50\text{TR}}$  of 325  $\mu\text{m}$ . The grain size distribution of the bed between MSL -6m and MSL -8m became more fine skewed ( $Sk_I$  of +0.2) in the October 30 measurements and more coarse skewed ( $Sk_I$  of -0.2) in the trough of the bar. This is in contrast with the other measurement occasions of the T6 survey for which a very small  $Sk_I$  was observed (Appendix B). Bed composition changes in the nearshore consisted of a wider and less pronounced peak with coarser bed material in the first survey (September 15), which was preceded by low northerly waves. Coarsening of the bed took place between the 2nd and 13th of October measurements at the seaward side of the sub-tidal bar (from

MSL-2m to MSL-5m) after a period with dominant wave conditions from the West ( $H_{m0}$  up to 2.8m).

The variability of the bed sediment composition in time was expected to be the result of the hydrodynamic conditions given the considerable (permanent or temporary) change in  $D_{50}$  after the October 22 storm, which is also in line with observed temporal variability in  $D_{50}$  by Stauble and Cialone (1996). Changes in  $D_{50}$  during the short-term T6 measurements are considered a proxy for the temporal variability of  $D_{50}$  as a result of hydrodynamics in other sediment sampling surveys at the Sand Motor, which also experienced similar normal conditions and a severe storm (Figure 4.5). The average significant wave height of the T6 survey was equal to the average of all surveys ( $H_{m0,off} = 1.2\text{m}$ ), while the storm was more severe during the T6 survey than for the other surveys ( $H_{m0,off} = 5.4\text{m}$  during the T6 survey and an average  $H_{m0,off} = 4\text{m}$  for the other surveys). The intra-survey variability was quantified as 2x the standard deviation of the variability in  $D_{50}$  of individual sample locations throughout the six week period of the T6 survey. This amounts to an estimate of  $40\ \mu\text{m}$  for the uncertainty in  $D_{50}$  of individual samples and  $10\ \mu\text{m}$  for  $D_{50\text{TR}}$ . The variability in the nearshore and offshore averaged median grain diameters ( $\Delta D_{50\text{TR,NS}}$  and  $\Delta D_{50\text{TR,OFF}}$ ) was respectively  $16\ \mu\text{m}$  and  $24\ \mu\text{m}$ .

#### LONG-TERM BED SEDIMENT COMPOSITION CHANGES

Bed sediment composition at the Sand Motor changed from a rather alongshore uniform bed composition (T0 survey) to a situation with considerable alongshore heterogeneity in  $D_{50}$  over the entire four year study period (Figure 4.8).

The pre-construction situation (T0; panel a in Figure 4.8) was characterized by a fining of the sediment in the offshore direction. Typically a median grain diameter of about 300 to 400  $\mu\text{m}$  was found at the waterline and  $\sim 200\ \mu\text{m}$  sand at MSL -7m contour and deeper. The alongshore variability in sediment size is largest in shallow water (MSL -2m) and decreases in the offshore direction, which is in line with other observations along the Holland coast (Wijnberg, 2002). The standard deviation of the grain size distribution ( $\sigma_I$ ) ranged from 0.6 to 0.8 for most samples, with largest  $\sigma_I$  for samples that were collected seaward of MSL -5m (Appendix B). Skewness ( $Sk_I$ ) ranged from -0.2 to 0.1 with slightly more positive skewness in shallow water (from MSL to MSL -3m).

Sediment samples at the dry beach that were collected during the construction of the Sand Motor (T1; panel b in Figure 4.8) typically had a median grain diameter ( $D_{50}$ ) between 250 and 310  $\mu\text{m}$  (278  $\mu\text{m}$  on average with  $\sigma_I$  of 30  $\mu\text{m}$ ). The relatively uniform bed at the dry beach is expected to be the result of mixing during the dredging and nourishing activities. Whether the underwater bed sediment was of similar composition is not known directly from measurements. It is expected that similar sand was used also offshore since the nourished material needed to adhere to the specifications with respect to grain size (i.e. between 200 and 300  $\mu\text{m}$ ). Suspension sorting (Slingerland and Smith, 1986) as a result of the dumping of the sediment may, however, have taken place. Consequently, some of the finest sand and silt fractions that were nourished may be missing from the underwater bed sediment of the Sand Motor.

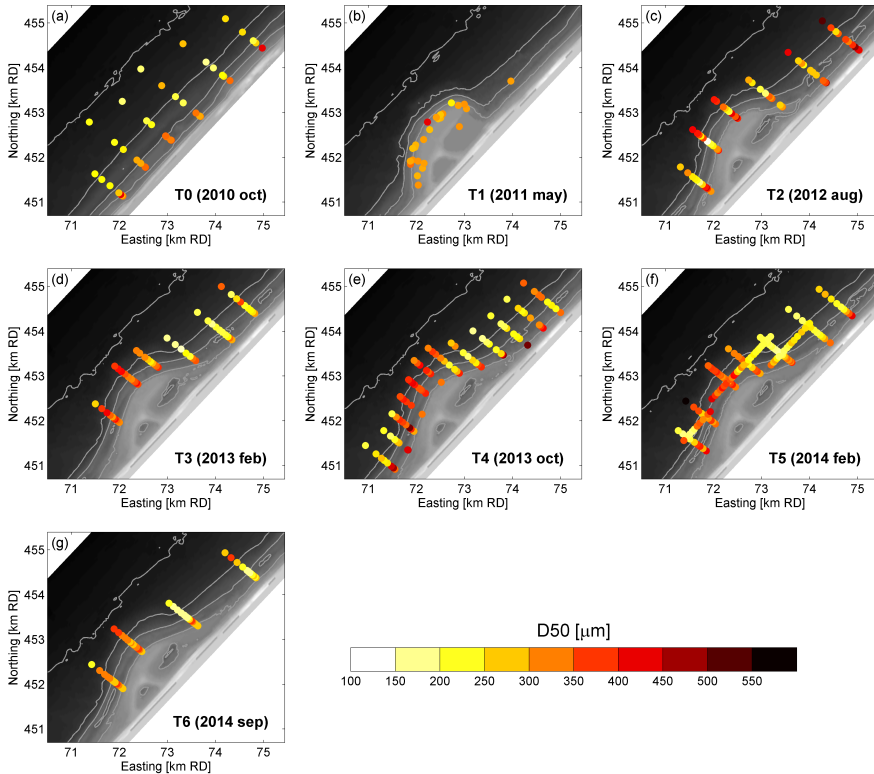


Figure 4.8: Median grain diameter of sediment samples for T0 to T6 surveys (respectively a to g)

The first survey after construction of the Sand Motor (T2; panel c in Figure 4.8) did not show the gradual fining in the offshore direction. Instead coarser sediment was found in shallow water (landward of MSL -2m) and deeper water (beyond MSL -6m), while finer sand was found at intermediate depths along the western side of the Sand Motor (i.e. 100 to 200  $\mu\text{m}$  from MSL -4m to MSL -8m). Overall, the average bed sediment composition ( $D_{50}$ ) of the T2 survey was considerably coarser than the natural bed (T0 survey), as well as coarser than the sediment that was used for construction (T1 survey). The  $D_{50}$  landward of MSL -2m typically was  $\sim 500 \mu\text{m}$ , while offshore  $D_{50}$  ranged from 300 to 500  $\mu\text{m}$ .

Considerably coarser sediment ( $D_{50}$ ) was observed at the central Sand Motor transects from about 1.5 years after construction of the Sand Motor (i.e. surveys T3 to T6) and a fining of the bed at the Northern and Southern flanks (panel d to g in Figure 4.8). This alongshore heterogeneity of the bed composition ( $D_{50,TR}$ ; Appendix C) had a length scale which is similar to the size of the Sand Motor ( $\sim 2 \text{ km}$ ; Figure 4.9). The coarsening of the transect-averaged median grain diameter ( $D_{50,TR}$ ) at the central transects of the Sand Motor (transect D and E) was up to +140  $\mu\text{m}$ , which was considerably coarser than the average  $D_{50,TR}$  of the T0 survey which was 220  $\mu\text{m}$ .  $D_{50,TR}$  was up to 50  $\mu\text{m}$  finer for the transects North of the Sand Motor (i.e. transects B and F). It is noted that a



more extensive fining of the bed may have been present in the area North of the Sand Motor, but this was possibly not captured by the sampling at the current transects.

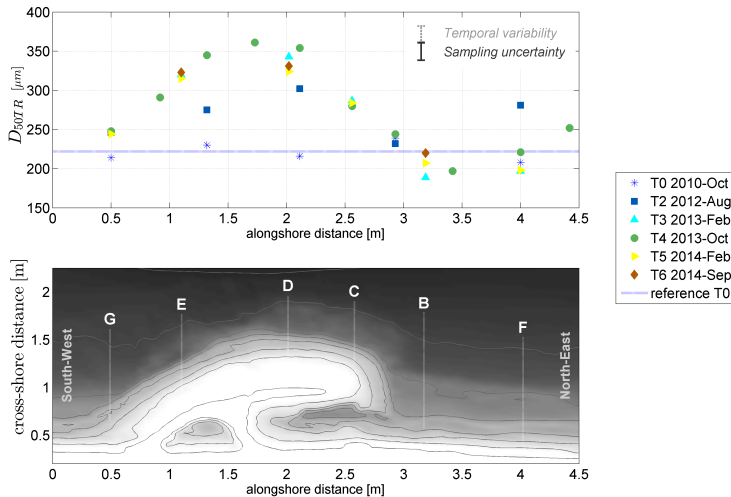


Figure 4.9: Alongshore variability in the transect-averaged median grain diameter ( $D_{50TR}$ ) at the Sand Motor.

The observed changes in  $D_{50TR}$  at the Sand Motor peninsula (transect D in Figure 4.9) well exceeded the uncertainty as a result of the analysis methodology ( $\sim 11 \mu\text{m}$  for  $D_{50TR}$ ) and short-term temporal variability of the bed composition ( $\sim 10 \mu\text{m}$  for  $D_{50TR}$ ) as observed in the T6 survey. The alongshore heterogeneity of the  $D_{50}$  after construction of the Sand Motor was substantially larger than for the reference survey (T0) which had a relatively spatially uniform bed composition ( $-10\%$  to  $+5\%$  deviation of  $D_{50TR}$  from the survey average). From T3 onward, the grain size distribution at the center transects of the Sand Motor was relatively narrow ( $\sigma_I$  of 0.4 to 0.6) compared to the grain size distribution of the nourished sediment, while more poorly sorted sand ( $\sigma_I$  of 0.7 to 0.9) was found in deeper water (from MSL  $-5\text{m}$  to MSL  $-10\text{m}$ ) North and South of the Sand Motor area. The reduction of  $\sigma_I$  at the Sand Motor provides an indication for changes in bed composition as a result of hydrodynamic sorting processes (e.g. due to differences in transport gradients or entrainment of sediment size fractions).

#### CROSS-SHORE AND ALONGSHORE VARIABILITY OF $D_{50}$

A more detailed investigation into the cross-shore sediment distribution at the Sand Motor peninsula and adjacent coast, showed that the cross-shore distribution of  $D_{50}$  was rather uniform at the central Sand Motor transects ( $D_{50}$  from 300 to 400  $\mu\text{m}$  at transects D) when compared to the natural fining in the offshore direction that was observed in the reference survey T0 (Figure 4.10). A natural fining of the sediment in the offshore direction was observed for the transects North and South of the Sand Motor (see example for transect B in Figure 4.10). A quantification of the cross-shore variability of the  $D_{50}$  by means of a linear regression for all samples in the active zone

(from MSL to MSL -8m) indicated an average cross-shore fining of  $\sim 24 \mu\text{m}$  per meter depth in the offshore direction ( $R^2 \geq 0.83$ ).

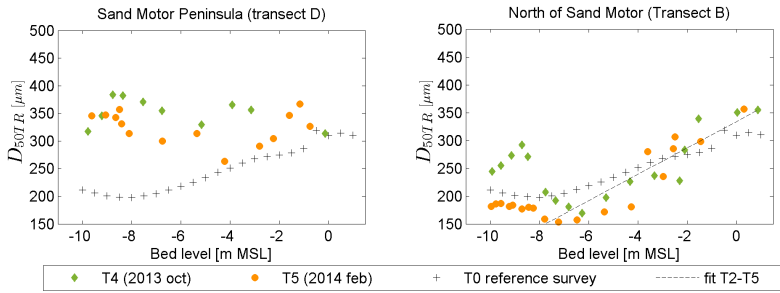


Figure 4.10: Cross-shore distribution of  $D_{50}$  at the Sand Motor peninsula and adjacent coast (transects B and D) before and after construction of the Sand Motor for a representative summer and winter survey (T0, T4 and T5).

Alongshore heterogeneity of the bed composition was most prominent in deeper water seaward of the sub-tidal bar ( $D_{50TR,off}$  of +90 to +150  $\mu\text{m}$  with respect to T0 survey; Figure 4.11) as a result of the relative coarse  $D_{50}$  in deeper water at the Sand Motor (Table 4.2). In the nearshore the  $D_{50TR,ns}$  at the Sand Motor (transects D and E) was only moderately coarser than  $D_{50TR,ns}$  at the adjacent coastal sections (0 to +70  $\mu\text{m}$  coarser).

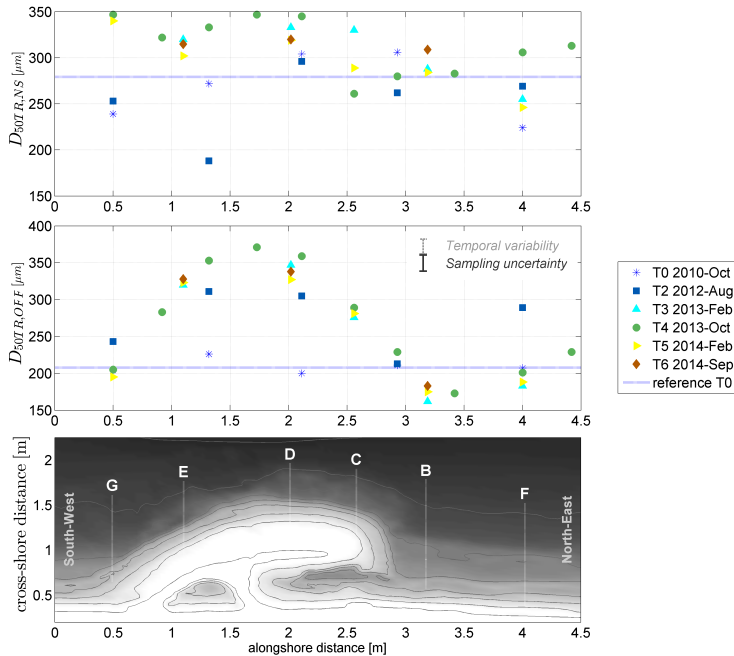


Figure 4.11: Alongshore variability in the offshore and nearshore averaged median grain diameter ( $D_{50TR,NS}$  and  $D_{50TR,OFF}$ ) at the Sand Motor.

### TEMPORAL DEVELOPMENT OF $D_{50}$

The temporal variation of the bed composition at the Peninsula of the Sand Motor (transect D) consisted of an initial increase of the  $D_{50TR}$  at T1 from about 216 to 278  $\mu\text{m}$  during construction of the Sand Motor (Figure 4.12, panel a) which was followed by additional coarsening of  $D_{50TR}$  from the T1 to T3 survey (up to  $\sim 340 \mu\text{m}$ ). The observed  $D_{50TR}$  (at transect D) was more steady after survey T3 with a small tendency towards a reduction of the coarsening after the T4 survey. The  $D_{50TR}$  of transects North of the Sand Motor (B and F) were either similar or somewhat finer than for the T0 survey (0 to  $-50 \mu\text{m}$  change compared to T0).

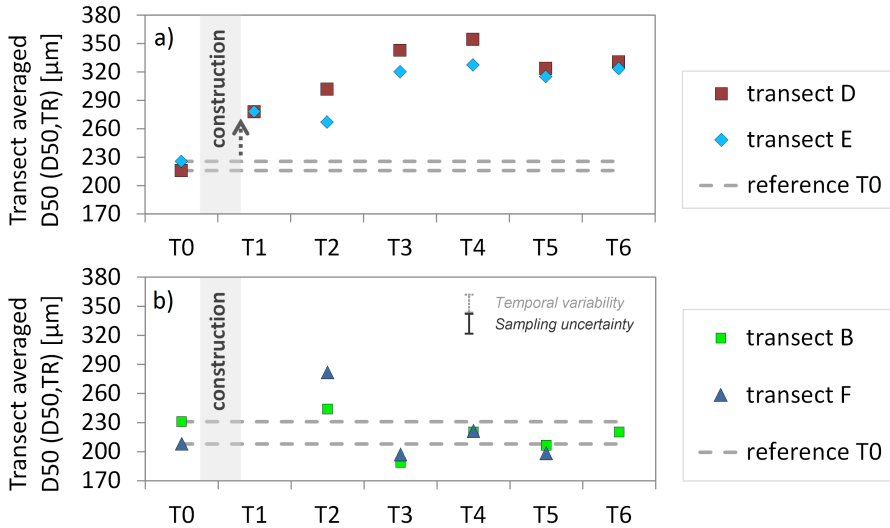


Figure 4.12: Transect-averaged median grain diameter ( $D_{50TR}$ ) over time at the center of the Sand Motor (panel a) and North of the Sand Motor (panel b).

The gradual increase in the  $D_{50TR}$  at the Sand Motor peninsula in the first two years (from T1 to T4) exceeded the uncertainty as a result of the analysis methodology and short-term temporal variability. Observed coarsening was therefore not considered due to initial construction of the Sand Motor alone, but partly also the result of a gradual process in time.

The longer-term behaviour of the  $D_{50TR}$  from survey T3 onward was much more subtle (Figure 4.12) and therefore makes it difficult to discern a trend. This may partly be due to a seasonal influence on the  $D_{50}$  of the measurement surveys, which was perceived to be present at transects North of the Sand Motor (panel b in Figure 4.12). These transects show  $\sim 30 \mu\text{m}$  coarser surveys in summer (T4 and T6) than in winter (T3 and T5). In order to filter out the bias of the surveys (e.g. due to seasonality) it is therefore proposed to use the difference in the  $D_{50TR}$  between the coarsest and finest transect of each survey (respectively  $D_{50TRmax}$  and  $D_{50TRmin}$ ) with respect to the average  $D_{50TR}$  of each survey ( $\overline{D_{50TR}}$ ) as a proxy for the 'degree of alongshore heterogeneity' of the  $D_{50}$  ( $S_{alongshore}$ ). The  $S_{alongshore}$  is given by the following equation :

$$S_{alongshore} = \frac{D_{50TRmax} - D_{50TRmin}}{\overline{D_{50TR}}} \quad (4.3)$$

Long-term development of  $S_{alongshore}$  for transects B and D (i.e. finest and coarsest transect) shows a considerably enhanced degree of alongshore heterogeneity ( $S_{alongshore}$ ) compared to the natural alongshore variability in the T0 survey (Figure 4.13). This  $S_{alongshore}$  decreased slowly over time since the T3 survey ( $\sim 30 \mu\text{m}$  decrease per year).

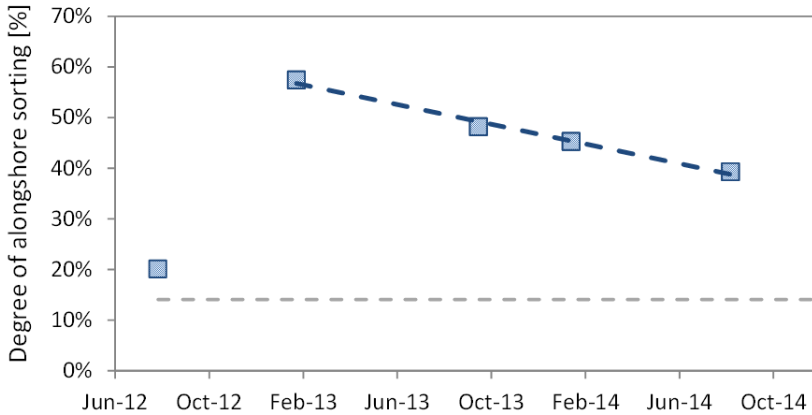


Figure 4.13: Time development of the degree of alongshore heterogeneity of the  $D_{50}$  ( $S_{alongshore}$ ) from the difference of transects B and D of surveys T2 to T6 [-] (with respect to  $\overline{D_{50TR}}$ ). The average natural alongshore variability of the  $D_{50TR}$  for all transects of the T0 survey is shown with the dashed grey line

#### 4.5. RELATION OF $D_{50}$ WITH BED SHEAR STRESSES

An inter-comparison was made of the alongshore heterogeneity of the  $D_{50}$  (using the transect-averaged  $D_{50TR}$ ) with monthly averaged bed shear stresses as a result of waves and currents ( $\bar{\tau}_{cw,mean}$  and  $\bar{\tau}_{cw,max}$ ) with the aim to investigate what hydrodynamic conditions (i.e. storm or normal conditions) are responsible for the observed large scale alongshore bed composition changes.  $\bar{\tau}_{cw,mean}$  is mainly influenced by the tide and moderate wave conditions, while the  $\bar{\tau}_{cw,max}$  is influenced predominantly by storm wave conditions. The typical summer and winter conditions are presented for October 2013 and February 2014 (i.e. T4 and T5 survey; Figure 4.14).

The largest bed shear stresses were present along the shoreline as a result of the waves and wave-induced longshore current, which is most evident for the more energetic February 2014 conditions ( $\bar{\tau}_{cw,max}$  in Figure 4.14d). Furthermore, a large area with enhanced bed shear stresses ( $\bar{\tau}_{cw,mean}$  ranging from 0.6 to 1 N/m<sup>2</sup>) was present in front of the Sand Motor as a result of tidal flow contraction (Figure 4.14a), which had a similar magnitude for both winter and summer conditions. This area extends approximately from MSL-13m till MSL-4m and has an alongshore extent of about 2 km.

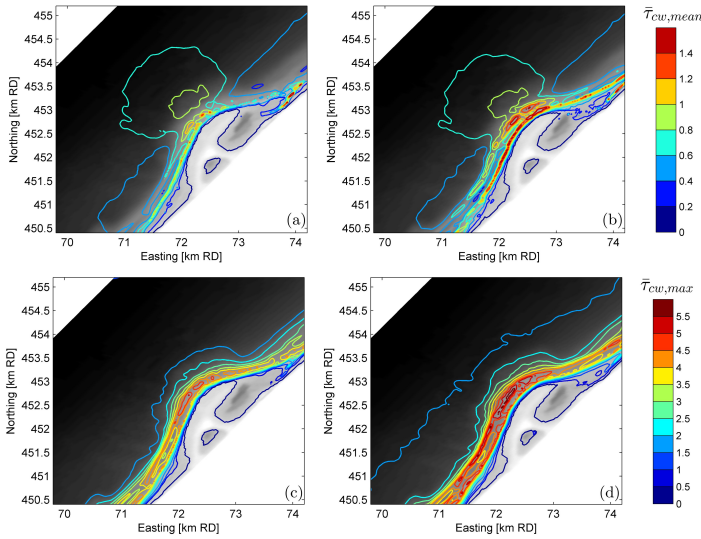


Figure 4.14: Mean and maximum bed shear stresses averaged over a month for October 2013 (T4) and February 2014 (T5). Panel a :  $\bar{\tau}_{cw,mean}$ (October 2013); Panel b :  $\bar{\tau}_{cw,mean}$ (February 2014) ; Panel c :  $\bar{\tau}_{cw,max}$ (October 2013); Panel d :  $\bar{\tau}_{cw,max}$ (February 2014)

The observed spatial pattern of the  $\bar{\tau}_{cw,mean}$  is considered qualitatively similar to the observed spatial  $D_{50}$  distribution at the Sand Motor (Figure 4.8). A positive relation between the transect-averaged mean bed shear stresses ( $\bar{\tau}_{cw,mean}$ ) and the transect-averaged median grain diameter ( $D_{50TR}$ ) was found for survey T4 (Figure 4.15,  $R^2 = 0.8$ ), while no correlation was found with the maximum bed shear stresses ( $\bar{\tau}_{cw,max}$ ). Note that the T4 survey is shown here since it has the most cross-shore transects (i.e. better alongshore resolution).

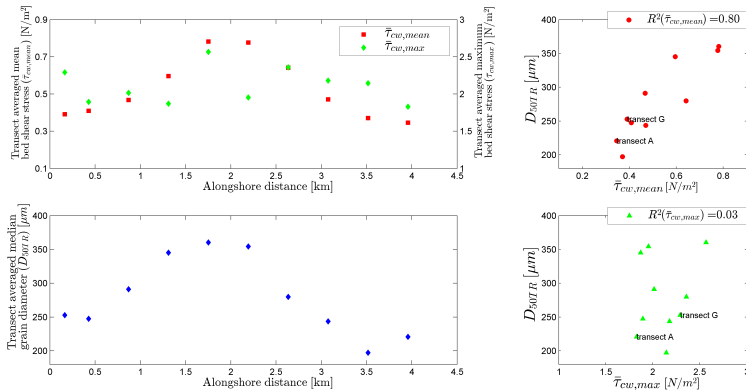


Figure 4.15: Inter-relationship between transect-averaged bed shear stress ( $\bar{\tau}_{cw,mean}$ ) and median grain diameter ( $D_{50TR}$ ) for the T4 survey transects. Top-left : Mean bed shear stress along the coast (using same alongshore distance reference as Figure 4.9). Lower-left :  $D_{50TR}$  along the coast. Top-right :  $\bar{\tau}_{cw,mean}$  versus  $D_{50TR}$ . Lower-right :  $\bar{\tau}_{cw,max}$  versus  $D_{50TR}$

Similar relations between  $D_{50TR}$  and transect-averaged bed shear stresses ( $\bar{\tau}_{cw,mean}$ ) were found for the other surveys (Figure 4.16). A positive correlation was found for surveys T3, T5 and T6 (respectively  $R^2$  respectively of 0.79, 0.65 and 0.64) and small correlation for the T2 survey ( $R^2$  of 0.3) which was preceded by a storm which followed a period with relatively quiet conditions. The correlation between  $\bar{\tau}_{cw,mean}$  and  $D_{50TR}$  suggests that enhanced hydrodynamic forcing conditions (due to tidal flow contraction) induce a mechanism which contributes to the development of the alongshore heterogeneity of the bed composition ( $D_{50TR}$ ) at the Sand Motor.

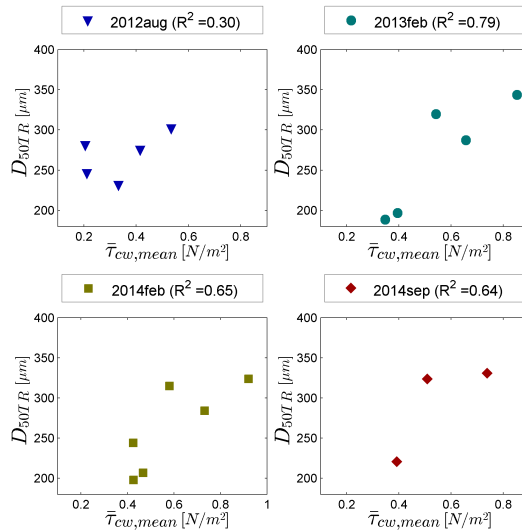


Figure 4.16: Inter-relation between transect-averaged bed shear stress ( $\bar{\tau}_{cw,mean}$ ) and median grain diameter ( $D_{50TR}$ ) for T2, T3, T5 and T6 surveys.

The local increase in the mean bed shear stresses ( $\bar{\tau}_{cw,mean}$ ) at the Sand Motor is considered a relevant driver for the generation of large-scale alongshore heterogeneity of the  $D_{50}$  at the Sand Motor peninsula on monthly to annual time scales. The locally higher potential to suspend sediment results in alongshore transport away from the Sand Motor which mainly consists of the finer sand fractions (referred to as 'preferential transport'). These finer sand fractions are mobilized more often than coarse sand fractions, because the thresholds for pick up of sand are more often exceeded as a result of the increased bed shear stresses. Van Rijn (1993) indicates a threshold value of  $\sim 0.4 \text{ N/m}^2$  for suspension of  $400 \mu\text{m}$  sand. This critical bed shear stress is in the range of the average shear stresses in deeper water (seaward of MSL-4m) of the Sand Motor (about  $0.4$  to  $1 \text{ N/m}^2$ ). The strong correlation of  $D_{50TR}$  with  $\bar{\tau}_{cw,mean}$  (which is dominated by the tidal current) suggests that the coarsening of the bed at the Sand Motor was influenced by a mechanism which coarsened the top-layer of the bed during normal conditions. The preferential transport of fine sand is expected to be responsible for coarsening in front of the Sand Motor peninsula from T1 to T3. The fining North and South of the Sand Motor is considered to be the result of the supply of relatively fine sand from the eroding sections of the Sand Motor.

A (partially) armored top-layer is expected to be present in front of the Sand Motor peninsula roughly between MSL-8m and MSL-13m as a result of the preferential transport/erosion of finer sand. This is in agreement with the observations of a narrower grain size distribution at the Sand Motor peninsula (standard deviation of the grain size distribution of  $\sim 0.5$  instead of 0.6 to 0.8 for the nourished material). The underlying substrate is, however, expected to be more poorly sorted as it is not yet affected by the hydrodynamic processes, which means that the fining of the Sand Motor during the October 22 storm (T6 survey) is most likely related to mixing of the top-layer sediment with the substrate. In short it is perceived that tidal flow contraction at the Sand Motor induces a mechanism of preferential transport which substantially affects the alongshore heterogeneity of the  $D_{50}$ .

## 4.6. DISCUSSION

A number of contributors for bed composition changes at the Sand Motor were identified on the basis of the survey results and hydrodynamic modelling. The main contributors are 1) preferential transport of finer sand fractions during moderate conditions, 2) mobilization of coarse sand fractions and cross-shore transport during storm events and 3) the initial disturbance of the bed composition during construction.

- I : Moderate conditions

Preferential transport of finer sand may take place during quiet and moderate wave conditions at the Sand Motor as a result of (tidal) flow contraction. This was shown from the strong correlation between the time-averaged mean bed shear stresses ( $\bar{\tau}_{cw,mean}$ ) and alongshore spatial heterogeneity of the  $D_{50}$  (Figure 4.15), which indicates that a mechanism is present during moderate conditions (mainly due to the tide) which considerably affects the development of the spatial heterogeneity of the  $D_{50}$ . The added sediment at the Sand Motor was similar to that of the surrounding coast, while the potential for mobilization was increased due to the tidal flow contraction at the peninsula. Consequently, the critical bed shear stresses for erosion of the fine fractions will be exceeded more frequently than for the coarser fractions, which results in a larger entrainment of the finer fractions in the water column (Komar, 1987) and enhanced alongshore transport rates (Steidtmann, 1982). For coasts with persistent erosion (i.e. larger outgoing than incoming flux of sediment), which is present at the large scale coastal disturbance of the Sand Motor, this will result in a coarsening of the bed in the coastal section with enhanced bed shear stresses and a fining of the bed at the adjacent coast where the flux of finer sand settles. The preferential transport of finer sand fractions will also be present when all fractions are mobilized, but it is expected to be strongest when the hydrodynamic forcing conditions are close to the critical bed shear stress of the considered sand fractions. On the basis of the observed gradual reduction of the  $S_{alongshore}$  (Figure 4.13) it is expected that the coarser bed composition at the Sand Motor will have a tendency to fade out over time. This is attributed to reduced tidal forcing conditions over time as a result of the smoothing of the morphology of the Sand Motor.

- II : Storm impact

Storm events can reduce the alongshore heterogeneity of the  $D_{50}$  at the Sand Motor, which is shown from the observed fining of the bed in the offshore zone during a severe storm condition (at 22 October 2014; T6 survey). This is in contrast with the coarsening of the bed (about  $30\ \mu\text{m}$  coarser  $D_{50}$ ) that was observed by Terwindt (1962) during a storm event. The changes in  $D_{50}$  of the bed at the Sand Motor also differed from observations by Stauble and Cialone (1996), who observed only nearshore coarsening of the  $D_{50}$  (landward of MSL-3m) and negligible changes in  $D_{50}$  at MSL-5m. These studies were, however, performed for natural coasts which lack the strong curvature of the coast and associated continuous erosion that is present at the Sand Motor. The observed finer  $D_{50}$  of the bed in deeper water as a result of the 22 October 2014 storm is expected to be related to high-wave conditions which mobilize all sand grains. This means that also the coarser bed material will be mobilized and distributed. Part of the armor layer may be removed resulting in exposure of (and mixing with) substrate layers and consequently in a relatively finer top-layer of the bed. This is especially of relevance in deeper water where more time is available to develop an armored bed during normal conditions (i.e. before high-energetic events mobilize the bed and partially remove the armoring). Additionally, storm events transport finer sediment in the offshore direction which will result in a coarsening of the (erosive) nearshore zone and a fining in deeper water at the toe of the storm deposition profile, as was observed in the wave flumes at the Großer WellenKanal (Broekema et al., 2016) and numerical modelling with Delft3D and Xbeach (Sirks, 2013; Reniers et al., 2013). Evidence of cross-shore transport of finer sand during storms was perceived to be present in the T2 survey for which a zone with relatively fine sand (i.e. 100 to  $200\ \mu\text{m}$ ) was observed at 4 to 8 meter water depth.

- III : Initial bed composition

A part of the observed alongshore heterogeneity of the  $D_{50}$  at the Sand Motor can be attributed to the initial disturbance of the bed sediment during construction (e.g. coarser sand applied locally or as a result of suspension sorting). The sediment used for construction ( $278\ \mu\text{m} \pm 60\ \mu\text{m}$ ) was significantly coarser than the bed composition of the T0 survey ( $\sim 220\ \mu\text{m}$ ). However, the gradual coarsening of the  $D_{50\text{TR}}$  at the Sand Motor peninsula in the first two years after construction (from  $278\ \mu\text{m}$  at T1 to 300 to  $400\ \mu\text{m}$  at T4) indicates that the development of alongshore heterogeneity of the  $D_{50}$  was affected considerably by the hydrodynamic sorting processes. An exact estimate of the contribution of the initial bed composition changes during construction cannot be given on the basis of the data alone, since T1 samples were only taken at the dry beach. It may require extra data of the initial bed composition at future large-scale coastal measures and/or well validated numerical modelling to further improve understanding on the initial bed composition as a result of dredging and nourishing activities.

It is recognized that sediment sampling and methodology for determining the grain size distribution may affect the measured  $D_{50}$  at the Sand Motor. For example, the application of the Van Veen grabber inherently means that only the first five to ten



centimeters of the bed sediment are sampled. Consequently, the underlying assumption in the interpretation is that a sufficiently thick layer of rather homogeneous sediment is present at the sample location. This does, however, seem like a realistic condition for a large-scale sand nourishment with persistent and steady patterns of erosion and sedimentation. The impact from the methodology for determining the grain size distribution was expected to be small for the current studies, since the current study focuses mainly on the median grain diameters ( $D_{50}$ ) which are shown to be better correlated for the different analysis techniques (Laser diffraction or sieving) than derived properties of the grain size distribution like Skewness and Kurtosis (Rodríguez and Uriarte, 2009; Murray and Holtum, 1996). Moreover, the observed changes over time were more considerable than the uncertainty in the analysis methodology, as derived from a data set of mechanically sieved samples and corrected Laser diffraction samples.

The observed development of alongshore heterogeneity of the  $D_{50}$  at the Sand Motor is considered a relevant mechanism which may also act at other large scale coastal measures which induce an increase in the hydrodynamic forcing conditions (e.g. due to tidal contraction). The  $D_{50}$  of the bed is likely to coarsen as a result of the new situation with enhanced bed shear stresses, which is even the case when nourishment sand with similar properties as the natural sediment is applied. The alongshore heterogeneity of the  $D_{50}$  at large-scale coastal measures, such as the Sand Motor, is expected to have a considerable impact on long-term morphological changes and ecological habitats of marine fish and benthos. It is envisaged that the long-term morphological changes of the Sand Motor are slowed-down by the coarsening of the bed at the exposed coastal sections due to reduced sediment transport of the coarser sand. Initial morphological changes, on the other hand, may have been enhanced as a result of the initially large erosion rates of the fine sand fractions (i.e. compared to the situation with a very narrow grain size distribution). Ecological impact is expected from the coarsening of the bed at the Sand Motor peninsula and fining of the bed at the adjacent coast. The actual impact differs per species and may either be beneficial or adverse (Alexander et al., 1993; McLachlan, 1996). For example, the coarsening of the bed at the Sand Motor may limit the body size of marine species and burrowing ability of juvenile Plaice (Gibson and Robb, 1992), while an improvement of the habitat suitability may be expected at the adjacent coast where sediment is finer. Given above considerations, it is considered relevant to account for bed composition changes in the environmental impact assessments of future large-scale coastal measures.

## 4.7. CONCLUSIONS

Bed sediment composition ( $D_{50}$ ) was surveyed and analysed at the large-scale 'Sand Motor' nourishment at the Dutch coast (~21.5 million m<sup>3</sup> sand) which is a large scale coastal perturbation which experiences continuous erosion. Significant spatial heterogeneity of the bed composition ( $D_{50}$ ) was observed, which consisted of a coarsening in front of the Sand Motor peninsula of +90 to +150  $\mu\text{m}$  and a fining of the sediment just north and south of the Sand Motor up to 50  $\mu\text{m}$  (referred to as 'alongshore heterogeneity of  $D_{50}$ '). Most pronounced alongshore heterogeneity of  $D_{50}$  was observed in

deeper water outside the surfzone (seaward of MSL -4m).

Spatial heterogeneity of the  $D_{50}$  can be induced by hydrodynamic forcing conditions at any large-scale coastal intervention which is sufficiently large to substantially affect the hydrodynamics of the tide. Alongshore spatial heterogeneity of the transect-averaged median grain size ( $D_{50TR}$  of coarsest and finest transect) was found to be strongly inter-related with the hydrodynamic forcing conditions as a result of the tide (i.e. time-averaged mean bed shear stresses). Preferential transport of finer sediment is a relevant mechanism for the coarsening of the bed at large scale coastal measures. The locally enhanced tidal forces mobilize in particular the finer sand fractions, while medium and coarse sand grains are hardly mobilized. The finer sediment is then transported to the adjacent coast. A requirement for this mechanism of preferential transport of finer sand fractions is a persistent pattern of erosion at the considered large-scale coastal measure, which means that the outgoing sediment flux exceeds the incoming flux of sand.

Storm conditions may reduce the coarsening of the bed in deeper water (i.e. outside the surfzone) for regions with enhanced bed shear stresses. This is the result of a mobilization of all of the bed sediment size fractions during storms and exposure of relatively fine substrate material as a result of the erosion. Additionally, storms may generate a cross-shore flux of finer sand from the surfzone to deeper water.

## APPENDIX A : COMPUTATION OF BED SHEAR STRESSES

Bed composition changes ( $D_{50,TR}$ ) at the Sand Motor are related either to the forcing conditions of the (tidal) currents or (storm) waves. For this purpose, the mean and maximum bed shear stresses as a result of combined waves and currents ( $\tau_{cw,mean}$  and  $\tau_{cw,max}$ ) are used as a proxy for respectively the net hydrodynamic force of the local currents and the maximum forcing as a result of the wave orbital motion. The combined contribution of waves and currents ( $\tau_{cw,mean}$  [ $N/m^2$ ]) is computed as follows according to Soulsby et al. (1993) :

$$\tau_{cw,mean} = Y(\tau_C + |\tau_W|) \quad (4.4)$$

Where  $\tau_C$  and  $\tau_W$  represent the current and wave related bed shear stress [ $N/m^2$ ]. The mean bed shear stress reduction factor ( $Y = X[1 + bX^p(1 - X)^q]$ ) is computed from the ratio of current and wave related bed shear stress ( $X = \tau_C / (\tau_C + \tau_W)$ ). Wave current-interaction coefficients b,p,q are set according to Van Rijn et al. (2004). The current related shear stress is computed on the basis of the average current velocity and friction with the bed.

$$\tau_C = \frac{1}{8} \rho_w f_c \vec{U} |\vec{U}| = \frac{\rho_w g \vec{U} |\vec{U}|}{C_{2D}^2} \quad (4.5)$$

With  $\rho_w$  the density of the water [ $kg/m^3$ ],  $g$  the acceleration of gravity [ $m/s^2$ ],  $f_c$  the dimensionless friction factor of Darcy-Weisbach,  $\bar{U}$  the depth averaged current velocity [ $m/s$ ] and  $C_{2D}$  the Chezy coefficient [ $m^{1/2}/s$ ]. The wave related bed shear stress ( $\tau_W$ ) is computed as follows :

$$\tau_W = \frac{1}{4} \rho_w f_w (U_{\delta,r}^2) \quad (4.6)$$

With  $U_{\delta,r}$  the orbital velocity of the waves [ $m/s$ ] according to Isobe and Horikawa (1982) and  $f_w$  the friction coefficient for waves [ $m$ ]. The friction factor for wave induced flow depends on the peak orbital excursion of the waves at the edge of the wave boundary layer ( $A_\delta$ ) and the bed form induced roughness ( $k_{s,w,r}$ ) which is related to the flow regime (e.g. sheet-flow or ripple regime; Van Rijn et al., 2004).

$$f_w = \exp\left(5.2 \left(\frac{A_\delta}{k_{s,w,r}}\right)^{-0.19} - 6\right) \quad (4.7)$$

Similar to the mean bed shear stress ( $\tau_{cw,mean}$ ) also the maximum bed shear stress ( $\tau_{cw,max}$ ) is computed :

$$\tau_{cw,max} = Z(\tau_C + |\tau_W|) \quad (4.8)$$

With maximum bed shear stress reduction factor ( $Z = 1 + aX^m(1 - X)^n$ ) and  $a, m$  and  $n$  as the wave current interaction coefficients (Soulsby et al., 1993).

## APPENDIX B : WIDTH AND SKEWNESS OF THE DISTRIBUTION

Graphical sample standard deviation ( $\sigma_I$ ) and graphical skewness ( $Sk_I$ ) of the grain size distribution (Folk and Ward, 1957) were computed as follows from the  $\phi$  values of the sediment (i.e.  $\phi = -\log_2(D)$ , with  $D$  as the grain diameter in millimeters).

$$\sigma_I = \frac{\phi_{84} - \phi_{16}}{4} + \frac{\phi_{95} - \phi_5}{6.6} \quad (4.9)$$

$$Sk_I = \frac{\phi_{16} + \phi_{84} - 2 \cdot \phi_{50}}{2(\phi_{84} - \phi_{16})} + \frac{\phi_5 + \phi_{95} - 2 \cdot \phi_{50}}{2(\phi_{95} - \phi_5)} \quad (4.10)$$

These derived properties can provide insight in the processes that were driving the bed composition changes. An overview of the observed graphical standard deviation ( $\sigma_I$ ) and skewness ( $SK_I$ ) of the grain size distribution are provided in [Figure 4.17](#) and [Figure 4.18](#).

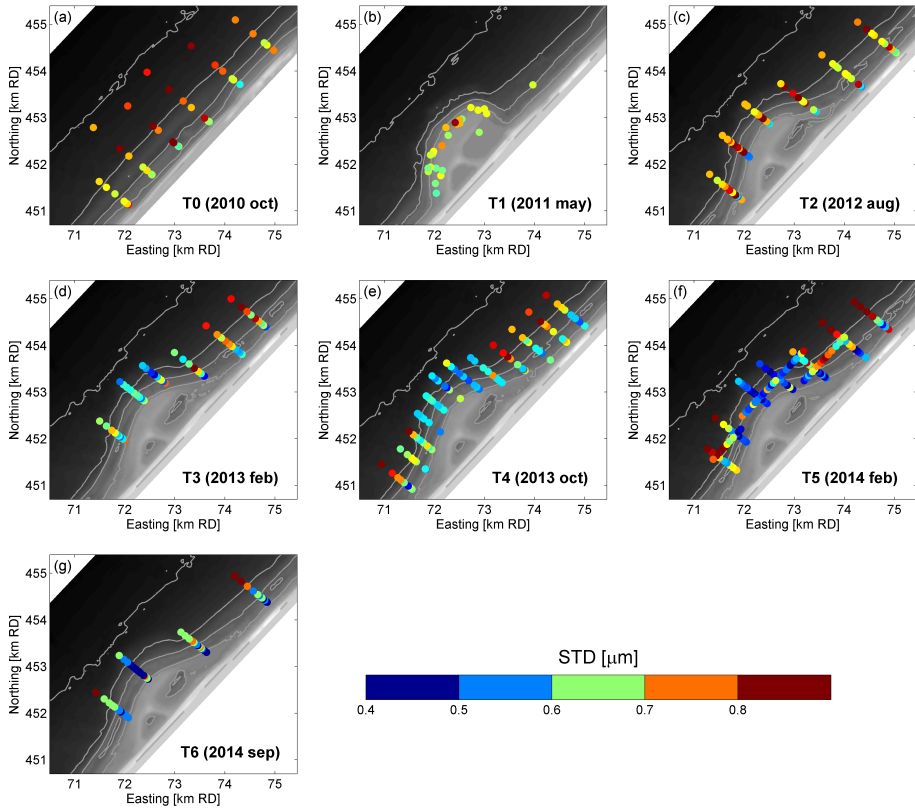


Figure 4.17: Standard deviation of sediment samples for T0 to T6 measurement surveys (blue colors indicate better sorted sand and red colors more poorly sorted sand)

The reference survey samples (T0) and original nourished material (T1) were moderately sorted to moderately well sorted (i.e.  $\sigma_I$  ranging from 0.6 to 0.8). This is in contrast with the situation from survey T3 onwards, which shows considerable spatial variability in the width of the grain size distribution ( $\sigma_I$ ). This spatial variability comprised a relatively narrow grain size distribution (i.e.  $\sigma_I$  of 0.4 to 0.6) at the center transect of the Sand Motor and more poorly sorted sand (i.e.  $\sigma_I$  of 0.7 to 0.9) in deeper water (from MSL -5m to MSL -10m) at the adjacent coast North and South of the Sand Motor. Noticeable is that the 10th weight percentile of the grain size ( $D_{10}$ ) at the center transect of the Sand Motor (transect D) has coarsened significantly after construction of the Sand Motor (from 124  $\mu\text{m}$  in the reference situation to  $\sim 220 \mu\text{m}$  from T3 survey onwards at transect D and E), which is an indication for sorting of the sediment by the transport processes (McLaren and Bowles, 1985; Masselink, 1992).

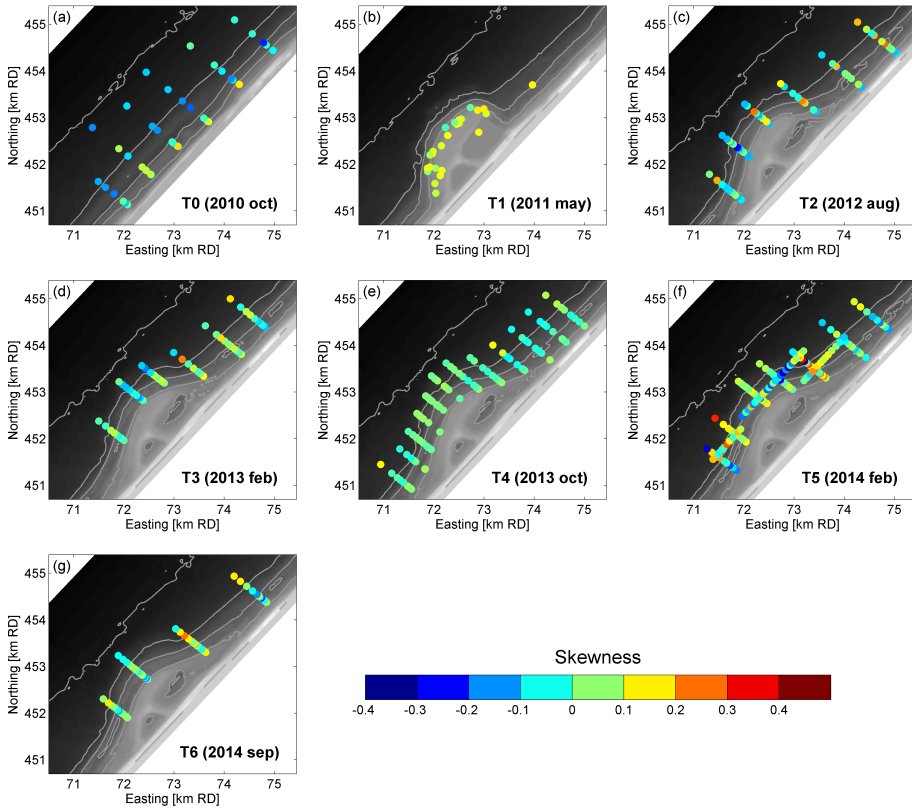


Figure 4.18: Graphical skewness of sediment samples for T0 to T6 measurement surveys (red indicates fine skewed sand; blue indicates coarse skewed sand)

Graphical skewness ranged from fine skewed to coarse skewed ( $Sk_I$  of -0.2 to +0.2) for the T0 survey (Figure 4.18) and was generally smaller in deeper water than near to the shoreline. Samples with an excess of fines were found landward of MSL -3m for the T0 survey. After construction of the Sand Motor some of the deep water sample locations of the T3 to T5 surveys were fine skewed to very fine skewed, which was typically the case for depositional areas where fine sand and silt from the Sand Motor accumulated.

Short-term temporal variability of the graphical standard deviation of the grain size distribution ( $\sigma_I$ ) was small during the T6 survey (Figure 4.19). The  $\sigma_I$  of the bed at the sub-tidal bar was  $\sim 0.4$  and increased in landward direction to  $\sim 0.8$  in the bar trough and in seaward direction to  $\sim 0.6$  at MSL -10m. Similarly, the temporal variability of the observed graphical skewness ( $Sk_I$ ) was also small. Only after the storm condition a more coarse skewed grain size distribution was observed in the bar trough ( $Sk_I \sim -0.2$ ) and a fine skewed distribution ( $Sk_I \sim +0.2$ ) at MSL -6m to MSL -8m.

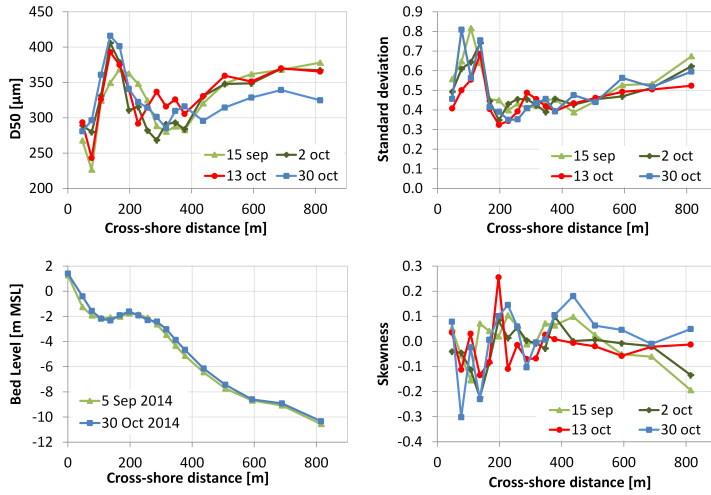


Figure 4.19: Median grain diameter ( $D_{50}$ ), graphical standard deviation ( $\sigma_I$ ), graphical skewness( $Sk_I$ ) and bed level for T6 measurement survey at transect D (i.e. center of Sand Motor)

### APPENDIX C : TRANSECT-AVERAGED MEDIAN GRAIN SIZE

The transect-averaged median grain diameters ( $D_{50TR}$ ) were computed for each of the transects from the waterline up to MSL -10m (Table 4.2). Additionally, also the median grain diameters were computed for the surfzone landward of MSL-4m ( $D_{50TR,NS}$ ) and the less active offshore part of the cross-shore profile ( $D_{50TR,OFF}$ ). Note that an average of nearby transects was used for some of the transects of surveys T0, T2 and T4 that did not exactly align with the transect positions of the T5 survey transects (A to G).

Table 4.2: Average median grain diameter per transect ( $D_{50TR}$ ) and differentiated for the zone seaward and landward of the MSL-4m ( $D_{50TR,OFF}$  and  $D_{50TR,NS}$ ) of the T0 to T6 surveys at the Sand Motor.

Transect	T0			T2			T3			T4			T5			T6		
	oct 2010			aug 2012			feb 2013			oct 2013			feb 2014			oct 2014		
	$D_{50TR}$			$D_{50TR}$			$D_{50TR}$			$D_{50TR}$			$D_{50TR}$			$D_{50TR}$		
	avg	OFF	NS	avg	OFF	NS	avg	OFF	NS	avg	OFF	NS	avg	OFF	NS	avg	OFF	NS
A	227	226	241	353	354	349	251	254	232	273	288	232	241	229	304	262	268	242
F	208	207	224	281	289	269	197	183	255	221	201	306	198	188	246			
B	231	210	285	245	233	264	189	162	288	220	201	282	207	175	284	220	183	309
C							287	276	330	280	289	261	284	281	289	268	248	275
D	216	200	304	302	305	296	343	347	333	354	359	345	324	327	319	331	338	320
E	226	220	263	267	293	205	320	320	320	321	318	327	315	323	302	323	328	315
G	214	204	239	246	243	253				248	205	347	244	195	340			
AVG*	220	211	260	282	286	273	264	257	293	275	266	304	259	245	298	281	273	292

\* Weighted average of all transects

# 5

## MODELLING SORTING PROCESSES

\* *The relevance of hydrodynamic conditions (e.g. horizontal tide and waves) for bed composition changes at the lower shoreface of the Sand Motor and driving sediment sorting processes was investigated using numerical modelling. A 3D multi-fraction morphological model was used to hindcast 2.5 years of observed spatial and temporal changes in  $D_{50}$  at the Sand Motor, which provided a good representation of the observed spatial pattern of  $D_{50}$  independent of the initial condition for the  $D_{50}$  of the bed. The alongshore variation of the  $D_{50}$  in both the 2DH and 3D models correlated significantly with the measurements ( $R^2$  of 0.84 to 0.94), but the observed cross-shore  $D_{50}$  variation was only represented well in the 3D model. The model computations showed that mild to moderate wave conditions at the lower shoreface can easily suspend the fine sand fractions, while the coarser sand fractions are hardly entrained, which was the main cause of the observed bed composition changes at the lower shoreface. Furthermore, the model shows that the extent and magnitude of the coarsening of the bed in front of the Sand Motor peninsula are related to the tidal contraction by the coastal measure which implies that large-scale bed composition changes can take place at any coastal structure which has a considerable impact on the tidal currents.*

### 5.1. INTRODUCTION

Spatial heterogeneity of bed sediment composition is observed at many coasts around the world (Holland and Elmore, 2008), but seldom accounted for in morphological or environmental impact studies of coastal interventions (e.g. modelling of sand nourishments; Capobianco et al., 2002). Knowledge of the potential spatial variability of the bed sediment (i.e. grain size and grading) is however considered essential for the understanding of the ecological impact of large-scale coastal interventions. Firstly, bed composition changes affect the ecological habitats for benthic species and fish (e.g. McLachlan, 1996; Knaapen et al., 2003). Small changes in the top-layer grain size can,

---

\*This chapter is based on the publication: Huisman, B.J.A., Ruessink, B.G., De Schipper, M.A., Luijendijk, A.P. and Stive, M.J.F. (2018). Modelling of bed sediment composition changes at the lower shoreface of the Sand Motor. *Coastal Engineering*, 132:33-49

for example, significantly affect the burrowing ability of juvenile plaice (Gibson and Robb, 1992). Secondly, long-term morphological changes are affected by bed coarsening when preferential transport of finer sand fractions takes place at large-scale sand nourishments (Van Rijn, 2007c; see [chapter 4](#)).

Spatial heterogeneity of the bed composition of natural coasts is characterized by a fining of sediment grain size in the offshore direction with coarsest sediment being found in the swash zone (Inman, 1953; Sonu, 1972; Liu and Zarillo, 1987; Pruszk, 1993; Horn, 1993; Stauble and Cialone, 1996; Kana et al., 2011). In the presence of sub-tidal bars the spatial pattern of the bed sediment composition can vary between different studies. Generally, coarser sediment is observed in the bar troughs and finer sediment on bar crests (Moutzouris et al., 1991; Katoh and Yanagishima, 1995), but Van Straaten (1965) and Guillén and Hoekstra (1997) observed coarser material on the bar crests for the Dutch coast. Considerable spatial heterogeneity of the sediment grain size is also observed at rip-bar systems with coarser sediment in the rip-channels (MacMahan et al., 2005; Gallagher et al., 2011; Dong et al., 2015). Coarsening of the bed (change in median grain diameter  $D_{50}$  of about  $+150 \mu\text{m}$ ) as a result of alongshore transport processes was observed at a large-scale sand nourishment at the Dutch coast ('The Sand Motor'). This study also showed that the alongshore changes in  $D_{50}$  are related to spatial variability in the hydrodynamic forcing conditions.

5

The impact of storm conditions at natural coasts consists of a coarsening of the sediment grain size. Most prominent coarsening of the median grain diameter ( $D_{50}$  up to  $100 \mu\text{m}$  coarser) during a storm event with offshore significant wave height of  $H_{m0} = 4 \text{ m}$  was observed in the swash zone (Stauble and Cialone, 1996). This coarsening gradually decreases in the offshore direction. Terwindt (1962) observed a quite uniform coarsening of  $\sim 30 \mu\text{m}$  from 2 to 6 meter water depth at the coast of Katwijk (The Netherlands) after a moderate summer storm ( $H_{m0} \approx 2\text{m}$ ). Numerical modelling of cross-shore transport sorting during storms also shows coarsening of the nearshore zone and subsequent fining of the offshore sediment at the toe of the deposition profile (Reniers et al., 2013; Sirks, 2013; Broekema et al., 2016). Seasonal variability of the cross-shore distribution of the grain size, as observed by Medina et al. (1994), comprised nearshore bed composition coarsening in winter ( $H_{m0,winter} \approx 4\text{m}$ ) and restoration to a finer bed composition in summer ( $H_{m0,summer} \approx 1\text{m}$ ). The largest annual variability in the measured  $D_{50}$  was observed in the swash zone (up to  $200 \mu\text{m}$ ) at mean sea level (MSL) which gradually decreased to a variability of  $\sim 20 \mu\text{m}$  at MSL -8 m. Seasonal variability of the  $D_{50}$  was, however, found to be almost negligible for a nourishment at the Dutch barrier island of Terschelling (Guillén and Hoekstra, 1996). Guillén and Hoekstra (1996) observed an 'equilibrium distribution' of the size fractions, which means that the cross-shore bed composition of each size fraction will be restored over time by the hydrodynamic processes to the natural equilibrium situation. An influence of the width of the littoral zone (which depends on the wave conditions) on the location of transitions in the cross-shore grading of the sediment was suggested by Guillén and Hoekstra (1997).

Spatial variability of the grain size (on cross-shore profiles or alongshore) is often the



result of differences in the behaviour of sediment grain size fractions for the same hydrodynamic forcing conditions (e.g. for bi-modal sand in Richmond and Sallenger, 1984). Sorting processes at the scale of the sediment grain can induce sorting mechanisms of which settling, entrainment and transport sorting are considered most relevant (Slingerland and Smith, 1986). Sorting due to settling, for example, plays a role in sedimentary environments where fine grains are deposited over a much larger distance than the coarse grains (Baba and Komar, 1981). Entrainment sorting is the result of differences in the suspension of sediment grain particles into the water column, which is affected by the size and weight of the particle (Komar, 1987) as well as the density of the grains (Steidtmann, 1982). Investigations on the critical limit for suspension of the sediment into the water column were made by Bagnold (1966) (and other researchers) who indicates that the 'initiation of suspension' is related to the shear velocity at the bed ( $u_*$ ) and the fall velocity ( $w_s$ ) of the sediment particle (see also Van Rijn, 1993). The finer sediment, that is suspended higher up in the water column (Rouse, 1950), is typically advected over a longer distance by the currents. The availability of the size fractions in the bed is also of relevance for the transport sorting as it determines the (reference) concentrations. These sorting processes may act together and induce a 'preferential transport' of (fine) sediment size fractions at locations where substantial gradients in the hydrodynamic forcing conditions are present. Hiding and exposure mechanisms (i.e. hiding of fine grains and exposure of coarse grains; Egiazaroff, 1965; Ashida and Michiue, 1973), on the other hand, may reduce the preferential transport for conditions which are at (or very close to) the critical shear stress for mobility of the sediment mixture. The individual sediment size fractions in the sand mixture (in unilateral flows) are then expected to behave similarly as they are mobilized at the same critical shear stress (Wilcock, 1993). Conditions in the marine environment are, however, typically above the mobility threshold and closer to the critical limit for initiation of suspension as a result of wave stirring (e.g. Holland coast; see [chapter 4](#)).

The modeling of changes in bed sediment composition can be performed either with data-driven models or numerical models. Data driven models use observed knowledge on the sediment distribution at the considered coast to derive the transport processes and/or predict future changes in bed composition. For example, Guillén and Hoekstra (1996) introduced the concept of an equilibrium cross-shore distribution of sediment size fractions for a beach at Terschelling (The Netherlands). Any change to the cross-shore distribution of a size fraction will result in a redistribution of sediment until the equilibrium cross-shore distribution is restored (Guillén and Hoekstra (1996)). McLaren and Bowles (1985) proposed a method to track the transport direction of (graded) sediment on the basis of spatial differences in the sediment grading. The derived properties of the grading (i.e. mean size, standard deviation and skewness) change in a logical way along the transport path. Other studies, however, suggest that only a better sorting provides a consistent proxy for the pathways of the sediment (Gao and Collins, 1992; Masselink, 1992).

Numerical models (e.g. Delft3D; Lesser et al., 2004) are more suitable than data-driven models for investigating situations where a local equilibrium is not available. Sedi-

ment transport rates and bed composition changes are computed per sediment size fraction on the basis of the forcing conditions in the numerical models (Van Rijn, 2007c). Typically an administration of bed composition changes is applied for a discrete number of layers of the bed (Ribberink, 1987). The capability of numerical modelling of sediment transport with multiple size fractions was shown, for example, by Van Rijn (1997a) for cross-shore sorting during storms. Furthermore, numerical modelling of sediment sorting was successfully validated against field and laboratory experiments for a river bifurcation in the Netherlands (Sloff and Mosselman, 2012) and detailed sorting at river dunes (Blom and Parker, 2004). Even the generation of river deltas was modelled by Geleynse et al. (2011) who found that models could reproduce the typical plan-form shapes of river deltas which depends both on the supply of sediment and local hydrodynamics. Applications of numerical modelling of the redistribution of non-uniform sediment are, however, missing for sand nourishments at natural coast where a large influence of alongshore redistribution of sediment can be expected.

## 5

The objective of this work is to assess the relevance of hydrodynamic conditions for the development of heterogeneity in  $D_{50}$  at mega nourishments and the differences in transport paths of sediment size fractions. This required a validation of the numerical model Delft3D against observed spatial and temporal changes in  $D_{50}$  over a period of 2.5 year after construction of the large-scale 'Sand Motor' nourishment (Stive et al., 2013). Simplified hydrodynamic conditions were then used in the model to exemplify the influence of individual conditions.



Figure 5.1: Aerial photograph of the Sand Motor after completion (September 2011). Note the clouds of fine-grained material moving to the North. Picture courtesy of Rijkswaterstaat / Joop van Houdt

## 5.2. STUDY AREA

The study area is located between Monster and Kijkduin on the southern part of the Holland coast (the Netherlands). A large-scale sand nourishment referred to as the 'Sand Motor' was constructed here from April to June 2011 (~21.5 million cubic meters; Stive et al., 2013). The plan-form design of the Sand Motor comprised of a hook-shape with a dune lake and open lagoon on the landward side (Figure 5.1) with an alongshore extent of about 2.5km and a cross-shore width of about 1 km at the water-line. The foot of the nourishment attaches to the natural bed at a depth of about 10 meters.

Bathymetric changes after construction of the Sand Motor were monitored at 1 to 3 month intervals. In the first period after completion a large morphological response of the Sand Motor was observed (De Schipper et al., 2016), as about 1.8 million  $m^3$  of sand was spread alongshore. The initial blunt shape was reformed in a smooth plan-form shape (see Figure 5.2). The nearshore bathymetry at the Sand Motor is characterized either by sections with a longshore uniform bar-trough system or transverse bars (Rutten et al., 2017).

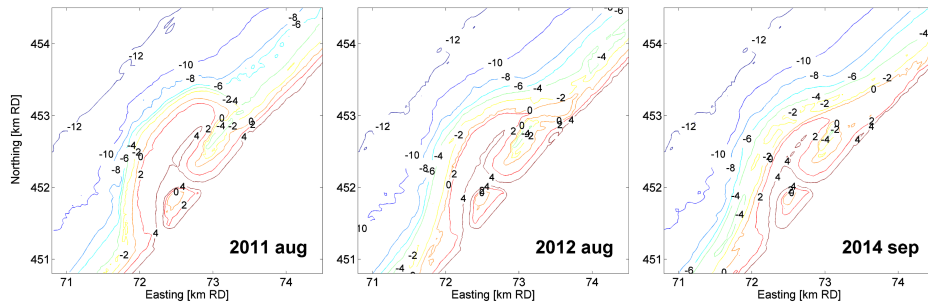


Figure 5.2: Sand Motor bathymetry directly after construction, after 1 year and after 3 year (bed level with respect to mean sea level).

The Holland coast wave climate is characterized by wind waves which originate either from the South-West (i.e. dominant wind direction) or the North-West (i.e. direction with largest fetch length). The average significant wave height ( $H_{m0}$ ) is about 1 meter in summer and 1.7 meter in winter (Wijnberg, 2002) with typical winter storms with wave heights ( $H_{m0}$ ) of 4 to 5 meter and a wave period of about 10 seconds (Sembiring et al., 2015). The severest storms originate from the North-West and coincide with a storm surge of 0.5 to 2 meter. Offshore wave data are available at an offshore platform ('Europlatform') at 32 m water depth. The horizontal tide is asymmetric with largest flow velocities towards the North during flood (~0.7 m/s) and a longer period with ebb-flow in southern direction (~0.5 m/s; Wijnberg, 2002). The tidal wave at this part of the North Sea is a progressive wave with largest flood velocities occurring just before high water. Tidal flow velocities at the Sand Motor are enhanced as a result of contraction of the flow (Radermacher et al., 2015). Mean bed shear stresses as a result of currents and waves ( $\tau_{cw}$ ) in the nearshore region of the Holland coast typically range from 0.1 to 10  $N/m^2$  (see chapter 4) which is an order of magnitude larger than

the critical threshold for mobilization of the grains ( $\tau_{crit}$  of about  $0.04 \text{ N/m}^2$  for sand with a  $D_{50}$  of  $300 \mu\text{m}$ ). The shear stresses in deeper water may, however, be insufficient to fully suspend all sediment grain size fractions in the water column during normal conditions (i.e. less than  $0.4 \text{ N/m}^2$  for  $300 \mu\text{m}$  sand; Van Rijn, 1993).

Sediment sampling at the Sand Motor nourishment revealed large spatial heterogeneity of the  $D_{50}$  which developed after construction (see [chapter 4](#)). Sediment data at the Sand Motor were collected prior, during and (half) yearly after construction of the Sand Motor over a time-frame of 4 years (see [Figure 5.3](#)). Surfzone sediment samples were collected with a Van Veen grab and dry beach samples from land. The Van Veen grab sampler had a radius of about 15 cm and collects sediment from the top 5 to 10 cm of the bed. Typically, about 5 to 12 samples were taken for each transect between MSL-1m and MSL-10m and a few samples on the dry beach. A special survey with short-term (bi-weekly) changes of the bed composition was performed in October 2014.

5

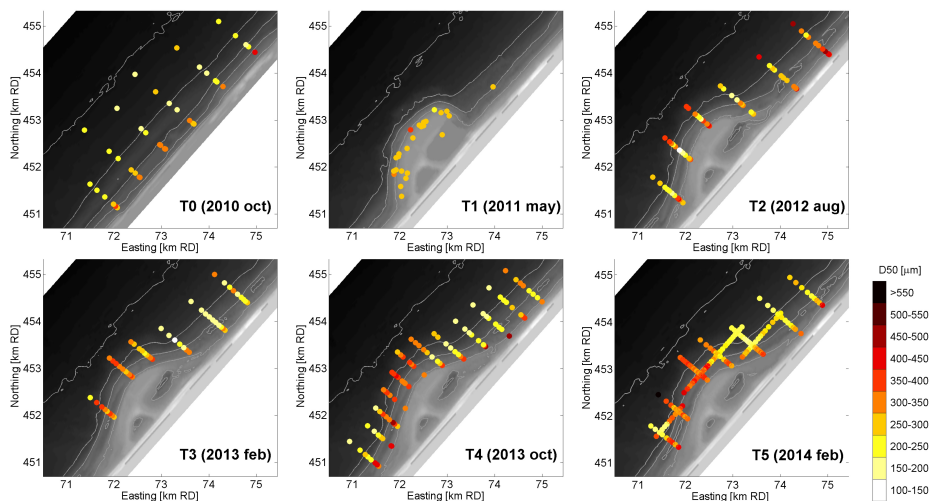


Figure 5.3: Median grain diameter of sediment samples for  $T_0$  to  $T_5$  surveys

The situation before construction of the Sand Motor ( $T_0$ ) was characterized by medium sand at the waterline ( $D_{50}$  of  $300$  to  $400 \mu\text{m}$ ; see [chapter 4](#)) which gradually fines in seaward direction to a  $D_{50}$  of about  $200 \mu\text{m}$  at MSL -7m and deeper (Van Straaten, 1965; see  $T_0$  situation in [Figure 5.3](#)). Dry beach and dune sediment generally consists of medium sand ( $200$  to  $300 \mu\text{m}$ ; Kohsiek, 1984). Nourished sediment ( $T_1$ ) was relatively uniform and well mixed with an average  $D_{50}$  of  $278 \mu\text{m}$ . The situation after construction of the Sand Motor ( $T_2$  and onwards) is characterized by significant coarsening of the bed sediment at the exposed part of the Sand Motor ( $\sim 150 \mu\text{m}$ ) and fining of the bed sediments just North and South of the Sand Motor (up to  $-50 \mu\text{m}$ ). This pattern was most clear from  $T_3$  survey onward ([Figure 5.3](#)), while a band with finer sediment was observed in the  $T_2$  survey between MSL -4m and MSL -8m. The  $T_2$  survey is, however, left out of consideration in this research as it deviated considerably from the

other surveys as a result of a storm which preceded the measurements (see [chapter 4](#)). A narrower grain size distribution was observed at the Sand Motor with a standard deviation (STD) of 0.4 to 0.6 after construction while the reference situation and nourished sediment were moderately well sorted (i.e. STD ranging from ~0.6 to 0.8). Note that this research uses kilometer marks to describe cross-shore profile sections at the 'Center of the Sand Motor Peninsula' (km 7), 'Northern flank' (km 8) and 'North of the Sand Motor' (km 9).

### 5.3. METHODOLOGY

The evolution of the bed composition at the Sand Motor was investigated with the aid of the numerical model Delft3D (Lesser et al., 2004). A 2.5 year hindcast of the bed sediment composition changes at the Sand Motor (with a focus on  $D_{50}$ ) was made, which was validated against observed  $D_{50}$  from sediment sampling surveys at the Sand Motor (see [chapter 4](#)). The computed bed composition changes over the hindcast period were used to provide insight in the transport rates for each of the sediment size fractions and vertical grading of the bed. The relevance of the hydrodynamic forcing conditions (i.e. tide and waves) for the development of heterogeneity in the  $D_{50}$  was then further investigated in models with simplified hydrodynamic conditions.

#### NUMERICAL MODEL SETUP

The Delft3D model (Lesser et al., 2004) uses the shallow water equations for 2DH and 3D computations of the flow and a wave energy transport model (SWAN) for the wave transformation towards the shore (Booij et al., 1999). The curvi-linear grid covers the southern section of the Holland coast (9 km in alongshore direction and 4 km in cross-shore direction) with a resolution of about 34m x 17m near to the Sand Motor ([Figure 5.4](#)). The initial Sand Motor bathymetry, as measured directly after construction of the Sand Motor on 3 August 2011, was used as a starting point for the numerical models. Both 2DH and 3D modelling approaches were applied (with 12 vertical layers for the 3D model). Measurements from a wave buoy and two ADCP stations were available for validation of the modelled hydrodynamics.

Flow boundary conditions were derived from the CoSMoS model (Sembiring et al., 2015; Barnard et al., 2014) which provides continuous forecasts of the tidal currents and water levels in the North Sea. The water level boundary condition was applied at the seaward boundary of the model, while tidal currents were included as a water level gradient (i.e. Neumann type boundary) at the lateral boundaries. Offshore wave boundary conditions consisted of a full time-series of wave conditions at the 'Europlatform' measurement station from August 2011 to February 2014 ([Figure 5.4](#)). The roller model (Roelvink, 1993a) was applied to distribute turbulence of the breaking waves over the surfzone.

Sediment transport was computed for predefined discrete size fractions (Van Rijn, 2007c) with the Transpor2004 formulation (Van Rijn et al., 2004; Van Rijn, 2007b). The reference concentrations of each of the size fractions are scaled according to their relative occurrence to make the transport rates of a sediment with multiple size fractions

comparable to uniform sediment (Van Rijn et al., 2004). This formulation performed well in the morphological hindcast of the first year development of the Sand Motor (Luijendijk et al., 2017).

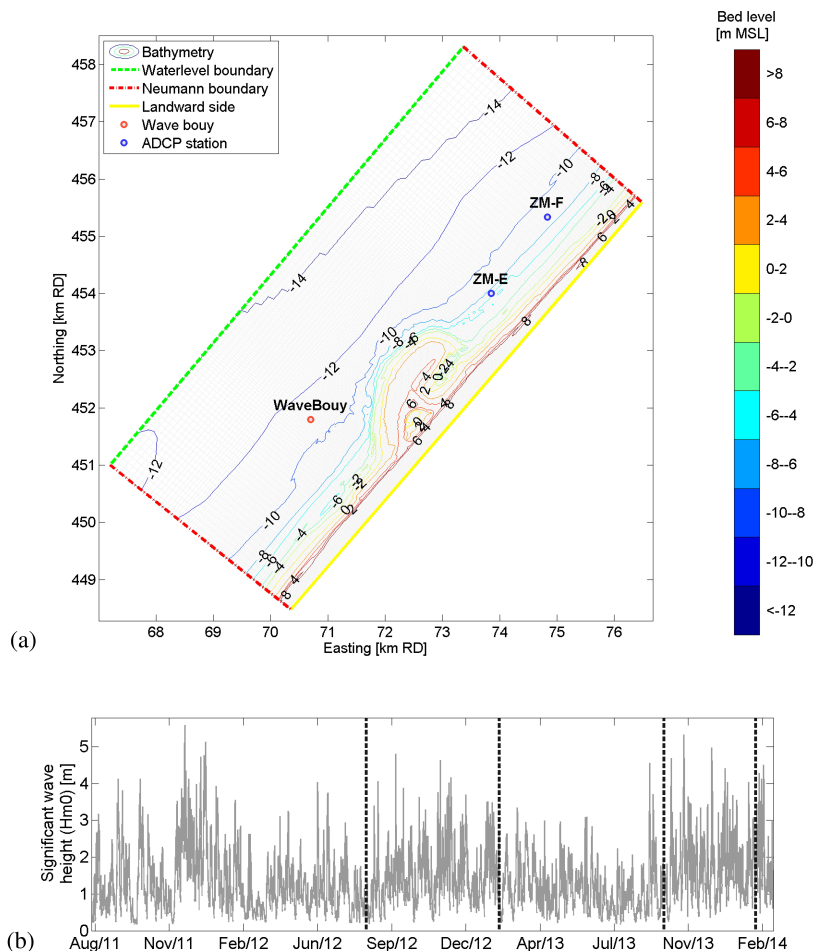


Figure 5.4: Model domain with initial bathymetry of August 2011 (a) and time-series of wave boundary conditions (b) from August 2011 to February 2014. Note that sediment sample surveys are shown as vertical dashed grey lines

The morphological time scale in the model is four times the hydrodynamic time scale (Ranasinghe et al., 2011). The introduced discrepancy between the phase of the tide and the waves was found to have no significant influence on the long-term sorting pattern from a half-year test simulation with a morphological factor of one. Transport rates were calibrated to 50% of the uncalibrated value for all simulations, which provided a good hindcast of the morphological changes at the Sand Motor for the model with a single sediment fraction (Luijendijk et al., 2017). Suspended transport due to currents and waves was set at respectively 100% and 20% for the 3D and 2DH simula-

tions, which corrects for the over-prediction of onshore sediment transport as a result of the absence of the offshore-directed undertow process in the 2DH models (Giardino et al., 2011).

A multi-layer approach was used to administrate the bed composition changes (Ribberink, 1987; Sloff and Mosselman, 2012), which means that the contribution of each of the sediment size fractions is administrated per layer and per grid cell. A 'transport layer' is present at the top of the bed for which the bed composition is adjusted over time as a result of erosion and/or accretion of the modelled sediment size fractions (Figure 5.5).

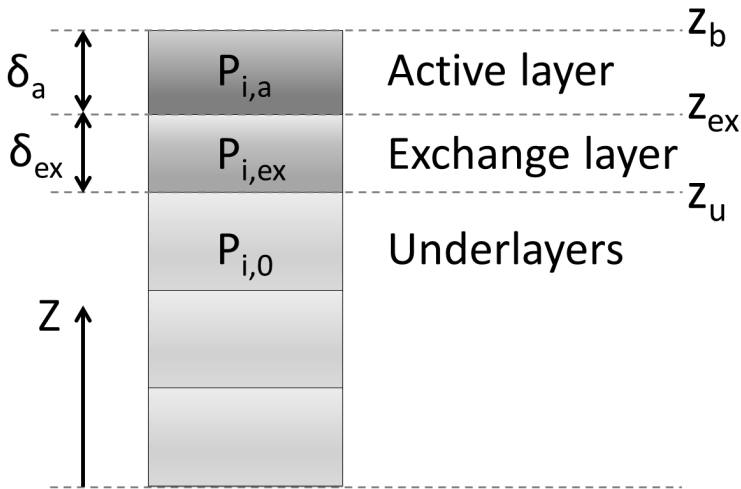


Figure 5.5: Multi-layer administration within Delft3D

The transport layer moves up and down with the bed when erosion or sedimentation takes place (i.e. with fixed thickness). During accretive situations the transport layer moves upward, which means that 1) newly accreted sediment is mixed proportionally with the existing material in the transport layer and 2) a representative part of the sediment of the transport layer is added to the layer underneath the transport layer (referred to as the 'exchange layer'). Analogously, sediment from the exchange layer is moved back to the transport layer when erosion takes place. The exchange layer has a variable thickness since its upper interface moves with the active layer, while layers below the exchange layer (referred to as 'underlayers') are vertically fixed. The vertical fixation of the underlayers prevents numerical diffusion of sediment into the substrate as a result of (temporary) changes in the morphology of the bed. A description of the mass balance for each sediment size fraction (Sloff and Mosselman, 2012) reads as follows:

$$\rho_s(1-\epsilon)\left(\frac{\partial(p_{i,a}\delta_a)}{\partial t} + p_i(z_0)\frac{\partial z_0}{\partial t}\right) + \frac{\partial q_{sxi}}{\partial x} + \frac{\partial q_{syi}}{\partial y} = 0 \quad (5.1)$$

in which the level of the substrate below the considered layer is denoted as  $z_0$  and the thickness of the layer as  $\delta_a$ . The top level of the considered layer is  $z_0 + \delta_a$ . The proportion of sediment of size fraction  $i$  at a layer is denoted as  $p_i$  which is taken equal to the proportion in the active layer ( $p_{i,a}$ ) when sedimentation occurs and equal to the proportion of the layer below the considered layer ( $p_i(z_0)$ ) during erosion.  $q_{sxi}$  and  $q_{syi}$  are mass sediment transport components per unit width for fraction  $i$  in the  $x$  and  $y$  direction, which is per definition zero for the exchange layer and underlayers.  $\rho_s$  is the density of the sediment and  $t$  is time.

A thickness of the active layer of 0.1 m was applied in the models, as this is considered the zone which is mixed by the waves (see also Sloff et al., 2001). It is noted, that the actual thickness of the top layer has an effect on the rate of initial  $D_{50}$  changes, but had only a small impact on overall  $D_{50}$  after a few years. Twenty underlayers with a thickness of 0.5 m were used in the models to represent the substrate material.

### MODEL RUN CONFIGURATIONS

Hindcast models were set up for the period from August 2011 to February 2014 to assess the performance of a Delft3D model in hindcasting bed sediment composition changes at the Sand Motor. The hindcast models differ with respect to the number of vertical layers in the water column (2DH or 3D) and initial bed composition (Table 5.1), while the same grid was used for each of the models (34m x 17m). Furthermore, a reference simulation was made with only 1 sediment fraction of 278  $\mu\text{m}$  sand ( $H_0$ ).

Table 5.1: Overview of hindcast model run configurations

Run	Vertical layers	Bathymetry* <sup>1</sup>	Transp. formula	Nr. frac.	Initial bed	Tide & Waves
$H_0$	2DH	ZM2011	Tr2004	1	uniform	Time-series (Aug 2011-Feb 2014)
$H_1$	2DH	ZM2011	Tr2004	5	uniform	Time-series (Aug 2011-Feb 2014)
$H_2$	3D (12)	ZM2011	Tr2004	5	uniform	Time-series (Aug 2011-Feb 2014)
$H_3$	3D (12)	ZM2011	Tr2004	5	inibed	Time-series (Aug 2011-Feb 2014)

\*<sup>1</sup> ZM2011 refers to the Sand Motor bathymetry of August 2011.

The models with a 'uniform' initial bed composition for the whole domain applied a  $D_{50}$  of 278  $\mu\text{m}$  (similar to the Sand Motor sand). The grain size distribution at the Sand Motor was classified in five size fractions according to Van der Zwaag (2014) (Table 5.2). The spatially varying initial bed composition ('inibed') consisted of the aforementioned sand mixture at the Sand Motor (i.e.  $D_{50}$  of 278  $\mu\text{m}$ ) and a natural fining of the sediment in the offshore direction at the adjacent coast (Figure 5.6). The applied 10th and 90th weight percentile diameter of the sand were respectively a factor 2.2x smaller or larger than the  $D_{50}$  which was similar to the ratio of the observed transect averaged  $D_{50}$ ,  $D_{10}$  and  $D_{90}$ . The sediment at the Sand Motor was specified as separate sediment fractions from those at the adjacent coast, with the aim of discerning the



behavior of the Sand Motor sand from that of the rest of the coast.

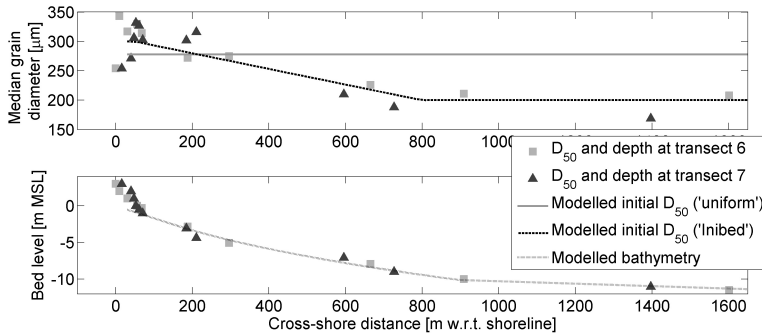


Figure 5.6: Cross-shore distribution of the measured  $D_{50}$  at the Sand Motor (T0 survey) and modelled initial bed

Table 5.2: Classification of the sediment distribution at the Sand Motor into five sediment size fractions

Class	Lower limit [ $\mu\text{m}$ ]	Median [ $\mu\text{m}$ ]	Upper limit [ $\mu\text{m}$ ]	Mass percentage
1	63	107	150	9.5
2	150	181	225	23
3	225	256	300	24
4	300	363	425	29
5	425	513	1180	15

The findings in the 3D model hindcast ( $H2$ ), which was envisaged to provide a good representation of alongshore and cross-shore transport processes, were substantiated more with model configurations with simplified hydrodynamics (i.e. adjusted tide or waves), which aimed at isolating the relative importance of hydrodynamic forcing conditions (i.e. tide, normal waves and storm conditions) on the development of spatial heterogeneity in the  $D_{50}$ . Besides an average climate condition with  $H_{m0}$  of 1 m from  $310^\circ N$  ( $W1$ ) also variations of climate conditions were made with a different wave height ( $H_{m0}$  of 3 m wave height,  $W2$ ) or with a sequence of a storm condition ( $H_{m0}$  of 3 m) after a moderate condition ( $H_{m0}$  of 1 m;  $W3$ ). Also the sensitivity of the  $D_{50}$  changes for the wave direction ( $\pm 30^\circ$ ) was evaluated ( $W4$  and  $W5$ ). Tidal conditions were investigated by simulating a situation without tide ( $C1$ ), with only the tide ( $C2$ ) or with a reduced or enhanced tidal velocity (at 80% or 120% of the actual tide;  $C3$  and  $C4$ ). Additionally, also the influence of a smaller seaward protrusion (of 200 or 400 m) of the nourishment bathymetry was modelled ( $B1$  and  $B2$ ). It is noted that the storm conditions ( $H_{m0}$  of 3 m) were present for 4 days, which is a realistic persistence for a year with relatively severe conditions along the Dutch coast.

## METHODS FOR QUANTIFYING MODEL PERFORMANCE

The actual performance of the hindcast models was quantified on the basis of an inter-comparison of the modelled and observed  $D_{50}$  (see chapter 4). Both the representation of the alongshore heterogeneity of the  $D_{50}$  and the cross-shore distribution of the

$D_{50}$  was evaluated. A weighted average of the median grain size per cross-shore transect ( $D_{50TR}$ ) was computed, both for the field surveys and the models, with the aim of comparing the alongshore heterogeneity of the  $D_{50}$ . This  $D_{50TR}$  is defined as :

$$D_{50TR} = \frac{1}{L} \sum_{i=1}^n D_{50,i} \Delta x_i \quad (5.2)$$

The contribution of each sample (landward of the MSL -10m contour) was computed by multiplying the median grain size of the sample ( $D_{50,i}$ ) with the representative cross-shore extent ( $\Delta x_i$ , i.e. half of distance to neighboring sample). The summed  $D_{50}$  contribution of each sample was divided by the length of the considered transect ( $L$ ). The agreement of the actual modelled and observed  $D_{50TR}$  was quantified by means of the squared correlation coefficient ( $R^2$ ). Uncertainty in  $D_{50TR}$  as a result of the sampling methodology was estimated at  $\sim 11 \mu\text{m}$  (see chapter 4), while uncertainty in  $D_{50}$  of individual samples was estimated at  $30 \mu\text{m}$ . Short-term temporal variability for moderate and storm conditions even amounted to a possible 40 to 80  $\mu\text{m}$  difference for individual samples.

5

#### 5.4. HINDCAST OF MORPHOLOGY AND BED COMPOSITION

Modelled currents and waves for the 2011-2012 winter period matched well with observations at local ADCP stations and a wave buoy (see calibration by Luijendijk et al., 2017). The patterns of erosion and sedimentation over the first two years after construction of the Sand Motor (from August 2011 till August 2013) were very similar, showing net erosion at the peninsula of the Sand Motor and accretion at the adjacent coast (Figure 5.7).

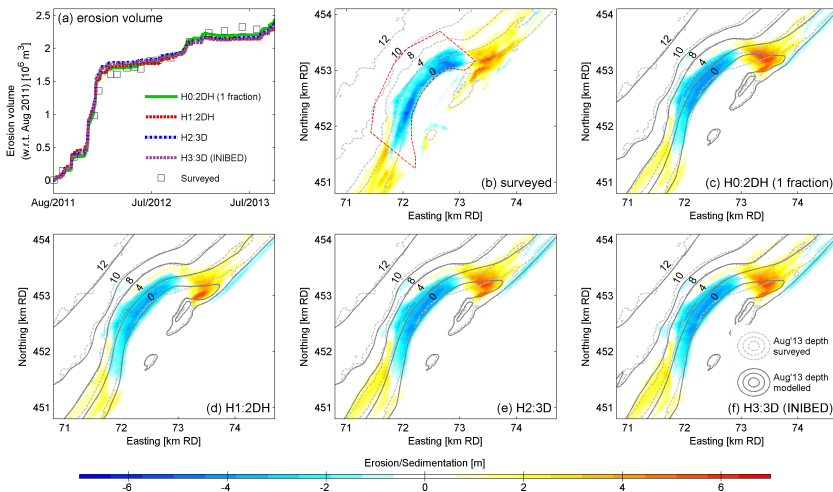


Figure 5.7: Bathymetric changes in the first two years after construction of the Sand Motor. Panel a shows the volume of erosion at the peninsula (i.e. within red dashed line in panel b), while panels b to f respectively show the surveyed and modelled bathymetric changes (from Aug 2011 to Aug 2013). Note that the MSL to MSL -12m contours for the surveyed and modelled bathymetries of August 2013 are presented respectively as dashed and continuous lines.

The erosion rates in a control area of  $\sim 2 \text{ km}^2$  at the Sand Motor peninsula (Figure 5.7b) were almost identical to the observed changes (see erosion volumes in Figure 5.7a). The modelled erosion volumes also aligned well with the observed erosion of about 1.8 million  $\text{m}^3$  by De Schipper et al. (2016) in the first year after construction of the Sand Motor. Models with multiple sediment fractions provided similar erosion rates as the model with a single sediment fraction ( $D_{50}$  of  $278 \mu\text{m}$ ). Computed erosion rates were, however, sensitive to the use of the roller model and the exact alignment of the integration area ( $\pm 0.2 \cdot 10^6 \text{ m}^3$ ), but do show similar behaviour over time for all models. Reference is made to Luijendijk et al. (2017) for more information on the roller model and morphological model performance of the single sediment fraction model.

The erosion and sedimentation patterns in the models (over the first two years) were also well represented in the models (Figure 5.7b to Figure 5.7f). The alongshore length of the region with erosion was very similar in the models and the survey, while the cross-shore distribution of the erosion was somewhat more gradual in the models. The most noticeable deviation concerned a seaward shift (of about 150 m) in the modelled location of the coastline on the northern flank of the Sand Motor (Figure 5.7), which can be seen from the difference between the modelled and surveyed depth contours (i.e. continuous and dashed gray lines). This dissimilarity between the model and observed changes was somewhat smaller in the simulations with multiple sediment fractions (compare panel c with panels d to f in Figure 5.7). Overall, the morphological performance of the models is considered adequate for an investigation of the redistribution of the sediment size fractions at the Sand Motor which is expected to depend on the large-scale bathymetric and hydrodynamic characteristics of the Sand Motor (e.g. cross-shore extent, wave transformation and tidal contraction).

Computed two-year averaged transport rates at the Sand Motor (Figure 5.8) showed positive transport gradients at the Sand Motor (i.e. erosive) and negative at the adjacent coast (deposition), which induced a transport away from the Sand Motor.

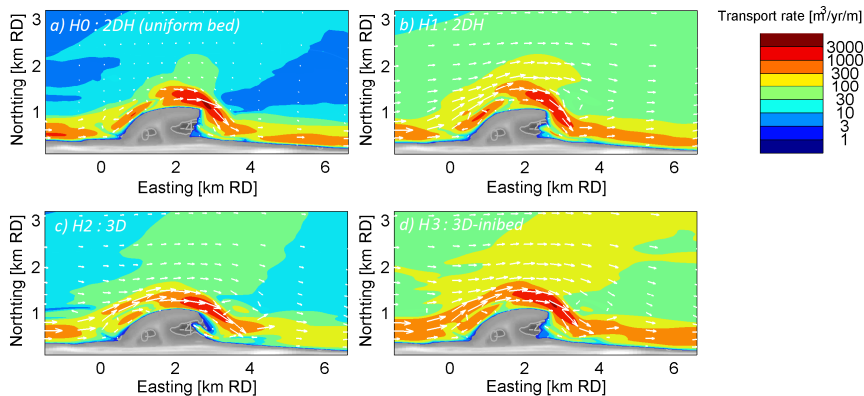


Figure 5.8: Time-averaged total transport for different model approaches of runs  $H0$  to  $H3$  (i.e. 2DH or 3D, single or multi-fraction approach and initially uniform or spatial varying bed composition). Note that transport is plotted with a logarithmic scale to visualize also the areas with moderate or low transport rates.

The transport rates of the single and multi-fraction models were similar in the near-shore region (from waterline to MSL-6m; compare  $H0$  and  $H1$  in Figure 5.8), which is in line with the observed similarities in the computed morphological changes. However, the transport rates in deeper water were enhanced considerably in the multi-fraction models ( $H1$  to  $H3$ ) as a result of the much larger mobility of the fine sediment fractions compared to the average sediment grain size in the single-fraction model ( $H0$ ). Additionally, overall transport rates were enhanced in the model with the initial spatially varying bed composition ( $H3$ ) which had more fine sand available in the bed.

The computed bed composition ( $D_{50}$ ) in the numerical models ( $H1$  to  $H3$  in Table 5.1) changed from a rather uniform initial  $D_{50}$  to a situation with considerable spatial heterogeneity in the  $D_{50}$  over a period of about 2.5 years (see time evolution of  $D_{50}$  in Figure 5.9).

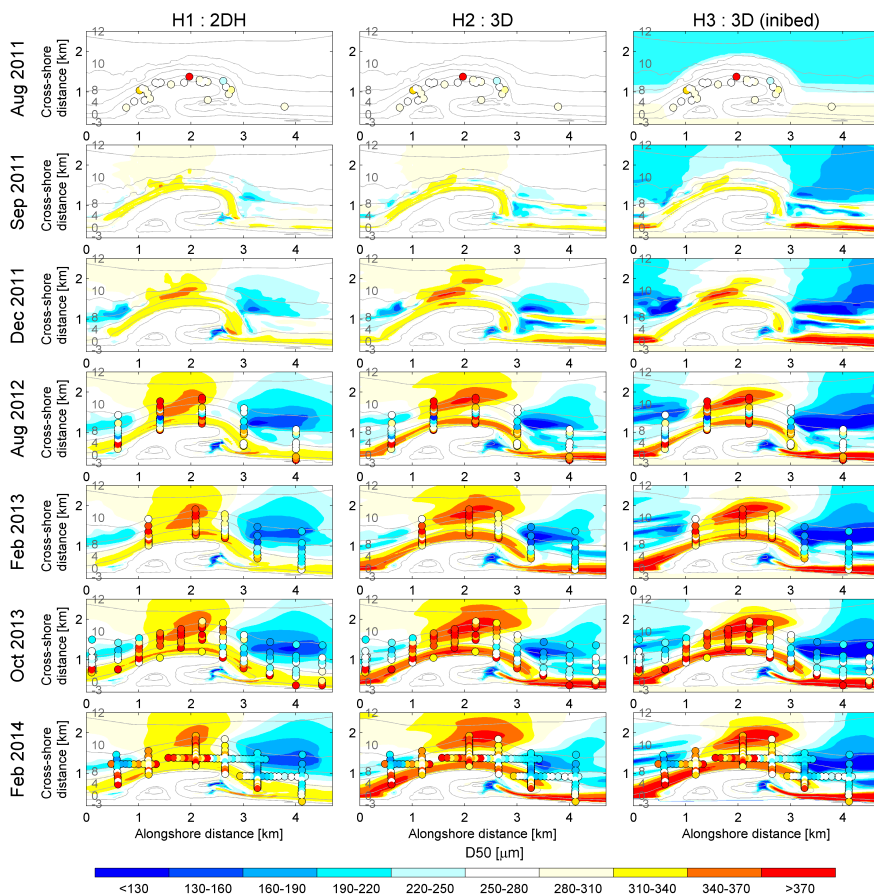


Figure 5.9: Development of spatial heterogeneity of the  $D_{50}$  over the first 2.5 years after construction of the Sand Motor for the 2DH, 3D and 3D-inibed models ( $H1$ ,  $H2$  and  $H3$ ). Sediment survey data are shown as coloured markers. Depth contours are shown as continuous grey lines as a bed level in m MSL.

The models show the development of a typical spatial pattern in the  $D_{50}$  which is also observed in the measurement surveys ( $T2$  to  $T5$ ). This consisted of (1) an area with coarser sediment in front of the Sand Motor peninsula (from MSL-4m to MSL-10m), (2) a finer sediment composition just North and South of the Sand Motor and (3) a cross-shore variation in the sediment size with coarse sediment in the breaker zone and a fining of the sediment in the offshore direction. Computed 10th and 90th percentile grain size diameter ( $D_{10}$  and  $D_{90}$ ) showed similar patterns as the  $D_{50}$ .

Qualitatively the 3D models (i.e.  $H2$  and  $H3$ ) provided the best agreement with the  $D_{50}$  patterns of the considered surveys (Figure 5.9), which represented both the magnitude of the coarsening of the  $D_{50}$  in front of the Sand Motor peninsula as well as the fining on the northern side of the Sand Motor. The model with 2DH hydrodynamics ( $H1$  in Figure 5.9) showed a less pronounced coarsening in front of the Sand Motor peninsula (MSL -4m to MSL -12m) than observed in the surveys (see February and October 2013). The initial bed composition was relevant for bed composition changes in deeper water (i.e. seaward of MSL -12m at the Sand Motor and seaward of MSL -8m at the adjacent coast).

The  $D_{50}$  patterns of the considered 3D models were very similar, irrespective of the initial condition that was used for the  $D_{50}$  of the bed (compare runs  $H2$  and  $H3$  in Figure 5.9). Consequently, the  $D_{50}$  patterns are considered to be the result of the hydrodynamic forcing conditions which acted on the models over the 2.5 year modelling period and subsequent morphological changes rather than the initial bed condition. Differences between the modelled and observed  $D_{50}$  patterns consisted of a relatively wide nearshore region with a coarse bed composition ( $D_{50}$  of 350 to 400  $\mu\text{m}$ ) and a smaller proportion of finer sand (200 to 250  $\mu\text{m}$ ) at  $\sim 4$  water depth at the northern side of the Sand Motor peninsula compared to the October 2013 and February 2014 surveys (Figure 5.9). This discrepancy is, however, expected to be related to the more seaward position of the modelled coastline on the northern flank of the Sand Motor compared to the observations (Figure 5.7) which results in a too seaward position of the surfzone with coarser  $D_{50}$ . A cross-shore shift of the modelled  $D_{50}$  of the bed was therefore used for transects at the northern flank of the Sand Motor in order to obtain an evaluation of the modelled alongshore and cross-shore bed sediment composition changes rather than the morphological performance. For this purpose the difference in depth of the modelled and observed bathymetry was minimized (i.e. the average distance between depth contours from MSL to MSL -10m).

A comparison of modelled transect averaged median grain diameters ( $D_{50\text{TR}}$ ) against observations showed that the aggregated model predictions were in good agreement with the data (comparison of  $D_{50\text{TR}}$  for October 2013 survey in Figure 5.10a). The 2DH model ( $H1$ ) reproduced a very similar trend of the  $D_{50\text{TR}}$  with small scatter (i.e. highest  $R^2$ ; Figure 5.10b), which suggests that 2DH processes provide a large contribution to the development of the alongshore  $D_{50}$  heterogeneity. The  $D_{50\text{TR}}$  at the flanks of the Sand Motor deviated more for the 3D models ( $H2$  and  $H3$ ) as a result of the mentioned cross-shore shift in the morphology. The absolute  $D_{50\text{TR}}$  (i.e. 1 on 1 line in the scatter plots) was, however, better represented in the 3D models ( $H2$  and  $H3$ ), which is shown

from a closer resemblance of the 1 on 1 line of the average modelled and observed  $D_{50TR}$  (Figure 5.10c and Figure 5.10d).

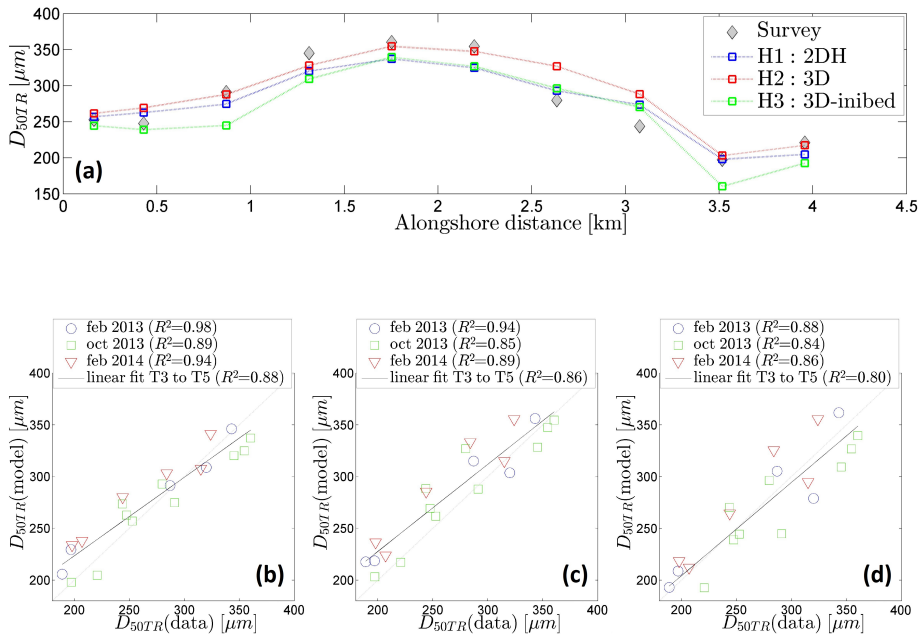


Figure 5.10: Measured and modelled transect averaged median grain diameter ( $D_{50TR}$ ) of the hindcast models H1 to H3 for surveys T3 to T5. (a) Alongshore variation of  $D_{50TR}$  for October 2013 survey; (b) Scatter plot of measured and observed  $D_{50TR}$  for H1: 2DH model, (c) H2: 3D model and (d) H3: 3D-inibed model.

The cross-shore variation of the  $D_{50}$  at three representative cross-shore transects (at the Peninsula, northern flank and North of the Sand Motor) was well represented in the models (i.e.  $R^2$  of 0.4 to 0.9; Figure 5.11). Especially the 3D models resolved the details of the cross-shore distribution of the sediment, such as the small depression in  $D_{50}$  (at  $x=300$  m) at the Sand Motor Peninsula in the February 2013 survey and the small increase in  $D_{50}$  North of the Sand Motor in the October 2013 survey. The 2DH models provided a more smoothed cross-shore distribution of the  $D_{50}$ . It is noted that a compensation was made for the bathymetric shift (of about 150 m) for the transect at the Northern flank of the Sand Motor, while transects at the Sand Motor Peninsula and North of the Sand Motor were shifted only marginally (i.e. typically  $\sim 40$  meters). Similar performance was observed for the February 2014 survey (with  $R^2$  ranging from 0.4 to 0.9) and the August 2012 survey ( $R^2$  of 0.3 to 0.6).

In summary, a 3D model is considered essential to represent both the alongshore and cross-shore patterns of the  $D_{50}$  at a mega nourishment and surrounding coast, while 2DH models can still reasonably represent the changes in the  $D_{50}$  of the bed in the alongshore direction. Additionally, an accurate initial (spatial varying) bed composition can be relevant for a precise representation of the magnitude of the  $D_{50TR}$

changes, but is not essential for the  $D_{50}$  in the nearshore (i.e. landward of MSL -8m).

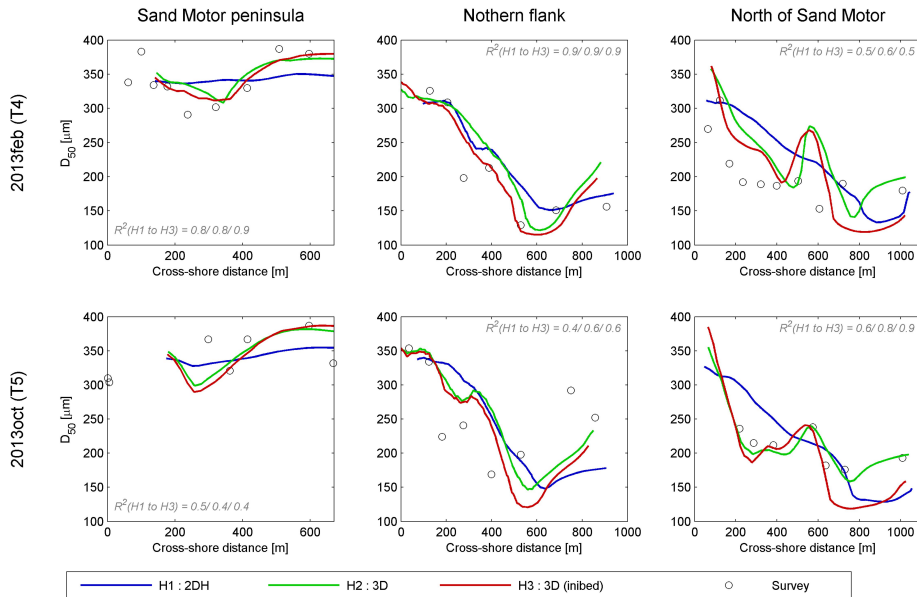


Figure 5.11: Median grain diameter on cross-shore transects at the center of the Sand Motor peninsula ( $tr=7$ ), northern flank ( $tr=8$ ) and North of the Sand Motor ( $tr=9$ ) for T3 and T4 surveys. Performance expressed as  $R^2$  is presented for H1, H2 and H3 respectively with grey text in the figure panels.

A closer look at the modelled  $D_{50}$  at the Sand Motor reveals that bed composition changes predominantly take place in the top-layer of the bed (Figure 5.12; H2 model). This is especially the case at the central Sand Motor transect, where erosion induced a coarsening of the top-layer material which extends well beyond the initial perimeter of the Sand Motor (Figure 5.12a). Furthermore, a thin layer of fine sand is present in deeper water just North and South of the Sand Motor (seaward of MSL -10m). On the other hand, a layer of up to a few meters of sediment accumulated at the landward side of the cross-shore profile (Figure 5.12, panel b and c). The coarser fractions accumulated in the nearshore region ( $D_{50} \sim 350 \mu\text{m}$ ) at the flanks of the Sand Motor while the finer sediment size fractions are transported to deeper water (100 to 200  $\mu\text{m}$  sand at MSL -10m) and further away in alongshore direction from the Sand Motor peninsula. Furthermore, a sequence of upward coarsening developed at the spit of the Sand Motor (see panel b of Figure 5.12 at  $x=3500 \text{ m}$ ). Finer sand fractions were deposited here initially, while over time the finer sand was covered by coarser sediment size fractions when the morphological footprint of the Sand Motor became wider. A very similar grading of the bed was found for the H3 model, but then super-imposed on the initial bed composition that was provided to the model.

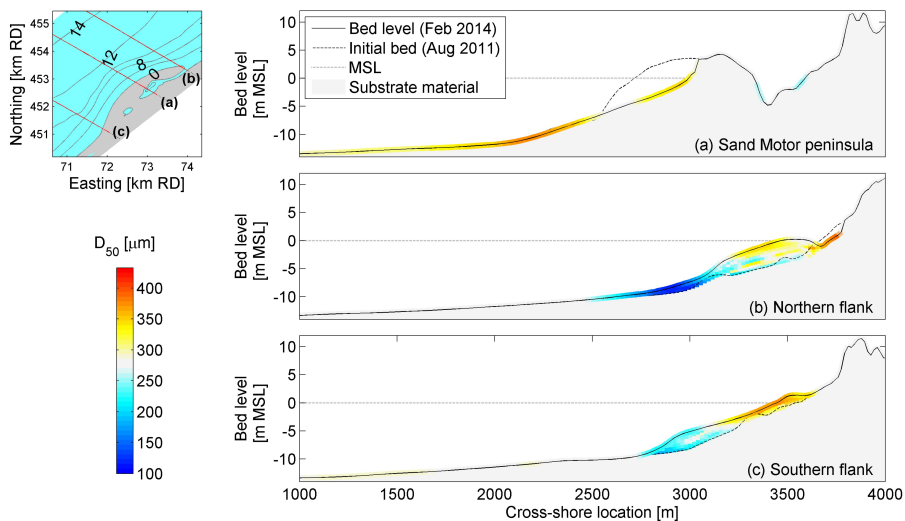


Figure 5.12: Vertical grading of the  $D_{50}$  of the bed at three cross-shore transects at the center of the Sand Motor and in the accumulation zones North and South of the Sand Motor (3D model : H2, February 2014).

The origin and destination of the Sand Motor sediment (which was marked as a separate fraction) was tracked for each of the size fractions, which shows that the fine sediment size fractions are redistributed over a much larger area than the coarse size fractions (Figure 5.13).

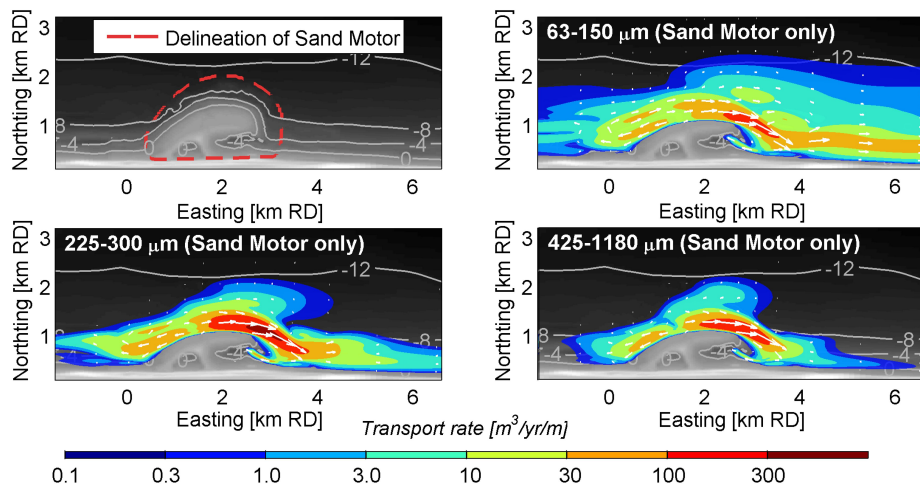


Figure 5.13: Time-averaged total transport for the considered sediment size fractions (H2 model). Note that transport is plotted with a logarithmic scale to visualize also the areas with moderate or low transport rates.

The finest sediment fraction (63 to 150  $\mu\text{m}$ ) was transported both inside and outside the surfzone (up to MSL-12m on the northern side of the Sand Motor), while



the medium and coarse fractions are transported almost exclusively in the nearshore (about 800 meter wide section on the northern and southern side of the Sand Motor). The fine-medium sand fraction (150 to 225  $\mu\text{m}$ ) had in-between behaviour and was still distributed partially by the tide. It is noted that the computed cross-shore width of the zone with transport of finer sediment size fractions is also in line with visual observations of fine sand plumes being expelled from the Sand Motor (Figure 5.1). The observed fining of the bed in deeper water North of the Sand Motor (Figure 5.12) is therefore expected to be also the result of the abundance of alongshore supply of the finer sand fractions (63 to 225  $\mu\text{m}$ ) from the Sand Motor body.

## 5.5. RELEVANCE OF HYDRODYNAMIC CONDITIONS

Model simulations with simplified hydrodynamics at the Sand Motor were used to identify the relevance of tide and waves for the generation of the coarsening at the Sand Motor and deposition regions at the adjacent coast. Simulations of storm and normal conditions (Figure 5.14a and Figure 5.14b) showed that coarsening of the  $D_{50}$  in front of the Sand Motor developed especially during normal wave conditions (run W1), while a less extensive coarsening of the bed developed as a result of the storm wave conditions (run W2).

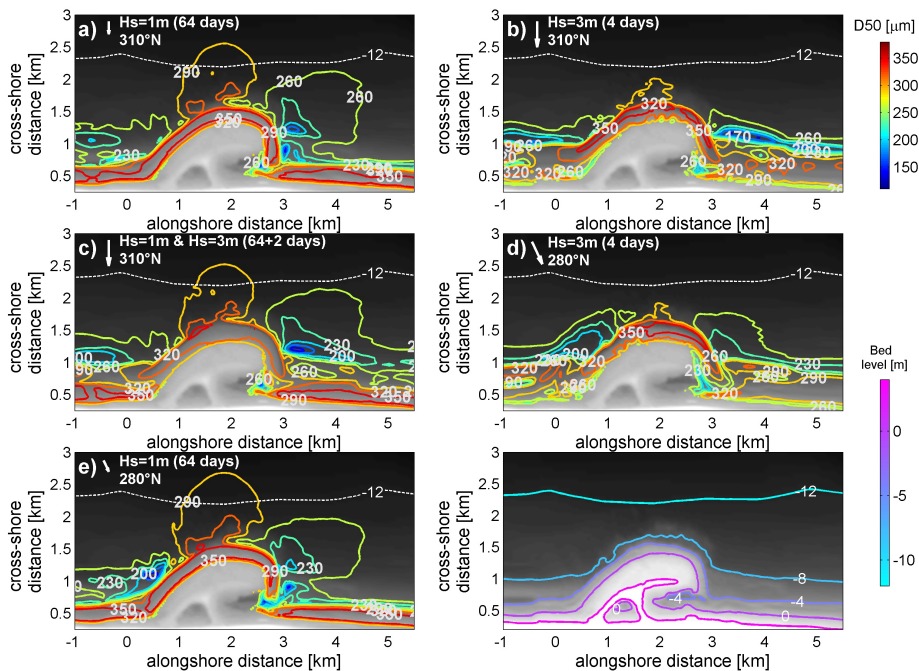


Figure 5.14: Modelled spatial pattern of  $D_{50}$  as a result of normal or storm conditions for shore-normal and oblique wave incidence. a) Run W1 with  $H_{m0}=1\text{m}$ ; b) Run W2 with  $H_{m0}=3\text{m}$ ,  $dur=4$  days; c) Run W3 with  $H_{m0}=3\text{m}$ ,  $dur=2$  days after 64 days with  $H_{m0}=1\text{m}$ ; d) Run W5 with  $H_{m0}=3\text{m}$ ,  $dur=4$  days from 280°N; e) Run W4 with  $H_{m0}=1\text{m}$  from 280°N.

It is noted that the duration of the conditions was scaled down to a realistic duration (respectively 64 and 4 days for the normal and storm wave condition). The precise duration of the simulations was, however, not of influence to the general finding that the storms contribute far less to the coarsening at the Sand Motor, because the size of the coarse patch was still relatively small after a storm condition of a month (i.e. run *W2* compared to run *W1*). This is also shown by a simulation of a storm condition after a period with normal conditions (run *W3*) which resulted in a small fining of the bed seaward of MSL -8m. The storm conditions, on the other hand, had a clear impact on the deposition regions North and South of the Sand Motor. The magnitude of the fining and area of this region was considerably larger for situations with storm conditions, which is related to the larger supply of sediment that is eroded from the coast. The direction of the incoming waves had a only small influence on the coarsening of the bed in front of the Sand Motor peninsula with slightly more coarsening for waves from the South-West (*W4*; [Figure 5.14f](#)). Wave direction did, however, affect the extent and magnitude of the deposition at the flanks of the Sand Motor during storm conditions (*W5*; [Figure 5.14e](#)), although the magnitude of the storm waves was still dominant.

## 5

Simulations with either only waves or tide (run *C1* and run *C2*) indicated that waves induce both a coarsening of the bed in the zone with the alongshore wave-driven current as well as patches with fine sand outside the surfzone on the flanks of the Sand Motor ([Figure 5.15a](#)), while tidal conditions were most relevant for the development of the coarsening of the bed outside the surfzone and induced a fining of the bed in deeper water at the adjacent coast ([Figure 5.15b](#)). The relevance of the tide is even further substantiated from simulations with enhanced and reduced tidal velocities (*C3* and *C4* in [Figure 5.15c](#) and [Figure 5.15d](#)) which show that the extent and magnitude of the coarse patch in front of the Sand Motor as well as the deposition region at the adjacent coast scale with the tidal velocities. The actual configuration of the Sand Motor also plays a role since spatial variation in  $D_{50}$  was hardly present for nourishment configurations with a (200 or 400 m) reduced cross-shore extent of the initial nourishment plan-form (*B1* and *B2* in [Figure 5.15e](#) and [Figure 5.15f](#)), which is related to a reduction of the contraction of the tide (i.e. less enhancement of tidal velocities) for these configurations.

In summary, a strong influence of the tidal velocities on the coarsening at the Sand Motor foreshore was found, which is the result of the enhanced forcing conditions due to the tidal contraction. It is expected that a preferential transport of fine sediment size fractions towards the adjacent coast is present which results in the coarsening of the top-layer of the bed (see [chapter 4](#)). The much smaller coarsening of the  $D_{50}$  for the bathymetries with a reduced seaward protrusion of the nourishment also suggests that the tidal contraction is an important cause for the coarsening of the  $D_{50}$  of the bed. Storm wave conditions on the other hand were found to reduce the coarsening of the bed at the Sand Motor as a result of the mobilization (and suspension) of all of the sediment size fractions as these conditions remove part of the relatively coarse top-layer. The extent of the deposition region at the flanks of the Sand Motor is, however, determined for a large part by the waves, which transport sediment with the undertow

current to intermediate water depths (i.e. MSL -4m to -8m).

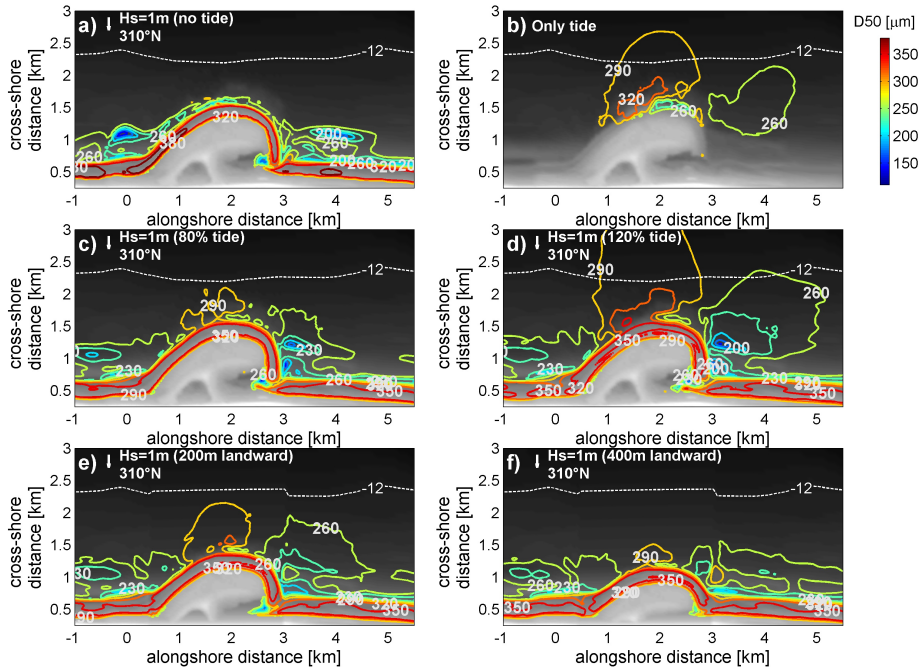


Figure 5.15: Modelled spatial pattern of  $D_{50}$  as a result of wave conditions ( $H_{m0}=1\text{m}$ , tide ( $\Delta H \approx 1.5\text{m}$  and  $\bar{U} \approx 1\text{m/s}$ ) or adjustments of the bathymetry (affecting the tide and waves). a) Run C1 with only waves; b) Run C2 with only tide; c) Run C3 with 80% tidal velocities; d) Run C4 with 120% tidal velocities; e) Run B1 with 200m landward shift of bathymetry; f) Run B2 with 400m landward shift.

## 5.6. DISCUSSION

Our results show that the development of large-scale alongshore  $D_{50}$  heterogeneity at the Sand Motor can be reproduced well with the present numerical model. The observed pattern of coarsening of the  $D_{50}$  in front of the Sand Motor peninsula and fining at the adjacent coast were reproduced in models with different initial conditions for the  $D_{50}$  of the bed, which suggests that the hydrodynamic processes are responsible for the changes in bed composition (Figure 5.9). The transect averaged median grain size ( $D_{50\text{TR}}$ ; Figure 5.10) was modelled well with 2DH and 3D models ( $R^2$  of 0.84 to 0.94), while the cross-shore distribution of the  $D_{50}$  and short-term variability during storms was reproduced best with a 3D modelling approach (Figure 5.11). The inclusion of the initial spatial varying bed composition provided a small improvement of the modelled alongshore heterogeneity of the  $D_{50}$  at the Sand Motor, but may be of large relevance if the applied nourishment sand is very different from the natural sediment or for situations where morphology is strongly influenced by the bed sediment condition (e.g. tidal estuaries or river bed dynamics; Dastgheib et al., 2008; Blom and Parker, 2004). The differences between the modelled and observed  $D_{50}$  patterns were small and mainly present on the flanks of the Sand Motor, which was also the loca-

tion where morphology of the bed was somewhat less well predicted (i.e. too small erosion on northern flank of Sand Motor). These secondary discrepancies may relate to a variety of processes, of which their relative importance is not yet known, such as 1) complex hydrodynamics in the nearshore bar-rip systems (MacMahan et al., 2005; Gallagher et al., 2011), 2) large-scale tidal eddy generation (Radermacher et al., 2015) and 3) secondary currents as a result of the fresh water plume of the Rhine (Visser et al., 1994). Long-waves also affect the nearshore morphology and bed composition during storm conditions (Van Thiel de Vries et al., 2008; Reniers et al., 2013), but are expected to have a relatively small impact on transport in deeper water (De Bakker et al., 2016).

Large-scale coarsening of the  $D_{50}$  of the bed just outside the surfzone (i.e. seaward of MSL -6m) of mega nourishments (such as the 'Sand Motor') is mainly the result of the tidal currents (Figure 5.14). The local contraction of the tide results in a more frequent exceedance of the critical bed shear stresses for suspension of the sediment (Van Rijn, 2007b) and subsequently also in a larger entrainment (Komar, 1987) and enhanced transport rate (Steidtmann, 1982) of the fine sand fractions. The difference in the suspension behaviour of the fine and coarse size fractions is expected to be largest during quiet and moderate wave conditions when the fine sand fraction is suspended while the coarse sand fraction is not, which is shown schematically in Figure 5.16 for a location on the lower foreshore of a mega nourishment.

5

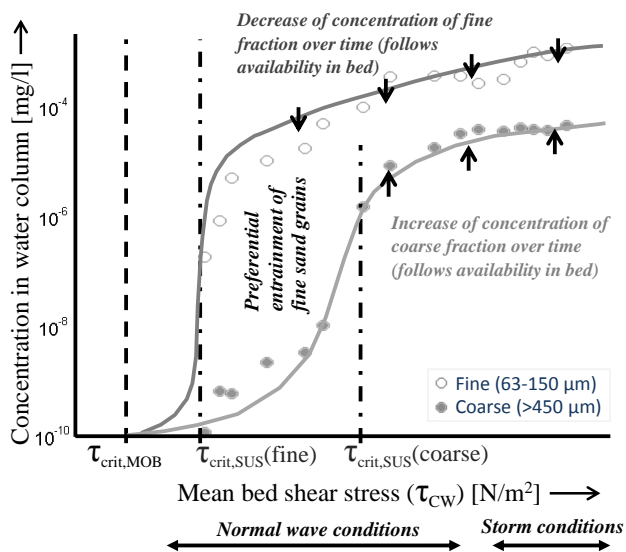


Figure 5.16: Schematic of the difference in suspension behaviour of fine and coarse sand fractions for moderate and storm conditions. The modelled time-averaged sediment concentrations at a location seaward of Sand Motor peninsula (E71856m, N453237m RD at 11 m water depth) of the 3D model (H2) are presented as circular markers for the coarse and fine sand fraction. The typical range of bed shear stresses for normal and storm conditions is shown below the graph.

A preferential transport of the finer sediment size fractions away from the Sand Motor

is present during normal conditions (see [chapter 4](#)), which removes the fine sediment size fractions from the top-layer of the bed at the Sand Motor foreshore ([Figure 5.12](#)). Over time the discrepancy in transport rates between fine and coarse size fractions is expected to reduce, as concentrations of fine material in the bed will decrease. A nourishment with a smaller seaward protrusion (i.e. reduction of 25% or 50%) shows a less pronounced coarsening of the bed since the tidal contraction -which is considered the principal driver for the erosion of the bed- is reduced considerably. This suggests also that alongshore heterogeneity in  $D_{50}$  is likely to develop at other coastal structures which induce a contraction of the tide (e.g. port structures). Eroded fine sediment from the foreshore of the Sand Motor is transported predominantly in northward direction to the adjacent coast ([Figure 5.13](#); MSL -8m to MSL -12m), which is the result of the tidal asymmetry with larger north-going flood velocities, which explains the relatively large size of the fine sediment patch on the northern side of the Sand Motor (compared to the small fine sediment patch at the southern side).

Wave conditions generate a coarsening of the  $D_{50}$  in the surfzone (Terwindt, 1962; Stauble and Cialone, 1996) as well as deposition of (relatively fine) sand at intermediate depths (i.e. between MSL -4m and -8m). Additionally, a reduction of the size of the coarse sediment patch in front of a mega nourishment will take place during storm conditions, which is the result of 1) the mobilization of all the size fractions and 2) mixing of the coarse top-layer with relatively fine substrate sediment. Consequently, both the fine sand as well as the coarse top-layer are (partly) removed during a storm event. The suspension behaviour of fine and coarse sand fractions is also considered more similar during high energy events (i.e. shear stress in [Figure 5.16](#) larger than  $\tau_{crit,SUS}$  of the medium and coarse sand fractions). This is also in agreement with observed fining of the bed in deeper water during the storm of 22 October 2014 (see [chapter 4](#)). The small influence of the direction of the waves on the coarse sediment patch is considered an indication that especially the stirring of the waves is of influence to the development of the coarse sediment patch. The development of the fine sediment patches at the flanks of the Sand Motor, on the other hand, is positively related to storm wave conditions, which transport a considerable amount of eroded fine sand from the surfzone to intermediate water depths (up to about MSL -8m) with the undertow current (Reniers et al., 2013; Broekema et al., 2016).

The cross-shore extent of the region with transport of the finer sand fractions at a mega nourishment is much wider than the cross-shore footprint of the coarser sand fractions ([Figure 5.13](#)). This indicates that the medium and coarser sand fractions (>225  $\mu\text{m}$ ) are transported mainly by the wave-driven alongshore current, while the finer sand fractions (65 to 225  $\mu\text{m}$ ) are also mobilized by the tide. Consequently, the redistribution behaviour of the coarse and fine sand fractions is different. Especially the sediment redistribution in the zone outside the surfzone will be dominated by the behaviour of the finest sand fraction, which means that an approach with a uniform sediment grain size will underestimate the transport rates in deeper water. Theoretically, the alongshore transport of different size fractions (in deeper water) may even be bi-directional (e.g. if the tide velocities are very a-symmetrical or when waves approach from one side), similar to the observed bi-directional cross-shore transport of

bi-modal sand at Duck (Richmond and Sallenger, 1984). Modelling of the morphological changes in deeper water therefore requires an approach with multiple sediment size fractions. The multi-fraction approach is therefore essential for the evaluation of the environmental impact of a mega nourishment (or port construction). Models with uniform sediment can, however, still be applied well for situations where all of the sediment size fractions are mobilized, such as the assessment of the lifetime of sand nourishments for which the dominant processes take place within the nearshore region. Initial erosion volumes at the Sand Motor could, for example, be hindcasted well with both the single and multi-fraction models (Figure 5.7; Luijendijk et al., 2017).

## 5.7. CONCLUSIONS

The numerical model Delft3D was applied for a 2.5 year hindcast of bed sediment composition ( $D_{50}$ ) at a large-scale sand nourishment ('Sand Motor'). Our findings indicate that the observed spatial pattern of the  $D_{50}$  at the Sand Motor (i.e. coarsening in front of the Sand Motor and fining at the adjacent coast) was reproduced well with the Delft3D model independent of the starting condition of the  $D_{50}$  of the bed. Both 2DH and 3D models reproduce alongshore variation in the  $D_{50}$  at such a mega nourishment ( $R^2$  of 0.84 to 0.94) while cross-shore variation is represented only in a 3D model.

The development of the coarsening of the (top-layer of the) bed in front of a mega nourishment (or other coastal structure) is attributed mainly to the contraction of the tide. The locally enhanced current velocities result in a more frequent exceedance of the critical bed shear stress for suspension of the sediment, which induces enhanced entrainment and transport of especially the fine sand fractions to the adjacent coast. Wave conditions, on the other hand, induce a coarsening in the surfzone and a potential fining in deeper water. At the flanks of the mega nourishment this fining is the result of cross-shore transport of fine sand by the undertow current, while storm wave conditions can induce a partial removal of the coarse top-layer of the bed on the lower foreshore (i.e. between MSL-6m and MSL-12m) in front of the mega nourishment. This is due to mobilization (and erosion) of both the coarse and fine sand fractions of the coarse top-layer and mixing with the relatively fine substrate sediment.

The finer sand fractions of a mega nourishment are distributed over a considerably larger (cross-shore) area than the coarser sand fractions. Typically, the coarse sand fractions are transported only in the surfzone by the wave-driven alongshore current while the fine sand travels also in deeper water with the tide. A modelling approach with multiple sediment size fractions is therefore required when the transport rates or morphological changes in deeper water are investigated. It is emphasized that this is of relevance for the assessment of the environmental impact (bed composition changes;  $D_{50}$ ) of any coastal measure with a large seaward protrusion (i.e. which creates contraction of the tide). An approach with a single sediment size fraction can, however, still provide a good performance for situations where all of the sediment size fractions are mobilized. For example, when the erosion volume of a nourishment is investigated which is mainly determined by sediment transport in the nearshore zone.

# 6

## CONCLUSIONS AND PERSPECTIVES

### 6.1. CONCLUSIONS

Sandy coastlines around the world are under threat of erosion as a result of natural causes and anthropogenic activities (Bruun, 1962; Bird, 1985; Hamm et al., 2002; Luijendijk et al., 2018). Maintenance of the coast is therefore essential to preserve the quality of the beaches for recreation and for the protection of the hinterland, for which purpose sand nourishments are commonly used (e.g. Leonard et al., 1990; Hanson et al., 2002; Cooke et al., 2012). Most studies focus on beach nourishments which are placed between the low water line and the dune foot, describing the influence of local environmental conditions and geometrical properties of the nourishment on its lifetime (Leonard et al., 1990). In the last decades, however, a shift was made from beach nourishments to larger scale sand nourishments which are placed at the shoreface seaward of the sub-tidal bar (from MSL -10 to -4 m; e.g. Van Duin et al., 2004) or as emerged mega feeder nourishments (from MSL -10 to +4 m; Stive et al., 2013) which can be considered as temporary land reclamations. However, efficient methods for the evaluation of the erosion and sediment redistribution of these nourishments are lacking, as their morphological behaviour is not sufficiently well understood. In addition, the sheer size of these measures poses questions regarding the impact on the environment. The objectives of this thesis are therefore to study 1) the erosion and sediment redistribution of shoreface and mega nourishments and 2) the effects of the disturbance by the nourishment on the sea bed. A combination of field measurements and numerical models are used to provide insight into sediment redistribution and sorting of sediment at the nourishments. Bathymetric data of nineteen shoreface nourishments at alongshore uniform sections of coast were used as well as the large-scale 'Sand Motor' nourishment at the Delfland coast (~21 million  $m^3$  of sand).

#### *Q1.1 : How do shoreface and mega nourishments redistribute over time?*

Shoreface nourishments evolve especially in cross-shore direction. A landward skewing of the cross-shore profile is typically observed consisting of a landward movement (and increase in height) of the nourishment crest and erosion of the seaward

edge of the nourishment. Some accretion takes place in the shallow nearshore region (MSL -3m to MSL) landward of the considered shoreface nourishments at the Dutch coast. An impact of the shoreface nourishment on the adjacent coast is not distinguishable, although it is expected that some sediment is supplied to the coast given the net loss of sand from the nourishment region. This is explained from the large capacity of the local forcing conditions (e.g. rip currents) to spread sand along the coast, which makes it difficult to measure the changes. In the first place the low impact of the shoreface nourishment during normal and mild conditions (when waves transform easily over the nourishment) results in a nearshore climate which diffuses any perturbations. Secondly, large eddies develop at the lateral sides of the shoreface nourishment during extreme wave conditions as a result of water-level setup behind the shoreface nourishment, which also spreads the sediment over a larger section of the coastline. Mega nourishments, on the other hand, reshape especially due to alongshore transport processes. In plan-form the mega nourishment reshapes towards a bell-shape which gradually becomes wider in alongshore direction and less pronounced in cross-shore direction. The redistributed sediment has a direct impact on the adjacent coast (i.e especially in the first kilometer) which accretes considerably in the first years after construction. A spit may even develop when the mega nourishment shape is sufficiently pronounced or when waves approach from a very oblique angle. On the longer term the sediment will continue to spread over a larger area, but the changes will take much longer (i.e. decades) as the rotation of the coastline will reduce at some distance of the nourishment. The lifetime (and erosion rate) of a mega nourishment depend especially on the energy of the waves, while wave direction plays a minor role for the considered nourishments at alongshore uniform coasts. In addition also the geometrical properties (e.g. length over width ratio) and median grain diameter of the sand mixture ( $D_{50}$ ) are of importance for the rate at which redistribution of sediment takes place. It is noted that the relevance of the cross-shore width for the lifetime of the mega nourishment is different from the design rules for beach nourishments, which relate the lifetime of beach nourishments to the alongshore length.

### *Q1.2 : What is the relative contribution of alongshore and cross-shore processes to the redistribution of shoreface and mega nourishments?*

Shoreface nourishments are influenced predominantly by severe wave conditions (especially  $H_{m0} \geq 3\text{m}$ ), which generate 1) onshore transport on the shoreface nourishment and at the coast, 2) some alongshore currents at the nourishment during oblique energetic events and 3) a water-level setup driven alongshore current behind the shoreface nourishment which feeds a rip current at the lateral sides. Cross-shore transport due to waves and water-level setup driven currents contribute most to the erosion of shoreface nourishments in the first years after construction (i.e. 60% to 85% for the considered nourishments in this thesis), while the alongshore transport contributes to a smaller extent. It is noted that a large portion of the erosion (75 to 95 %) is represented even when purely shore-normal incident wave conditions are applied, which suggests that wave direction is not very important for the lifetime of a shoreface nourishment. The alongshore current dominates the morphological response of a mega nourishment, which takes place in the surfzone. Tidal currents on



the other hand affect the (alongshore) redistribution of sediment of a mega nourishment outside the surfzone ( $\sim$  MSL -8m to MSL -14m), which is shown clearly for the hindcasts of bed composition changes at the Sand Motor. However, the volume of sediment transported by the tidal currents is relatively small compared to the wave-driven alongshore transport in the surfzone (landward of  $\sim$ MSL -4m). Especially the sensitivity of the alongshore transport for a small re-orientation of the coastline (with respect to the waves) determines the erosion rate of a mega nourishment. Most of the wave-driven alongshore transport at large scale nourishments (at the Dutch coast) is driven by moderate wave climate conditions ( $H_{m0}$  1 to 2 m).

### *Q1.3 : How can the lifetime of nourishments be assessed efficiently?*

A model resolving extreme wave conditions is needed to model the erosion rates at a shoreface nourishment (e.g. the Xbeach model), which requires a calibrated set of parameters for the wave skewness and asymmetry as they provide a substantial contribution to the cross-shore transport at the shoreface nourishment. This study used wave skewness and asymmetry parameters that were derived for the safety assessments of the Dutch coast, which provided a good basis for the modelling of the erosion of five shoreface nourishments. A calibration of a stable profile shape for the undisturbed coastal profile will be needed when such a parameter set is absent for the considered coast. Remarkable is that a good estimate of erosion rates of shoreface nourishments can be obtained using just the initial sedimentation-erosion rates based on a single post-construction bathymetry. On the other hand, the response of a mega nourishment can be described well with a model that resolves the alongshore wave-driven current, such as a shoreline model (e.g. UNIBEST). These coastline models have the advantage that no trade-off has to be made with respect to the schematization of the wave climate (e.g. representation of the wave energy for storm events), which is often required for detailed process-based Reynold Averaged Navier Stokes (RANS) models. Some reduction of the modelling complexity may, however, be made, because the lifetime of a mega nourishment was found to be rather insensitive to the wave direction. In fact, the most relevant parameter for the lifetime of a mega nourishment at alongshore uniform beaches is the sensitivity of the alongshore sediment transport to a small adjustment of the coast angle. This makes it easier to evaluate the behaviour of mega nourishments worldwide, as the wave energy is more easily determined than the wave incidence angle. In some cases it can be sufficient to use lookup tables for the lifetime of permanent and temporary 'land reclamations' as discussed in this thesis. For example, when a first order estimate of the lifetime of a nourishment is required for an initial planning stage of a coastal maintenance project.

### *Q2.1 : What impact do sand nourishments have on the bed sediment composition of the surrounding coast?*

Considerable alongshore heterogeneity of the median grain size of the bed ( $D_{50}$ ) can take place after construction of a mega nourishment, which effectively is a large cross-shore perturbation of the coastline. Field measurements at the Sand Motor showed (1) coarsening of the region seaward of the Sand Motor (a  $D_{50}$  change of +90 to +150  $\mu\text{m}$ ) and (2) a deposition area with relatively fine material (50  $\mu\text{m}$  finer) just North and

South of the Sand Motor. The alongshore heterogeneity of the  $D_{50}$  is most evident outside the surfzone (i.e. seaward of MSL -4 m), while alongshore variation in  $D_{50}$  was relatively small in the surfzone (i.e. landward of MSL -4 m). Considerable bed composition change can take place also seaward of the toe of the nourishment at the natural seabed (i.e. ~ up to MSL -14 m at the Sand Motor). The measurements also show the impact of a storm, which consists of a ~40  $\mu\text{m}$  finer  $D_{50}$  of the offshore bed composition in front of the Sand Motor (i.e. where a considerably coarser bed was in place), which suggests that especially the mild to moderate conditions affect the development of spatial heterogeneity in the  $D_{50}$  of the bed. The alongshore spatial heterogeneity of the  $D_{50}$  is expected to reduce over time as the cross-shore perturbation by the mega nourishment becomes smaller.

### *Q2.2 : What processes affect sediment sorting at nourishments?*

The observed coarsening of the bed offshore from the Sand Motor is attributed to the enhanced bed shear stresses due to the local tidal contraction. This leads to an erosive gradient seaward of the nourishment, which transports predominantly the finer grains to the low-energy regions in deeper water at the adjacent coast. Consequently, a coarse top layer of the bed develops at the lower shoreface in front of the nourishment. The preferential transport of the finer sand grains results from the higher likelihood of suspension of the fine grains compared to the coarse grains for the forcing conditions that are present at the lower shoreface of the Sand Motor. The coarse sand grains are mobile at the bed (i.e. above critical threshold of motion), but are still not transported well as they are only suspended during energetic storm events. The finer sand grains, on the other hand, are suspended in the water column for all environmental conditions. These sediment sorting processes are especially relevant outside the surfzone (i.e. seaward of MSL-4m) during mild to moderate wave conditions, while a reduction of the local coarsening of the bed takes place during storms (i.e. when the mode of transport of the size fractions is more similar). In addition, storms also induce additional mixture of the top-layer of the bed with the underlying (undisturbed) substrate sediment. Similarly, also breaking waves reduce the effect of the sediment sorting processes in the nearshore, because breaking waves easily suspend both the coarse and fine sand grains into the water column which results in more similar transport of the size fractions. Similar sorting processes as observed at the Sand Motor can be present at other coastal structures at sandy coasts (e.g. mega nourishment or port breakwater) when the structure has a sufficiently large cross-shore extent which affects the tidal currents.

### *Q2.3 : What are the implications of sediment sorting at mega nourishments for morphological modelling?*

Morphological models using only a representative median grain size ( $D_{50}$ ) are often sufficient to represent the initial morphological evolution of nourishments. At the Dutch coast, the local breaking of the waves in the nearshore easily suspends all grain size fractions, which means that the transport mode is similar. Consequently, only a small difference in transport potential of the size fractions is present in the surfzone. This justifies the use of a single representative grain size fraction. The small differ-

ence in suspension behaviour of the size fractions in the surfzone also implies that a relatively small impact of the sorting processes is present on the bulk of the morphological change of nourishments, which takes place predominantly in the surfzone due to wave-driven alongshore and cross-shore transport processes. The (less active) sediment outside the surfzone (i.e. seaward of MSL -4 m) is, however, influenced by sorting processes, as shown for the Sand Motor. A good model representation of the sediment transport in this region requires the inclusion of 1) differential transport and suspension behaviour of the size fractions using transport computations for multiple size fractions of the same mixture as well as 2) a multi-layer bed administration to track the proportion of each size fraction in the bed. Using such an approach, larger transport potential of the fine sand fraction and armouring of the top-layer of the bed are accounted for in the model. A good representation of the initial bed composition was not crucial for the Sand Motor, but it is envisioned that a precise spatially varying initial bed composition may be needed for small scale nourishments or investigations of the transport rates at the lower shoreface of a natural coast. The observed and computed variations in bed composition underline the importance of sorting processes for the assessment of bed composition changes at large-scale coastal structures and deep-water morphology of the lower shoreface.

## 6.2. DISCUSSION AND PERSPECTIVES

Ongoing urbanization and enhanced sea level rise will increase the pressure on the land use of sandy coasts in the future (Defeo et al., 2009), which makes it likely that more and more sand nourishments are needed for the protection of beaches. Policy makers are, however, still in need of information on the behaviour and modelling of nourishments to draw the outlines of sustainable and cost-effective future coastal management strategies. The observations and modelling of sand redistribution of shoreface and mega nourishments in this thesis provide necessary building blocks for 1) the evaluation of the efficiency of large-scale shoreface and mega nourishments in mitigating coastal erosion and 2) the effects of large-scale nourishments on the seabed composition. The results are considered useful for wave dominated sandy coasts around the world, even though data from Dutch field sites is used in the thesis. For example, the guidelines for mega-nourishments can be used also for coasts with less wave energy (e.g. sites in the Middle East, South-East Asia or Australia) or more severe waves (e.g. United States or Namibia) as long as the local Longshore Transport Intensity parameter (*LTI*) and active height are defined appropriately. Similarly, also the methods for prediction of the erosion of shoreface nourishments are expected to be applicable at other coast based on the good performance for the five considered nourishments, although the settings for onshore transport processes may need to be calibrated. It is therefore suggested to do similar modelling of shoreface nourishments for other sites in the world to obtain confidence in the approach.

A remaining challenge is still the long-term morphological change of shoreface nourishments (>5 years after construction) after the cross-shore adaptations have taken place. It is envisioned that these longer term changes are dominated by alongshore processes as is the case for mega nourishments, but this could not be verified for the

considered shoreface nourishments in this thesis as disturbances by other measures are often present in the data after a few years. The gap in knowledge may either be filled in with a well monitored set of shoreface nourishments over a longer period (i.e. >5 years) or by means of detailed numerical computations for complex situations where nourishments overlap (i.e. using precise reconstructions based on the currently available data). The physics involved in the spreading of shoreface nourishments should then be resolved well in the numerical models, which will require especially a better representation of hydrodynamic and morphological processes at the sub-tidal bar, since the current model physics have the tendency to flatten out the bars over time (e.g. Grunnet et al., 2004; Van Duin et al., 2004). This problem is overcome in this thesis by fixing the morphology of the bar, but this is not considered valid at longer time-frames. If a parameterization can be made of the local hydrodynamic and morphological processes at the sub-tidal bar, this would make it possible to enhance the performance of morphological models substantially. A detailed investigation of the flow patterns at the bar and trough will be needed to estimate the net transport processes. It is envisioned that the importance of driving processes for bar-growth, such as time lags of hydrodynamics and sediment suspension, additional turbulence and converging flow, can be investigated most efficiently using detailed numerical models (e.g. Navier-Stokes type models; Jacobsen and Fredsoe, 2014b). Measurements in the field and laboratory flume experiments can also provide a useful addition for the verification of the models, but are practically difficult to realize. A wide range of environmental conditions and beach morphologies needs to be studied, which is easier to achieve with numerical models.

## 6

The modelling of shoreface and mega nourishments is narrowed down in this thesis to the most essential physical processes (e.g. the wave-driven current only) in order to reduce computational costs, which is very efficient (i.e. taking a few minutes of computational time) compared to detailed morphological field models which run for days. It is, however, recognized that other processes, such as cross-shore transport and tide induced transport, may also provide a contribution to the spreading of the sand of mega nourishments (Luijendijk et al., 2017). A relevant aspect that may need to be accounted for at some sites is the influence of coastal structures (or sediment blocking elements) on the redistribution of sand at mega nourishments, which effectively means that a coastline model (which also accounts for wave direction and shielding) is needed instead of the design-graphs. However, in practice the effects of most of the omitted processes (e.g. tidal water levels) are often smaller than the uncertainty in the redistribution of the sand by the wave-driven current (e.g. partly due to uncertainty in future wave conditions and/or uncertainty in the formulations) or these processes are only present for a small period of time. For example, it took a few months for the cross-shore profile at the Sand Motor peninsula to change from a relatively steep profile to a more natural mild sloped beach, which means that alongshore sediment transport is enhanced only for a relatively short period of time. In some cases it may, however, be very relevant to use more complex modelling, which is the case for beaches close to tidal inlets, where considerable erosion (or accretion) can take place due to the tidal currents. Furthermore, other processes than the wave-driven along-shore current are relevant when detailed morphological features such as spits or bed

composition change due to placement of the nourishment are relevant.

It should be noted that the use of efficient dedicated models, which narrow down problems to the essential physical processes, puts a large weight on the experience of the modeler, who needs to judge the relevance of the transport processes and applicability of the methods for the local situation. The constraints of the methods are therefore described extensively in the discussions of the chapters on the lifetime of shoreface and mega nourishments. For example, wave direction needs to be accounted for at enclosed beaches or coastal sections with structures, while an adjustment of the rate of spreading may be needed for beaches with varying types of sediment (e.g. sand nourishment on shingle beaches). The most crucial system characteristic for morphological modelling of mega nourishments is the rate of alongshore transport in relation to a coastangle adjustment (*LTI*) which is difficult to assess. In order to aid coastal modelers, it is suggested to extend the current handbooks with hydrodynamic forcing conditions (e.g. 1/100 year wave conditions) with site specific coastal properties. The *LTI* parameter (expressing the sensitivity of the wave climate to a rotation of the beach) is a useful site-specific parameter which contains both the relevant local forcing conditions as well as the coastal properties (e.g. sediment size, profile shape). In this way a morphological boundary condition is provided to modelers. In addition the *LTI* from the handbook will also be useful as a reference for coastal modelers using more complex models.

The recent increase in the size of nourishments and expected application of these large-scale measures in the near future also poses a question about the effects on the marine habitat for benthos and fish (Post et al., 2017). For this reason it is suggested to make assessments of the expected bed composition changes as a result of long-term maintenance strategies of the coast, since similar sorting processes as observed at the Sand Motor are likely to be present also at other mega nourishments. Especially the regions outside the surfzone are expected to be influenced by the measures, and therefore need more attention. In addition, it is suggested to evaluate bed composition change of the seabed also for other coastal structures, as similar sorting processes as observed at the Sand Motor are likely also present at other structures with a sufficiently large cross-shore extent to affect the tidal current.

In order to ease the evaluation of the impact of future large-scale nourishments on bed composition, it is necessary to improve the computational efficiency of the numerical models computing the multi-fraction transport rates and administration of sediment in the bed. Instead of using a detailed time-series of wave conditions, which is not available for future forecasts, it is expected that a set of representative average climate conditions can also be used to predict the changes of the seabed. Even a single average climate condition can provide a decent representation of the large-scale longer-term development of spatial heterogeneity in  $D_{50}$  as shown for the Sand Motor. The selection of this single condition will, however, be difficult to make in most practical situations for which reason a set of representative conditions is recommended. In addition a speed up of the bed changes can be obtained using a Morphological factor (Ranasinghe et al., 2011), which accelerates the bed level changes by multiplying

the accretion and erosion of the bed with a fixed factor. Thus allowing more efficient evaluation of the effects of nourishments on bed composition. On the longer-term it is recommended that design graphs are made of bed composition change at mega nourishments and/or coastal structures (e.g. port breakwaters), which will depend on the local environmental conditions (average wave height, percentage of occurrence of storms, tidal currents), geometry of the beach, shape of coastal measures (influencing the contraction of the tidal flow) and natural characteristics of the sand (especially the  $D_{50}$  and width of the distribution). These design graphs will make it feasible to come up with ballpark numbers of structure induced bed composition changes in the initial planning phases of new measures.

When it comes to detailed hindcasts of bed composition changes due to nourishments, it is expected that improvements can still be made to the model representation of bed composition changes during storms. The current concept using a fixed thickness of the transport layer in the bed administration, which does not account for mixing of the top-layer of the bed by waves (during storm events). For example, Meirelles et al. (2016) show that bed forms during storm conditions are much larger than during mild conditions, suggesting that a different mixing of the top-layer of the bed may take place. This may also explain why the numerical modelling of sediment sorting at the Sand Motor is somewhat less accurate during temporary storm conditions, as the additional mixing with the substrate is not represented. It is therefore suggested to use a 'mixing routine', which can move top-layer sediment deeper into the bed and/or expose deeper located finer sand fractions to the currents. At the Sand Motor this process was, however, somewhat less relevant as mild to moderate wave conditions (which have a smaller mixing depth than the modelled transport layer thickness) are dominant for the development of the bed composition changes, but mixing during storm events can be relevant for other regions. Another important aspect of the bed composition modelling that plays a role in different environments than the Sand Motor, is the potential underestimation of transport of fine sand fractions in the current modelling approach when the relatively fine sand moves over a coarse bed. Currently, the numerical modelling with multiple fractions uses a concept of availability of sediment in the bed for the scaling of the transport rates of each of the size fractions. This concept does work well when the bed composition has sufficient time (and space) to adapt to the supply (and export) of sediment, which means that the considered condition should last sufficiently long (e.g. days to weeks) to influence the top-layer bed composition. However, for situations with local armouring of the bed this approach is not suitable, in analogy with coarsening of the top-layer of the bed by aeolian transport processes (Hoonhout, 2017). For example, at entrance channels of tidal basins the fine sediment passes over a coarse bed with armouring. The current approach will tend to mix the new sand in the bed, which slows down the movement of the sediment (as it will only be transported as soon as a considerable part of the top layer consists of the finer sand). In order to move finer sand over an armoured bed, it will therefore be needed to scale the transport of the separately computed size fractions in the numerical model based on the presence of the considered fractions in the updrift supply of sediment.

# REFERENCES

- Alcamo, J., Moreno, J. M., Novaky, B., Bindi, M., Corobov, R., Devoy, R. J. N., Giannakopoulos, C., Martin, E., Olesen, J. E., and Shvidenko, A. (2007). *Climate Change 2007: Impacts, Adaptation and Vulnerability : Europe. Contribution of Working Group II to the Fourth Assessment Report of the Intergovernmental Panel on Climate Change, Europe*. Cambridge University Press, Cambridge, UK.
- Alexander, R. R., Stanton, R. J., and Dodd, J. R. (1993). Influence of sediment grain size on the burrowing of bivalves. *Palaios*, 8:289–303.
- Anthony, E. J., Brunier, G., Besset, M., Goichot, M., Dussouillez, P., and Nguyen, V. L. (2015). Linking rapid erosion of the mekong river delta to human activities. *Scientific Reports*, 5:Article number 14745.
- Arriaga, J., Rutten, J., Ribas, E., Falqués, A., and Ruessink, B. G. (2017). Modeling the long-term diffusion and feeding capability of a mega-nourishment. *Coastal Engineering*, 121:1–13.
- Ashida, K. and Michiue, M. (1973). Studies on bed load transport rate in alluvial streams. *Japan Society of Civil Engineers*, 4.
- Ashton, A., Murray, A. B., and Arnoult, O. (2001). Formation of shoreline features by large-scale instabilities induced by high-angle waves. *Nature*, 414:296–300.
- Baba, J. and Komar, P. D. (1981). Measurements and analysis of settling velocities of natural quartz sand grains. *Journal of Sedimentary Petrology*, 51:631–640.
- Bagnold, R. A. (1966). An approach to the sediment transport problem from general physics. *Geological Survey Professional Papers, Washington, USA*, 422-1:1–37.
- Barnard, P. L., Van Ormondt, M., Erikson, L. H., Eshleman, J., Hapke, C., Ruggiero, P., Adams, P. N., and Foxgrover, A. C. (2014). Development of the Coastal Storm Modeling System (CoSMoS) for predicting the impact of storms on high-energy, active-margin coasts. *Natural Hazards*, 74 (2):1095–1125.
- Bart, L. J. C. (2017). Long-term modelling with xbeach: combining stationary and surfbeat mode in an integrated approach. Master's thesis, Delft University of Technology.
- Battjes, J. A. and Janssen, J. P. F. M. (1978). Energy loss and set-up due to breaking of random waves. In *16<sup>th</sup> International Conference on Coastal Engineering*, volume 1, pages 570–587, Hamburg, Germany. ASCE.

- Battjes, J. A. and Stive, M. J. F. (1984). Calibration and verification of a dissipation model for random waves. *Proceedings of the 19th Coastal Engineering Conference Houston*, pages 649–660.
- Benedet, L., Finkl, C. W., and Hartog, W. M. (2007). Processes controlling development of erosional hot spots on a beach nourishment project. *Journal of Coastal Research*, 23(1):33–48.
- Bird, E. C. F. (1985). *Coastline changes: A global review*. Wiley Interscience, Chichester, New York.
- Blom, A. and Parker, G. (2004). Vertical sorting and the morphodynamics of bed form-dominated rivers: A modeling framework. *Journal of Geophysical Research*, 109(F2):2156–2202.
- Booij, N., Ris, R. C., and Holthuijsen, L. H. (1999). A third-generation wave model for coastal regions 1. Model description and validation. *Journal Of Geophysical Research*, C4, 104(C4):7649–7666.
- Brinkkemper, J. A., Aagaard, T., De Bakker, A. T. M., and Ruessink, B. G. (2018). Short-wave sand transport in the shallow surf zone. *Journal of Geophysical Research: Earth surface*, 123:1145–1159.
- Broekema, Y. B., Giardino, A., Van der Werf, J. J., Van Rooijen, A. A., Vousdoukas, M. I., and Van Prooijen, B. C. (2016). Observations and modelling of nearshore sediment sorting processes along a barred beach profile. *Coastal Engineering*, 118:50–62.
- Brown, J. M., Phelps, J. J. C., Barkwith, A., Hurst, M. D., Ellis, M. A., and Plater, A. J. (2016). The effectiveness of beach mega-nourishment, assessed over three management epochs. *Journal of Environmental Management*, 184 (2):400–408.
- Bruun, P. (1962). Sea level rise as a cause of shore erosion. *Journal Waterways and Harbours Division*, 88(1-3):117–130.
- BS812 (1975). *Sampling, Shape, Size and Classification, part I*. British Standards (BS) 812.
- Capobianco, M., Hanson, H., Larson, M., Steetzel, H., Stive, M. J. F., Chatelus, Y., Aarninkhof, S., and Karambas, T. (2002). Nourishment design and evaluation: applicability of model concepts. *Coastal Engineering*, 47(2):113–135.
- Cooke, B. C., Jones, A. R., Goodwin, I. D., and Bishop, M. J. (2012). Nourishment practices on Australian sandy beaches: a review. *Journal of Environmental Management*, 113:319–327.
- Cruz, R., Harasawa, H., Lal, M., Wu, S., Anokhin, Y., Punsalmaa, B., Honda, Y., Jafari, M., Li, C., and Ninh, N. H. (2007). *Climate Change 2007: Impacts, Adaptation and Vulnerability: Asia. Contribution of Working Group II to the Fourth Assessment Report of the Intergovernmental Panel on Climate Change*. Cambridge University Press, Cambridge, UK, 469–506.



- Dastgheib, A., Roelvink, J., and Wang, Z. (2008). Long-term process-based morphological modeling of the marsdiep tidal basin. *Marine Geology*, 256(1–4):90–100.
- Davis, R. A., Wang, P., and Silverman, B. R. (2000). Comparison of the performance of three adjacent and differently constructed beach nourishment projects on the gulf peninsula of florida. *Journal of Coastal Research*, 16 (2):396–407.
- De Bakker, A. T. M., Brinkkemper, J. A., Van der Steen, E., Tissier, M. F. S., and Ruessink, B. G. (2016). Cross-shore sand transport by infragravity waves as a function of beach steepness. *Journal of Geophysical Research: Earth Surface*, 121(10):1786–1799.
- De Ronde, J. (2008). Toekomstige langjarige suppletiebehoefte. delft: Deltares. Technical report, Deltares.
- De Schipper, M. A., De Vries, S., Ruessink, G., De Zeeuw, R. C., Rutten, J., Van Gelder-Maas, C., and Stive, M. J. F. (2016). Initial spreading of a mega feeder nourishment: Observations of the Sand Engine pilot project. *Coastal Engineering*, 111:23–38.
- De Vincenzo, A., Covelli, C., Molino, A., Pannone, M., Ciccaglione, M., and Molino, B. (2018). Long-term management policies of reservoirs: Possible re-use of dredged sediments for coastal nourishment. *Water*, 11(1):15.
- De Vriend, H. J., Zyserman, J., Nicholson, J., Roelvink, J. A., Pdchon, P., and Southgate, H. N. (1993). Medium-term 2DH coastal area modelling. *Coastal Engineering*, 21:193–224.
- Dean, R. G. and Yoo, C. H. (1992). Beach-nourishment performance predictions. *Journal of Waterway, Port, Coastal, and Ocean Engineering*, 118(6):567–586.
- Defeo, O., McLachlan, A., Schoeman, D. S., Schlacher, T. A., Dugan, J., Jones, A., Lastra, M., and Scapini, F. (2009). Threats to sandy beach ecosystems: a review. *Estuarine, Coastal and Shelf Science*, 81:1–12.
- Deltacommissie (2008). *Samen werken met water [in Dutch]*.
- Deltares (2011). *UNIBEST-CL+ manual Manual for version 7.1 of the shoreline model UNIBEST-CL+*.
- Dong, P., Chen, Y., and Chen, S. (2015). Sediment size effects on rip channel dynamics. *Coastal Engineering*, 99:124–135.
- Egiazaroff, I. (1965). Calculation of non-uniform sediment concentrations. *Journal of Hydraulic Division ASCE*, 91(HY4):225–247.
- Eisma, D. (1968). Composition, origin and distribution of Dutch coastal sands between Hoek van Holland and the Island of Vlieland. *Netherlands Journal of Sea Research*, 4:123–267.
- Falques, A. and Calvete, D. (2005). Large-scale dynamics of sandy coastlines: Diffusivity and instability. *Journal of Geophysical Research-Oceans*, 110(C3).

- Field, C. B., Mortsch, L. D., Brklacich, M., Forbes, D. L., Kovacs, P., Patz, J. A., Running, S. W., and Scott, M. J. (2007). *Climate Change 2007: Impacts, Adaptation and Vulnerability: North America. Contribution of Working Group II to the Fourth Assessment Report of the Intergovernmental Panel on Climate Change*. Cambridge University Press, Cambridge, UK, 617–652.
- Folk, R. L. and Ward, W. C. (1957). Brazos River bar: a study in the significance of grain size parameters. *Journal of Sedimentary Petrology*, 27:3–26.
- Gallagher, E. L., MacMahan, J. H., Reniers, A. J. H. M., Brown, J. A., and Thornton, E. B. (2011). Grain size variability on a rip-channeled beach. *Marine Geology*, 287:43–53.
- Gao, S. and Collins, M. (1992). Net sediment transport patterns inferred from grain-size trends based upon definitions of "transport vectors". *Sedimentary Geology*, 80:47–60.
- Geleynse, N., Storms, J. E. A., Walstra, D. J. R., Jagers H R A Wang, Z. B., and Stive, M. J. F. (2011). Controls on river delta formation; insights from numerical modelling. *Earth and Planetary Science Letters*, 302(1-2):217–226.
- Giardino, A., Briere, C. D. E., and Van der Werf, J. J. (2011). Morphological modelling of bar dynamics with delft3d. the quest for optimal parameter settings. Technical Report 1202345-000, Deltares.
- Gibson, R. N. and Robb, L. (1992). The relationship between body size, sediment grain size and the burying ability of juvenile plaice, pleuronectes platessa l. *Journal of Fish Biology*, 40:771–778.
- Grunnet, N. M. and Ruessink, B. G. (2005). Morphodynamic response of nearshore bars to a shoreface nourishment. *Coastal Engineering*, 52(2):119–137.
- Grunnet, N. M., Ruessink, B. G., and Walstra, D. J. R. (2005). The influence of tides, wind and waves on the redistribution of nourished sediment at Terschelling, The Netherlands. *Coastal Engineering*, 52(7):617–631.
- Grunnet, N. M., Walstra, D. J. R., and Ruessink, B. G. (2004). Process-based modelling of a shoreface nourishment. *Coastal Engineering*, 51(7):581–607.
- Guillén, J. and Hoekstra, P. (1996). The "equilibrium" distribution of grain size fractions and its implications for cross-shore sediment transport: A conceptual model. *Marine Geology*, 135:15–33.
- Guillén, J. and Hoekstra, P. (1997). Sediment Distribution in the Nearshore Zone: Grain Size Evolution in Response to Shoreface Nourishment (Island of Terschelling, The Netherlands). *Estuarine, Coastal and Shelf Science*, 45:639–652.
- Hallermeier, H. J. (1981). A profile zonation for seasonal sand beaches from wave climate. *Coastal Engineering*, 4:253–277.

- Hamm, L., Capobianco, M., Dette, H. H., Lechuga, A., Spanhoff, R., and Stive, M. J. F. (2002). A summary of European experience with shore nourishment. *Coastal Engineering*, 47(2):237–264.
- Hanson, H., Brampton, A., Capobianco, M., Dette, H H abd Hamm, L., Laustrup, C., Lechuga, A., and Spanhoff, R. (2002). Beach nourishment projects, practices, and objectives - a European overview. *Coastal Engineering*, 47:81–111.
- Hanson, H. and Kraus, N. C. (1989). Genesis: Generalized model for simulating shore-line change. report 1. technical reference. Technical Report CERC-89-19, U.S. Army eng. Waterw. Exp. Station, Coastal Eng. Res. Center, Vicksburg, Miss.
- Hanson, S., Nicholls, R., Ranger, N., Hallegatte, S., Corfee-Morlot, J., Herweijer, C., and Chateau, J. (2011). A global ranking of port cities with high exposure to climate extremes. *Climatic Change*, 104:89–111.
- Hartog, W. M. (2006). Nourishment behavior Delray beach. Possible mechanisms for local anomalous behaviour. Master's thesis, Delft university of Technology.
- Hartog, W. M., Benedet, L., Walstra, D. J. R., Van Koningsveld, M., Stive, M. J. F., and Finkl, C. W. (2008). Mechanisms that influence the performance of beach nourishment: A case study in delray beach, florida, u.s.a. *Journal of Coastal Research*, 24(5):1304–1319.
- Hassan, W. N. and Ribberink, J. S. (2005). Transport processes of uniform and mixed sands in oscillatory sheet flow. *Coastal Engineering*, 52:745–770.
- Hinton, C. and Nichols, R. J. (1998). Spatial and temporal behaviour of depth of closure along the holland coast. *Proceedings of the International Conference on Coastal Engineering (ICCE)*, pages 2913–2925.
- Hoefel, F. and Elgar, S. (2003). Wave-Induced Sediment Transport and Sandbar Migration. *Science*, 299(5614):1885–1887.
- Hoekstra, P., Houwman, K. T., Kroon, A., Ruessink, B. G., Roelvink, J. A., and Spanhoff, R. (1996). Morphological development of the terschelling shoreface nourishment in response to hydrodynamic and sediment transport processes. In *In: Edge, B.L. (Ed.), Proc. 25th Int. Conf. on Coastal Engineering. ASCE, New York, pp. 2897–2910.*
- Holland, K. T. and Elmore, P. A. (2008). A review of heterogeneous sediments in coastal environments. *Earth-Science Reviews*, 89:116–134.
- Hoonhout, B. M. (2017). *Aeolian Sediment Availability and Transport*. PhD thesis, Delft University of Technology.
- Horn, D. P. (1993). Sediment dynamics on a macrotidal beach, Isle of Man (U.K.). *Journal of Coastal Research*, 9:189–208.
- Hsu, T. and Liu, P. L. (2004). Toward modeling turbulent suspension of sand in the nearshore. *Journal of Geophysical Research: Oceans*, 109(C6):2156–2202.

- Huisman, B. J. A., De Schipper, M. A., and Ruessink, B. G. (2016). Sediment sorting at the sand motor at storm and annual time scales. *Marine Geology*, 381:209–226.
- Huisman, B. J. A., Ruessink, B. G., De Schipper, M. A., Luijendijk, A. P., and Stive, M. J. F. (2018). Modelling of bed sediment composition changes at the lower shoreface of the Sand Motor. *Coastal Engineering*, 132:33–49.
- Huisman, B. J. A., van Thiel De Vries, J. S. M., Walstra, D. J. R., Roelvink, J. A., Ranasinghe, R., and Stive, M. J. F. (2013). Advection and diffusion of shore-attached sand nourishments. In *In P Bonneton and T Garlan (Eds.), International conference on coastal dynamics, 2013, France, pp. 845-858.*
- Huisman, B. J. A., Walstra, D. J. R., Radermacher, M., De Schipper, M. A., and Ruessink, B. G. (2019). Observations and modelling of shoreface nourishment behaviour. *Journal of Marine Science and Engineering*, 7(3):59.
- Inman, D. L. (1953). Areal and seasonal variations in beach and nearshore sediments at La Jolla, California. Technical report, U.S. Army Corps Eng. Beach Erosion Board, Technical Memorandum 39.
- Inman, D. L. (1987). Accretion and Erosion Waves on Beaches. *Shore & Beach*, 55:61–66.
- Isobe, M. and Horikawa, K. (1982). Study on water particle velocities of shoaling and breaking waves. *Coastal Engineering in Japan*, 25:109–123.
- Jacobsen, N. G. and Fredsoe, J. (2014a). Cross-shore redistribution of nourished sand near a breaker bar. *Journal of Waterway, Port, Coastal and Ocean Engineering*, 140:125–134.
- Jacobsen, N. G. and Fredsoe, J. (2014b). Formation and development of a breaker bar under regular waves. Part 2: Sediment transport and morphology. *Coastal Engineering*, 88:55–68.
- Janssen, G. M. and Mulder, S. (2005). Zonation of macrofauna across sandy beaches and surf zone along the Dutch coast. *Oceanologia*, 47:265–282.
- Kana, T. W., Rosati, J. D., and Traynum, S. B. (2011). Lack of evidence for onshore sediment transport from deep water at decadal time scales: Fire Island, New York. *Journal of Coastal Research*, SI 59:61–75.
- Karambas, T. V. and Samaras, A. G. (2014). Soft shore protection methods: The use of advanced numerical models in the evaluation of beach nourishment. *Ocean Engineering*, 92:129–136.
- Katoh, K. and Yanagishima, S. (1995). Changes of sand grain distribution in the surf zone. In Zeidler, R. B. and Dally, W. R., editors, *Coastal Dynamics 1995: Proceedings of the International Conference on Coastal Research*, pages 639–650, Gdansk, Poland. Am. Soc. of Civ. Eng.

- Knaapen, M. A. F., Holzhauer, H., Hulscher, S. J. M. H., Baptist, M. J., De Vries, M. B., and Van Ledden, M. (2003). On the modelling of biological effects on morphology. *River, Coastal and Estuarine Morphodynamics*, Barcelona:773–783.
- Kohsiek, L. (1984). The grain size characteristic of the most seaward range of dunes along the dutch coast (in dutch). Technical Report nota WWKZ-84G.007, Rijkswaterstaat. Dutch title : De korrelgrootte karakteristiek van de zeereep (stuifdijk) langs de Nederlandse kust.
- Komar, P. D. (1987). Selective grain entrainment by a current from a bed of mixed sizes: a reanalysis. *Journal of Sedimentary Petrology*, 57 (2):203–211.
- Komar, P. D. (1998). *Beach Processes and Sedimentation*. Prentice Hall, Upper Saddle River (New Jersey), 2nd edition.
- Konert, M. and Vandenberghe, J. (1997). Comparison of laser grain size analysis with pipette and sieve analysis: a solution for the underestimation of the clay fraction. *Sedimentology*, 44:523–535.
- Kroon, A., Van Leeuwen, B., Walstra, D. J. R., and Loman, G. (2015). Dealing with uncertainties in long-term predictions of a coastal nourishment. In *ICE Coastal Management, 7 - 9 September 2015, Amsterdam, the Netherlands*.
- Krumbein, W. C. and James, W. R. (1965). A lognormal size distribution model for estimating stability of beach fill material. Technical report, Northwestern Univ. Evanston Ill.
- Larson, M. and Kraus, N. C. (1991). Mathematical modeling of the fate of beach fill. *Coastal Engineering*, 16(1):83–114.
- Leonard, L., Clayton, T., and Pilkey, O. H. (1990). An analysis of replenished beach design parameters on U.S. East coast barrier islands. *Journal of Coastal Research*, 6(1):15–36.
- Lesser, G. R., Roelvink, J. A., Van Kester, J. A. T. M., and Stelling, G. S. (2004). Development and validation of a three-dimensional morphological model. *Coastal Engineering*, 51(8-9):883–915.
- Liu, J. T. and Zarillo, G. A. (1987). Partitioning of shoreface sediment grain-sizes. In *Coastal Sediments, New Orleans, USA, pp. 1533–1548*.
- Ludka, B. C., Guza, R. T., and O'Reilly, W. C. (2018). Nourishment evolution and impacts at four southern california beaches: A sand volume analysis. *Coastal Engineering*, 136:96–105.
- Luijendijk, A. P., Hagenaars, G., Ranasinghe, R., Baart, F., Donchyts, G., and Aarninkhof, S. G. J. (2018). The state of the world's beaches. *Scientific Reports*, 8(1):6641.

- Luijendijk, A. P., Ranasinghe, R., Schipper, M. A. D., Huisman, B. J. A., Swinkels, C. M., Walstra, D. J. R., and Stive, M. J. F. (2017). The initial morphological response of the Sand Engine: A process-based modelling study. *Coastal Engineering*, 119:1–14.
- MacMahan, J., Stanton, T. P., Thornton, E. B., and Reniers, A. J. H. M. (2005). RIPEX-Rip Currents on a shore-connected shoal beach. *Marine Geology*, 218:113–134.
- Masselink, G. (1992). Longshore variation of grain-size distribution along the coast of the Rhone Delta, Southern France - a test of the McLaren model. *Journal of Coastal Research*, 8 (2):286–291.
- McCall, R., Van Santen, R., and Huisman, B. J. A. (2014). Coastline modelling - Phase III : Investigation of the influence of model schematisation on a hindcast for the coast of Domburg. Technical report, Deltares.
- McCall, R. T. and Van Santen, R. (2013). Modelling coastline maintenance - A review of three coastline models. Technical report, Deltares.
- McLachlan, A. (1996). Physical factors in benthic ecology: Effects of changing sand particle size on beach fauna. *Marine Ecology Progress Series*, 131:205–217.
- McLachlan, A. and De Ruyck, A. M. C. (1993). Survey of sandy beaches in diamond area I. contract report to cdm, oranjemund, namibia. Technical report.
- McLaren, P. A. and Bowles, D. (1985). The effects of sediment transport on grain-size distributions. *Journal of Sedimentary Petrology*, 55:457–470.
- Medina, R., Losada, M. A., Losada, I. J., and Vidal, C. (1994). Temporal and spatial relationship between sediment grain size and beach profile. *Marine Geology*, 118 (3):195–206.
- Meirelles, S., Henriquez, M., Souza, A. J., Horner-Devine, A. R., and Pietrzak, J. D. (2016). Small scale bedform types off the south-holland coast. *Journal of Coastal Research*, 75 (sp1):423–426.
- Moutzouris, C. I., Kraus, N. C., Gingerich, K. J., and Kriebel, D. L. (1991). Beach profiles versus cross-shore distributions of sediment grain sizes. *Advances in Coastal Modeling*, pages 860–874. American Society of Civil Engineers, New York, NY.
- Mulder, J. P. M. and Tonnon, P. K. (2010). Sand engine : Background and design of a mega-nourishment pilot in the netherlands. *Proceedings of the International Conference on Coastal Engineering*, 1(32).
- Murray, D. M. and Holtum, D. A. (1996). Technical note: Inter-conversion of malvern and sieve size distributions. *Minerals Engineering*, 9 (12):1263–1268.
- Nicholls, R. J. (2004). Coastal flooding and wetland loss in the 21st century: changes under the SRES climate and socio-economic scenarios. *Global Environmental Change*, 14:69–86.

- Nicholson, J., Broker, I., Roelvink, J. A., Price, D., Tanguy, J. M., and Moreno, L. (1997). Intercomparison of coastal area morphodynamic models. *Coastal Engineering*, 31:97–123.
- Ojeda, E., Ruessink, B. G., and Guillen, J. (2008). Morphodynamic response of a two-barred beach to a shoreface nourishment. *Coastal Engineering*, 55:1185–1196.
- Pape, L., Kuriyama, Y., and Ruessink, B. G. (2010). Models and scales for nearshore sandbar behavior. *Journal of Geophysical Research-Earth Surface*, 115 (F03043).
- Park, J., Stabenau, E., Redwine, J., and Kotun, K. (2017). South florida's encroachment of the sea and environmental transformation over the 21st century. *Journal of Marine Science Engineering*, 5(31).
- Pelnard-Considere, R. (1956). Essai de théorie de l' evolution des formes de rivage en plages de sable et de galets. *4th Journees de l'Hydraulique, Les Energies de la Mer, Question III*, Rapport No. 1:74–1–74–10.
- Post, M. H., Blom, E., Chen, C., Bolle, L. J., and Baptist, M. J. (2017). Habitat selection of juvenile sole (*Solea solea* l.): Consequences for shoreface nourishment. *Journal of Sea Research*, 122:19–24.
- Pruszk, Z. (1993). The analysis of beach profile changes using dean's method and empirical orthogonal functions. *Coastal Engineering*, 19:245–261.
- Radermacher, M., De Schipper, M. A., Price, T. D., Huisman, B. J. A., Aarninkhof, S. G. J., and Reniers, A. J. H. M. (2018). Behaviour of subtidal sandbars in response to nourishments. *Geomorphology*, 313:1–12.
- Radermacher, M., Zeelenberg, W., De Schipper, M. A., and Reniers, A. J. H. M. (2015). Field Observations of Tidal Flow Separation at a Mega-Scale Beach Nourishment. In *The Proceedings of the Coastal Sediments 2015*. San Diego, USA, 11–15 May 2015.
- Ranasinghe, R., Duong, T. M., Uhlenbrook, S., Roelvink, J. A., and Stive, M. J. F. (2013). Climate change impact assessment for inlet-interrupted coastlines. *Nature Climate Change*, 3:83–87.
- Ranasinghe, R., Swinkels, C. M., Luijendijk, A. P., Roelvink, J. A., Bosboom, J., Stive, M. J. F., and Walstra, D. J. R. (2011). Morphodynamic upscaling with the MORFAC approach: Dependencies and sensitivities. *Coastal Engineering*, 58(8):806–811.
- Reniers, A. J. H. M., Gallagher, E. L., MacMahan, J. H., Brown, J. A., Van Rooijen, A. A., Van Thiel de Vries, J. S. M., and Van Prooijen, B. C. (2013). Observations and modeling of steep-beach grain-size variability. *Journal of Geophysical Research: Oceans*, 118 (2):577–591.
- Reniers, A. J. H. M., Roelvink, J. A., and Thornton, E. B. (2004a). Morphodynamic modeling of an embayed beach under wave group forcing. *Journal of Geophysical Research*, 109(C01030):1–22.

- Reniers, A. J. H. M., Thornton, E. B., Stanton, T. P., and Roelvink, J. A. (2004b). Vertical flow structure during Sandy Duck: Observations and modeling. *Coastal Engineering*, 51:237–260.
- Ribberink, J. S. (1987). *Mathematical modelling of onedimensional morphological changes in rivers with nonuniform sediment*. PhD thesis, Delft University of Technology.
- Richmond, B. M. and Sallenger, A. H. J. (1984). Cross-shore transport of bimodal sands. *Proceedings of the 19th International Conference on Coastal Engineering*, 2:1997–2008.
- Rijkswaterstaat (1999). Modelbeschrijving kuststrook-fijn model. Technical report.
- Rijkswaterstaat (2017a). Database of nourishment locations, volumes and characteristics.
- Rijkswaterstaat (2017b). The yearly coastal measurements (in Dutch : De JAaRlijks KUSmetingen or JARKUS).
- Rodríguez, J. G. and Uriarte, A. (2009). Laser diffraction and dry-sieving grain size analyses undertaken on fine- and medium-grained sandy marine sediments: A note. *Journal of Coastal Research*, 25 (1):257–264.
- Roelse, P. (1990). Beach and dune nourishment in the Netherlands. In *Proc. 22nd Int. Conf. on Coastal Engineering*, pages 1984–1997, New York. ASCE.
- Roelvink, D., Reniers, A., Van Dongeren, A., Van Thiel de Vries, J., McCall, R., and Lescinski, J. (2009). Modelling storm impacts on beaches, dunes and barrier islands. *Coast. Eng.*, 56(11-12):1133–1152.
- Roelvink, J. A. (1993a). Dissipation in random wave groups incident on a beach. *Coastal Engineering*, 19:127–150.
- Roelvink, J. A. (1993b). *Surfbeat and its effect on cross-shore profiles*. PhD thesis, Delft University of Technology.
- Roelvink, J. A. (2006). Coastal morphodynamic evolution techniques. *Coastal Engineering*, 53:277–287.
- Roelvink, J. A. and Stive, M. J. F. (1989). Bar-Generating Cross-Shore Flow Mechanisms on a Beach. *Journal Of Geophysical Research*, 94(C4):4785–4800.
- Rouse, H. E. (1950). *Engineering hydraulics*. New York, John Wiley and Sons.
- Rubin, D. M. (2004). A simple autocorrelation algorithm for determining grain size from digital images of sediment. *Journal of Sedimentary Research*, 74 (1):160–165.
- Ruessink, B. G. and Kroon, A. (1994). The behaviour of a multiple bar system in the nearshore zone of Terschelling: 1965-1993. *Marine Geology*, 121:187–197.



- Ruessink, B. G., Kuriyama, Y., Reniers, A. J. H. M., Roelvink, J. A., and Walstra, D. J. R. (2007). Modeling cross-shore sandbar behavior on the timescale of weeks. *Journal of Geophysical Research-Earth Surface*, 112(F3):1–15.
- Ruessink, B. G., Wijnberg, K. M., Holman, R. A., Kuriyama, Y., and van Enckevort, I. M. J. (2003). Intersite comparison of interannual nearshore bar behavior. *Journal of Geophysical Research*, 108(C8):3249.
- Ruggiero, P., Buijsman, M., Kaminsky, G. M., and Gelfenbaum, G. (2010). Modeling the effects of wave climate and sediment supply variability on large-scale shoreline change. *Marine Geology*, 273(1–4):127–140. Large-scale coastal change in the Columbia River littoral cell.
- Rutten, J., Ruessink, B. G., and Price, T. D. (2017). Observations on sandbar behaviour along a man-made curved coast. *Earth Surface Processes and Landforms*.
- Sembing, L. E., Van Ormondt, M., Van Dongeren, A. R., and Roelvink, J. A. (2015). A validation of an operational wave and surge prediction system for the Dutch Coast. *Natural Hazards and Earth System Sciences Discussions*, 2:3251–3288.
- Shand, R. D., Bailey, D. G., and Shepherd, M. J. (1999). An inter-site comparison of net offshore bar migration characteristics and environmental conditions. *Journal of Coastal Research*, 15(3):750–765.
- Sirks, E. E. (2013). Sediment sorting at a large scale nourishment. Master's thesis, Delft University of Technology.
- Slingerland, R. and Smith, N. D. (1986). Occurrence and formation of water-laid placers. *Annual Review of Earth and Planetary Sciences*, 14:113–147.
- Sloff, C. J., Jagers, H. R. A., Kitamura, Y., and Kitamura, P. (2001). 2d morphodynamic modelling with graded sediment. *Proceedings of 2nd IAHR Symposium on River, Coastal and Estuarine Morphodynamics*, pages 10–14.
- Sloff, C. J. and Mosselman, E. (2012). Bifurcation modelling in a meandering gravel-sand bed river. *Earth Surface Processes and Landforms*, 37(14):1556–1566.
- Sonu, C. (1972). Bimodal composition and cyclic characteristics of beach sediment in continuously changing profiles. *Journal of Sedimentary Petrology*, 42:852–857.
- Sorensen, R. M., Douglass, S. L., and Weggel, J. R. (2011). Results from the Atlantic City, N.J., beach nourishment monitoring program. In *Coastal Engineering Proceedings, [S.l.], n. 21, jan. 2011. ISSN 2156-1028*.
- Soulsby, R. L., Hamm, L., Klopman, G., Myrhaug, D., Simons, R. R., and Thomas, G. P. (1993). Wave-current interaction within and outside the bottom boundary layer. *Coastal Engineering*, 21:41–69.
- Spee, E. and Vatvani, D. (2009). Evaluatie van de nieuwe bodem v61-04 voor het kuststrookmodel - wti hr-zout, 1200103-023. Technical report, Deltares.

- Stauble, D. K. and Cialone, M. A. (1996). Sediment dynamics and profile interactions: Duck94. *Coastal Engineering*, 4:3921–3934.
- Steidtmann, J. R. (1982). Size-density sorting of sand-size spheres during deposition from bedload transport and implications concerning hydraulic equivalence. *Sedimentology*, 29:877–883.
- Stive, M. J. F., De Schipper, M. A., Lujendijk, A. P., Aarninkhof, S. G. J., Van Gelder-Maas, C., Van Thiel de Vries, J. S. M., De Vries, S., Henriquez, M., Marx, S., and Ranasinghe, R. (2013). A New Alternative to Saving Our Beaches from Sea-Level Rise: The Sand Engine. *Journal of Coastal Research*, 29 (5):1001–1008.
- Stive, M. J. F., De Vriend, H. J., Nicholls, R. J., and Capobianco, M. (1993). Shore nourishment and the active zone: A time scale dependent view. In *Proceedings of the Twenty-third International Conference on Coastal Engineering*, pages 2464–2473, Venice, Italy.
- Stive, M. J. F., Nichols, R. J., and De Vriend, H. J. (1991). Sea-level rise and shore nourishment : a discussion. *Coastal Engineering*, 16:147–163.
- Stolk, A. (1989). Zandsysteem kust, een morfologische karakterisering. Geopro report 1989.02, Rijksuniversiteit Utrecht, Vakgroep Fysische Geografie. 97 pp. (In Dutch).
- Svendsen, I. A. (1984). Mass flux and undertow in a surf zone. *Coastal Engineering*, 8:347–365.
- Szmytkiewicz, M., Biegowski, J., Kaczmarek, L. M., Okroj, T., Ostrowski, R., Pruszek, Z., Rozynski, G., and Skaja, M. (2000). Coastline changes nearby harbour structures: comparative analysis of one-line models versus field data. *Coastal Engineering*, 40 (2):119–139.
- Terwindt, J. H. J. (1962). Study of grain size variations at the coast of Katwijk 1962 (in Dutch). Report K-324, Rijkswaterstaat, The Hague, The Netherlands.
- Thevenot, M. M. and Kraus, N. C. (1995). Longshore sand waves at Southampton Beach, New York: observation and numerical simulation of their movement. *Marine Geology*, 126:249–269.
- Tonnon, P. K., Huisman, B. J. A., Stam, G. N., and Van Van Rijn, L. C. (2018). Numerical modelling of erosion rates, life span and maintenance volumes of mega nourishments. *Coastal Engineering*, 131:51–69.
- Trembanis, A. C. and Pilkey, O. H. (1998). Summary of beach nourishment along the us gulf of mexico shoreline. *Journal of Coastal Research*, pages 407–417.
- Trembanis, A. C., Pilkey, O. H., and Valverde, H. R. (1999). Comparison of Beach nourishment along the U.S. Atlantic, Great Lakes, Gulf of Mexico, and New England Shorelines. *Coastal Management*, 27 (4):329–340.

- Valverde, H. R., Trembanis, A. C., and Pilkey, O. H. (1999). Summary of beach nourishment episodes on the U.S. East Coast barrier islands. *Journal of Coastal Research*, 15:1100–1118.
- Van der Spek, A. J. F., de Kruijf, A. C., and Spanhoff, R. (2007). Guidelines shoreface nourishments. Technical report, National Institute for Coastal and Marine Management/RIKZ, Report RIKZ/2007.012, The Hague, (in Dutch).
- Van der Spek, A. J. F. and Elias, E. P. L. (2013). The effects of nourishments on autonomous coastal behaviour. In *7th International Conference on Coastal Dynamics, Arcachon, France*, number 221.
- Van der Zanden, J., Van der A, D. A., Hurther, D., Caceres, I., O'Donoghue, T., and Ribberink, J. S. (2016). Near-bed hydrodynamics and turbulence below a large-scale plunging breaking wave over a mobile barred bed profile. *Journal of Geophysical Research: Oceans*, 121 (8):6482–6506.
- Van der Zwaag, J. (2014). Development of sediment sorting at the large scale nourishment 'The Sand Motor'. Master's thesis, TU Delft and Deltares. Additional MSc Thesis.
- Van Duin, M. J. P., Wiersma, N. R., Walstra, D. J. R., Van Rijn, L. C., and Stive, M. J. F. (2004). Nourishing the shoreface: Observations and hindcasting of the Egmond case, The Netherlands. *Coastal Engineering*, 51 (Issue 8-9):813–837.
- Van Enckevort, I. M. J. and Ruessink, B. G. (2003). Video observations of nearshore bar behavior. Part 1: alongshore uniform variability. *Continental Shelf Research*, 23:501–512.
- Van Geer, P., Den Bieman, J., Hoonhout, B., and Boers, M. (2015). XBeach 1D - Probabilistic model: ADIS, settings, Model uncertainty and Graphical User Interface. Technical report, Deltares.
- Van Koningsveld, M. and Mulder, J. P. M. (2004). Sustainable Coastal Policy Developments in the Netherlands. A Systematic Approach Revealed. *Journal of Coastal Research*, 20(2):375–385.
- Van Rijn, L. C. (1993). *Principles of Sediment Transport in Rivers, Estuaries and Coastal Seas*. Aqua Publications, Amsterdam.
- Van Rijn, L. C. (1997a). Cross-shore modelling of graded sediments. Technical Report Z2181, WL | Delft Hydraulics.
- Van Rijn, L. C. (1997b). Sediment transport and budget of the central coastal zone of Holland. *Coastal Engineering*, 32:61–90.
- Van Rijn, L. C. (2007a). Unified View of Sediment Transport by Currents and Waves I: Initiation of Motion, Bed Roughness, and Bed-Load Transport. *Journal of Hydraulic Engineering*, 133(6):649–667.

- Van Rijn, L. C. (2007b). Unified View of Sediment Transport by Currents and Waves II: Suspended Transport. *Journal of Hydraulic Engineering*, 133(6):668–689.
- Van Rijn, L. C. (2007c). Unified View of Sediment Transport by Currents and Waves III: Graded Beds. *Journal of Hydraulic Engineering*, 133(7):761–775.
- Van Rijn, L. C. (2014). A simple general expression for longshore transport of sand, gravel and shingle. *Coastal Engineering*, 90:23–39.
- Van Rijn, L. C., Ribberink, J. C., Reniers, A., and Zitman, T. J. (1995). Yearly averaged sand transport at the -20 m and -8 m NAP depth contours of the Jarkus profiles 14, 40, 76 and 103. Report H1887, WL | Delft Hydraulics, Delft, The Netherlands.
- Van Rijn, L. C., Walstra, D. J. R., and Van Ormondt, M. (2004). Description of TRANSPORT2004 and implementation in Delft3D-ONLINE. Report Z3748.00, WL | Delft Hydraulics.
- Van Straaten, L. M. J. U. (1965). Coastal barrier deposits in South- and North Holland in particular in the area around Scheveningen and IJmuiden. *Mededelingen van de Geologische Stichting*, 17:41–75.
- Van Thiel de Vries, J. S. M. (2009). *Dune erosion during storm surges*. PhD thesis, Delft University of Technology, Delft, The Netherlands.
- Van Thiel de Vries, J. S. M., Van Gent, M. R. A., Walstra, D. J. R., and Reniers, A. J. H. M. (2008). Analysis of dune erosion processes in large-scale flume experiments. *Coastal Engineering*, 55(12):1028–1040.
- Visser, A. W., Souza, A. S., Hessner, K., and Simpson, J. H. (1994). The effect of stratification on tidal current profiles in a region of freshwater influence. *Oceanologica Acta*, 17(4):369–381.
- Walstra, D. J. R. (2016). *On the anatomy of nearshore sandbars: A systematic exposition of inter-annual sandbar dynamics*. Delft University of Technology.
- Walstra, D. J. R., Hoekstra, R., Tonnon, P. K., and Ruessink, B. G. (2013). Input reduction for long-term morphodynamic simulations in wave-dominated coastal settings. *Coastal Engineering*, 77:57–70.
- Walstra, D. J. R., Reniers, A. J. H. M., Ranasinghe, R., Roelvink, J. A., and Ruessink, B. G. (2012). On bar growth and decay during interannual net offshore migration. *Coastal Engineering*, 60:190–200.
- Weber, O., Gonthier, E., and Faugères, J. C. (1991). Analyse granulométrique de sédiments fins marins: comparaison des résultats obtenus au sédiograph et au malvern. *Bulletin de l'Institut de Géologie du Bassin d'Aquitaine*, 50:107–114.
- Wijnberg, K. M. (2002). Environmental controls on decadal morphologic behaviour of the Holland coast. *Marine Geology*, 189:227–247.
- Wijnberg, K. M. and Kroon, A. (2002). Barred beaches. *Geomorphology*, 48:103–120.

- Wijnberg, K. M. and Terwindt, J. H. J. (1995). Extracting Decadal Morphological Behavior from High-Resolution, Long-Term Bathymetric Surveys Along the Holland Coast Using Eigenfunction Analysis. *Marine Geology*, 126(1-4):301–330.
- Wijsman, J. W. M. and Verduin, E. (2011). T0 monitoring Zandmotor Delftlandse kust: Benthos ondiepe kustzone en natte strand. Technical report, IMARES / Wageningen UR.
- Wilcock, P. R. (1993). Critical shear stress of natural sediments. *Hydraulic Engineering*, 119(4):491–505.
- WL | Delft Hydraulics, Boussinesqweg1, D. T. N. (1994). *UNIBEST, a software suite for the simulation of sediment transport processes and related morphodynamics of beach profiles and coastline evolution. Programme manual.*
- Zonneveld, P. C. (1994). Comparative investigation of grain-size determination (sieve/Malvern). Technical Report OP 6500, State Geological Survey, Haarlem, The Netherlands.



# ACKNOWLEDGMENTS

The writing of a PhD thesis has been a challenge exceeding expectations. The freedom to pursue new ideas about the coastal system and the dynamics of the interaction with colleague scientists have been greatly inspiring. It was like unpacking a present when unexpected behaviour could be transformed to understandable mechanisms, while expected behaviour was ruled out. Having more endurance than the problems that were faced proved to be the most successful strategy, which could be aided with suitable data analyses and/or modelling. Of course, it has also been tough work at times. Here I was fortunate to have support from family, friends and colleagues at Deltares, Delft University of Technology and Utrecht University. You helped me greatly in keeping a positive view on the research even when the pressure of unfinished work was piling up.

I would like to thank my promotor Marcel Stive who has provided the excellent conditions for this research through ERC-Advanced Grant 291206-NEMO, as well as to Wiel Tilmans and Klaas-Jan Bos who were very supportive in providing me an opportunity to spend time on this PhD thesis. You all had great confidence in a positive outcome of the PhD work, which was experienced as sailing with the wind in the back. The thorough reading and pleasant discussions on results with many of you were also valued, for which I would like to express my special gratitude to Gerben Ruessink, Matthieu de Schipper, Dirk-Jan Walstra, Leo van Rijn, Max Radermacher and Arjen Luijendijk. I really appreciate the kind words you had before pointing out the gaps that had to be filled in. The fact that the work was read and appreciated also helped me a great deal in finding motivation for the finalization of the work, for which relief was also provided by SO programme leaders Peter van den Berg and Wiebe de Boer. Being part of the NEMO team with Bas Hoonhout and Saulo Meirelles and Max Radermacher also made the PhD trajectory a lot lighter in a sense that different opinions could be shared directly or indirectly using flyers, while unplanned road trips to the Noord-Oost polder also fitted well into our schedules. On the practical side, a great number of people have been supporting the work extensively. Daan Wouwenaar has been an accurate and decisive navigator who dared to sail even unto MSL depth contour during high waters, not bothering about running aground in the troughs of the waves. I also really enjoyed working with Emma Sirks, Jelle van der Zwaag and Laurens Bart on the collection of sediment samples, initial analyses and modelling. Your work has formed the data foundation for the conceptual thinking of the sorting processes that act at the lower shoreface. It all sorted out well in the end, and I hope that you can also look back at an adventurous period at sea and working on the thesis. While the numeric explorations of Gerwin Stam, Victoria Curto and Astrid Vargas Solis were also very interesting and a very much valued cooperation. Many more people could be added who provided me with information on relevant literature, data processing or additional data from

other research programmes, of which I would limit myself here to Jeroen Wijsman of Wageningen Marine Research and Pieter-Koen Tonnon of Deltares who provided relevant data on sediment samples in the framework of the Sand Motor monitoring programme of the European Fund for Regional Development (EFRO). The collaboration with researchers from the NatureCoast project (no. 12686) also proved to be very useful, for which the Dutch Technology Foundation STW is acknowledged, which is part of the Netherlands Organisation for Scientific Research (NWO), and which is partly funded by the Ministry of Economic Affairs.

Not the least, I would like to express my special gratitude for the support that was provided by my wife Christine throughout the whole period, even when things were very busy at home. Having Nathan, Lucas and Lois around has made our lives even more energetic, and receiving them in our midst truly provided the most special moments in these years. I hope to have ample time for the kids in the coming period. Moreover I am thankful to God for the skills and daily health he provided, which helped me a great deal in the research and writing of this thesis, as well as the perspective that is provided towards the research work. Not exaggerating the importance of the PhD work in view of greater things, even though it has been a very useful occupation.



## ABOUT THE AUTHOR

Bas Huisman was born with the Dutch nationality on the 22nd of June 1980 in Slie-drecht. Bas Huisman attended the secondary school in Rotterdam (Atheneum) after which he studied at Delft University of Technology. The fundamental physics and practical engineering in the Department of hydraulic engineering of the Faculty of Civil Engineering and Geosciences had a strong appeal to Bas Huisman, which resulted in a Cum Laude Master of Science degree in the field of river engineering in August 2005. After the Master thesis it was possible to continue work at Rijkswaterstaat (within the former insitute on fresh water RIZA) studying the Water quality of the Dutch rivers and lakes on the basis of measurements. From 2006 onwards Bas Huisman became advisor/researcher at WL | Delft Hydraulics (and later Deltares) within the department of Harbour Coastal and Offshore engineering with a focus on morphological impacts of coastal infrastructure. Experience was gained in wave, tide and morphological modelling (e.g. Swan, Pharos, Unibest, Delft3D, Xbeach), software coding (e.g. Fortran and Matlab), laboratory experiments, scientific writing and project management. A decision was quickly made when the opportunity came up to join in a part-time PhD position at Delft University of Technology starting in fall 2012. The ERC advanced grant of Marcel Stive on Nearshore Monitoring and Modelling (NEMO) at Delft University has provided an excellent opportunity to study coastal morphological processes. This thesis is the result of the studies made within the PhD. Currently, Bas Huisman is part of the department of Applied Morphodynamics at Deltares, working on wave, flow and morphological modelling and field data analysis of estuaries and sandy coasts in a large number of countries around the world.



# LIST OF PUBLICATIONS

31. **B.J.A. Huisman, D.J.R. Walstra, M.A. de Schipper, M. Radermacher, B.G. Ruessink (2019)**, *Observations and Modelling of Shoreface Nourishment Behaviour*, Journal of Marine Science and Engineering. 2019; 7(3):59
30. **J.A. Roelvink, B.J.A. Huisman, A. Elghandour (2019)**, *Efficient modelling of complex coastal evolution at monthly to century time scales*, International Journal of Sediment Research. 2019 (in review)
29. **C. Hallin, B.J.A. Huisman, M. Larson, D.J.R. Walstra; H. Hanson (2019)**, *Impact of sediment supply on decadal-scale dune evolution - Analysis and modelling of the Kennemer dunes in the Netherlands*, Geomorphology (accepted)
28. **B.T. Grasmeijer, L.C. van Rijn, J.J. van der Werf, F. Zijl, B.J.A. Huisman, A.P. Luijendijk, R.J.A. Wilmink, A.P. de Looff (2019)**, *Method for calculating annual sand transports on the Dutch lower shoreface to assess the offshore boundary of the Dutch coastal foundation*, Proceedings of the Coastal Sediments Conference. 2019
27. **B.J.A. Huisman, B.G. Ruessink, M.A. de Schipper, A.P. Luijendijk, M.J.F. Stive (2018)**, *Modelling of bed sediment composition changes at the lower shoreface of the Sand Motor*, Coastal Engineering, Vol. 132 pp. 33-49
26. **J.A. Roelvink, B.J.A. Huisman, A. Elghandour (2018)**, *New approach to modelling coastal evolution in the context of global change*, Proceedings of the Sixth International Conference on Estuaries and Coasts (ICEC-2018), August 20-23, 2018, Caen, France
25. **C. Fredriksson, B.J.A. Huisman, M. Larson, H. Hanson (2018)**, *Long-term dune evolution under interacting cross-shore and longshore processes*, Coastal Engineering Proceedings, [S.l.], n. 36, p. sediment.73, dec. 2018. ISSN 2156-1028.
24. **Y.S. Chang, B.J.A. Huisman, W.P. de Boer, J. Yoo (2018)**, *Hindcast of Long-term Shoreline Change due to Coastal Interventions at Namhangjin, Korea*, Journal of Coastal Research, SI 85
23. **P.K. Tonnon, B.J.A. Huisman, G.N. Stam, L.C. van Rijn (2018)**, *Numerical modelling of erosion rates, life span and maintenance volumes of mega nourishments*, Coastal Engineering, Vol. 131, pp. 51-69
22. **M. Radermacher; M.A. de Schipper, T.D. Price, B.J.A. Huisman, S.G.J. Aarninkhof, A.J.H.M. Reniers (2018)**, *Behaviour of subtidal sandbars in response to nourishments*, Geomorphology, Vol. 313, pp. 1-12
21. **Y.S. Chang, B.J.A. Huisman, W.P. de Boer, J-S. Sim, R.T. McCall, K. Do, J. Yoo (2017)**, *Modelling the Shoreline Response to a Submerged Breakwater at Anmok Beach in Korea with Single Line Theory*, Journal of Coastal Disaster Prevention, Vol. 4, pp. 161-175

20. **B.J.A. Huisman, A. Vargas Solis, M.A. de Schipper, M. Radermacher, R. Ranasinghe (2017)**, *Impact of beach states on alongshore transport*, Proceedings of the Coastal Dynamics Conference 2017
19. **J. Stronkhorst, B.J.A. Huisman, A. Giardino, G. Santinelli, F.D. Santos (2017)**, *Sand nourishment strategies to mitigate coastal erosion and sea level rise at the coasts of Holland (The Netherlands) and Aveiro (Portugal) in the 21st century*, Ocean and coastal management, pp. 1-11
18. **M. Radermacher, G. Wessel, M.A. de Schipper, B.J.A. Huisman, S.G.J. Aarninkhof and A.J.H.M. Reniers (2017)**, *Evolution of alongshore bathymetric variability around a mega-scale beach nourishment*, Proceedings of the Coastal Dynamics Conference 2017
17. **Wiebe de Boer, Bas Huisman, Jeseon Yoo, Kideok Do, Yeon S. Chang, Robert McCall, Freek Scheel, Arjen Luijendijk, Cilia Swinkels, Panos Athanasiou, Dirk-Jan Walstra (2017)**, *Relative impact of natural processes and anthropogenic interventions on the variability in shoreline position at the Korean East coast*, Proceedings of the Coastal Dynamics Conference 2017
16. **A.P. Luijendijk, R. Ranasinghe, M.A. de Schipper, B.J.A. Huisman, C. Swinkels, D.J.R. Walstra and M.J.F. Stive (2017)**, *The initial morphological response of the Sand Engine: A process-based modelling study*, Coastal Engineering, Vol. 119, pp 1-14.
15. **B.J.A. Huisman, M.A. de Schipper and B.G. Ruessink (2016)**, *Sediment sorting at the sand motor at storm and annual time scales*, Journal of Marine Geology, Volume 381, 1 November 2016, pp. 209–226.
14. **B.J.A. Huisman, V. Curto, R. Hoekstra and M.A. De Schipper (2015)**, *Reshaping of realistic beach nourishments under high angle wave conditions*, 36th IAHR world Congress, 2015.
13. **A.P. Luijendijk, B.J.A. Huisman, and M.A. De Schipper (2015)**, *Impact of a storm on the first-year evolution of the sand engine*, Coastal Sediments conference 2015, Sand Diego, US.
12. **B.J.A. Huisman, J. v.d. Zwaag, A.P. Luijendijk, and B.G. Ruessink (2015)**, *Practical considerations on numerical modelling of sediment sorting at a large scale sand nourishment*, Coastal Sediments conference 2015, Sand Diego, US.
11. **A. Giardino, M. di Leo, G. Bragantini, H.J. de Vroeg, P.K. Tonnon, B.J.A. Huisman, M. de Bel (2015)**, *An Integrated Sediment Management Scheme for the Coastal Area of Batumi (Georgia)*, MedCoast 2015 Conference.
10. **P.K. Tonnon, G.N. Stam, B.J.A. Huisman, L.C. van Rijn (2014)**, *Initial sand losses and life span predictions for mega-nourishments along the Dutch coast*, International Conference on Coastal Engineering (ICCE).
9. **B.J.A. Huisman, E.E. Sirks, L. van der Valk and D.J.R. Walstra (2014)**, *Time and Spatial Variability of Sediment Gradings in the Surfzone of a Large Scale Nourishment*, Journal of Coastal Research, Special Issue No. 66.
8. **B.J.A. Huisman, J.S.M. van Thiel De Vries, D.J.R. Walstra, J.A. Roelvink, R. Ranasinghe and M.J.F. Stive (2013)**, *Advection and diffusion of shore-attached sand nourishments*, In P Bonneton and T Garlan (Eds.), International conference on coastal dynamics, 2013, France, (pp. 845-858).

7. **B.J.A. Huisman, Z.B. Wang, J.G. De Ronde, J. Stronkhorst and C.J. Sprengers (2013)**, *Coastline modeling for nourishment strategy evaluation*, Proceedings of the 6th conference on Applied Coastal Research (SCACR), June 2013.
6. **A. Giardino, W.P. de Boer, C. den Heijer, B.J.A. Huisman, J.P.M. Mulder, D.J.R. Walstra (2013)**, *Innovative approaches and tools for erosion control and coastline management*, Proceedings of Medcoast 2013 Conference, Marmaris, Turkey, Vol. 2.
5. **C. Den Heijer, D.J.R. Walstra, J.S.M. van Thiel de Vries, B.J.A. Huisman, B.M. Hoonhout, F.L.M. Diermanse, P.H.A.J.M. Van Gelder (2011)**, *Importance of dune erosion influencing processes*, Seventh International Symposium on Coastal Engineering and Science of Coastal Sediment Processes (ICS 2011).
4. **M. Schroevers, B.J.A. Huisman, M. van der Wal (2011)**, *Measuring ship induced waves and currents on a tidal flat in the Western Scheldt Estuary*, Current, Waves and Turbulence Measurements (CWTM), 2011 IEEE/OES 10th, pp. 123-129.
3. **B.J.A. Huisman, D. Rudolph, A. Kanand, M. Möschen (2009)**, *Scour protection performance of an innovative composite rubber mat at offshore wind turbine foundations*, Proceedings of the European Offshore Wind conference, 2009.
2. **B.J.A. Huisman, A.P. Luijendijk (2009)**, *Sand demand of the Eastern Scheldt: morphology around the barrier*, Deltares report Z4581, February 2009.
1. **Driesprong-Zoeteman, A.; Huisman, B.J.A.; Van Hal, M. (2006)**, *Afwenteling rijkswateren : eerste verkenning van effectiviteit KRW maatregelen in rijkswateren Schelde en Rijn-West*, RIZA werkdocument, 2005.154X. Rijkswaterstaat.